UNSW SYDNEY

Cortical N-methyl-d-aspartate receptor in schizophrenia: Characterising molecular changes at the cellular and sub-cellular level

Author:
Derminio, Dominique

Publication Date:
2015

DOI:
https://doi.org/10.26190/unsworks/18196

License:
https://creativecommons.org/licenses/by-nc-nd/3.0/au/
Link to license to see what you are allowed to do with this resource.

Downloaded from http://hdl.handle.net/1959.4/54473 in https://unsworks.unsw.edu.au on 2024-04-27

Cortical N-methyl-d-aspartate receptor in schizophrenia: Characterising molecular changes at the cellular and sub-cellular level

Dominique Suzanne Derminio

A thesis in fulfilment of the requirements for the degree of

Masters in Science by Research

School of Psychiatry

Faculty of Medicine

University of New South Wales

21 April 2015

ORIGINALITY STATEMENT

'I hereby declare that this submission is my own work and to the best of my knowledge it contains no materials previously published or written by another person, or substantial proportions of material which have been accepted for the award of any other degree or diploma at UNSW or any other educational institution, except where due acknowledgement is made in the thesis. Any contribution made to the research by others, with whom I have worked at UNSW or elsewhere, is explicitly acknowledged in the thesis. I also declare that the intellectual content of this thesis is the product of my own work, except to the extent that assistance from others in the project's design and conception or in style, presentation and linguistic expression is acknowledged.'

Signed .....

Date 21/04/2015 .....

Acknowledgements

I would like to take some time to thank people who have helped me get to where I am today.

First, I would like to thank my undergraduate professors whom were always available. To my advisor and professor Dr. Carroll, who allowed me to take more courses than he would have preferred because he believed in my capabilities to handle the extra work and always having his door open to talk about everything that was needed. To my first research advisor, Dr. Sellers, who peaked my interest in asking questions and teaching me to think like a scientist.

Next, I would like to thank my mentor and co-supervisor. Professor Cyndi Shannon Weickert, I can never thank you enough for the opportunity you have provided me. When I originally e-mailed you asking for an internship at NeuRA, I would have never imagined the life changing opportunity you would provide in such an amazing country. Being in this laboratory has opened my perspective to the science community by going to conferences and speaking with world-renowned researchers in the field of schizophrenia. I feel as though I have grown as a scientist being in your laboratory. Also, to Dr. Vibeke Catts, thank you for all your time and patience you have had with me. You have been someone who I have always felt comfortable coming to you and asking anything. The feedback I have received from you has allowed me to grow as a researcher, and I can never thank you enough for all you have done.

Now, for the rest of the Schizophrenia Research Laboratory, I first want to thank Debora Rothmond and Inara Bebris for all of the e-mails back and forth helping me get set up at UNSW and for Debora picking me up at the airport in a country where I didn't know anyone at that time. You made me feel at home as

soon as I got off of that 14-hour plane ride. Next, I want to thank Alice Rothwell and Debora, again, for the immunohistochemistry help. Dr. Sam Fung, thank you for your help with all of the in situ questions I had. Thank you Yiru Zhang as well, for helping me find images to show the PFC, part of your research. Also, I want to thank everyone else in the SRL laboratory for being there for questions, laughs, and for welcoming me into this lab the way you did.

Outside of the lab, I want to thank my mom and dad for allowing me travel across the world to take this wonderful opportunity. Also, I want to thank my Aunt Marlene for just random laughs and jokes when I was stressed out. Finally, I want to thank all my friends, and my boyfriend Jeff, who were there who supported me along the way from every part of the world.

Manuscripts in preparations and conference presentations

Manuscripts in Preparation:

Post-synaptic density NMDA-receptor NR1 subunit in the prefrontal cortex of patients with schizophrenia. For submission to Schizophrenia Research

Conference presentations

Decreased NMDA receptor NR1 subunit in post-synaptic density from prefrontal cortex in patients with schizophrenia. *Australia Neuroscience Society Annual Meeting*, January 2013, Melbourne, Victoria, Australia.

Increased autoantibodies against brain tissue in schizophrenia. *Brain Sciences* UNSW, August 2012, Randwick, New South Wales, Australia.

Increased autoantibodies against brain tissue in schizophrenia. *Society of Biological Psychiatry*, May 2012, Philadelphia, Pennsylvania, United States of America.

Abstract

Schizophrenia is a mental disorder that affects approximately 1% of the world's population. The N-methyl-d-aspartate receptor (NMDAR) seems likely to play a prominent role in schizophrenia; as when NMDAR antagonists are introduced, psychosis occurs in individuals with no mental disorders. This thesis explores how NMDAR may be endogenously changed in the brains of people with schizophrenia. By using tissue fractionation, discussed in chapter 3, to examine the post-synaptic density (PSD) specifically one can specifically examine the NMDAR protein at the synapse of the neuron. Also, one can examine the NMDAR mRNA level in the brains of people with schizophrenia compared to controls.

My Masters' thesis research covers four broad areas, namely subcellular tissue fractionation of human cerebral cortex, the determination of the NMDAR subunit NR1 protein levels specifically in the PSD, analysis of NR1 mRNA transcript across cortical lamina, and the quantification of NMDAR NR1 mRNA at the cellular level. It is hypothesized that the NMDAR NR1 protein will be decreased in the PSD and mRNA will be decreased in neurons in schizophrenia patients. There are four main aims of this study. The first aim is to extract the postsynaptic density fraction from human brains in the BA10 region. Using the New South Wales Tissue Resource Centre Cohort (37 schizophrenia patients and 37 controls). Tissue fractionation, discussed in chapter two, was completed in order to obtain total homogenate and PSD-enriched fractions from the PFC [Brodmann's Area (BA) 10]) from individuals with schizophrenia and controls.

The second aim was to measure NMDAR NR1 protein levels in schizophrenia compared to controls in the total homogenate and PSD associated

homogenate from the BA10 region. The amounts of NMDAR NR1 protein were determined using Western blotting techniques, described in chapter four.

The third aim was to examine examining the laminar expression of NMDAR NR1 mRNA in BA46 in schizophrenia compared to controls using a riboprobe GRIN1 (human genome designation for the NMDAR NR1 subunit). Film from in situ hybridization was used to determine the amount of mRNA from NMDAR NR1 in each cortical layer in the BA46 in patients with schizophrenia and controls, discussed in chapter five.

The fourth aim was to measure the cellular expression of NMDAR NR1 mRNA in BA46 in schizophrenia compared to controls in three laminar layers. In addition, silver grain analysis (corresponding to the amount of NMDAR NR1 mRNA/cells) of individual large and small neurons was analysed to determine if changes in mRNA could be localised to specific cell types within cortical layer V. mRNA for the NR1 subunit was studied in the PFC using in situ hybridization, discussed in chapter six.

Through the process of Western blotting, it was concluded that our fractionation samples containing the synapse were indeed enriched for proteins (including NR1) known to be enriched in the PSD. From there, analysis of the PSD fractions revealed a statistically significant decreased NR1 protein (39%) in the PSD in people with schizophrenia compared to controls. There were no significant diagnostic differences in NR1 mRNA expression when analysing the individual layers of the cortex from the autoradiographic films. However, when delving deeper and looking at individual neurons, I found that pyramidal neurons were significantly lower in NR1 mRNA expression in people with schizophrenia, and thus may play a role in the hypoglutamatergia in schizophrenia.

Future work required would be to determine which neurons are responsible for the NR1 protein changes at the PSD. A comprehensive examination of NR1 mRNA expression across more cortical layers at a microscopic level in BA46 is warranted.

Table of Contents

Title Page …….. Page 1

Originality Statement …….. Page 2

Acknowledgements …….. Page 3

Manuscripts in preparation and conference presentations…….. Page 5

Abstract …….. Page 6

Table of Contents …….. Page 9

List of Figures …….. Page 14

List of Tables …….. Page 17

List of Abbreviations …….. Page 20

Chapter 1- Introduction to Schizophrenia …….. Page 24

Mental illness and schizophrenia …….. Page 24

What is schizophrenia? …….. Page 25

The human brain …….. Page 29

Prefrontal cortex in relation to schizophrenia …….. Page 30

Brodmann Areas 10 and 46 …….. Page 32

Neuron types, glutamatergic pyramidal cells and GABAergic interneurons…… Page 36

The N-methyl-d-aspartate receptor …….. Page 37

Molecular biology of the N-methyl-d-aspartate receptor …. Page 40

Studies of the NMDAR in schizophrenia …… Page 43

Subcellular tissue fractionation……..Page 45

The postsynaptic density……Page 46

NMDAR NR1 subunit……..Page 49

mRNA……..Page 50

in situ hybridisation……...Page 51

Silver grains……Page 51

Aims of my thesis …….... Page 53

Chapter 2- New South Wales Tissue Resource Centre Cohort……..…….. Page 55

UNSW Research Ethics Approval……Page 55

Cohort information……...Page 55

Overview……Page 62

Chapter 3- Methods in Post-Mortem Tissue Fractionation……Page 63

Consideration of Tissue Fractionation Techniques……..Page 63

Aims of this study……..Page 65

Material and Methods ……..…….. Page 65

Tissue pulverisation……...Page 65

Subcellular fractionation of post-mortem brain tissue …….. Page 65

Day 1……..…….. Page 66

Day 2……..…….. Page 68

Day 3……..…….. Page 70

Day 4……..…….. Page 71

BCA protein analysis ……..…… Page 72

Protein measurement……..…… Page 72

Results for Tissue Analysis……Page 73

Discussion……..…...Page 77

Chapter 4- Western Blotting Study…..……Page 81

Introduction……..Page 81

Material and Methods……..……..Page 81

TRC Cohort……...…Page 81

Western blot procedure……...Page 81

Day 1…….…… Page 82

Day 2……..……...Page 83

Day 3 …….. Page 84

Chemidoc analysis …….. Page 84

Quantity One analysis …….... Page 85

Data and statistical analysis ……..…….. Page 85

Results for NMDAR NR1 PSD protein analysis……...Page 86

Antibody signal decreased overtime……Page 86

Demographic/clinical effects of NR1……..……Page 89

Diagnosis related effects of NR1 in fractionation……Page 91

Discussion……Page 93

Future research……Page 97

Limitations of the study……Page 97

Chapter 5-NR1 mRNA Assessment of Expression Laminar Film Analysis Page 100

Introduction……Page 100

Material and Methods……..…..Page 100

In situ hybridisation film quantification…….....Page 101

Determining the µCi/g of NMDAR NR1/cortical layer……...Page 101

Excel…..…….....Page 102

Data Analysis……Page 103

Results……...Page 103

Film analysis for NMDAR RN1 mRNA expression level…….Page 103

Statistical analysis……..……...Page 105

Discussion……...Page 114

Chapter 6- NR1 Silver Grains in Interneurons and Pyramidal Neurons....Page 118

Introduction.....Page 118

Method.....Page 119

In situ hybridization silver grain analysis.....Page 119

Cell counts and nuclear diameter measurements.....Page 120

Silver grain counts.....Page 121

Data analysis.....Page 122

Results.....Page 122

Cortical width of BA46.....Page 122

Silver grain analysis of layer III in BA46.....Page 123

Silver grain analysis of layer II in BA46.....Page 123

Silver grain analysis of layer V in BA46.....Page 123

Number of cells counted in layer V.....Page 123

Density of glial cells.....Page 124

Density of interneurons.....Page 125

Density of pyramidal neurons.....Page 126

Nuclei size of neurons.....Page 127

Binning for neurons analysis.....Page 128

Discussion.....Page 151

Limitations.....Page 161

Chapter 7- Overall Discussion: What does this mean to schizophrenia?....Page 164

Experimental limitations and future directions.....Page 167

References.....Page 170

Appendix 1- Solutions.....Page 199

Appendix 2- Methods related to Thesis, carried out by others.....Page 209

Appendix 3- Methods related to Thesis carried out in thesis……...Page 215

List of Figures

Figure 1.1: The prefrontal cortex in relation to overall brain size……... Page 31

Figure 1.2: Shows view of the PFC and its different regions……....Page 34

Figure 1.3: AMPA and NMDA receptors functioning together as a coincidence detector ……..Page 38

Figure 1.4: Structure of the NMDAR and common molecules ……Page 41

Figure 3.1: An overview of Day 1 for the tissue fractionation procedure…Page 68

Figure 3.2: An overview of Day 2 for the tissue fractionation procedure…Page 69

Figure 3.3: An overview of Day 3 for the tissue fractionation procedure…Page 71

Figure 3.4: An overview of Day 4 for the tissue fractionation procedure.. Page 72

Figure 3.5: Western blot to analyse specific tissue fractions……...Page 74

Figure 3.6: Quantitative analysis of Western blot of fractionation using NR1, Synaptophysin, and NeuN…….....Page 76

Figure 4.1 Western blot transfer cassette procedure……...Page 83

Figure 4.2: NR1 protein and housekeeping protein expression over time using the same lots of antibodies……...Page 87

Figure 4.3: Westing blot showing NR1 antibody non-functional……Page 88

Figure 4.4: Amount of NR1 protein from the PSD homogenate comparing schizophrenia patients and controls……Page 92

Figure 5.1: Example of placement of lines for lamina analysis in BA46…Page 102

Figure 5.2: Different cortical layers in the DLFPC expressed by the NDMAR NR1 mRNA……..Page 104

Figure 5.3: Comparison between diagnostic group for NMDAR NR1 mRNA in the DLPFC for layers II, III, IV, V, and VI……...Page 106

Figure 5.4: Comparison between schizophrenia patients and controls for NR1 mRNA for the sum of all laminar layers……...Page 107

Figure 5.5: Comparison between diagnostic group for NMDAR NR1 mRNA in the DLPFC at each individual in every layer……..……..……..……...Page 108

Figure 5.6: Comparison between a possible locations of the NMDARs in schizophrenia patients compared to healthy controls……..…...Page 116

Figure 6.1: Comparing overall number of cells counted for individual controls and schizophrenia patients……..……..…..……Page 124

Figure 6.2: Number of glial cells in layer V per μm^3 comparing schizophrenia patients and controls……..…Page 125

Figure 6.3: Number of interneurons in layer V per μm^3 comparing schizophrenia patients and controls……..…..Page 126

Figure 6.4: Number of pyramidal cells in layer V per μm^3 comparing schizophrenia patients and controls……...Page 127

Figure 6.5: Comparing the nuclei sizes of glial cells, interneurons, and pyramidal neurons……..……Page 128

Figure 6.6: Original bins for small interneurons comparing schizophrenia patients and controls for silver grain analysis……...…..……Page 130

Figure 6.7: Original bins for large pyramidal neurons comparing schizophrenia patients and controls for silver Grain analysis……..Page 131

Figure 6.8: No expression, low expression, medium expression, and high expression of NR1 mRNA for interneurons……..…..……Page 135

Figure 6.9: No expression, low expression, medium expression, and high expression of NR1 mRNA for pyramidal cells……...Page 140

Figure 6.10: The average number of silver grains per interneuron per bin expression group……...Page 144

Figure 6.11: The average number of silver grains per pyramidal neuron per bin expression group……..……..……...Page 145

Figure 6.12: The amount of total expressing pyramidal neurons comparing schizophrenia patients vs controls. ……..……..……..Page 146

Figure 6.13: The amount of total expressing interneurons comparing males and females……..……..……..……..……..……..……..……...Page 146

Figure 6.14: Layer II, III, and V showing pyramidal neurons and interneurons variations between layers……..……Page 151

Figure 6.15: Potential interconnections between pyramidal neurons and interneurons……..……...Page 153

Figure 6.16: Differences between interneurons and pyramidal neurons in normal individuals and schizophrenia patients……..……..……..…Page 154

Figure 6.16: Comparing size between the "small" interneurons and the "large" pyramidal cells in layer II……Page 163

List of Tables

Table 1.1: Previous published studies investigating NR1 in PFC from patients with schizophrenia……..……..…….Page 45

Table 2.1: Detailed TRC cohort information for controls……..Page 59

Table 2.2: Detailed TRC cohort information for schizophrenia patients.....Page 60

Table 2.3: Detailed clinical information for schizophrenia patients in the TRC cohort……Page 61

Table 2.4: Summary of demographics of schizophrenia patients and matched controls of the TRC cohort……..Page 62

Table 3.1: An overview of the protein amounts in each tissue fractionation in the TRC cohort……Page 75

Table 4.1: Correlation of demographics variables with NR1 protein in the total homogenate and the PSD fraction……..……..Page 89

Table 4.2: Correlation of clinical variables for schizophrenia patients with NR1 protein in the total homogenate and the PSD fraction samples……..Page 90

Table 5.1: Correlation between each layer of BA46……..…….....Page 105

Table 5.2: Demographics correlated with layers II, III, IV, V, and VI in total cohort……..……..…Page 112

Table 5.3: Demographics correlated in layers II, III, IV, V, and VI in the schizophrenia diagnostic group…….....Page 112

Table 5.4: Demographics correlated in layers II, III, IV, V, and VI in the control group……..……..Page 113

Table 5.5: Correlations examining age of onset, duration of illness, and antipsychotic medication was correlated with NR1……..……..Page 114

Table 6.1: Demographics correlated with no, low, medium, and high expressing interneurons in the total cohort……..…....Page 133

Table 6.2: Demographics correlated with no, low, medium, and high expressing interneurons in the schizophrenia diagnostic group……..……..…....…Page 134

Table 6.3: Demographics correlated with no, low, medium, and high expressing interneurons in the control group……..……..……..Page 134

Table 6.4: Demographics correlated with no, low, medium, and high expressing pyramidal neurons in the total cohort……..……..……..…....Page 136

Table 6.5: Hemispherical differences in no, low, medium, and high expressing interneurons and pyramidal neurons……..……..……..…....Page 136

Table 6.6: Demographics correlated with no, low, medium, and high expressing pyramidal neurons in the schizophrenia diagnostic group……..…....Page 137

Table 6.7: Demographics correlated with no, low, medium, and high expressing pyramidal neurons in the control group……..……..……..…....Page 137

Table 6.8: Correlations with no, low, medium, and high expressing interneurons with age of onset, duration of illness, and CPZ……..……..Page 138

Table 6.9: Correlations with no, low, medium, and high expressing pyramidal neurons with age of onset, duration of illness, and CPZ……..……..…Page 139

Table 6.10: Demographics correlated with total expressing interneurons and pyramidal neurons in the total cohort……..Page 142

Table 6.11: Demographics correlated with total expressing interneurons and pyramidal neurons in the schizophrenia diagnostic group……..……..…Page 142

Table 6.12: Demographics correlated with total expressing interneurons and pyramidal neurons in the control group……..…Page 143

Table 6.13: Demographics correlated with average number of silver grains per cell per expression group in interneurons and pyramidal neurons in the total cohort……Page 147

Table 6.14: Demographics correlated with average number of silver grains per cell per expression group in interneurons and pyramidal neurons in the schizophrenia diagnostic group……Page 148

Table 6.15: Demographics correlated with average number of silver grains per cell per expression group in interneurons and pyramidal neurons in the control group……Page 148

Table 6.16: NR1 silver grains/cell for neurons for different expressers in the total cohort compared by two-way ANOVA by gender……Page 150

Table A3.1: Standard values used for analysis using ImageJ……Page 231

List of Abbreviations

1°	Primary
2°	Secondary
A	Accidental
Abs	Antibodies
AMPA	α-amino-3-hydroxy-5-methyl-4-isoxazo lepropionic acid
ARVD	Arrhytmogenic right ventricular dysplasia
As	Asian
ASCVD	Atherosclerotic cardiovascular disease
BA	Brodmann's Area
BCA	Bicinchoninic Acid
BT	Bipolar type
C	Cytosolic fraction
Ca	Caucasian
$CaCl_2$	Calcium Chloride
CCD	Charge couple device
CNS	Central nervous system
Con	Control Case
COPD	Chronic obstructive pulmonary disease
CPZ	Chlorpromazine equivalent neuroleptic dose
D	Disorganised
DSM	*Diagnostic and Statistical Manual of Mental Disorder*
DDT	Dichlorodiphenyltrichloroethane
DiH_2O	Deionized water
DLPFC	Dorsal lateral prefrontal cortex

DT	Depressive type
Dx	Diagnosis
ECL	Chemiluminescence
EtOH	Ethanol
F	Female
Fab	Fragment antigen-binding
Fc	Crystallise fragment
H	Homicide
H_2O	Water
H_2O_2	Hydrogen peroxide
HCl	Hydrochloric Acid
Hemi	Hemisphere
HEPES	4-(2-hydroxyethyl)-1-piperazineethanesulfonic acid
HRP	Horseradish peroxidase
KCl	Potassium chloride
LFC	Lateral frontopolar cortex
LTP	Long term potentiation
M	Male
Med	Medium
MeOH	Methanol
mg	Milligrams
mGlu	Metabotropic glutamate
MI	Myocardial infraction
MPFC	Medial prefrontal cortex
N	Nuclear enriched fraction

$NaHCO_3$	Sodium Bicarbonate
NaOH	Sodium Hydroxide
Nat	Natural
NIM	Nuclear isolation media
NLB w/ high NaCl	Nuclear lysis buffer with high sodium chloride
NLB w/ no NaCl	Nuclear lysis buffer with no sodium chloride
NMDAR	N-methyl-d-aspartate receptor
NSW TRC or TRC	New South Wales Tissue Resource Centre
P	Paranoid
P#	Pellet #
PBSB or 1x PBS	1x Phosphate Buffered Saline
PCP-	Phencyclidine
PFC	Prefrontal cortex
PKC	Protein kinase C
PMI	Post-mortem interval
PPE	Personal protective equipment
PPF	Presynaptic membrane fraction
PSD	Post synaptic density
PVDF	Polyvinylidene difluoride
R	Residual
RIN	RNA integrity number
rs	Reference SNP
S	Suicide
S#	Supernatant #
Scz	Schizophrenia case

Scz-A	Schizoaffective patient
SDB	Sucrose density barrier
SDS	Sodium dodecyl sulfate
Sol A	Solution A
SPM	Synaptic membrane fraction
SV	Synaptic vesicle fraction
T	Total homogenate
TBST	Tris-buffered saline with Tween 20
TD	Tardive dyskinesia
TEMED	Tetramethylethylenediamene
U	Undetermined
Un	Undifferentiated
VLPFC	Ventral lateral prefrontal cortex

Chapter 1: Introduction

This chapter focuses on schizophrenia, a major mental illness characterised by psychosis, and on molecular changes in the human brain of patients with schizophrenia. In this introduction, I will explain what schizophrenia is and how disabling the illness is to patients. Then, I will describe which parts of the brain could be affected and which neuronal receptors may be altered in the brains of people with this disease.

Mental illness and schizophrenia

Psychiatrists use the *Diagnostic and Statistical Manual of Mental Disorders* (DSM) to diagnose mental illness. The incidence of mental illness as a whole can range from the low end of 4.3% of people living in Shanghai, to as many as 26.4% of people living in the United States[1], which means that mental illness research is important because it affects so many people worldwide. From this, a subgroup of individuals will have schizophrenia. It is known that approximately 1% of people worldwide are affected by schizophrenia[2,3], which means more people are disabled by this disease than by many types of cancers and other common illnesses[4]. Thinking of this number in a different way, this 1% of people account for approximately 70 million people. Individuals diagnosed with a mental disorder are likely to have a shortened lifespan, dropping from an average age at death of 78.5 years to 66.3 years of age in Australia[5]. The shortened lifespan in people with schizophrenia can be attributed to suicides that are seen at higher rates (10-13%)[6] compared to the general population in which the suicide rate is 12 times less[4], along with comorbid factors that include cardiovascular disease, obesity, poor diet, lack of physical activity, and smoking[7,8]. In addition to a shorter life span, patients have a lower quality of life with many years of productive life lost due to disability

[5]. Thus, schizophrenia carries a tremendous economic and societal burden for the individual, family and community.

What is schizophrenia?

Schizophrenia is one of the costliest and one of the least understood psychiatric disorders to date[7,9]. The name schizophrenia was coined by a Swiss psychiatrist in the early 1890's and is derived from some of the first symptoms recognised in people with the illness[10]. Many people with this illness have a disconnection from a normal functioning life prior to illness and their bizarre psychotic experiences; so, because of this, it was said that individuals with schizophrenia had a split (schizo-) mind (-phrenia)[10].

Schizophrenia is a disabling brain disease with a variety of different symptoms, including positive symptoms[11], negative symptoms[8,11,12], affective symptoms[8,13], and cognitive symptoms[8,13]. Positive symptoms include hallucinations and delusions or strange perceptions, ideas and beliefs that the patients do not generally understand, but begin to believe over time[13]. Examples of this are inner voices saying "The government is watching the person's every move through hidden video cameras", or "some one believing and acting as if he or she is a vampire". As part of the negative symptoms, people withdraw from social interactions, have a lack of motivation, and a reduction in or derailment of normal speech[8,12,13]. This can be distressing to people who are close to the patients, as well as the person suffering from schizophrenia. Affective symptoms include feelings of fatigue, guilt, hopelessness, empty moods, or thoughts of suicide[13]. Cognitive symptoms, such as impaired ability to learn and interpret information, being more unfocused, deficits in working memory of patients with schizophrenia, can also greatly contribute to vocational disability[8,13,14]. It has been noticed when the N-

methyl-d-aspartate receptors (NMDARs) are blocked in healthy individuals, these people have similar deficits as people with schizophrenia [15-17]. The NMDAR will be discussed in more detail later in this chapter.

There are some people who have brief (up to six months) periods in which their psychosis is extremely active, but then symptoms gradually wane off and the person can go on to live a normal life. However, most patients meeting the previously mentioned diagnostic criteria for schizophrenia experience episodes of psychosis throughout their entire life[13]. Throughout the duration of the illness, negative symptoms are seen to generally be stable but sometimes worsen[18]. Therefore, the symptoms of schizophrenia can vary along a continuum from fairly normal behaviour to extreme disorder and can vary even within an individual's lifetime.

According to DSM-IV, schizophrenia can be broken down into subtypes: paranoid, schizotypal disorder, delusional disorders, schizoaffective, psychotic disorders, and other unspecific nonorganic psychosis[13]. The utility of these subtypes has been questioned, and they are not used in the most current DSM-V. Many patients with the diagnosis of schizophrenia also have other disorders that affect their every day lives[18]. Substance abuse alone is considered a mental illness, but it has been seen that abuse of illicit drugs and alcohol occur in approximately 47% of schizophrenia cases, and smoking in up to approximately 80% of cases[18], making management and treatment of schizophrenia more problematic. The subtypes of schizophrenia with different symptoms and potential comorbidities makes schizophrenia a difficult disease to begin to investigate, as the clinical picture and the biological picture is heterogeneous.

Schizophrenia is thought to arise from a mixture of genetic changes, both normally occurring polymorphisms and mutations, such as chromosomal deletions, and from environmental factors, both physical and social. Currently, it seems that no single gene defect alone is sufficient to cause schizophrenia. Besides genetics, there are deleterious factors around birth, i.e. premature birth, low birth weight, perinatal hypoxia conditions[19], and maternal immune complications during pregnancy[20], which increase the risk for schizophrenia. There are also negative factors associated with growing up, i.e. social isolation, immigration, and urban lifestyles[7] that can increase the risk of developing schizophrenia. The likelihood of developing schizophrenia has been found to be greater in individuals with multiple contributing causes, such as high stress and drug abuse[2,3,8,18]. With so many factors potentially contributing to the development of schizophrenia, it is hypothesized that there are different biological pathways leading to this illness.

While there are common phenotypic traits of schizophrenia, the clinical picture can vary a great deal between patients, likely due to the numerous etiopathological differences[3]. Although schizophrenia is a common illness with some symptoms that are similar from person to person, the variations cause no two people with schizophrenia to have identical symptom profiles[18] and that could be problematic for psychiatrists and researchers alike. Currently, clinical interviews are the diagnostic measure in place to diagnose schizophrenia[13]. Other potential diagnostic measures, such as Electroencephalograph (EEG), Magnetic Resonance Imaging (MRI), blood biomarkers, or genetic testing hopefully is going to be useful in the future for diagnosis[21-23].

There are no clinically utilised precise biological markers for schizophrenia at this time. With different psychiatrists diagnosing patients in different ways and

relying on reported symptoms and clinical history, it is possible that patients with similar symptoms could be classified into different DSM subgroups of schizophrenia. In fact, the recently published DSM-V no longer identifies subtypes as these changes over time with change in clinical presentation and thus were deemed to have low validity. [24] Heterogeneity in clinical presentation at the time of death could lead to variability in research findings from post-mortem studies, especially if each subtype presentation has a different underlying molecular pathology. Understanding these differences could potentially bring researchers closer to understanding the underlying causes of schizophrenia as a whole. This will require understanding how the human brain functions normally, compared to how it functions in patients with schizophrenia; thus, more research in this field is needed.

Since the onset of schizophrenia generally is during late adolescence or early adulthood, the age when the body and brain is going through many physical changes, understanding what is functionally occurring in this time period is a great place to begin[25]. Men, on average, are diagnosed with schizophrenia between the ages of 18 and 25, whereas women are generally diagnosed around age 25, but some women are diagnosed later in life during menopause (age of diagnosis averages: men- 21yrs, women- 27yrs), but the age range can vary[25] since women are diagnosed schizophrenia on average four to five years later than males, but some studies report a difference of up to 11.2 years[26,27]. Being able to study the brain of people with schizophrenia at the time when the illness is first manifesting may provide better insight into which parts of the brain are involved in the initial onset and which parts of the brain become damaged due to putative misfiring of neurons over time. However, the information provided in this thesis demonstrates

that molecular changes can be found in the brains of schizophrenia patients after being diagnosed for an extended period of time (3-52 years). Most brain studies during the early onset of schizophrenia are limited to brain scanning, which by its nature is limited to elucidating gross volumetric changes (structural MRI), or differences in activation (functional MRI or EEG). Being able to understand what is occurring during this crucial time of disease onset and how schizophrenia may vary according to age or duration of illness may help researchers understand schizophrenia to a greater extent.

Besides age of onset, there are also other gender differences associated with schizophrenia. Firstly, it is common that women will have a less severe disease course than men, with less intense psychosis[28]. Secondly, males develop schizophrenia more often compared with females (1.4:1)[29]. In both the clinical and post-mortem cohorts used for research studies, there are more men than women, which is a reflection of what is occurring in the overall patient population. When attempting to understand the underlying cellular and molecular changes leading to schizophrenia, it is critical that I examine human brain tissue to see how the illness impacts brain areas responsible for rational thought and language, functions present in humans that other species are thought to not possess.

The Human Brain

The human brain is one of the most complex systems in the entire body, with over a 100 billion neurons and it is a tissue that undergoes many dramatic changes throughout life at both the cellular and molecular levels, which makes it challenging to study[4,30-33]. With technology, scans of human brains can be taken while subjects perform tasks providing researchers a better understanding of what physiological changes may be occurring in the brain under different circumstances.

But looking at the human brain via imaging will not show what is occurring at the cellular and molecular level. So, along with examination of brain scans of living people, human brain tissue can be obtained and analysed in post-mortem studies. This allows a direct examination of the molecules and cells contributing to human thoughts and actions. This thesis focuses on post-mortem studies of human brains.

People with schizophrenia tend to have volume differences in certain brain regions compared to people without psychosis. Looking at a meta-analysis study, along with other articles, of regional deficits in brain volume measured using MRI; it was shown that the temporal gyrus, insula, temporal lobe, and frontal cortex have significantly decreased amounts of grey matter in schizophrenia patients[34-37]. Specifically to this thesis, the prefrontal cortex (PFC) has been extensively studied[38-43] and has been found to have decreased volume in schizophrenia patients[44]. Our laboratory is at the forefront of studying the molecular pathology in the PFC in people with schizophrenia, which has been the primary focus of my study.

Prefrontal Cortex in Relation to Schizophrenia

There are sulci and gyri that define the frontal lobe, in particular the PFC. The PFC is significantly larger and more complex in humans and non-human primates than in other mammals, seen in Figure 1.1[14,45]. It has been suggested that this larger PFC could be one of the reasons why humans have a unique, more abstract, way of thinking, compared to other animals[45]. The PFC is the rostral part of the frontal lobes of the brain. Within the PFC, there are several subregions: dorsal lateral prefrontal cortex (DLPFC), ventral lateral prefrontal cortex (VLPFC), anterior cingulate cortices, and lateral frontopolar cortex (LFC)[43,46]. These subregions are demarcated by sulci [Figure 1.2]. Based on differences in cell

composition and layering (cytoarchitecture) between brain regions, an alternative way to divide the cortex is by using Brodmann's classification from 1909[47-49]. The Brodmann areas (BA) associated with the DLPFC (BA46/BA9) and the frontal pole (BA10) are the focus of the post-mortem work in my thesis.

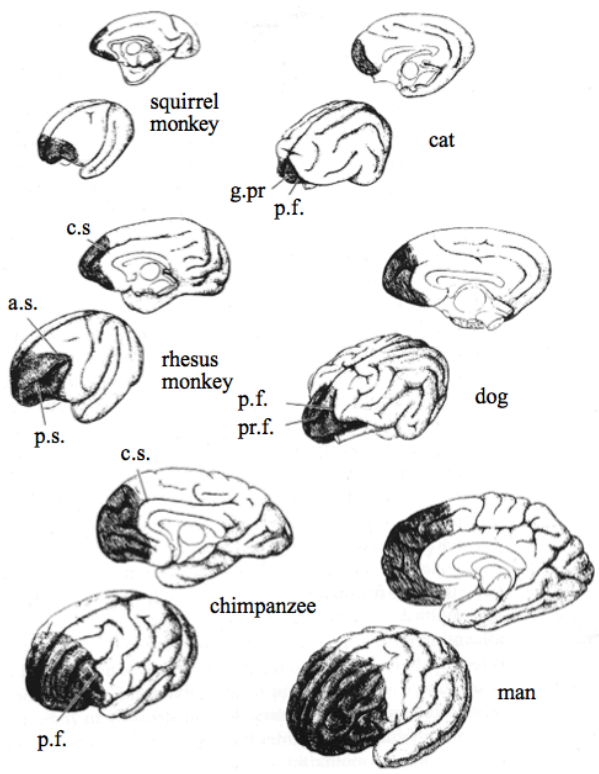

Figure 1.1: The prefrontal cortex in relation to overall brain size. The abbreviations are: a.s., arcuate sulcus; c.s., cingulate sulcus; g.pr., gyrus proreus; p.f., presylvian fissure; p.s., principal sulcus; pr.f., proreal fissure. "Man" in this figure is showing all humans. This figure is used, with written consent, from Fuster, 1995.

The PFC in humans is large and it has been noted that it has a key role in regulating cognition and dealing with abstract information[45]. Also, this part of the human brain deals with planning complex cognitive behaviour, personality expression, decision-making, and moderating social behaviour[43], as well as providing goal directed tasks, reward-related signals[36,5836,57], orderliness, and self-discipline[40,45]. It has been observed that damage to the PFC causes people to behave sporadically and impulsively, which can lead to an unawareness about how their actions will affect others[40,45,50-54]. Many of the cognitive deficits observed with

PFC damage are seen in people with schizophrenia, including lack of attention, distractibility, working memory problems, and disorganized and inappropriate social behavior[43,50-54]. Consistent with this, the PFC has been shown to be dysfunctional in people with psychotic disorders[43,55], and altered PFC brain activity has been linked to schizophrenia[37,68,67]

Due to the similarities between symptoms induced by damage to the PFC and schizophrenia symptoms, the PFC is a region of interest. In the human PFC, numerous cellular changes normally take place during young adulthood[55,56]. This is important because schizophrenia generally has first onset around late adolescence/young adulthood, and the normative cellular changes could be malfunctioning at this stage to bring about symptoms. Understanding the molecular malfunction underlying symptoms could lead to understanding schizophrenia at a more in depth level. In schizophrenia, malfunctioning could occur in specific cortical neurons, involving glutamatergic and GABAergic neurons, which will be discussed in more detail.

Brodmann Areas 10 and 46

The human brain tissue used in my study came from two separate PFC regions: Brodmann Area 10 (BA10), which consists of the frontal pole [57], and Brodmann Area 46 (BA46), which can be found along of the middle frontal gyrus and the inferior frontal sulcus, seen in Figure 1.2[58]. The PFC is one of the largest brain regions in humans[59], consisting of the caudal, dorsal, lateral, medial, and ventral PFC[33], seen in Figure 1.2. The grey matter cortex of the PFC consists of six neural layers[60]. The approximate proportionate width of the layers across the total PFC are as follows: layer I- 12%, layer II- 6%, layer III- 36%, layer IV-6%, layer V 15%, and layer VI 25%[58]. Layer III has small to medium size pyramidal neurons

that typically project to other cortical regions and layers[61]. Layer Va has more medium to large sized pyramidal neurons that typically project to the striatum, and layer VI has more varied neuronal types and includes pyramidal neurons projecting to the thalamus[61].

In much of the frontal cortex, layer IV is granular and well developed and has distinct borders between layers III and V[58,61]. Both BA10 and BA46 have small to medium pyramidal neurons in layer III and medium sized neurons in layer V[61]. In BA46 layer V, pyramidal neurons may be a little more difficult to clearly identify due to the compact neurons in the layer[58]. However, there is much variability from one normal human brain to the next when examining the neurons in layer III and V. Some brains have larger pyramidal neurons than others, with the arrangement of these neurons being less distinct[58].

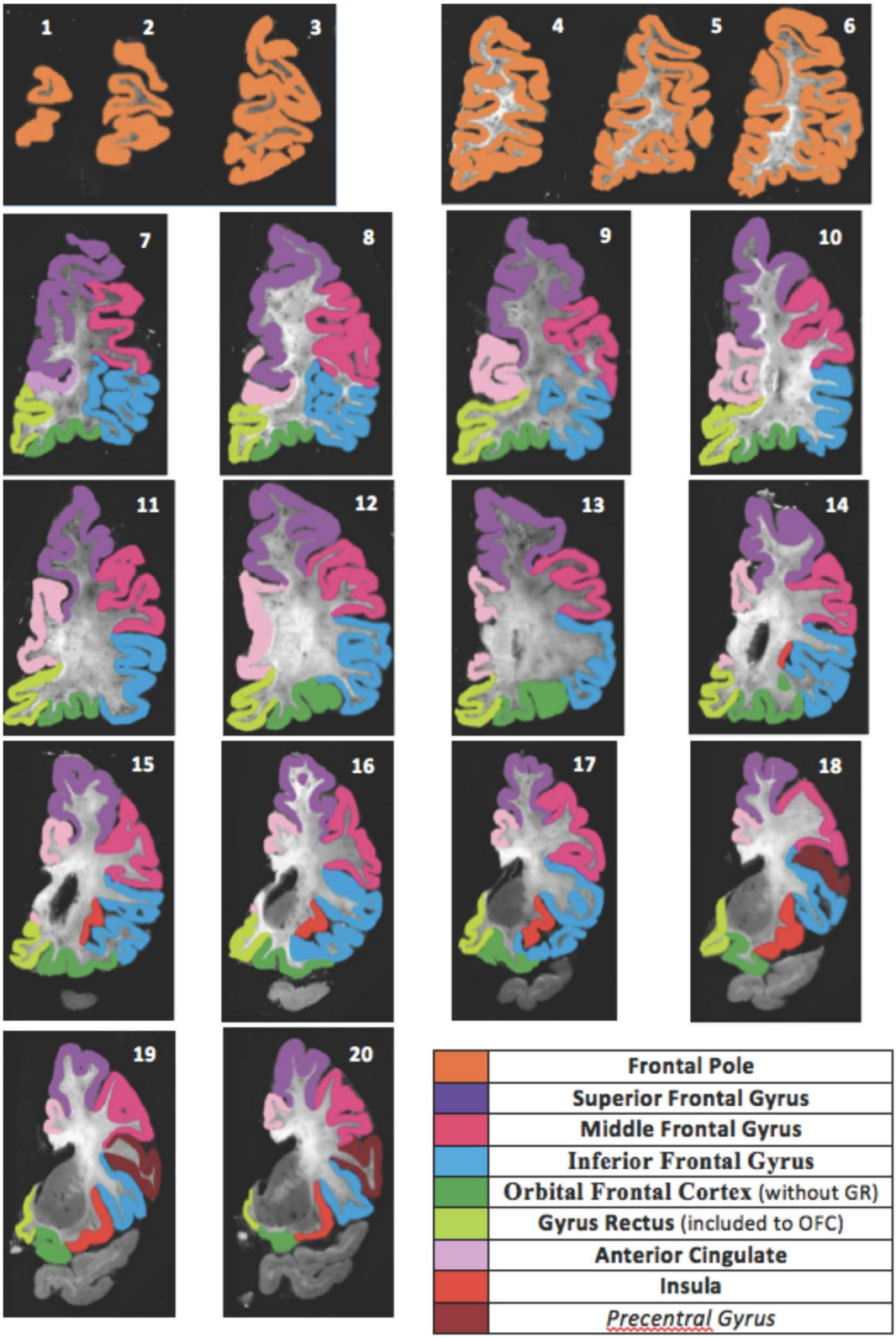

Figure 1.2: Prefrontal Cortex:. Images 1 through 20 moves progressively in an anterior to posterior direction. Precentral gyrus and temporal lobe do not belong to the PFC. (Figure completed by Yiru Zhang).

BA10 accounts for about 1.2% of the entire brain volume, but uses approximately 20% of the total oxygen required for the brain[33,34,62,63]; thus a great deal of energy is used to keep this region functioning potentially because of the constant and ongoing information processing that occurs within this region. Compared to other primates, BA10 in humans is larger with more extensive neuronal connectivity which allows for better cognitive and logical thinking[33,38,39,62,64]. With the large size and specialised neurons, cognitive aspects, like memory and learning, are thought to be associated with BA10. Unlike BA10, BA46 is a highly studied region of the brain in schizophrenia.. BA46 occupies a more posterior region of the middle frontal gyrus compared to BA10, and a large part of this region is below the surface in the inferior frontal sulcus[61]. BA46 is located between BA10, which is more anterior, and BA45, which is more posterior. This region lies mainly on the middle frontal gyrus within the DLPFC, even though this area is based solely on the cytoarchitecture of the brain, not the function this region has (however, structural differences are thought to give rise to functional differences)[58,65].

The PFC region has many important cognitive functions associated with it. Burgess states that the prefrontal region of the brain is least understood of all brain regions[66]. However, activation of the PFC occurs when attention and cognitive processes, especially working memory, are occurring[67]. Mentioned above, this region deals with decision-making, reasoning, problem solving, memory, and impulsive behaviour; impairment of these cognitive processes occur on a daily basis for schizophrenia patients[2,3,64,68-70].

People with lesions in this the PFC have been found to have short-term memory problems, impulse control problems, difficulty understanding relevance of

a situation, and have organizational difficulties[71]. By using fMRI, activation of BA46 is found to be enhanced during information processing[72]. Also, it has been found that retrieving memories and doing tasks require this area of the brain[73].

Neuron types, Glutamatergic pyramidal cells and GABAergic interneurons

There are two main types of neurons that will be discussed throughout this thesis; both reside in the cerebral cortex and hippocampus. One type is the pyramidal neuron, and the other type is the interneuron. In mammals, approximately 70% of all neurons are pyramidal neurons[56,74]. The cell body of pyramidal neurons are triangular or pyramid shape, hence the name. Surrounding their pyramid-shaped cell body (soma), there are many long dendrites that are off the apical end, along with shorter dendrites on the basal end [56]. The pyramidal neurons are excitatory neurons, which means they release glutamate into the synaptic cleft[56], triggering excitation of adjacent neurons carrying glutamatergic receptors. There are a several subgroups of pyramidal neurons, but throughout this thesis, the types of pyramidal neurons will all be grouped together.

Interneurons, the other neuronal type discussed herein, constitute about 20% of neurons in the cerebral cortex, are smaller than pyramidal neurons, and they have a different function; these interneurons, that typically send axonal projection within the area of origin, are inhibitory[75]. Unlike pyramidal neurons that synthesise and release glutamate, interneurons synthesise and release The interneurons' job is to signal to local neurons where they send inhibitory signals[75] that help maintain homeostasis in the brain and modulate the excitation of pyramidal neurons[75,76]. To date, there are approximately 20 different classes of interneurons[75,77], but work being done in this thesis will consider them as one class, inhibitory. GABA dysfunction is thought to play a key role in

schizophrenia[76,78]. Looking at the GABAergic neurons' mRNA expression of key neurotransmitter receptors can help our understanding of this neuron type, which is known to contribute to cortical pathology in schizophrenia[79-81,82].. Schizophrenia could be associated with reduced N-methyl-d-asparate receptor (NMDAR) receptors[82,83] on either pyramidal neurons leading to the hypoglutamatergic (less glutamate) and or interneurons hyperglutamatergic (more glutamate) theories, which will be discussed later on in detail.

N-Methyl-D-Aspartate Receptor

The NMDAR is an ionotropic glutamate receptor[43,84] that allows the passage of cations into the intracellular space. The NMDAR is robustly expressed throughout the brain[85-88] and impacts a wide variety of behaviours, including expression of personality, decision-making, learning, memory, and social behaviours[43,89], which schizophrenia patients are seen to have more difficulty with than someone without schizophrenia. NMDARs are thought to regulate the synaptic strength and the action potential amplitude, of neurons[89], and NMDARs have been found to be critically involved with learning and memory[77,78,90].

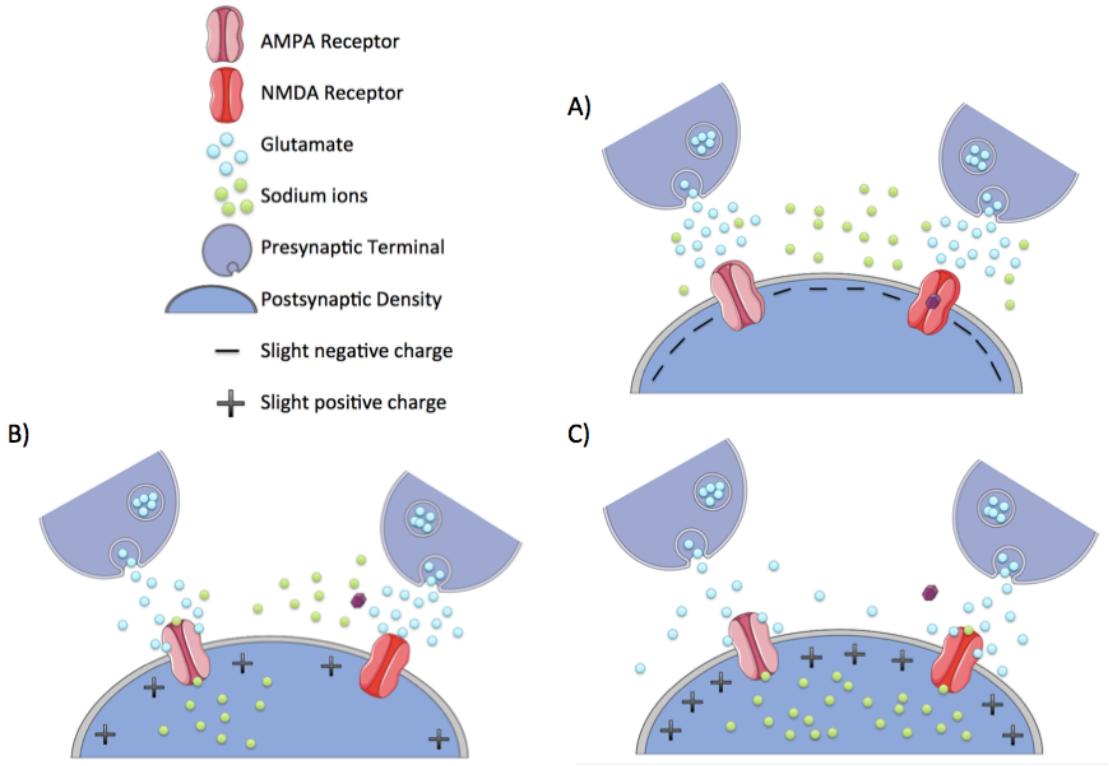

Figure 1.3: Coincidence detectors with two different neurons acting upon another to open both the AMPAR and NMDAR. When the AMPAR is opened, the inside of the neuron becomes partially positive kicking out the NMDAR Mg block (in purple). When this occurs, the NMDAR is now open to be used. A) A neuron at resting potential. B) AMPA receptors are stimulated caused depolarisation of the interior of the neuron. C) NMDAR is now active causing a greater influx of sodium ions.

NMDARs are generally found in the membrane on the postsynaptic density[85,87], seen in Figure 1.3. NMDARs are known to have specific binding sites for glycine and glutamate[48,91] (Figure 1.4), both of which (co-agonists) are required to bind for the NMDAR ion channel to open. Other exogenous molecules that bind to the NMDAR are L-aspartate, phencyclidine (PCP), ketamine, MK-801, and N-methyl-D-aspartate acid[78,90], seen in Figure 1.4. At resting membrane potential of neurons, magnesium ions block the NMDAR channel and stop cations from diffusing through it (Figure 1.3A). Ions are only able to diffuse through the NMDAR

ion channel when stimulus (commonly activation of 2-amino-3-(3-hydroxy-5-methyl-isoxazol-4-yl) propanoic acid receptors (AMPARs)) first depolarizes the cell through an influx of Na^+ ions[48,89], which dislodges the magnesium block on the NDMAR (Figure 1.3B). This feature is what makes the NMDAR have unique properties and allows it to function as a coincidence detector (Figure 1.3C).

A coincidence detector is when more than one neuron fires at the same time to the PSD, in the case of a glutamate afferent, this allows the AMPA channel to react causing neuronal depolarisation of the neuron, and in turn, through the depolarisation, the NMDAR block, Mg^{2+}, is "kicked out" allowing other cations to rush into the cell. The main positively charged ions that pass through the NMDAR ion channels include potassium, calcium, and sodium[78,90,92]. Inside the cell, the ability of NMDARs to activate key second messenger signalling is calcium dependent[89,90,93], which means it relies on calcium to start the signalling cascade. Calcium signalling influences many cellular components and can promote plasticity[90,93,94], including long term potentiation (LTP)[6,95-97], and thus, it is influx of Ca^{2+} that occurs with opening of the NMDAR channel that is significant and distinct from many other glutamate receptors leading to more long-term changes in neurons.

While the first pharmacological theory in schizophrenia was based around dopamine receptors because all known antipsychotics bind to the dopamine D2 receptor, more recently there has been a greater focus on the glutamate system. This is in part because a recognised pharmacological model for schizophrenia implicates hypofunction of the NMDAR[94,95]. This theory first came about in the 1980s[6,91,95,97-99], when two explanations about how less glutamate neurotransmission could occur in people with schizophrenia were put forward: 1)

dopaminergic receptor hyperactivity could inhibit glutamate release and/or 2) damage to glutamatergic neurons could result in less glutamate release[95,100-103]. From these two explanations above, schizophrenia research began to examine glutamate related changes in the brains of people with schizophrenia compared to controls.

Other evidence in support of the role of glutamate in schizophrenia, and NMDARs more specifically came from pharmacology. There are binding sites of the NDMAR that have more than one known ligand, like the PCP binding site in the ion channels[91,98,99,104]. Drugs like PCP, ketamine, and MK-801, which act as antagonists, all bind to this site[98,100-103]. Each of these drugs can cause a psychotic state in healthy people that appears to be similar to the symptoms observed in schizophrenia patients[100,104], mimicking positive, negative, and cognitive symptoms[98,105]. When NMDAR antagonists are given to schizophrenia patients, the symptoms intensify[100,104,106]. Because of these symptoms that occur when the NMDAR is blocked, this receptor seems like a viable target of interest in schizophrenia research[107,108]. Thus, the NMDAR hypofunction is hypothesized to be associated with schizophrenia[109,110]. Therefore, there is a need to understand the NMDAR in more detail.

Molecular Biology of the NMDA Receptor

NMDARs are made up of subunits, generally seen as heterotetrameric ionotropic glutamate receptors[72,77,111] that contain two NR1 subunits[78,98,112] and a combination of two NR2 or NR3 subunits[72,78,111]. Altogether, it is known that there are eight splice variants of the NR1 subunit[78,98,112-114], but this thesis looks at all NR1 subunits as a whole. The NR2 and NR3 subunits have different splice variants as well[78,109]. Figure 1.4 shows the structure of the NMDAR and the binding sites

associated with the specific subunits. The NR1 subunit is the obligatory subunit of the NMDAR[92,96], and will be discussed in further detail later in this thesis. According to some studies, there also needs to be at least one NR2 subunit as part of the complex since NMDARs with only NR1 and NR3 subunits do not function as they have no glutamate binding site (on NR2 subunits only). While these receptors can not function as a glutamate receptor, it is possible that they could function as a glycine receptor.[78,109,113,114]. One interesting finding is substituting just one of the non-obligatory subunits on the NMDAR will not always change the function of the receptor as a whole[84,109], but substituting or removing an NR1 subunit can make the receptor non-functional[86,109], meaning that the NR1 subunit is an important contributor to a functioning receptor, but may not be the only reason for malfunctions to occur.

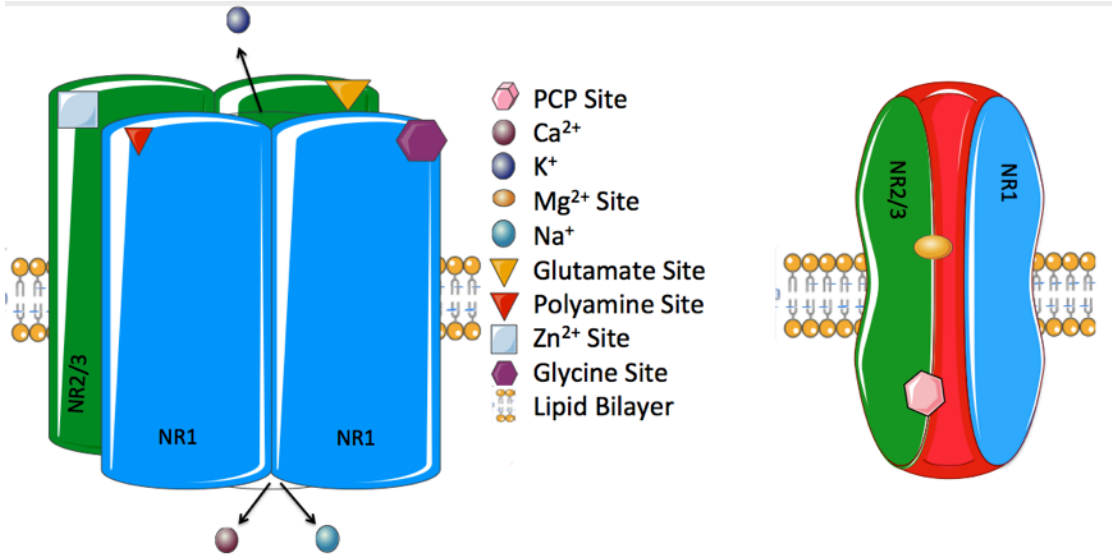

Figure 1.4: Structure of the NMDAR and common molecules associated with it. The NMDAR is a heterotetrameric ionotropic glutamate receptor that contains four receptor subunits. The subunit of interest in the study was the obligatory NR1 subunit.

In this thesis, post-mortem brain tissue is used to measure the protein levels

of the NMDAR NR1 subunit by Western blots, along with in situ hybridisation to measure GRIN1 (NR1) mRNA expression. There have been differences seen with the NMDAR receptor, as a whole, and at the subunit levels, along with abnormal levels of mRNAs, between people with psychosis and control groups. [Refer to Table 1.1]. It is recognised that the NMDAR may be imperfect in schizophrenia in some way; however, it is currently unknown in which way(s) the NMDAR is altered and which specific subunits play a role in mental illness.

It is known that at the PSD, protein or receptor trafficking can change rapidly[89]. There is a hypothesis in schizophrenia research that proposes there could be a problem with NMDAR-associated postsynaptic proteins in the PFC[91]. There is little work on the NMDAR in the PSD in schizophrenia, so studying how the NDMAR on the PSD specifically differs between a healthy state and psychosis would bring research one step closer to understanding what is occurring in schizophrenia. One other study examining NMDAR NR1 protein on the PSD in schizophrenia patients was by Hahn. [115] He found that it is possible to separate the PSD fraction from the total homogenate of human brain tissue, along with an abundance of NMDARs on the PSD. [115] He found that there was an increase in NRG1 signalling in PSD proteins in schizophrenia patients. [116] This is thought to lead to NMDAR hypofunction in schizophrenia. [116]

Determining how much NR1 protein is on the PSD specifically is vital to how much of the total NR1 protein is actually inserted into the synaptic membrane and has the potential to be functional. Looking only at the total homogenate amount of protein will be looking at protein derived from everywhere in the cell, i.e. the Golgi apparatus, endoplasmic reticulum, and vesicles. Knowing what is available for use

at the synapse is the most vital information to have to understanding the potential differences between diagnostic groups.

Studies of the NMDAR in Schizophrenia

The pathophysiology of schizophrenia is poorly understood. One of the possible theories behind schizophrenia is an alteration in the glutamate receptors, more specifically the NMDAR. [74] Previous findings of the NMDARs have examined many different regions of the brain in schizophrenia patients. Looking at the NMDAR NR1 mRNA transcript, most cortical studies find either a decrease [91,117-121] or no change [107,122-125], with the exception of two studies which found an increase [106,126]. Several studies focused on elderly individuals with schizophrenia [106,121,124], which is potentially problematic because the expression of the NMDA receptor NR1 subunit is known to decrease with age [127-131] and if you only look at elderly individuals, the results obtained could be skewed particularly if people with schizophrenia aged differently compared to controls. For the NMDAR NR1 protein product in the cortex of people with schizophrenia, two studies have observed a decrease [117,132], one study found an increase, but only in a particular splice variant [133], and the majority of studies find no statistically significant change [72,105,124,134-136] However, the differential changes could be occurring on or exaggerated in the PSD only and when studying the cell as a whole, there may be no overall net change. Differences throughout the various brain regions can lead to discrepancies between studies, and may be one of the reasons why the results between various studies are inconclusive. One reason why so many studies have found no change possibly is due to differential changes occurring at the intracellular level versus what is specifically occurring on the PSD. While some individuals with schizophrenia have a net decrease in NR1 mRNA or protein levels, this obviously

may not the case for all individuals with schizophrenia investigated. It may be that some of those individuals with no net decrease in NR1 expression may have deficits in the trafficking of the NMDA receptor complex to the postsynaptic density, which could result in fewer functional receptors at the synapse. Alternatively, or additionally, there may be multiple molecular pathways to the development of schizophrenia, with NMDA receptor function being just one of them. More post-mortem studies are needed to examine these NMDAR subunits in more detail at a protein and mRNA level in the same individuals, which is completed in this thesis.

Thus, previous studies done looking at NR1 at the protein and mRNA levels in the cortex in schizophrenia have shown inconsistent results. These inconsistencies could be due to variations of schizophrenia subtypes in cohorts, looking at a slightly different brain region, or using different methodologies. Table 1.1 provides a brief summary of the previous NR1 results from the PFC comparing schizophrenia patients to controls. It is noteworthy that sample size may be a limiting factor in identifying statistically significant changes in mRNA and protein expression in many post-mortem studies, this affects especially the earlier studies [120,125,134], and that the largest study to date [117], from our laboratory found a decrease in both NR1 mRNA and protein expression in the dorsolateral prefrontal cortex (BA46) of patients with schizophrenia. However, it is not known which neuron type or types are contributing to this decrease in mRNA in the PFC. Determining specific neuron types will show whether schizophrenia could be a hyperglutamatergic or hypoglutamatergic system. Currently, both theories are being studied in the schizophrenia field.

Table 1.1: A brief summary of previous studies investigating NR1 in PFC from patients with schizophrenia. Black represents mRNA, green represents protein. A rhombus represents no differences between schizophrenia patients and controls, whereas the arrows indicate a significant up or down regulation in patients compared to controls.

Brain Area	Findings	References
Prefrontal Cortex	↓↓	91,132
Frontal Cortex	◆	134
Frontal Pole	◆	122
DLPFC	↑↓↓↓◆◆	77,106,117,121,133
Middle Frontal Cortex	◆	125
Anterior Cingulate	↑	133
Orbitofrontal Cortex	◆	135

Looking at the variation in what has been found previously in the NR1 mRNA and protein studies, my thesis aims to investigate the NR1 subunit in a large Australian post-mortem brain cohort. It seeks to extend previous homogenate work (mRNA and protein) using in situ hybridisation to measure mRNA in individual cortical lamina and neuronal subtypes and tissue fractionation followed by Western blotting to determine NR1 protein at the PSD.

Sub-Cellular Tissue Fractionation

Cellular fractionation is the method of separating post-mortem human brain tissue into different subcellular parts, the most important in this thesis being the PSD since this region is where the active NDMARs lie. I wanted to study how the functionally poised NMDAR NR1 subunits on the PSD differ between schizophrenia patients and control individuals, discussed in more detail throughout chapters three and four.

The Postsynaptic Density

The PSD is a highly organized structure that is attached to the postsynaptic membrane typically found on the dendrites of mature neurons. This subcellular structure on the dendritic spines was first noticed by electron microscopy as a dense thickening juxtaposed to the neuronal cell membrane directly across from the pre-synaptic terminal axon[137,138]. While the initial functional significance of the PSD was not known, it was clear that this thickening occurred preferentially on terminals that were also excitatory [139]. It is now known that the PSD is a scaffolding complex made up of many different proteins allowing different groups of signalling molecules to come together and interact[115,138,140,141].

One important feature of the PSD is that it anchors glutamatergic receptors: N-methyl-D-aspartic acid receptors, AMPA, the group I metabotropic glutamate (mGlu) receptors and other signalling molecules[89,115,142,143]. The PSD is particularly interesting due to the fact that synapses contain many of the protein products of multiple genes implicated in psychoses and mood disorders, which implicate glutamate signalling mechanisms in particular[115,144-147]. The NMDARs are highly concentrated on the PSD[89,115,148,149] and understanding how the level or action of NMDARs may be changed, particularly in the PSD, may provide insight to glutamate neurotransmission at the molecular level in schizophrenia.

It is known that NMDARs are not just found on the PSD but are trafficked throughout different parts of the neurons (the endoplasmic reticulum, Golgi apparatus, and vesicles), and can be found on the cell membrane sometimes at a distance from synapses often via lateral and extrasynaptic movements[150]. At the cell surface, there are three main membrane areas where the NMDARs are generally located: 1) synaptic, 2) perisynaptic, and 3) extrasynaptic [151]. It is noted

that the NMDAR cycles between being on the surface of the PSD and the endosomal compartments responsible for recycling new receptors to the surface[115,137,142,143].

NMDARs are found on postsynaptic membranes throughout the central nervous system (CNS)[89] and the outer cell membrane is in a dynamic state where insertion and removal of receptors from the synapse occurs[152]. Thus, the NMDARs do not just stay in place on the PSD, but can be found within vesicular pools within the cytoplasm[89]. However, the NMDARs that are available to be activated by presynaptic functional release of glutamate are thought to be restricted to those being present on the outer cell membrane and in the PSD in particular [153]. Being able to examine the amount of NMDAR proteins poised to react, i.e. those located at the PSD, is a useful way of testing the states of responsiveness to coincident firing of glutamatergic synapses. [154]

It is known that each dendrite can transport from tens to hundreds of glutamate receptors under normal circumstances[155]. If certain neuronal dendrites should have hundreds of receptors, but in fact only have tens of receptors, the functionality of this synapse could be dramatically reduced. For instance, the glutamatergic system is critical for memory formation, so if there are less glutamate receptors at the PSD, specifically the NMDAR, this could cause lack of memory retention or lack of learning capability. The PSD plays a role in molecular adhesion, controlling the clustering and regulation of glutamate receptors[156]. One hypothesis is the NMDAR diffuses to the outer cell membrane neuron surface to always have a specific amount of NDMARs present, but an influx occurs when needed, and when the NMDAR is positioned at the cell surface, memory and learning can occur[157]; so if malfunctioning of trafficking to the PSD occurs, the cognitive processes of individuals affected could be reduced. However, the

activation of the NMDAR is not passive, but an active process, as protein kinase C (PKC) activates new NDMARs to be brought to the PSD at the cell surface of the neurons in the brain[158]. Overall, if the activation process of bringing new receptors to the PSD is not functioning correctly, there could be a lack of receptors being brought to the PSD, which could result in memory deficiency.

The NMDAR has special trafficking abilities due to their location in synaptic spines[159]. The mobility of the NMDAR is due to the cycle it takes between the cell surface and the endosomes, where intracellular materials are brought to be sorted before degradation occurs[160]. If the endocytic zone where sorting occurs is not functioning properly, the fast and effective internalization of receptors, along with stopping of diffusion may not occur correctly[137]. When NMDARs were completely removed from a synapse experimentally, it was found that about 40% of the receptors were already replaced within 20 minutes[89]. This finding suggests recovery is not due to unbinding or insertion of new receptors since this process would take a longer time, but functional NMDARs can diffuse laterally to the synapse from extrasynaptic outer cell membrane when needed[161]. Lateral diffusion is important for maintaining and delivering proteins of interest to the synapse at a fast rate. This suggests that NMDARs have distinctive trafficking routes under different control.

The trafficking of the entire NMDAR complex is thought to be partly controlled by the NR1 subunit. [162] Thus less NR1 subunit in the PSD could lead to the lack of the movement of the entire NMDAR that could cause fewer NDMARs to actually arrive at the desired destination on the PSD. Also, the movement of the NMDARs off of the synapse could be occurring at a quicker rate than it should be in schizophrenia patients. The insertion and removal of NMDA receptors are crucial in

the regulation of synaptic strength, so if something is malfunctioning, major complications could occur. An example of this would be NMDAR encephalitis when upon autoantibody binding to the receptor, the NDMARs are internalised off the membrane into vesicles, causing psychosis [163]. Because the PSD is a specialised region where NMDAR can bring about changes in membrane potential and promote action potential generation, it is key to understand how the NMDAR at the PSD may be changed in schizophrenia.

NMDAR NR1 Subunit

NMDARs are complex ionotropic glutamate receptors[91,117,121,133,164-166] on which genetic and environmental risks may converge to cause dysfunctions in neurological and neuropsychiatric disorders[89,115,138,164,167]. The critical question is at which level should NMDAR function in individuals with schizophrenia be studied: genetic, mRNA expression, protein level, or functional studies? For this thesis, I examined how the NMDAR NR1 subunit protein varies between schizophrenia patients and controls. It is known that NMDARs can be altered at the protein level when looking at the specific subunit NR1 in the PFC in schizophrenia patients[91,117,121,168,169] and that the NMDARs are localized to the PSD [74,170], where they interact with ligands leading to a calcium influx and changes to multiple intracellular signalling pathways[74,168,169,171,172]. NMDARs are believed to be a part of the pathophysiology of many psychiatric illnesses, and in addition to schizophrenia, there is bipolar, depression, and autism[74,90,115,173-176]. In schizophrenia, there is a controversy between what is actually happening to the NMDARs: are there more, are there less, are they localised to specific subcellular locations? One hypothesis is that there is a reduced amount of NMDAR protein at the PSD, where it is functional; however, there may be a greater amount of

NMDARs in storage areas, in the Golgi apparatus, endoplasmic reticulum, and in vesicles. Another prospect would be that there are increased NMDARs at the PSD, but with less in reserve in other parts of the cell.

Specifically to schizophrenia, some studies suggest that NMDAR hypofunction facilitates symptoms[74,99,171,172,177], while another study suggests that hyperfunction of this receptor could be the cause[178]. Experiments using genetically modified mice with a deficiency in NR1 protein show schizophrenia-like behaviours such as hyper-locomotion, stereotypy, and sensorimotor problems [99,177,179]. In the current study, I seek to quantify the obligatory NR1 subunit protein of the NMDAR in total homogenate to see if there is an overall decrease in the NMDAR NR1 protein and in the PSD. I study the PFC in schizophrenia brain tissue using Western blotting. By focusing on both the total and PSD fractions, I aim to confirm in BA10 the previous observations of decreased NR1 protein in the same cohort in the DLPFC (middle frontal gyrus), a neighbouring region to BA10, and to determine if there is a change in the NMDAR NR1 subunit level more specifically in the PSD and I hypothesise that the NMDAR NR1 protein will be decreased at the PSD. The aim of this study was to assess NR1 protein expression, specifically in the total homogenate and in the PSD fraction, in schizophrenia patients compared to the control group.

mRNA

There are pros and cons to studying mRNA expression, as opposed to protein levels; while mRNA allows the study of the functional genes and is often more quantitative than protein studies, mRNA is further removed from the functional protein. Post-mortem studies mRNA are known for being possible because of mRNA degradation. Some factors associated with mRNA degradation

include pH and PMI, both of which can impact on RIN (RNA integrity number)[180,181]. In my studies, I find that tissue pH is critical and diagnostic groups are well matched for tissue pH, RIN, and PMI such that no systematic group difference exists. In addition, the length of time tissue in frozen storage can impact on mRNA quality[182].

In situ hybridisation

In situ hybridisation is conducted for the purpose of localising specific fragments of mRNA[183,184], DNA, or protein[185,186]; RNA-RNA probe-target interactions are the strongest interactions and are the basis for in situ hybridisation[183,187].

In human brain subcellular tissues, the cells that are thought to express NMDARs are most likely interneurons and pyramidal neurons. [91] The NMDAR is a relatively abundant mRNA and is fairly easily detected by in situ hybridisation giving a strong and distinct signal with only a few days of exposure time to film. Using in situ hybridisation, allows for examining NMDAR mRNA in each cortical layer. The DLPFC has six layers and each Brodmann's has distinctive cytoarchitecture the can be used to differentiate between human cortical regions discussed in depth in Rajkowska and Goldman-Rakic, 1995 [58].

Silver grains

Silver grain analysis involves looking at the expression of mRNA at a cellular level. The cell types investigated depend on which mRNA is being examined and in which brain region. For example, looking at cortical NMDAR mRNA, it is found that both interneurons and pyramidal neurons produce the mRNA of interest. These two neurons are contrasting one another due to interneurons being inhibitory and pyramidal neurons being excitatory. Examining NMDARs in excitatory and

inhibitory neurons in schizophrenia is an important step in understanding which type of neuron, if not both, could be one of the underlying causes of reduced NMDAR in schizophrenia.

Of the six cortical layers, NR1 mRNA is most robustly expressed in layers III and V in the PFC One study shows there are no differences between control and schizophrenia groups in the frontal cortices[91,106]. Layer II, III, and V were examined first in chapter 6 because these layers are of critical interest in schizophrenia. In a previous study, a 7% decrease in neuronal size was found in layer III[188]. Also, in the DLPFC of schizophrenia patients, it was found that there was a significant decrease in layer III pyramidal cell size comparing them to both normal controls and other, non-schizophrenic, psychiatrically ill patients[189]. However, in one study it was observed that lower amounts of silver grains were present for NR2A grains in layers III and IV in schizophrenia patients[91,181]. Moreover, it was found that PSD proteins were different in specific neuron types, pyramidal cells, in layers III and V[91,190]. Knowing that differences in PSD proteins were found on specific neurons, I decided to look at individual neurons, interneurons and pyramidal neurons, to determine if NMDAR NR1 mRNA was changed in specific cell types. Here, I will discuss how I examined three specific layers of BA46 for both pyramidal neurons and interneurons: layer II, where there are more condensed pyramidal neurons that are quite small; layer III, where pyramidal neurons are bigger and more spread out than layer II; and layer V, where there are a lot of large pyramidal neurons; interneurons are seen throughout all those layers making up about 20 percent of all neurons [191,192]. Modifications were made throughout my project to create a better protocol for analysis; however, throughout this thesis, I will be

focusing on the analysis of layer V only where a consistent protocol was applied throughout the measurements.

It is known that the DLPFC inhibitory interneurons help synchronise pyramidal neuron actions[82]. These two neuron types work hand in hand with one another to maintain a health balance in cortical excitation and inhibition. The integrity of the NMDARs in cortical interneurons is known to be vital during development to maintain GABAergic functions[193]. Indeed a deletion of the NMDARs in corticolimbic interneurons during early life is enough to prompt future problems including behavioral and pathophysiological qualities in mice, which mimic human schizophrenia[193]. However, it is not know if interneurons or pyramidal neurons or both contribute to the putative NMDAR NR1 reductions in the cortex of patients with schizophrenia.

Aims of my thesis:

My Masters' thesis research covers four broad areas, namely subcellular tissue fractionation of human cerebral cortex, the determination of the NMDAR subunit NR1 protein levels specifically in the PSD, analysis of NR1 mRNA transcript across cortical lamina, and the quantification of NMDAR NR1 mRNA at the cellular level. It is hypothesized that the NMDAR NR1 protein will be decreased in the PSD and mRNA will be decreased in neurons in schizophrenia patients.

The following are the four aims of this thesis that will test the hypothesis above:

1) To extract the postsynaptic density fraction from human brains. Post-mortem human brain tissue from BA10 was separated into seven different fractions: total homogenate, cytosolic fraction, nuclear fraction, synaptic membrane fraction, post-synaptic density, presynaptic membrane, and synaptic vesicles. Bicinchoninic acid

(BCA) analysis was performed to measure yield of protein in the samples and Western blotting was used to confirm the identity of subcellular compartments.

2) To measure NMDAR NR1 protein levels in schizophrenia compared to controls. NR1 protein levels in total and PSD associated homogenate from the BA10 region from patients with schizophrenia and controls were examined by Western blotting. This investigation was done to confirm or refute whether or not the previously observed deficit in NR1 protein is evident as decreased NMDAR NR1 subunits at the synapse where they are most functional..

3) To measure laminar expression of NMDAR NR1 mRNA in schizophrenia compared to controls. GRIN1 (human genome designation for the NMDAR NR1 subunit) mRNA expression in specific laminar layers in the DLPFC was examined by analysis of films from in situ hybridization experiments to determine which cortical layers demonstrate a change.

4) To measure cellular expression of NMDAR NR1 mRNA in schizophrenia compared to controls. Cellular GRIN1 mRNA transcripts in three laminar layers in the DLPFC were measured to determine whether an observed deficit in GRIN1 mRNA expression is specific to interneurons or pyramidal cells. This was achieved by counting of silver grains on microscopic images of BA46 cortex labeled for GRIN1 mRNA by in situ hybridization.

Addressing these four aims will provide insight as to how the NMDAR differ between schizophrenia patients and controls at a protein and mRNA level at a more detailed level than have previously been reported.

Chapter 2- New South Wales Tissue Resource Centre Cohort

This cohort was used throughout my entire thesis project. The different demographics variables discussed in this chapter will be used as covariates in different statistical analyses such as ANCOVAs if they are found to influence or vary with the measurement of interest.

UNSW Research Ethics Approval

Tissues were received from the New South Wales Tissue Resource Centre [NSW TRC] at the University of Sydney, which is supported by the National Health and Medical Research Council (NHMRC) of Australia, Schizophrenia Research Institute, National Institute of Alcohol Abuse and Alcoholism (NIH (NIAAA) R24AA012725). All post-mortem tissue research was approved under the guidelines of the Human Research Ethics Committee at the University of New South Wales (HREC 07261 for 2007-2012 and HC12435 from November 2012-2017).

Subjects[194]

The NSW TRC provided post-mortem brain tissue from 37 individuals with schizophrenia and 37 matched controls who did not have a psychiatric diagnosis. All demographic and clinical information from this cohort was documented as previously described in Weickert et al[194]. The next of kin gave consent to the brains being donated for research purposes and the Coroners Designated Officer gave approval for the NSW TRC. Without these approvals, tissue cannot be used. The ethics committees from Sydney South West Area Health Service (Protocol number X07-0074) and the University of Sydney (Reference Number 555) have approved the collection of the tissue used in experiments for this thesis.

In order to be a donor, there are certain criteria that must be met: the donor must be over the age of 17 with no significant history of developmental or

compounding neurological disorders, and no infectious disease. They also have to be free of any head trauma in the five years prior to death. If any cases had a history of substance use, these cases were individually examined to see if the individual could be used in the cohort, and were only used if they did not show excess use of any substance. Another factor in not being included in the cohort is if an individual had a prolonged agonal status or assisted ventilation within 24 hours of death. Tables 2.1 and 2.2 show detailed demographic information of the TRC cohort for schizophrenia patients and controls, respectively. Table 2.3 shows the detailed clinical information for schizophrenia patients.

Age at Death and Post-mortem Interval[194]

To verify the age at death and the birth date of the deceased in the TRC cohort, the next of kin was contacted and medical records obtained. The post-mortem interval (PMI), the time from death until brain freezing, was calculated in one of two different ways: (1) the time of death, if known, or (2) the midpoint between last time anyone saw the person alive to the time brain dissection occurred.

pH Measurement[194]

pH in the TRC cohort was measured by dissecting 1.0g of fresh cerebellum tissue and tissue homogenisation using 10mL of dH_2O. Using a pH meter (MP220, Mettler Toledo), all tissue sample pH was measured in triplicate and if any of these samples were consistently below a pH of 6.00, the sample was generally removed, though this also depended on whether the RNA quality was deemed to be acceptable. The importance of pH is that it is an indicator of the quality of tissue and RNA from the tissue sample.

Manner of Death[195]

Subjects' manner of death were categorised into five different groups: (1) natural (Nat), (2) accidental (A), (3) suicide (S), (4) homicide (H), and (5) undetermined (U). This information, along with any other related causes or medical conditions that could be linked to death, was obtained from the Coroner's documentation. In the TRC cohort, all schizophrenia patients were included; however, control cases were omitted from the cohort if they had death by suicide, due to possible psychiatric disorders.

Agonal State[195]

Agonal state ratings follows the guidelines from previous papers[115,196,197]. The ratings (1) excellent, (2) good, or (3) poor were established on the information received from the police report, Coroner's office, and autopsy report. Each person was rated individually. To determine the rating for each case, specific requirements needed to be met. For an excellent rating, the agonal phase needed to be short and/or the individual to be in good physical condition prior to death, for a good rating, the person needed to have a moderate agonal phase and/or be in moderate physical condition, and for a poor rating, they needed a long agonal phase and/or to be in poor physical condition. However, a fourth rating has been used in other papers where individuals were known to be on a respirator for a prolonged periods[115,196,197], but our cohort had no patients or controls with an extended hospital stay prior to death, so this agonal state was excluded in this study.

Schizophrenia Subtype

The information in Table 2.3 below shows the different clinical information about the patients. This information is included these for historical reasons and allows one to form an impression of the kind of patients that are included in the post-

mortem brain collection. However, subtype specific analyses of my data were not completed because the assigned subtype may not reflect the clinical state of the deceased person at the time of death.

Psychiatric Medication

For all medical records available, neuroleptic medications were noted and then converted into a common reference scale in chlorpromazine (CPZ) dose, a common antipsychotic, equivalent doses in milligrams (mg). This conversion was done using a software program, Neuroleptic Conversion Calculator (Version 1.2.1, 2002, Addat Pty Ltd). From this single dose in mg, a lifetime dosage of CPZ and the original medication was estimated by multiplying the average daily dose with the duration of illness in days. Patient's medical records were examined to determine when the last dosage and type of antipsychotic medication taken.

Smoking History

Nicotine is known to activate different receptors, including the NMDAR on the PSD. [198] It has been found that smoking can lead to cognitive [199] and sensory processing difficulties, [200] which is also seen in schizophrenia patients. This could be due to the differential modulation of different genes being affected on the NMDAR at the PSD. [198] Smoking history was broken down into four categories: (1) non-smoker, (2) moderate (less than 25 cigarettes per day), (3) heavy smoker (25 cigarettes or more per day), and (4) ex-smokers who have not smoked in at least a year. Data were collected using medical records and by interviewing the next of kin. Only 59 of the 74 people in this cohort had data available for assessment of smoking histories.

Table 2.1: Detailed TRC cohort information for normal controls. Abbreviations: Con=Control, L=Left, R=Right, Y=Yes, n=No, X=Ex-smoker, U=Unknown, PMI=Post-mortem interval, PFC=Prefrontal cortex, RIn=RNA Integrity number, Hr=Hours, StdDev=Standard Deviation, Ave=Average

Diagnosis	Age at Death	Gender	Cerebellum pH	PMI (hrs)	RIN	Ethnicity	Hemisphere	Brain Volume	Brain Weight	Cause of death	Agonal State	Smoking
CON	38	Male	6.26	13.5	7.7	Caucasia	L	1610	1620	Atherosc	2	Yes
CON	60	Male	6.59	21	7.8	Caucasia	L	1431	1440	Acute my	2	Unknown
CON	37	Male	6.64	21	7.6	Caucasia	L	1600	1610	Ischaemi	2	Unknown
CON	18	Male	6.06	33	7	Caucasia	L	1729	1740	Probable	2	No
CON	50	Male	6.68	29	8.1	Caucasia	R	1315	1320	Ischaemi	2	No
CON	56	Male	6.53	24	7.1	Caucasia	R	1627	1635	Coronary	2	Yes
CON	59	Male	6.56	20	7.4	Caucasia	R	1355	1360	Coronary	2	Yes
CON	43	Male	6.43	13	7.4	Caucasia	R	1432	1500	Thrombot	2	Ex-smoke
CON	37	Male	6.37	24	7.5	Caucasia	R	1497	1520	Electroc	2	Unknown
CON	46	Male	6.65	25	7.3	Caucasia	R	1493	1490	Mitral v	1	Unknown
CON	58	Male	6.46	12	7.6	Caucasia	L	1323	1350	Ischaemi	1	Yes
CON	60	Female	6.8	13	7.4	Caucasia	L	1191	1200	Ischaemi	2	Unknown
CON	50	Male	6.26	19	6.9	Caucasia	L	1537	1500	Ischaemi	2	Ex-smoke
CON	74	Male	6.22	10	7.4	Caucasia	L	1536	1528	Respirat	2	No
CON	34	Male	6.73	20.5	7.1	Caucasia	R	1508	1580	Acute ex	2	Yes
CON	56	Female	6.65	23	7.1	Cauc/Uni	R	1335	1360	Pulmonar	2	Ex-smoke
CON	33	Female	6.77	24	8	Caucasia	L	1407	1390	Cardiac	1	No
CON	44	Male	6.6	50	7.2	Caucasia	L	1271	1220	Ischaemi	2	Ex-smoke
CON	73	Male	6.8	48	8.1	Caucasia	R	1380	1380	Dilated	2	Yes
CON	46	Male	6.12	29	6.7	Caucasia	L	1331	1320	Acute My	1	Ex-smoke
CON	53	Male	6.64	27	7.1	Caucasia	R	1391	1450	Acute my	1	Unknown
CON	24	Male	6.27	43	7.1	Caucasia	R	1490	1490	Undeterm	2	Yes
CON	21	Female	6.83	39.5	8.1	Caucasia	R	1510	1570	Primary	1	No
CON	64	Male	6.68	39.5	7	Caucasia	R	1470	1470	Coronary	1	No
CON	62	Male	6.56	37.5	7.5	Caucasia	R	1421	1480	Acute my	2	Unknown
CON	49	Female	6.93	15	8.3	Caucasia	R	1282	1330	Probable	1	Unknown
CON	60	Male	6.7	25	7.1	Caucasia	R	1598	1610	Bacteria	3	No
CON	78	Female	6.3	11	6.1	Caucasia	R	1345	1320	Respirat	2	No
CON	78	Male	6.2	6.5	7.5	Caucasia	L	1463	1320	Dehydrat	3	No
CON	57	Male	6.6	18	8.4	Caucasia	L	1401	1360	Ischaemi	1	Ex-smoke
CON	60	Male	6.66	21.5	6.9	Caucasia	R	1560	1620	Ischaemi	1	No
CON	54	Male	6.8	29	6	Asian/In	R	1526	1510	Coronary	1	No
CON	56	Male	6.76	37	6.2	Caucasia	R	1554	1510	Left ven	2	Yes
CON	55	Male	6.5	20	7.3	Caucasia	L	1391	1400	Cardiac	3	Ex-smoke
CON	61	Male	6.25	27.5	6.6	Caucasia	R	1379	1438	Ischaemi	1	No
CON	37	Male	5.3	11	6.9	Caucasia	R	1279	1280	Pulmonar	1	Yes
CON	51	Female	6.92	37.5	7.7	Caucasia	R	1246	1294	Acute my	1	No
Ave	51.14	30 M	6.52	24.80	7.30	A=2, C=35	R=23, L=14	1438.22	1446.35		1=14, 2=20	Y=9 N=13
Stdev	14.62	7 F	0.31	10.97	0.57			121.74	127.15		3=3	X=7 U=8

Table 2.2: Detailed TRC cohort information for schizophrenia patients in the TRC cohort. Abbreviations: Schizoaf= Schizoaffective, SCZ= Schizophrenia, L=Left, R=Right, M=male, F=Female, Y=Yes, n=No, X=Ex-smoker, U=Unknown, PMI=Post-mortem interval, PFC=Prefrontal cortex, RIn=RNA Integrity number, Hr=Hours, StdDev=Standard Deviation, Ave=Average

Diagnosis	Age at Death	Gender	Cerebellum pH	PMI (hrs)	RIN	Ethnicity	Hemisphere	Brain Volume	Brain Weight	Cause of death	Agonal State	Smoking
SCZ	67	Male	6.36	5	8.4	Caucasia	L	1391	1400	Ischaemi	1	Unknown
SCZ	27	Male	6.5	10	7	Caucasia	L	1411	1420	Clozapin	3	Unknown
SCZ	51	Female	5.7	12	6.2	Caucasia	R	1153	1160	Lithium	3	Unknown
SCZ	51	Male	6.02	21	6.9	Caucasia	L	1481	1490	Ischaemi	2	Yes
SCZ	27	Male	6.25	33	8.2	Caucasia	R	1490	1500	Hanging	2	Yes
SCZ	57	Male	6.35	38	7.5	Caucasia	L	1580	1590	Consequn	2	Yes
SCZ	27	Male	6.22	38.5	8	Cauc/Uni	L	1663	1700	Myocardi	2	Unknown
SCZ	52	Male	6.1	8.4	7.7	Caucasia	R	1125	1140	Ischaemi	2	Yes
SCZ	56	Female	6.59	39	7.6	Caucasia	R	1011	1020	Undeterm	3	Yes
SCZ	44	Male	6.55	29.5	7.3	Caucasia	L	1372	1420	Hanging,	2	No
SCZ	67	Female	6.23	27	6.3	Caucasia	L	1119	1130	Empyema,	3	Yes
SCZ	30	Male	6.6	24	7.3	Caucasia	L	1394	1390	CO poiso	2	No
Schizoaf	61	Female	6.37	17	6.8	Caucasia	R	1366	1290	Myocardi	2	Yes
SCZ	56	Male	6.22	15	6.7	Caucasia	L	1302	1310	Chronic	3	No
SCZ	32	Male	6.24	26	7.9	Caucasia	L	1538	1540	Hanging	2	Unknown
SCZ	58	Female	6.14	19	6.8	Caucasia	R	1122	1120	Sepsis a	3	Unknown
SCZ	51	Male	6.62	18	7.9	Caucasia	L	1550	1560	Ischaemi	3	Yes
SCZ	66	Female	6.52	12.5	6.6	Caucasia	R	1235	1220	Faecaloi	3	Yes
SCZ	40	Male	6.2	21.5	7.6	Caucasia	L	1332	1360	Combined	2	Unknown
SCZ	55	Male	6.34	72	6.6	Caucasia	R	1510	1500	Ischaemi	2	Yes
SCZ	75	Male	6.36	36	6.9	Caucasia	L	1455	1440	Ischaemi	3	Yes
SCZ	54	Male	6.17	27.5	6.3	Caucasia	R	1508	1460	Coronary	2	Yes
SCZ	57	Male	6.66	48	6.5	Caucasia	R	1468	1420	Atherosc	2	Yes
Schizoaf	73	Male	6.8	14	7	Caucasia	L	1640	1590	Asphyxia	2	Yes
Schizoaf	73	Female	6.85	20	7.2	Caucasia	L	1457	1400	Right ve	3	No
Schizoaf	57	Male	6.6	28	7.4	Caucasia	R	1429	1400	Chronic	2	Yes
SCZ	56	Female	6.56	34	7.7	Caucasia	L	1548	1360	Pulmonar	3	No
SCZ	61	Female	6.65	42	6.8	Caucasia	R	1197	1140	Ischaemi	2	Yes
Schizoaf	30	Male	6.75	26	7.2	Caucasia	L	1601	1550	Hanging	2	Yes
SCZ	54	Female	6.5	29	7.2	Caucasia	R	1550	1490	Asthma	2	Yes
SCZ	33	Male	6.65	48	8.3	Caucasia	L	1544	1480	Hanging	2	No
Schizoaf	34	Male	6.7	26	7.3	Asian/Vi	R	1554	1500	Hanging	2	Yes
SCZ	52	Male	6.43	46	7.1	Caucasia	R	1536	1548	Cardiome	2	Yes
SCZ	55	Female	6.69	33.5	7.6	Caucasia	L	1192	1120	Combined	2	Yes
Schizoaf	33	Female	6.95	50	8.1	Caucasia	R	1371	1420	Hanging	2	No
Comorbid	68	Female	6.43	32	7.5	Caucasia	L	1377	1426	Acute pa	2	Yes
SCZ	59	Male	6.48	26.5	7.6	Caucasia	R	1526	1586	Ischaemi	2	Yes
Ave	51.32	24 M	6.44	28.46	7.27	A=1, C=36	R=17,L=20	1408.05	1394.32		1=1, 2=25	Y=23, N=7
Stdev	14.13	13 F	0.26	13.77	0.58			165.48	163.99		3=11	X=0, U=7

Table 2.3: Detailed clinical information for schizophrenia patients in the TRC cohort. Abbrev: B-Bipolar, D-Depression, DO-Disorganised, P-Paranoia, R-Residual, U-Undifferentiated, C-Chronic, E-Episodic, Pos- Positive, Neg-Negative, Y-Yes, N-No, CPZ-Chlorpromazine, TD-Tardive Dyskinesia, StdDev= Standard Deviation, Ave= Average.

Diagnosis	Diagnosis Subclass	Disease Course	Syndrome	Age of Onset	Duration of Illness	Last CPZ	Lifetime CPZ	TD	Auditory Hallucinations	Visual Hallucinations	Paranoia	Grandiose	Thought Disorder	Catationia	Polydipsia
Comorbid	Undifferentiated	Chronic	Positive	23	45	190	3679200	No	Yes	No	Yes	No	Yes	No	No
Schizoaf	Bipolar	Chronic	N/A	31	30	100	20438175	No	Yes	No	No	Yes	Yes	No	No
Schizoaf	Depressi	Chronic	N/A	21	52	380	12337000	yes	Yes	No	Yes	No	Yes	No	No
Schizoaf	Depressi	Chronic	N/A	36	37	300	4051500	No	Yes	No	Yes	No	Yes	No	No
Schizoaf	Bipolar	Chronic	Positive	30	27	415	10840500	No	Yes	Yes	Yes	Yes	Yes	No	No
Schizoaf	Depressi	Chronic	N/A	27	3	285	205312.5	No	No	No	Yes	No	Yes	No	No
Schizoaf	Bipolar	Chronic	Positive	27	7	250	498225	No	Yes	No	Yes	Yes	Yes	No	No
Schizoaf	Depressi	Chronic	N/A	14	19	95	1126938	No	Yes	No	Yes	No	No	No	No
SCZ	Undifferentiated	Chronic	Positive	26	41	1340	19454500	No	Yes	Yes	Yes	No	Yes	No	No
SCZ	Undifferentiated	Chronic	Positive	18	9	300	2133608	No	Yes	No	Yes	No	Yes	No	No
SCZ	Residual	Chronic	Negative	35	16	570	3248500	yes	Yes	No	Yes	No	Yes	No	No
SCZ	Residual	Chronic	Negative	27	24		3504000	No	Yes	No	Yes	No	Yes	No	No
SCZ	Paranoid	Chronic	Positive	19	8		919800	No	No	No	Yes	No	Yes	No	No
SCZ	Paranoid	Chronic	Positive	30	27	700	2463750	No	Yes	No	Yes	No	Yes	No	No
SCZ	Undifferentiated	Chronic	Negative	23	4	200	419750	No	Yes	Yes	Yes	No	Yes	No	No
SCZ	Paranoid	Chronic	Positive	21	31	680	4865450	No	Yes	No	Yes	Yes	Yes	No	No
SCZ	Paranoid	Chronic	Positive	24	32	580	4088000	No	Yes	No	Yes	No	Yes	No	No
SCZ	Undifferentiated	Chronic	Positive	27	17	500	3567875	No	Yes	No	Yes	No	No	Yes	No
SCZ	Disorgan	Chronic	Negative	21	46	350	10493750	yes	Yes	No	Yes	No	Yes	No	No
SCZ	Paranoid	Episodic	Positive	26	4	300	806650	No	Yes	No	Yes	No	Yes	No	No
SCZ	Disorgan	Chronic	Negative	21	35	450	5429375	yes	Yes	No	No	No	Yes	No	No
SCZ	Disorgan	Chronic	Positive	19	13	190	3701100	No	Yes	No	No	No	Yes	No	No
SCZ	Paranoid	Episodic	Positive	19	39	450	4982250	No	Yes	No	Yes	No	Yes	No	No
SCZ	Paranoid	Chronic	Positive	21	30	150	8760000	yes	Yes	No	Yes	Yes	Yes	No	No
SCZ	Paranoid	Chronic	Positive	19	47		31736750	yes	Yes	No	Yes	No	No	No	No
SCZ	Paranoid	Chronic	Positive	17	23	986	8499938	No	Yes	No	Yes	Yes	Yes	No	No
SCZ	Paranoid	Chronic	Positive	30	25		8212500	No	Yes	No	Yes	Yes	Yes	No	No
SCZ	Paranoid	Chronic	Negative	32	43	500	10986500	yes	Yes	No	No	Yes	Yes	Yes	No
SCZ	Paranoid	Episodic	Positive	19	35	1560	4151875	yes	Yes	No	Yes	No	Yes	No	No
SCZ	Paranoid	Chronic	Positive	40	17	618	3723000	No	No	No	Yes	No	Yes	No	No
SCZ	Disorgan	Chronic	Positive	17	39	760	14235000	No	Yes	Yes	No	No	Yes	No	No
SCZ	Paranoid	Chronic	Positive	19	42	1200	17629500	No	Yes	No	Yes	No	Yes	No	No
SCZ	Paranoid	Chronic	Positive	19	35	700	9740938	yes	Yes	No	Yes	Yes	Yes	No	No
SCZ	Paranoid	Chronic	Positive	22	11	250	891330	No	Yes	No	Yes	Yes	Yes	No	No
SCZ	Undifferentiated	Chronic	Positive	19	33	500	7116186	yes	Yes	No	Yes	No	Yes	No	No
SCZ	Undifferentiated	Chronic	Positive	17	38	1300	32767875	No	Yes	Yes	Yes	No	Yes	No	No
SCZ	Disorgan	Chronic	Negative	21	38	750	10874080	No	Yes	No	Yes	No	Yes	No	yes
Average	B=3, D=4=DO=5	C=34	P=25, N=7	23.7	27.62	542.4	7907586	Y=9	Y=34	Y=5	Y=32	Y=10	Y=34	Y=2	Y=1
Std Dev	P=16, R=2,U=7	E=3	N/A=5	6.07	13.82	373.9	7953627	N=28	N=3	N=32	N=5	N=27	N=3	N=35	N=36

Table 2.4 shows an overall summary of the TRC matched cohort

Table 2.4: The demographics of schizophrenia patients and matched control subjects in the New South Wales Tissue Resource Centre post-mortem brain tissue cohort. Abbreviations: F=Female, M=Male, R=Right, L=Left, PMI=post-mortem interval.

	Schizophrenia (n=37)	Controls (n=37)
Ages in years (mean (range))	51.5 (27-75)	51.1 (18-78)
Gender	13F/24M	7F/30M
pH cerebellum (mean±s.d).	6.44±0.26	6.52±0.31
PMI (hours) (mean±s.d.)	28.46±13.77	24.80±10.97
Brain weight (grams) (mean±s.d.)	1394.32±163.99	1446.35±127.15
Brain volume (mL) (mean±s.d.)	1408.05±165.48	1438.22±121.74
Hemisphere	17R/20L	23R/14L
Freezer storage duration (mean±s.d.)	78.89±37.24	69.62±42.71
Smoking (yes/no/unknown/ex-smoker)	23/7/7/0	9/13/8/7
Suicide	8	0
Age (years) at onset (mean (range))	23.70 (14-40)	
Duration of illness (years) (mean± s.d.)	27.62±13.82	
Chlorpromazine lifetime dose (mg) (mean±s.d.)	7907585.91± 7953626.65	
Chlorpromazine median dose (mg) (mean±s.d.)	691.64±502.20	

Overview

This matched 37 and 37 cohort was used for the entire thesis. This cohort, ranging in age from 27 to 75, along with a large sample size, is different than other cohorts in this field. Using this cohort, I hope to further advance knowledge in this field.

Chapter 3- Novel Post-Mortem Tissue Fractionation Technique

Consideration of Post-Mortem Tissue Fractionation Techniques

Studying sub-cellular microdomains, like the PSD, provides an opportunity to better understand how proteins work in certain environments rather than in a conglomeration of total tissue, which is similar to what occurs in vivo[115,140,141,144,146]. Knowing how to isolate the PSD in human post-mortem brain tissue helps with understanding the NMDAR in healthy people along with how the NMDAR differs in mental illness. Throughout the previous studies looking at the PSD, the numbers of proteins found on the PSD have varied greatly from only a few hundred to over one thousand[89,115]. This difference may be attributable to a difference in sensitivities of the techniques, or to collecting a slightly different or more varied region of the brain that could consist of different PSDs that have different proteins, or a combination of both. As isolating the PSD can be difficult and time consuming, and because of the amount of tissue needed to get an adequate fraction of PSD material to study, not many research laboratories have applied sub-cellular fraction techniques to the study of the human brain [89,115].

The ability to isolate the PSD using tissue fractionation allows us to measure levels of proteins and receptors located in this important membrane region. In 1974, Cotman and colleagues were among the first to describe a method to isolate the PSD using homogenised rodent brain tissue[196,197,201]. Using sucrose and calcium chloride buffer, tissue was subjected to an osmotic shock to lyse the cell membranes and the homogenate centrifuged to pellet the insoluble material, which was removed. They then employed a sucrose gradient, consisting of 0.8, 1.0, and 1.2M sucrose, to obtain the synaptic membrane fraction (SPM) which following centrifugation was situated between the 1.0 and 1.2M sucrose layers. Isolation of

different proteins between layers of different molecular concentrations of sucrose exploits differences in the densities of fractions of interest. Next, to obtain the PSD, a detergent similar to sodium dodecyl sulfate (SDS) buffered to a pH of 7.5 can be added to the SPM and the homogenate centrifuged. Cotman confirmed they isolated the PSD by electron microscopy of the SPM and the final PSD fraction[201]. In the original photos of the SPM fraction, the PSD was seen as a dense structure attached to the presynaptic membrane. After detergent treatment and centrifugation, the electron microscopy showed there was a dense structure isolated from the SPM, presumed to be the PSD.

Later in 2001, Phillips and colleagues further refined the methods by showing that pH played a major role in the isolation of the PSD[202]. They noted that when the pH of a solution the tissue was in was 6, the pre- and post-synaptic regions remained connected, but when the pH was raised to 8, the two membranes separated more fully. Recently, Hahn and colleagues optimized three different methods of post-mortem brain tissue fractionation, based on the above methods, to isolate the PSD from human post-mortem brain tissue. The most extensive method in the Hahn et al. paper, method 3, obtained six fractions: 1) total homogenate, 2) cytosolic fraction, 3) synaptic membrane fraction, 4) synaptic vesicles, 5) pre-synaptic fraction, and 6) post-synaptic density fraction[115]. For these fractions, pH is important because proteins are very sensitive to their environment, and if the pH is too high or too low, the proteins can unfold to the point of denaturing causing samples to be unusable for later studies. Our laboratory was interested in retrieving the PSD fraction, along with other fractions, so I used a modification of method 3, which also isolated a nuclear fraction from an otherwise discarded component[196,197,203].

Aims of this study:

The aim in this chapter is to try and understand what is occurring in the total homogenate and at the PSD in our cohort specifically. In this section of the study, human prefrontal brain tissue (BA10) was separated into subcellular components which starts with the total homogenate, then isolating six other components: cytosolic fraction, nuclear fraction, synaptic membrane fraction, synaptic vesicles, pre-synaptic fraction, and the post-synaptic density fraction. The two main components that will be used in future chapters are the total homogenate and the post-synaptic density fraction.

Material and Methods

The chemical compositions of solutions are described in Appendix 1.

Tissue Pulverisation:

BA10 samples were kept on dry ice. Samples were weighed (Mettle Toledo XS105 Dual Range scale). Approximately 400mg of frozen tissue chunks were then poured back into the 50mL Falcon tube until later pulverisation. For pulverisation, the brain tissue was smashed into small, fine pieces. All of the labelled samples were frozen at -80°C.

Subcellular Tissue Fractionation of Post-mortem Brain Tissue:

Throughout the entire tissue fractionation procedure, all centrifugation was done at 4°C and all of the samples and solutions, excluding the Protease inhibitor (Sigma P8340), were kept at 4°C. This procedure required four days to fully process one sample. Seven fractions were obtained for each sample. The seven samples included the total homogenate (T), the cytosolic fraction (C), the nuclear fraction (N), the synaptic membrane fraction (SPM), the PSD, the synaptic vesicular fraction (SV), and the presynaptic membrane fraction (PPF).

Day 1:

An overview of Day 1 is seen in Figure 3.1. Day one required seven solutions: 2.0M sucrose, 2.3M sucrose, nuclear isolation media (NIM), sucrose density barrier (SDB), solution A (Sol. A), nuclear lysis buffer with no sodium chloride (NLB with no NaCl), and nuclear lysis buffer with high sodium chloride (NLB with high NaCl), Sucrose solutions had to be used within 24hrs of being made due to the high risk of bacteria contaminations in these solutions.

In a Class 1 fume hood in a PC2 laboratory, a Potter-Elvehjem homogeniser (Kontes Glass Co., Vineland, NJ, US) was used to homogenise approximately 0.4g of post-mortem brain tissue in 5mL of solution A. The total sample (T) was stored in a -80°C freezer. The remaining T fraction was centrifuged at 1400×g (RCF) for 15min at 4°C in the Eppendorf centrifuge (refrigerated microcentrifuge Eppendorf 5415R). After centrifugation, the supernatant (S1) from the tubes were combined and placed on ice. The pellets (P1) from the tubes were then rehomogenised with small plastic pestles in 1mL of solution A (250µl/tube). Next, the resuspended pellets were centrifuged at 710×g in the Eppendorf centrifuge for 10min at 4°C. The approximate 1.5mL of supernatant (S2) was then added to S1. The pellet (P2) was placed on ice to be used later on in the procedure.

The pooled S2 samples were centrifuged at 16000×g in the Eppendorf centrifuge for 20mins at 4°C. After centrifugation, the supernatant (S3) was considered to be the cytosolic (C) fraction. The C fraction was placed into the -80°C freezer, along with an aliquot for bicinchoninic acid (BCA) quantification of the protein. The pellets (P3) were saved for later in the procedure.

A crude suspension of the pellet P2 was prepared using NIM. Six mL of 2M SDB was added, along with the NIM/sample mixture and mixed. Four mL of 2.3M

sucrose was added to the sample tubes, which were then was placed in the ultracentrifuge rotor (SW41Ti, 09E2800). The NIM/SDB mixture was carefully overlayed on top. This was spun for 1hr at 100,000xg (24,200RPM) at 4°C in order to separate the nuclei from the rest of the mixture.

After one hour, any material floating on the meniscus was removed and the supernatant liquid was poured off to leave the nuclear pellet (P4). P4 was resuspended in NLB with high NaCl. The P4 in solution was vortexed quickly. This was then placed on a rotation wheel to incubate at 4°C for 20mins. Thereafter, NLB with no NaCl (low salt) was added and the solution allowed to precipitate on ice for 20mins causing the nuclei to lyse under hypertonic conditions. The samples were then centrifuged at 14,000xg in the Eppendorf centrifuge for 10mins at 4°C. The supernatant (S4) was considered to be the N fraction. S4 was collected and saved for analysis with an aliquot saved for BCA protein determination. The pellet (P5) received after the 14,000xg centrifugation contained DNA, lipids, and other nuclear contents, which was discarded.

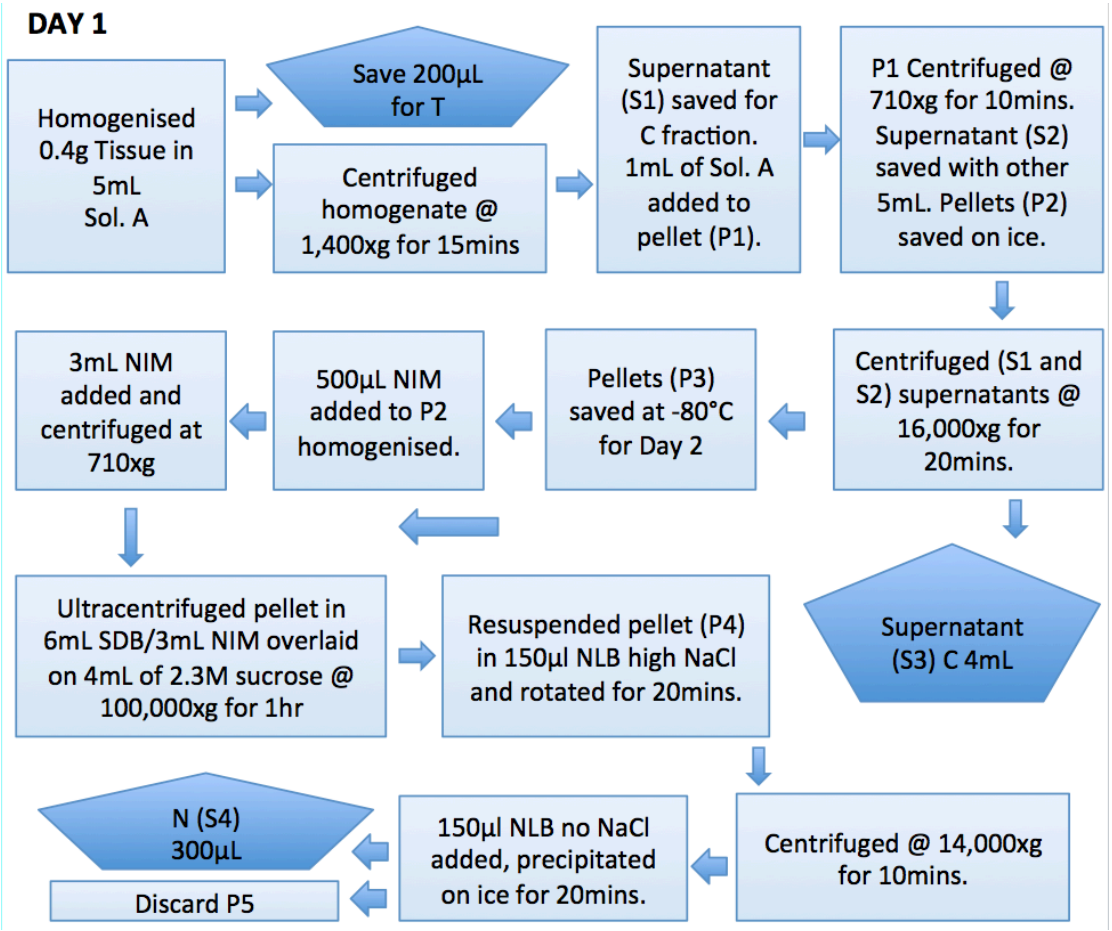

Figure 3.1: An overview of Day 1 for the tissue fractionation procedure. T: total fraction, C: cytosolic fraction, N: nuclear fraction

Day 2:

An overview of Day 2 is seen in Figure 3.2. P3 from Day 1 were resuspended in total volume of 750µL of solution B. A three-layer sucrose gradient (5mLs of 1.2M, and 3mLs of each 1M and 0.85M sucrose) was pipetted into ultracentrifuge tubes (99U4065), taking great care to not allow mixture of the layers. The solution B mixture was added on top, then centrifuged for 3hrs at 100,000×g (24,200RPM) in a SW41Ti rotor in Beckmann ultracentrifuge at 4°C.

After the 3hr centrifugation the white band (P6) between the 1.0M and 1.2M sucrose was removed using a syringe and needle (18GA 3.5in, Ref: 405248). P6 contained synaptosomes, and was diluted with 5X volume of solution B and centrifuged 30mins at 35,000×g (19,500RPM) at 4°C. The supernatant (S5) was removed and the pellet resuspended with 0.1mM $CaCl_2$ and centrifuged at 15,000×g (RCF) at 4°C for 20mins. $CaCl_2$ was used as a wash. After the $CaCl_2$ solution was removed, the pellet (P7) was resuspended in 20mM Tris pH 7.4, triple detergent to dissolve the pellet. The samples were then placed on the rotation wheel for 60mins at 4°C. This fraction was designated as the synaptic membrane fraction (SPM). A proportion of this sample was set aside for the SPM fraction and frozen at -80°C, and 150ml was further fractionated on day three

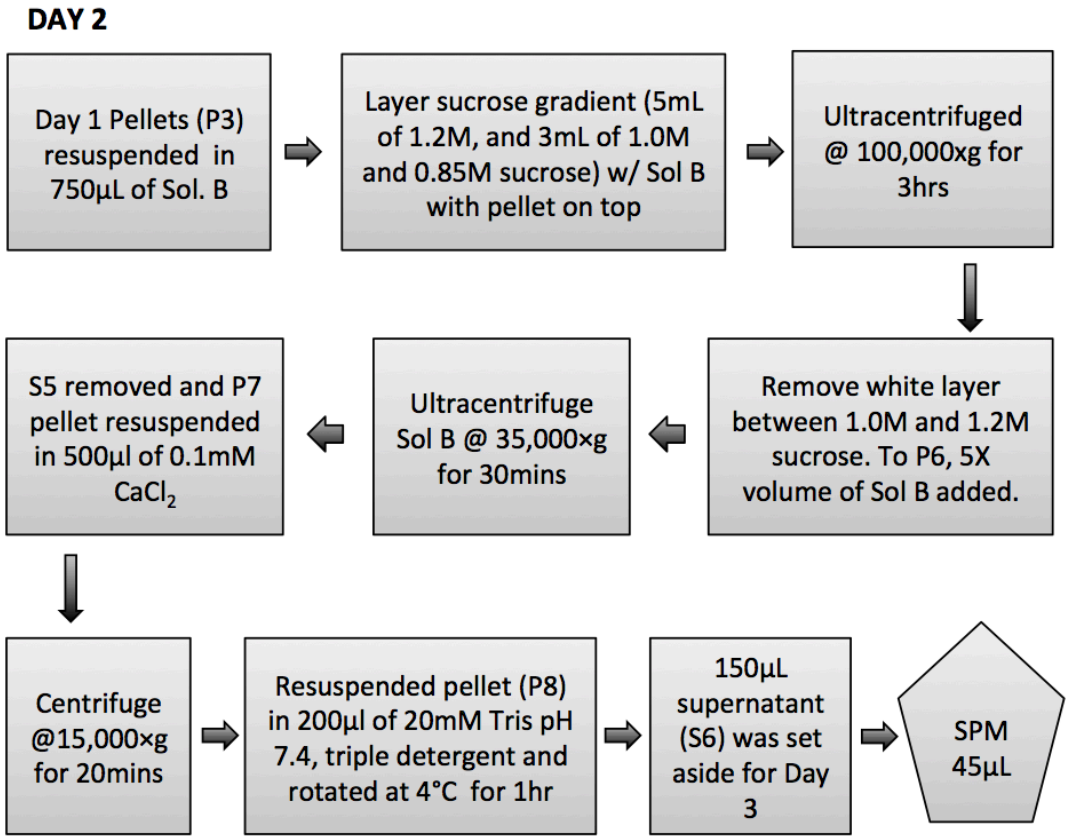

Figure 3.2: An overview of Day 2 for the tissue fractionation procedure. SPM: synaptic membrane fraction.

Day 3:

An overview of Day 3 is seen in Figure 3.3. The 150ml aliquot of SPM was diluted with ice-cold 0.1mM $CaCl_2$. The sample had 40mM Tris-HCl pH 6 supplemented with 2% Triton-X 100 added to each tube. The samples were then left on the rocker at 4°C for 30mins for precipitation. After 30mins, the samples were transferred to the 70.1Ti rotor and centrifuged at 35,000×g (19,500 RPM) for 20mins at 4°C.

The supernatant (S6) was designated as the SV fraction. S6 was removed and protein was precipitated in 5X volume ice-cold acetone. The samples were vortexed and placed in -20°C freezer overnight. The pellet (P8) from the prior centrifugation was dissolved in 1mL 0.1mM $CaCl_2$. These samples had 40mM Tris pH 8, 2% Triton-X 100 added to each tube. These samples were agitated on a rocker for 60mins at 4°C. Afterwards, the samples were centrifuged at 140,000×g (39,000RPM) for 30mins at 4°C.

The supernatant (S7) contained the less dense synapse component and was designated as the presynaptic membrane fraction (PPF), leaving a pellet of the denser PSD protein (P9). S7, the PPF fraction, was precipitated in 5X volume ice-cold acetone and then left in a -20°C freezer overnight. The pelleted (P9) PSD fraction was allowed to air dry and it was dissolved in 20mM Tris pH 7.4 triple detergent. The PSD fraction was set aside for the BCA assay.

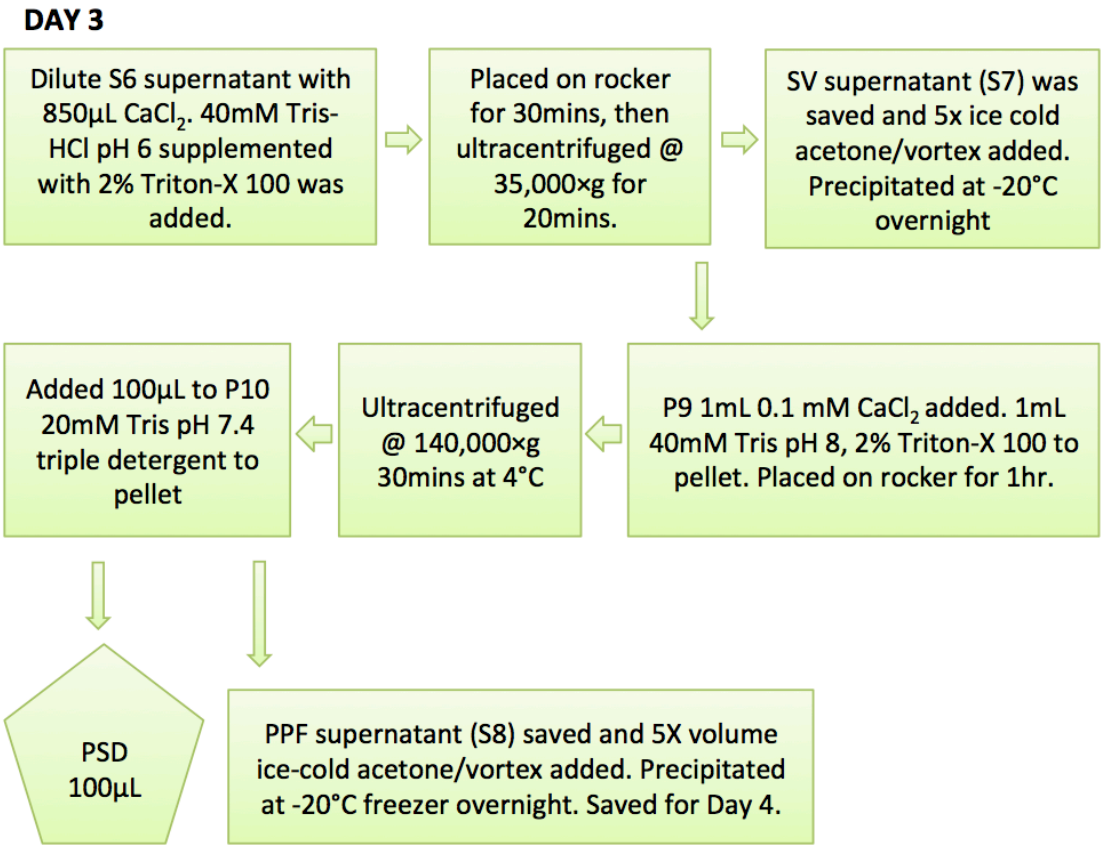

Figure 3.3: An overview of Day 3 for the tissue fractionation procedure. SV: vesicular fraction, PPF: presynaptic membrane fraction, PSD: postsynaptic density fraction.

Day 4:

An overview of Day 4 is seen in Figure 3.4. The SV and PPF fractions were centrifuged at 24,000×g (11,800RPM) 30mins at 4°C. Once centrifuged, the supernatants were discarded and the tubes inverted to air dry for 30mins. The pellets were then dissolved in 20mM Tris pH 7.4, triple detergent. Six µL of each fraction were set aside for BCA protein quantification.

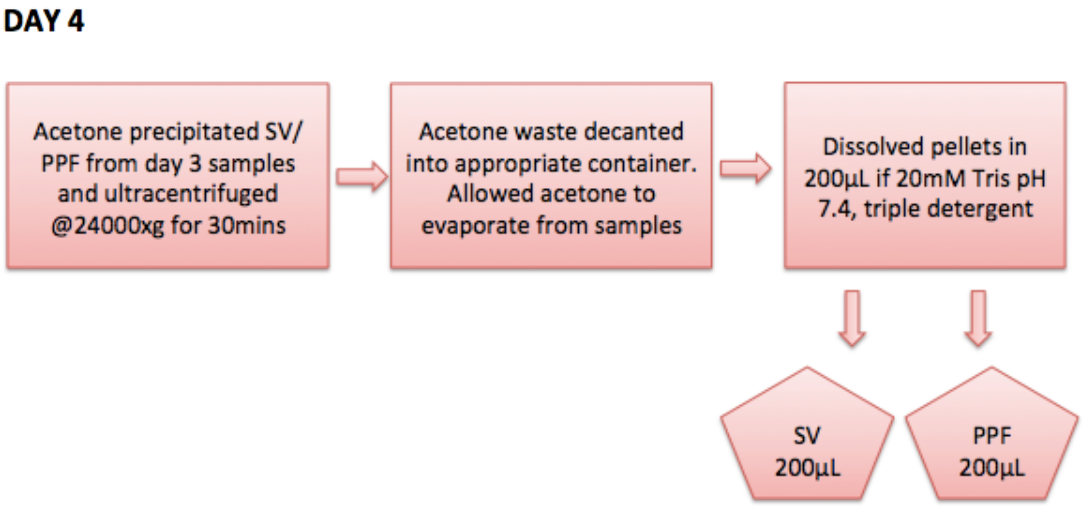

Figure 3.4: An overview of Day 4 for the tissue fractionation procedure. SV: vesicular fraction, PPF: presynaptic membrane fraction.

BCA Protein Analysis:

The protein concentrations were determined for T, C, N, SPM, SV, PPF and PSD fractions by BCA method (Pierce). NLB (175mM NaCl), Solution A and Tris pH 7.4, triple detergent with inhibitors was used as appropriate dilutes for standards.

For BCA analysis, 5µL of each standard at different concentrations (0.1 to 1.4mg/mL) was pipetted in triplicate into a 96-well plate. Five µL of each sample, in either singlet (SPM, PSD, PPF, or SV) or triplicate (T, C, N), were then loaded into the plate. The BCA kit was run using the manufacturers protocol. The plate was incubated at 45°C for 30mins. Using a plate reader, the absorbance was measured at 562nm.

Protein Measurement

Protein amounts were measured by first running a Western blot, then using the ChemiDoc, and finally running the Quantity One program on two samples. This

was completed to check the reliability of the tissue fractionation method being used. Only two samples were used to check the reliability of the fractionation methodology because some fractions produced low amounts of protein. Some samples from the tissue fractionation were removed due to lack of tissue material or because during certain stages of fractionation where a pellet should have formed, there was no visible pellet. The 1° Abs used was NR1-NMDAζ1 monoclonal Ab (Santa Cruz) at 1:1000 in 5% milk in TBST, synaptophysin (MAB368, Merck Millipore) was used at 1:10000 in 5%milk in TBST, and NeuN (MAB377, Merck Millipore) was made 1:1000 in 5% milk in TBST. The membrane was incubated with the 1° at 4°C overnight on a rocker.

Results for Tissue Fractionation

Enrichment of Tissue Fractions

Figure 3.5 shows a Western blot wins different antibodies to check for the presence of proteins that should be in each fraction. The PPF was not tested in the Western blot below. NMDA NR1 molecular weight is approximately 120kD. [117] Synaptophysin is approximately 38kD. [204]. NeuN is found to have up to three bands with molecular weight being approximately 46kD, 48kD, and 70kD. [205] Finally, α-tubulin is seen at approximately 55kD. [117] Figure 3.6 shows the approximate amount of protein calculated by dividing the protein of interest by the housekeeping protein, α-tubulin.

Relationship between protein yields for different fractions and demographic and clinical variables were examined using Pearson correlations. Across the total cohort, freezer storage time had a major effect on yield of protein in five of the seven fractions, including the PSD fraction. Due to some samples being greater than two standard deviations away from the average protein amount, some samples

were considered outliers were removed. Correlations showed that the C fraction, (r=-.340, p=0.004, n=71), N fractions (r=-.345, p=0.003, n=70), SPM fractions (r=-.445, p=0.000, n=72), and SV fraction (r=-.282, p=0.023, n=65) were negatively correlated with length of freezer time. However, the PSD fraction was positively correlated (r=.298, p=0.014, n=68). Even though the data was normally distributed, a closer look at the data showed that a small group of data points in the C, SPM, and SV using Pearson's correlations were likely causing the significance. It was also found that PMI, in hours, was positively correlated with protein yield in the N fraction (r=.250, p=0.037, n=70). Also, there was a highly significant correlation between the starting material and how much protein was received in the T fraction (r=.307, p=0.009, n=72).

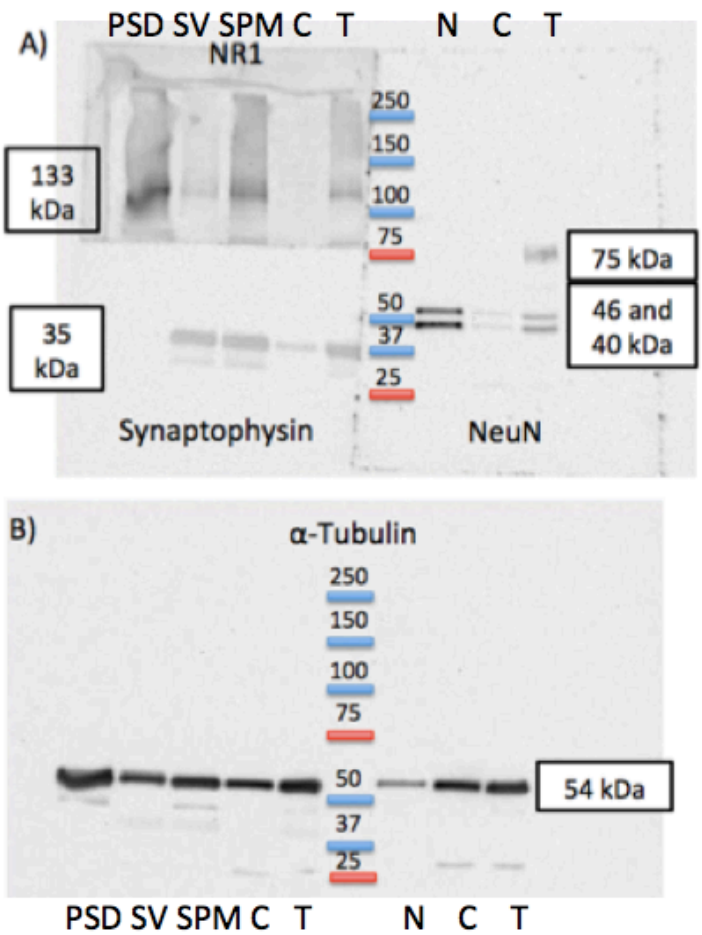

Figure 3.5: A) Western blot using three antibodies against NR1, synaptophysin, and NeuN that are known to be in specific tissue fractions. B) Western blot looking at the housekeeping protein, α-tubulin. NMDA NR1 molecular weight ~ 120kD, Synaptophysin is ~38kD, NeuN ~46kD, 48kD, and 70kD, and α-tubulin is seen at approximately 55kD. Abbreviations for fractions: T=Total, C=Cytosolic, n=Nuclear, SPM=Synaptic membrane fraction, SV=Synaptic vesicles, PSD=Post synaptic density, kDa=Kilodalton

Table 3.1: An overview of the TRC cohort tissue fractionation protein yields in each fraction. Abbreviations: SD= Standard deviation, T=Total fraction, C=Cytosolic fraction, n=Nuclear fraction, SPM=Synaptic membrane fraction, SV=Synaptic vesicles, PSD=Post synaptic density, and PPF= presynaptic membrane fraction

		Fraction						
	Starting Material (SM)	**T**	**C**	**N**	**SPM**	**SV**	**PSD**	**PPF**
Average (µg)	429130.8	128687.8	1248.6	137.8	309.4	167.7	54.2	29.4
SD (µg)	74101	33944.1	285.6	97.7	147.2	249.4	27.5	27.9
Range (high) (µg)	629000	187464.4	1752.1	488.1	198.0	1445.2	115.8	229.6
Range (low) (µg)	301000	28697.3	1.0	28.5	5.70	10.70	10.50	4.40
Percent of SM		30.4	1.33	0.05	0.15	0.04	0.01	0.01
Percent of SM SD		8.2	0.31	0.02	0.17	0.06	0.007	0.006
Percent of T			24.4	0.55	1.39	0.68	0.21	0.16
Percent of T SD			15.0	0.47	1.13	0.84	0.16	0.47
Number of Samples	74	72	72	70	72	71	69	67

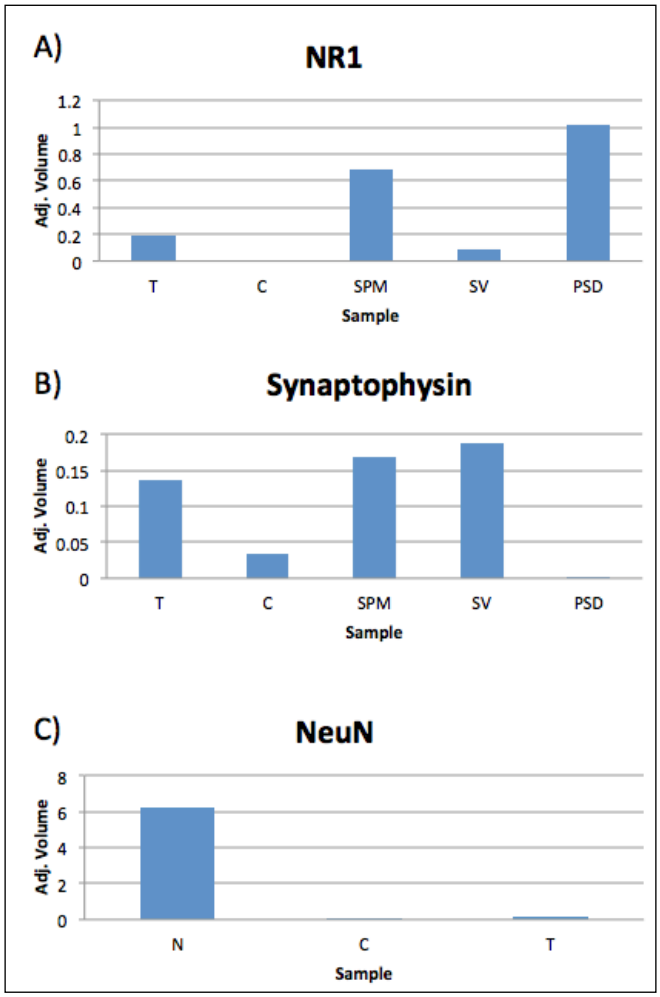

Figure 3.6: A chart showing different fractions for each of the proteins of interest. Adjusted values are calculated by dividing the protein of interest by the housekeeping protein, α-tubulin. A) NR1 protein showing the PSD fraction has the most concentrated amount over the other fractions. B) Showing there are no synaptophysin proteins in the PSD and very little in the C fraction. C) NeuN protein showing that the N fraction is where NeuN is located at a high concentration, where it should be.

Yield of Tissue Fractions

The average amount of starting material for the post-mortem tissue fractionation, along with the yields of T, C, N, SPM, SV, PSD, and PPF fractions are seen in Table 3.1.

In the control group alone, there was a negative correlation for two fractions and negative trend for two other fractions with the freezer storage time: C (r=-.293, p=0.087, n=35), N (r=-.421, p=0.012, n=35), SPM (r=-.468, p=0.005, n=35), and SV (r=-.342, p=0.059, n=31). Also, PMI was positively correlated with the yield in the N fraction (N: r=.380, p=0.024, n=35) and SPM (r=.566, p=0.000, n=35). The T Fraction protein yield also correlated positively with brain volume (mL) (r=.375, p=0.027, n=35) and brain weight (mg) (r=.380, p=0.024, n=35).

For the schizophrenia patient group, the amount of starting material (mg) correlated positively with the T fraction protein yield (r=.396, p=0.015, n=37). There were also a few correlations with freezer storage time, which may have impacted on brain tissue quality. The freezer storage time played a role in how much protein was in four of the seven fractions; three fractions were negatively correlated (C (r=-.401, p=0.015, n=36), N (r=-.347, p=0.041, n=35), and SPM (r=-.440, p=0.006, n=37)) and one fraction was positively correlated (PSD (r=.410, p=0.016, n=34)).

Age of onset and CPZ equivalent correlations

Besides just tissue quality based on post-mortem variables, the age of illness onset and chlorpromazine dose equivalents correlated with the amount of protein for different fractions. Age of onset was positively correlated with yield in the PSD fraction (r=.387, p=0.024, n=34). The last recorded amount of medication (CPZ) that schizophrenia patients received was positively correlated with the SPM fraction yield (r=.359, p=0.040, n=33). SV fractions yield correlated with lifetime amount of medication taken (r=.652, p=.000, n=34), the highest amount of medication prescribed (r=.715, p=0.000, n=34), and the mean amount of medication given (r=.714, p=0.000, n=34). Consequently, the last recorded medication that schizophrenia patients received, correlated positively with the SPM fraction yield (r=.359, p=0.040, n=33).

Discussion

There are a many different methods to extract the total protein from human brain tissue. Our laboratory extracts total protein in two different ways in addition to the method I used for my thesis. Other ways total protein extraction has been completed in our laboratory (by Shan Yuen Tsai) utilises either a Poly-tron, or a

mortar and pestle to mechanically break up the tissue into a Tris buffer (14.68mL 0.1M Tris buffer, 300µL of protein inhibitor cocktail, 18.65µL aprotinin, and 15mL glycerol). Using the Poly-tron, approximately 14mg/mL of protein was obtained from a total amount of 50mg of starting material and 500µL buffer. Using the plastic mortar and pestle, roughly 4.5mg/mL of protein was obtained from approximately 50mg of starting material and 500µL of buffer. For the protein extraction protocol used in this thesis, for 400mg of brain tissue, 5mL of Sol. A was used. My total homogenisation fraction had a protein concentration of approximately 30mg/mL. Since the maximum amount of protein the Poly-tron and mortar and pestle techniques would retrieve is 14mg protein/100mg stating material (=14% yield) and the method used in this thesis would have a maximum of 150mg protein/400mg stating material (=37.5% yield), it can be concluded that the method by Hahn et al.[115] had the best proportion of extracted protein to homogenising buffer (mortar and pestle: 9%; Poly-tron: 14%; tissue fractionation method: 37.5%). This could be due to the fact that the Hahn method consisted of using a glass homogeniser, whereas the other methods used a plastic homogeniser or a metal machine. Also, another difference is the homogenising buffer used. For my homogenisation, I used Sol. A, a high molar sucrose solution, whereas the other two methods use a Tris solution. Buffers can have a wide variety of effects depending on the specific proteins' properties[206]. Using Tris, the pH will either cause stabilisation or destabilisation of the protein of interest[206]. Sucrose was used in my work since it helps with the solubility of tissue fractions and can help to separate subcellular compartments based on density.

The lab that optimised the method which was modified for the tissue fraction that was used in this thesis had a higher yield than I did for the SPM, SV,

PPF, and PSD fractions, using 500mg starting material[115], where my tissue fractionation had on average 400mg per sample. For the SPM fraction, approximately 0.8mg protein was yielded[115]. My SPM total amount was 0.3mg. The SV fraction yielded 0.5mg, along with 0.25mg of the PPF fraction[115,133,164-166]. My SV fraction had a total amount of protein of 0.17mg and my PPF fraction had 0.029 mg. Finally, the PSD fraction yielded approximately 0.25mg of protein[115,164]. My PSD fraction had 0.054mg. However, in the published results of the Hahn method, it is unclear what the final amount of protein collected for each fraction was[115].

Several factors in the protocol could affect the measure of protein yield in the laboratory procedure. For the PSD and PPF fractions, the acetone evaporation step may not have been complete as any remaining acetone could inhibit the protein from being dissolved completely within the samples. As well it was noted that the BCA kit used was highly sensitive to particles in the wells of the 96-well plates. This could cause potential problems, for the T fraction particularly, if there were minimal undissolved particles floating in the wells, as the BCA plate reader could misinterpret the amount of protein in each well. Other variability could be due to the amount of starting material, which was taken into account for by weight, but some tissue samples could have more lipids or blood causing the weight to be slightly heavier. These are some of the possible reasons why yield variability could have occurred between samples

I did confirm the purity of a subset of the samples (n=2) by analyzing the difference fractions, T, C, N, PSD, SPM, and SV, by Western blots. My purity check for enrichment of specific proteins in the different fractionations worked well. From the literature, it is known that very little NR1 should be seen in the C fraction[207]. Synaptophysin, a synaptic vesicle protein, should be absent from the

PSD fraction[208] and enriched in the SPM[208] and SV fraction[208], which is consistent with my observations. Finally, NeuN is a neuronal specific nuclear protein, which was observed mainly in the N fraction[209], with considerably less NeuN protein in the T and C fractions. The centrifugation process of the C fraction might not have pelleted all of the N fraction particles leading to some NeuN proteins being seen, however from immunohistochemistry, it is known that some NeuN is also found in the cytoplasm of neurons. [205,210]

Chapter 4: Western Blotting Study

Introduction

Western blotting is used when one needs to detect if specific proteins of interest are in a sample. This technique provides information about whether the protein of interest is in the sample, the approximate molecular weight, and quantity of an antigen recognised by antibodies.

In this chapter, I focus on protein analysis of the NMDA NR1 protein in schizophrenia patents and controls. The total homogenate and PSD fractions in schizophrenia. The method for how the fractions were obtained were described in chapter 3. The aim of this study is to identify if there is a decrease in schizophrenia patients in NMDAR NR1 protein at the PSD level.

My hypothesis is that there would be a decrease in protein in schizophrenia patients at the PSD level, but not in the total homogenate. The aim of this study is to identify if there is a decrease in schizophrenia patients in NMDAR NR1 protein at the PSD level. Using the method of Western Blotting is for identification of specific proteins and the protein's molecular weight.

Material and Methods

TRC Cohort:

The NSW TRC cohort, consisting of 37 schizophrenia patients and 37 controls were used for the Western blotting studies. The demographic details are described in Chapter 2 (Tables 2.1 and 2.1) and summarised in Table 2.4 (derived from Weickert et. al.[117]).

Western Blotting Procedure:

All solution compositions used for Western blots can be found in Appendix 1.

Day 1:

An 8% polyacrylamide gel with the appropriate number of wells, generally 15, was made. An 8% gel was used because of the molecular weight size of NMDAR NR1 protein (~130kD). Appendix 1 shows how to make the 8% Western Blot gel. For the total homogenate (T) samples, 10μg of protein (5μL) was used and for PSD samples 1μg of protein (10μL) was used. Samples were combined with an equal volume of Laemmli sample buffer that contains 5% β-mercaptoethanol (1:1). An internal control consists of, a pooled sample of five control samples and five schizophrenia samples, was used to ensure efficiency of the run. Protein was loaded onto the gels. The gels were run at 150 V for 40mins up to 1.25hrs. The protein was transferred from the gel onto nitrocellulose membrane at 100 V for 3hrs to ensure all the protein was completely transferred.

Once the transfer was complete, the membrane was stained with Ponceau S Solution (Sigma, P7170-1L), which rapidly stains protein bands, to confirm transfer. Five percent non-fat skim milk was added to the container holding the membrane, which was left for a minimum of 1hr on a rocker in the refrigerator at 4°C. Primary antibody (1° Ab) was added to the nitrocellulose membrane after an hour and it was incubated at 4°C overnight on a rocker. The 1° Ab used was NR1-NMDAζ1 monoclonal Ab (Santa Cruz) at 1:1000 in 5% milk in TBST. .

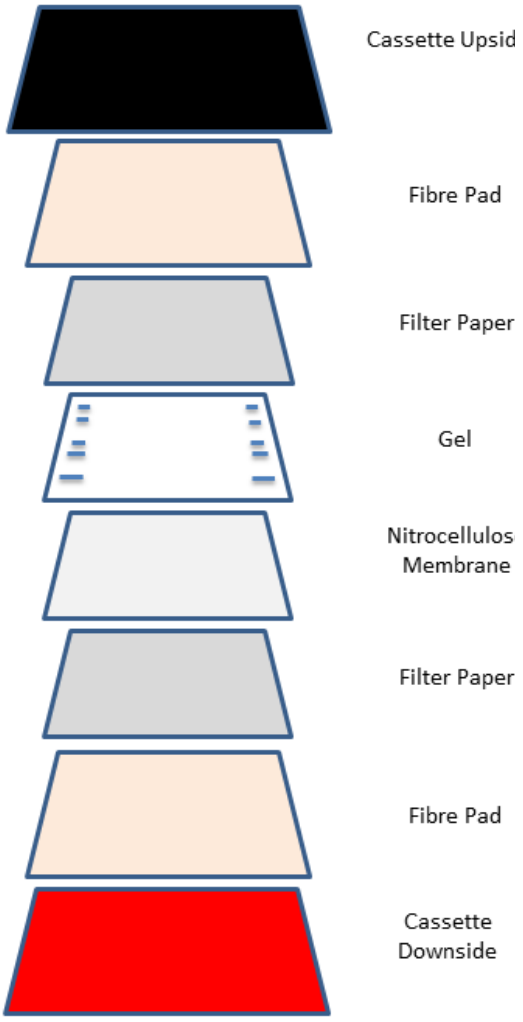

Figure 4.1: The order in which Western blot transfer components are placed in the cassettes.

Day 2:

The 1° Ab was rinsed off with TBST (3 x 10 minutes), then a secondary antibody (2°Ab), AP106P rabbit anti-goat IgG antibody HRP conjugate (Merck Millipore), at a 1:5000 dilution was made in blocking solution- 5% milk in TBST The membrane was incubated with the 2°Ab at room temperature on the rocker for 1hr. Then the 2°Ab was rinsed off with TBST. After this, analysis of the membrane was done using film and a Chemidoc (described in detail in Appendix 3).

If a second set of antibodies is applied and the 1°Ab or 2°Ab would react to the first set, then stripping buffer was used to remove the first 1°Ab and 2°Ab.

Stripping buffer was added and rotated on a platform to mix. Next, the membrane was blocked for 1 to 2hrs with Block at 4˚C.

A housekeeping protein was examined to confirm how much protein was actually added to each well. The control 1°Ab (T3952-100UG, Anti-β-Tubulin III antibody) (Sigma Aldrich) was made at 1:10,000 in 5% milk in TBST added to the membrane, which was incubated on a rocker overnight at 4˚C. Anti-β-Tubulin III antibody was used because all eukaryotic cells contain this form of tubulin. [211]

Day 3:

The 1° Ab for the housekeeping control protein was rinsed off with TBST. A 2° Ab (AP192P donkey anti-mouse IgG antibody, HRP conjugate) (Merck Millipore) was made at 1:5000 dilution in the Western blocking solution. The membrane was incubated at room temperature for 1hr. The 2° Ab was rinsed off with TBST. The analysis of the membrane was done using film and a Chemidoc (described below).

Chemidoc Analysis

The membrane was placed on to an overhead plastic sheet. For each membrane, 500µL of lumin (Millipore Immobilin, Cat. no. WBKLS0500) and 500µL of perox (Amersham ECL, Cat no PRN2209) was mixed was and pipetted onto the membrane. After waiting 30secs to one minute for the chemical reaction to occur, the excess solution was poured off and the blots were moved to the Chemidoc to start the exposures. Using Quantity One Chemidoc XRS, exposers of the NMDA NR1 antibody with the chemiluminescence chemicals were taken for between 120secs. to 300secs. For tubulin, a 30sec exposure was used. ,

After the Chemidoc procedure was completed, another 1mL per blot of the Lumin/Perox mixture was made and placed on the membrane again for 30secs to a minute to allow the luminescence quality to be stronger. The membrane was

exposed to film to obtain a permanent image of the protein band of interest (time varied between 1sec and 1hr), the film was developed using an automatic film processor.

Quantity One Analysis

Chemidoc Quantity One program version 4.6.5 was used. Each band of interest was captured in boxed regions to measure the density of it. One additional box was made and placed over a region of the membrane where there were no protein bands; this was used for a background calibrator. The data was exported to excel, and the volume was then found by dividing the adjusted volume of the protein of interest by the volume of the housekeeping protein.

Data and statistical analysis

The T sample data were not normally distributed comparing the amount of NMDAR NR1 protein/tubulin protein, so Spearman correlations were used; whereas the PSD sample data were normally distributed so Pearson correlations were run. For protein analysis, independent sample Student's t-tests, ANOVAs, and ANCOVAs were completed. These fractions were correlated with PMI, RIN, pH, freezer storage, age, and brain volume. Using the Western blotting method, the T samples were run on five separate occasions, (however, the diminishing expression of the signal on protein bands suggested the antibody was deteriorating, and most of these runs were deemed not reliable). The PSD samples gave a more consistent signal and were run on three separate occasions. The averages of all runs, excluding two standard deviations outliers, are reported, providing data for 69 samples.

Results for NMDAR NR1 PSD Protein Analysis

The Western blots completed showed that there was one clearly identifiable band at the 135kDa mark, which is the expected size for the NR1 protein. For the housekeeping antibody, bands for α-tubulin appeared at approximately the 45kDa mark, though some samples showed a doublet slightly smaller to the known tubulin size. (See Figure 4.2)

Antibody signal decreased over time

An investigation was completed to see how well the NMDAR NR1 antibody was working over time. Figure 5.6 shows a slow decrease in the signal from NMDAR NR1 Westerns over time (with A being the first gel (run 1) followed by B (run 2), then E (run 3) followed by F (run 4)) for the total homogenate sample with similar running conditions and exposure times. Before each Western blot was completed, a new batch of antibody from the original stock solution was made. The deterioration could be due to a potential contamination of the stock or an unstable antibody for this protein.

Next, I checked to see if the transfer did not work in the molecular weight range of the NR1 protein (approximately 135kDa) because larger proteins remained in the gel. I tested another antibody specific to Neuregulin 1 and confirmed that bands showed up at the expected molecular size of up to 180kDa (seen in Figure 4.3).

We concluded that the antibody had lost antigenicity when used over a prolonged period of time. Thought this testing, I determined the total homogenate samples were not reliable to use for statistical analysis. Refer to Figures 4.2 and 4.3. The quantity of NMDAR NR1 in each sample was not consistent over replicate trials showing low correlations (r=0.1-0.5) across assay runs. This section will just

discuss the PSD fraction of the Western blotting procedure, which was performed first and which gave a reliable signal.

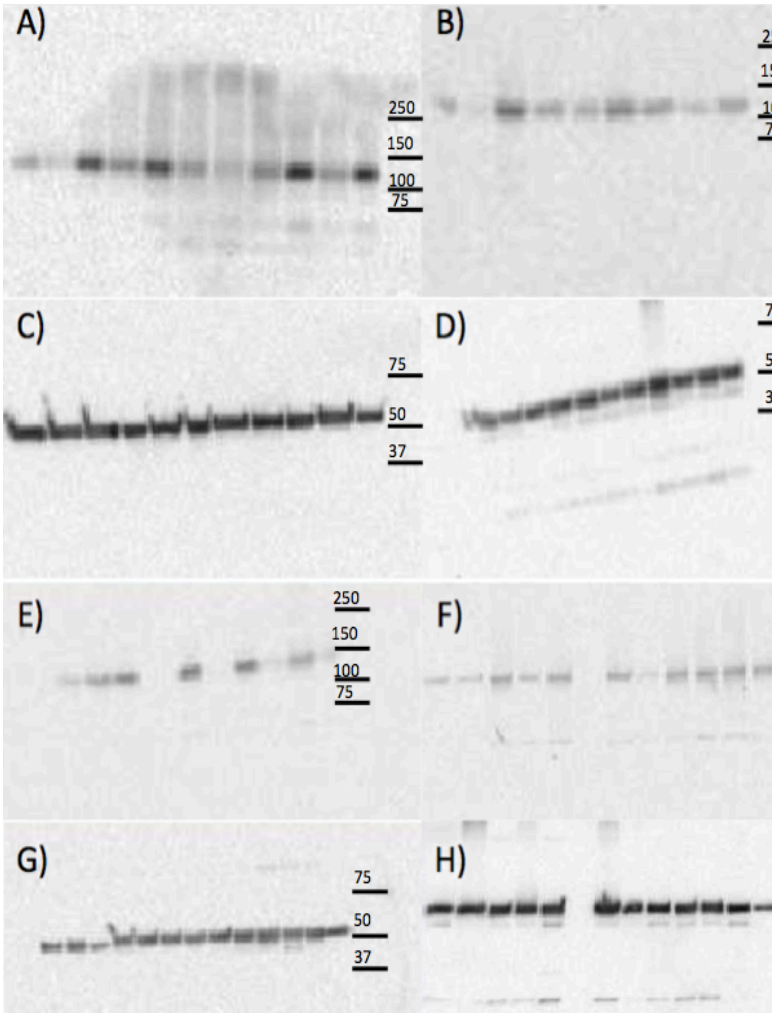

Figure 4.2: A-H are Western blot run on both schizophrenia patients and controls in BA10. A) Run 2 for NR1 protein T fraction, 2-minute exposure. B) Run 3 for NR1 protein, 2-minute exposure. C) House keeper α-tubulin for Run 2. D) House keeper α-tubulin for Run 3. E) Run 4 for NR1 protein, 2-minute exposure. F) Run 5 for NR1 protein, 5-minute exposure. G) House keeper α-tubulin for Run 4. H) House keeper α-tubulin for Run 5.

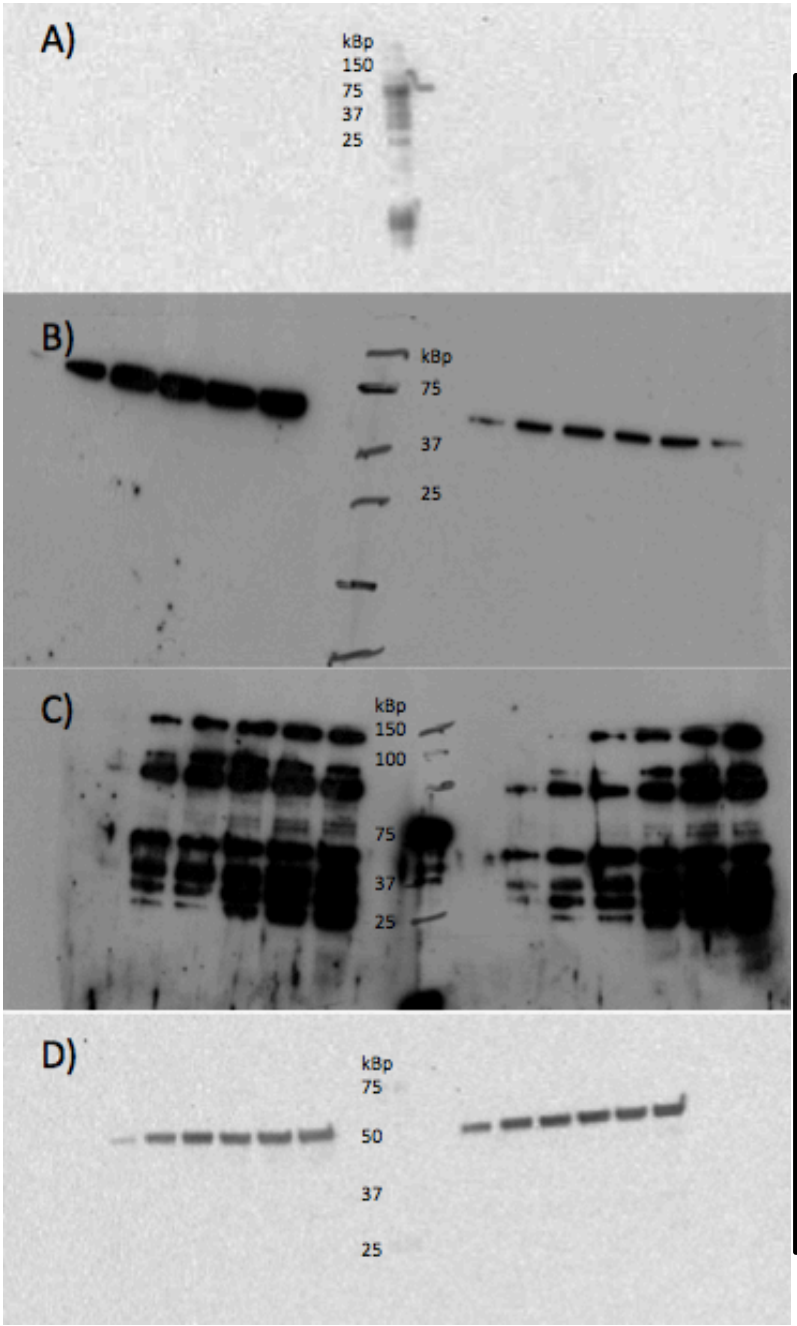

Figure 4.3: A) Western blot with no signal using NR1 antibody and two different secondaries (AP106P- left and SC2033- right). B) Western blot on the same membrane using HSP60 antibody and the same secondary antibodies as NR1 (AP106P- left and SC2033- right). C) Western blot on the same membrane showing expression at similar molecular weight as the NR1 protein using NRG1 antibody. (SC-348) D) House keeper α-tubulin for membrane.

Therefore, I tested whether the primary antibody against NR1 or the secondary antibody had deteriorated. Firstly, I investigated whether the secondary antibodies were working optimally. In this case, I tested two 2° antibodies that were expected to bind to the NR1 specific antibody. As seen in Figure 5.7a there was no signal for NR1 with either 2° antibody, but when the secondary antibodies were applied to blots probed with a different primary antibody (for HSP60, also raised in rabbit), strong bands were detected. From this test, I was able to conclude

that the secondary antibody was not the likely contributor to the loss of signal in the NR1 Western blots.

Demographic and clinical related effects on NR1 subunit expression in subcellular tissue fractionation:

Table 4.1 shows correlations between demographic variables and quantities of NR1 in the PSD for the full cohort, only schizophrenia patients, and only controls. It is noted that age at death was a significant factor in the total cohort having a negative correlation with NR1 in the PSD (r=-.247, p=0.020, n=69). The older the individual, the less NMDAR NR1 subunit was detectable at the PSD. Also, PMI had a negative correlation with NR1 in the PSD for the total cohort (r=-.233, p=0.027, n=69).

Table 4.1: Correlation of demographic variables with the NR1 protein in the PSD for the full cohort, only schizophrenia patients, and only controls. R-values are shown. * p<0.05, # p<0.10, which statistically significant are bolded. Abbreviations: Yr= years, Hrs=houres, Mo=months, g=grams, PSD = post-synaptic density, PMI=post mortem interval, RIn= RNA integrity number

	PSD Full Cohort	PSD Control	PSD Schizophrenia
Age of Death (Yr)	**r=-.247***	r=-.271#	r=-.235#
pH of PFC	r=.-132	r=-.041	r=-.279#
PMI (Hr)	**r=-.233***	r=-.119	r=-.232#
RIN	r=.023	r=.009	r=.018
Freezer Storage (Mo)	r=.102	r=-.063	r=.209
Brain volume (g)	r=.009	r=.128	r=-.239#

When doing a independent sample Student's t-tests for amount of NR1 in the PSD between men and women in the entire cohort, there was no difference between the sexes (t=.130, df=67, p=0.897). When co-varying for age of the cohort and PMI, there was also no significant difference found (F=.059, df=1, p=0.809). When doing a independent sample Student's t-tests for NR1 at the PSD between left and right brain hemisphere, there was no statistically significant difference by

independent sample Student's t-tests (t=-1.313, df=66, p=0.194). However, there was a strong trend towards statistical significance when an ANCOVA was completed, co-varying for age and PMI (F=3.715, df=1,64, p=0.058), indicating there is 30% more NMDAR NR1 protein at the PSD in the right hemisphere. Being a smoker also seemed to influence the amount of NMDAR NR1 protein in the PSD fraction (F=4.131, df=2,52, p=0.022), showing that smokers had 44% less NR1 protein at the PSD (p=0.008, LSD post-hoc text). This remained significant when co-varying for PMI and age at death (F=4.323, df=2,50, p=0.019).

For the schizophrenia group, there were no statistically significant correlations seen, but there were four noteworthy negative correlations at trend levels between NR1 protein at the PSD and age at death (r=-.235, p=0.090, n=34), pH (-.279, p=0.055, n=34), PMI (r=-.232, p=0.093, n=34), and brain volume (r=-.239, r=0.087, n=34). Table 5.3 shows correlations between clinical variables and quantities of NR1 in the PSD fractions for all schizophrenia patients. Looking at the clinical data in Table 4.2, there was also a trend towards significance stating that the more CPZ a patient had over the course of a lifetime, the less PSD NMDAR NR1 protein a patient had.

Table 4.2: Correlation of clinical variables comparing the NR1 protein in the PSD fraction in schizophrenia patients. p<0.10 are #.

	PSD Schizophrenia
Age of Onset	p= -.035
Duration of Illness (years)	p= -.221
CPZ (Lifetime)	p= -.238#
CPZ (Low)	p= -.064
CPZ (High)	p= -.190
CPZ (Mean)	p= -.200

For the controls for the PSD samples, it was found that there were no significant correlations in NR1 amount and any of the demographic variables. However, there was a negative trend seen for age of death (r=-.271, p=0.057, n=35).

Diagnosis related effects of NR1 subunit expression in subcellular tissue fractionation: I found at statistically significant 39% decrease in amount of NR1 protein in the PSD fraction from schizophrenia patients compared to controls (t=-2.874, df=66, p=0.005), shown in Figure 4.4. This remained statistically significant when an ANCOVA was completed co-varying for age at death and PMI (F=5.186, df=1,64, p=0.026). Also, high and equal amount of alpha-tubulin were seen for all subjects used, with no statistically significant difference between the diagnostic groups found (t=-1.681, df=72, p=0.097; Figure 4.5). When examining suicide versus natural death in schizophrenia patients, there was no statistical significant difference in the amount of NMDAR NR1 protein observed (t=-1.185, df=32, p=0.245).

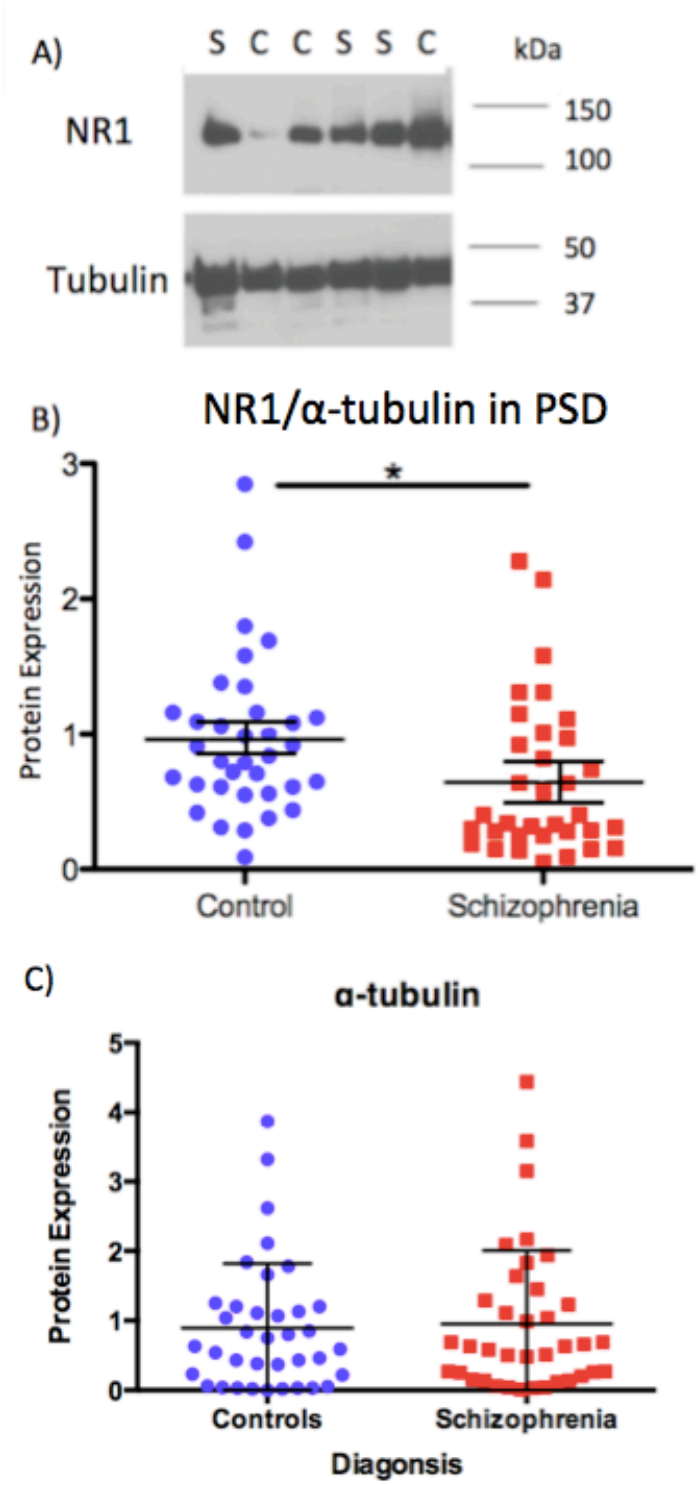

Figure 4.4: A) Western blot images showing the variation of NR1 in the PSD in BA10 in both schizophrenia patients and controls. I noted a single band for NR1 and α-tubulin at the expected size. B) The PSD fraction comparing schizophrenia patients and controls show a significant decrease in NR1 in the schizophrenia group. C) α-tubulin protein expression levels between the control group and schizophrenia patients. α-tubulin is used as a housekeeping protein. There was no significant difference between diagnostic groups. Error bars are showing SEM.

Discussion

Our lab examined NRI in has the largest post-mortem cohort to date. Despite other evidence implicating NMDARs having potential structural and functional differences in schizophrenia, examining NMDAR NR1 in the PFC could be the next step forward in understanding what is occurring in this illness. I found evidence that the PSD fraction from BA10 in schizophrenia patients have lower amounts of NR1 protein compared to the control group in our laboratory cohort over a wide age range, even after taking into consideration of reduced NR1 protein in the PSD in both controls and people with schizophrenia with age. If this important subunit is underrepresented in the postsynaptic signalling regions, then it is possible that fewer NMDA receptors are out on the PSD in people with schizophrenia, and this would interfere with glutamate signal transduction between neurons. So, even if the neurons have an overall equivalent amount of NMDAR NR1 protein in controls and in schizophrenia, if the NR1 protein is in an inoperative area or is maldistributed, the neurons will not be optimally functional. With decreased levels of NR1 proteins in the PSD in schizophrenia patients, this helps further the knowledge in the field and suggests that the NMDAR function may be changed in schizophrenia patients[135,136,212-215], and as a result could contribute to neuropsychiatric disease[117,135,136,213-215].

Shown previously in Table 1.1, other studies have shown that total NR1 protein levels between schizophrenia patients and controls were unchanged, increased, or decreased[77,91,106,117,122,212,216]. Less NR1 protein can mean limited function of the NMDAR, which could mean less binding potential to the receptors overall and less NMDARs functioning correctly. [117,175] Too much of a decrease in NMDAR NR1 could cause death prenatally, because it is known that mice without

any NR1 subunits never survive until birth. [217,218] However, if some NMDAR NR1 protein subunits in mice are decreased by 5-10%, this could potentially cause an increase in motor activity and have behaviour that would compare to schizophrenia. [219] Some suggest that if there are either too many or too few NMDARs functioning, this could lead to a decline in behaviour[117,118,124,175]. When looking at the PSD in our cohort, there was evidence of altered NR1 protein. Since this receptor is a cation channel allowing calcium and sodium into the cell and potassium out, if there is a decrease in NMDARs, this could limit the postsynaptic activation and or allow the balance of signalling at the postsynaptic site to be altered. Without glutamate signals, especially ones from the NMDAR receptor that are critical for learning and memory, functioning correctly, schizophrenia symptoms could occur. For example, administration of NMDAR antagonists, like ketamine, to healthy controls can cause schizophrenia-like symptoms [100]. However, from our laboratory studies I only know that the level of NR1 is lower in the PSD, but I do not know anything about the state of the NMDAR function. Previous studies from post-mortem brain of people with schizophrenia, pioneered by Hahn et al., do show that the NMDAR may be under-activated upon indirect stimulation with growth factors. [115] Our studies suggest that a reduced level of NMDAR NR1 can be a component of this dysfunction, at least in our cohort.

I found a relationship in my study between NMDAR NR1 subunit and hemisphere, following results seen by other groups who have found that the left hemisphere of schizophrenia patients have decreased NR1 protein levels. [117,118,124] I also found no difference in protein levels between men and women, whereas other data shows schizophrenic women have increased NR1 protein levels and schizophrenia males have decreased levels compared to controls[124,220]. However,

our laboratory has published a paper as well showing that there were no differences seen between mend and women for NMDAR NR1 mRNA or protein in the same cohort. [117]

Another observation was looking at the possible effects of antipsychotics treatments prior to death may relate specifically to decreased NMDAR NR1 protein levels. One study shows that there is an association between the Positive and Negative Symptom Scale examination while patients are taking antipsychotics [221], meaning that something is affecting how the brain is functioning. Some studies show no difference in antipsychotic medication and brain function [117,222], but other studies show that antipsychotics could downregulate the long-term amount of NMDAR NR1 at the mRNA and protein levels [223], along with in other prefrontal cortex mRNA. [224] This shows that antipsychotics could be altering the brain at a cellular level over the course of a patient's lifetime.

Smoking may also have an effect on how much NMDAR NR1 protein there is in the PSD. In this study, it was found that smokers had less NMDAR NR1 protein. In one study, it was found that smoking might differentially modulate glutamatergic function, specifically the NMDAR, in both schizophrenia patients and control subjects.[198] However, an alternative explanation for how NMDAR may differ between schizophrenia patients compared to controls could be related to the increased smoking that is typically displayed by schizophrenia patients. [198] It is possible that smoking or altered lifestyle associated with smoking could cause an even great loss NMDAR NR1 protein and mRNA over time in the prefrontal cortex

Moving more specifically to cortical layer III, it has been found that there are decreased somal sizes in pyramidal neurons in individuals with schizophrenia. Since pyramidal neurons play a central role in corticocortical connectivity, it was

hypothesized that these neurons could be playing a role in schizophrenia. [225,226] In layer III in BA10, a 9-12% decrease in dendritic spines of pyramidal cells have been observed[226]. This decrease did not correlate with antipsychotic medication leading one to believe that it is attributable to a pathophysiological cause[226] . The decrease in dendritic spines would likely result in less PSD proteins including the NMDAR. Since I saw a decrease in percent yield of NMDAR NR1 protein in people with schizophrenia, this would help support my argument. It may also mean that there would be fewer spines overall in the cortex of people with schizophrenia and less NR1 protein/spine in schizophrenia patients. Reduced NR1 protein may be due to deficiencies in synthesis and may relate to a significant difference in NMDAR NR1 at the mRNA level, which will be discussed in later chapters. Layer III is discussed in more detail in chapters five and six.

When looking at possible confounders, it was found that PMI could play a role in how much NR1 there was at the PSD. This is important because PMI it has been found that the longer the PMIs, the more difficult it is to get reliable and usable data[227]. The finding that there is a negative correlation with NMDAR NR1 protein and PMI is consistent with this because schizophrenia patients were matched with healthy controls in my study. PMI is unlikely to explain the diagnostic differences.

More studies would be needed in order to make sure that decreased NMDAR NR1 is the direct cause to cognitive and behavioural actions that is common in schizophrenia patients.

Future research

In future research, being able to capture the NMDARs proteins on the interneurons and pyramidal neurons separately would be ideal since it is thought these neurons, either inhibitory or exhibitory respectively, could have a differential impact in schizophrenia. It is hypothesised that due to inhibitory interneurons being more easily manipulated by action potential compared to the pyramidal neurons, this could be the focus of where the deficit in protein lies[91,220], along with extensive pathology documented in this neuronal subset[228].

Limitations of the study

In chapter three and four, NR1 protein was isolated, examined and quantified in BA10. Chapters five and six will focus on NR1 mRNA in BA46. Because of the overlapping function, shared developmental history, and similar neuropathology across cortical regions in schizophrenia, whatever is occurring in BA46 should most likely be reflected in BA10 as well. The Schizophrenia Research Laboratory began focusing on BA10 from two points of view: from a theoretical point, i.e. theories suggesting this region differs between schizophrenia patients and normal controls, and from a practical point of view, due to tissue fractionation needing a great deal of tissue, BA46 did not have enough tissue, so I moved to an adjacent region of the brain with similar function, BA10.

Western blots are laborious and there are many processes that need to be completed consistently in order for this method to work. In the current study, I investigated how the NMDA NR1 subunit expression differs in total homogenate and in the PSD from people with schizophrenia and people without any neurological/psychiatric disorders. In a previous paper published by my laboratory 36% less NMDAR NR1 protein in total homogenate from the DLPFC of

schizophrenia patients compared to controls was observed[117]. I was not able to confirm this difference due to technical issues detailed earlier in this chapter.

Other issues with both primary and secondary antibodies include contamination of the antibodies, storing at an incorrect temperature, and prolonged storage. Contamination can include bacterial and fungal issues, but there are also other compounds that will not allow the antibody to function correctly if there are even trace amounts in the antibody solutions, including sodium azide and thiomersal. For temperature storage, if long-term storage is needed, most primary antibodies should be kept at -20°C. If the antibodies are being used often, keeping them at 4°C should suffice for the antibody to stay stable for at least a few months, or even years, depending on the specific antibody. It has been found that some antibodies should never be kept below 4°C as freezing can destroy the antigen binding site. Finally, as noted above, antibodies can lose reactivity to epitopes within a few months to a few years, even with proper storage. Having them at colder temperatures will keep the antibodies stable for a longer period of time. The importance of these factors varies among antibodies and caution must be used while using antibodies so false results do not occur in experiments.

When used in the laboratory, antibody-antigen affinity can vary greatly with changes in temperature, pH, and use of different buffers and solvents[179]. The measurement called avidity is the strength of the interaction between an antibody and its antigen[179]. In the case of Western blots, both low and high avidity binding molecules can be used. However, due to the majority of antibodies recognising only six amino acids or less on a peptide, specific binding can become tricky. This is due to the vast number of known proteins and the limited number of amino acid combinations there can possibly be. When doing Western blots, most of the time

when more than one band appears, they are at considerably different molecular weight. One should not ignore these bands, but try to find reasons these bands might be occurring.[229] Another thing to consider is that unexpected immunoreactive bands upon Western blotting does not always signify antibody cross reactivity with unrelated proteins as proteins can often be synthesised as parts of larger precursors and be cleaved to yield smaller peptides[230]. It is possible that the microdomain of the protein recognised by the antibody is still intact in these different isoforms of protein and thus multiple immunoreactive bands could still represent different forms of the protein of interest[230].

Chapter 5- NMDAR NR1 mRNA Assessment of Expression using Laminar Film Analysis

Introduction

In this chapter, I performed film analysis for laminar mRNA expression in the DLPFC. This method gives an overview of the mRNA expression of each layer of the cortex. mRNA is important because this is the link between our genetics and the functional proteins being produced. If there is a problem with too much or too little mRNA, then there can be too much or too little protein produced, which can affect brain function.

This thesis uses in situ hybridisation to analyse the NMDAR NR1 subunit mRNA levels in the DLPFC of 37 people with schizophrenia and 37 controls. In the previous reports about the NMDAR in brain tissue, it has been found that schizophrenia patients have a significant decrease in NR1 mRNA, along with a significant decreased in NR2C mRNA in the PFC[91,85,95,14784,94,146]. However, others found no changes in the NMDAR mRNA expression[101,106,122]. More specifically in the DLPFC, the NMDAR NR1 mRNA was found to be increased[106], decreased[194], or not changed [216]. Because of these variations between studies, I wanted to see if there was more or less of a decrease in mRNA in certain cortical layers. The aim of this study to examine if there is a difference between the amounts of mRNA for NR1 being produced in schizophrenia patients' brains compared to controls. It is hypothesised that the schizophrenia patients will have less NR1 mRNA than the control group and that this difference will be greater in specific layers.

Material and Methods

Prior to my analysis, members of the Schizophrenia Research Laboratory designed the NMDAR NR1 mRNA probes and performed the actual wet lab

experiment. From this experiment, the films and emulsion dipped slides were provided to me for analysis. My thesis work entailed the quantitative analysis of NMDAR NR1 mRNA from the autoradiographic films and of the quantification of the cellular level of expression through microscopic examination of the slides. The in situ hybridisation protocol is shown in Appendix 2.

In situ hybridisation film quantification:

In situ films were scanned using a Canon CanoScan8600F scanner. Next, Adobe Photoshop (Adobe Photoshop CS5 extended version 12.0x64), was used for the cropping process and to check for background consistencies between samples. A radioactive standard curve was used to obtain the correct calibration for the amount of mRNA hybridisation in μCi/g using ImageJ. The standard values are used for specific curve fitting models that the program can adjust for. The aim was to get an R^2-value for the standard curve as close to 1.0 as possible. Each image was then calibrated using the best-fit exponential function and converting the OD of each image to μCi/g.

Determining the μCi/g of NMDAR NR1/cortical layer

The line tool was chosen for analysis of mRNA levels within BA46 cortex. The line width was set to 10 pixels, and drawn from the pial surface to the white matter. The areas used for calculation was based on Professor Cyndi Shannon Weickert's and Alice Rothwell's work locating the correct cytoarchitecture area prior to the start of my thesis work. An example of where the grey matter from BA46 was measured is in Figure 5.1. The lines drawn are much longer spanning beyond the pial surface and into the white matter than the area of interest (layers I-VI) so when doing the calculation of individual layers, there would be a boundary on either side of the grey matter. Any data outside the grey matter area of interest was

not included in the final calculations. The μCi/g was then measured by averaging the signal from three lines of the same width and approximate length. The counting box area, view under the microscope, is approximately 1,900,000 pixels. Each large circle is approximately 962 pixels and each small circles is approximately 177 pixels.

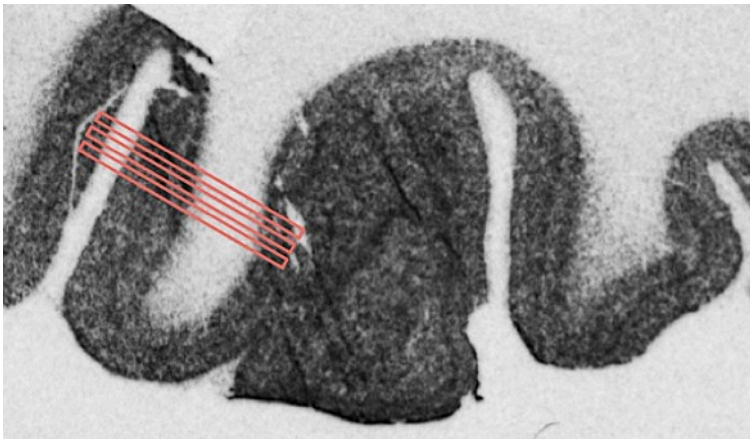

Figure 5.1: An example of placement of lines for lamina analysis placed in the DLPFC (BA46) for quantification of optical density. White matter was used to show where the boundaries of the grey matter was using Excel because the signal was approximately zero. Only one area was used because Professor Cyndi Shannon Weickert and Alice Rothwell concluded this cytoarchitecture of the area was correct prior to the start of my thesis work.

Excel

Next, the raw data density was copied into excel. A previously developed macro program [231] was used. Adjustments were made to best fit the data to the common cortical width. It was important not to "overfit" the data and it was important to compare the results to the picture of the brain section. The layers were then lined up, based on the percentage area assigned by Rajkowska 1995.[58]

Data Analysis

Kolmogorov-Smirnov test of normality was used to check if we should use parametric or non-parametric statistics. Two-way ANCOVAs were used to examine mRNA expression levels across laminar between schizophrenia patients compared to controls. One-way ANCOVAs were completed to examine the expression level on a layer-to-layer basis between schizophrenia patients and controls. Correlations were completed to examine how diagnostic data, along with demographics affected the mRNA expression levels per cortical layer.

Results

Film Analysis for NMDAR NR1 mRNA Expression Levels

NMDAR NR1 mRNA was located throughout most of the grey matter in the DLPFC in the cortical layers II, III, IV, V, and VI, seen in Figure 5.2.

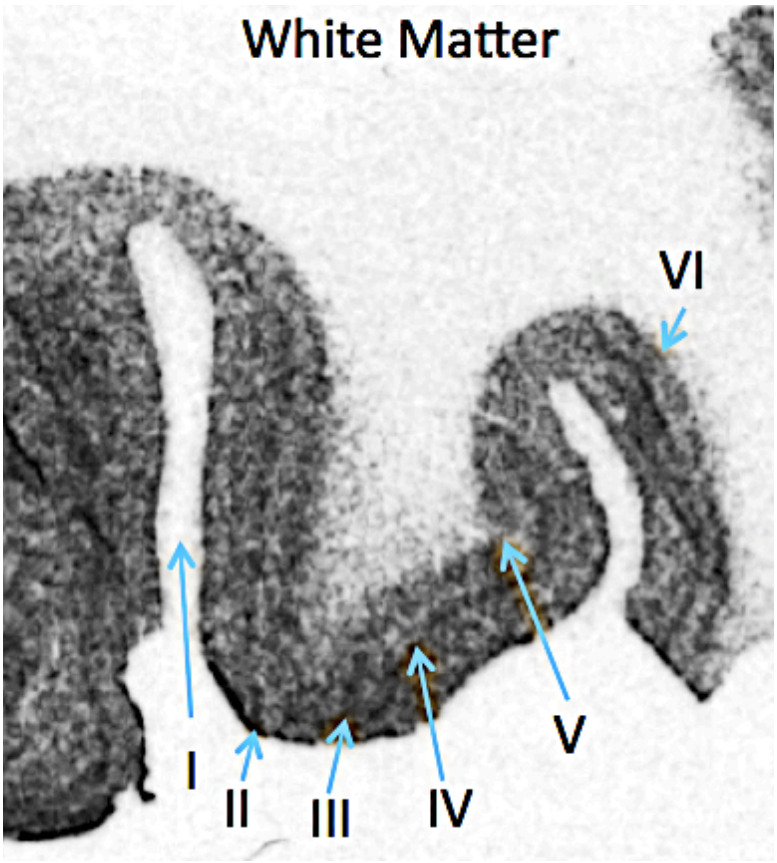

Figure 5.2: Shows the different cortical layers in the DLPFC and their NMDAR NR1 mRNA expression.

Laminar analysis was completed by looking at layers II, III, IV, V, VI and the sum of these layers in the DLPFC of post-mortem human brain tissue. After exploring the cortical layers, I found that when looking at the patient and control groups separately, the NMDAR NR1 mRNA levels from the film based analysis were normally distributed using Kolmogorov-Smirnov test of normality ($p>0.092$), thus enabling the use of parametric statistics. I found that NMDAR NR1 mRNA levels in each layer correlated $p<.001$ with one another, data seen in Table 5.1.

Table 5.1: Correlations between each layer of BA46 region in the TRC total cohort.

	Layer II	Layer III	Layer IV	Layer V	Layer VI
Layer II		r=.788, p=0.000	r=.681, p=0.000	r=.678, p=0.000	r=.624, p=0.000
Layer III	r=.786, p=0.000		r=.913, p=0.000	r=.786, p=0.000	r=.807, p=0.000
Layer IV	r=.681, p=0.000	r=.931, p=0.000		r=.800, p=0.000	r=.844, p=0.000
Layer V	r=.678, p=0.000	r=.786, p=0.000	r=.800, p=0.000		r=.830, p=0.000
Layer VI	r=.624, p=0.000	r=.807, p=0.000	r=.844, p=0.000	r=.830, p=0.000	

Because of this reason, and to reduce the number of statistical tests required, the expressions across layers were summed prior to exploring the relationship between NR1 expression and demographic and clinical variables using film analysis. After combining the data, it was found that when looking at the full cohort, it was normally distributed using Kolmogorov-Smirnov test of normality ($D(69)=.081$, $p>0.200$). The data for the controls alone ($D(34)=.118$, $p>0.200$), and for patients with schizophrenia ($D(35)=.097$, $p>0.200$) were normally distributed as well so parametric tests were utilised, except for looking at medication effects, when Spearman correlations were done because data for the amount of medication was not normally distributed.

Statistical Analysis

For the laminar film analysis, no differences were seen in NMDAR NR1 mRNA expression levels across laminar between schizophrenia patients compared to controls doing a 2-way ANCOVA, co-varying for age and pH (diagnosis $F= 1.934$, $p=0.165$, $df=1$, with a significant difference according to cortical laminar between layers $F= 9.079$, $p<0.001$, $df=5$, but no interaction effect between layers and diagnosis: $F=.247$, $p=0.941$, $df=5$), seen in Figure 5.3. The sum of the laminar layers is seen in Figure 5.4.

By doing a Tukey post-hoc test on an ANOVA, since using SPSS post-hoc tests cannot be completed on ANCOVAs, there were significant differences between

layer II and layer VI (0.1152±0.02601,p=.000), layer III and layer VI (0.0818±0.02601, p=.002), layer IV and layer VI (0.1318±0.02610, p=.000), and layer V and layer VI (0.1007±0.02610, p=.000). All other data are not shown.

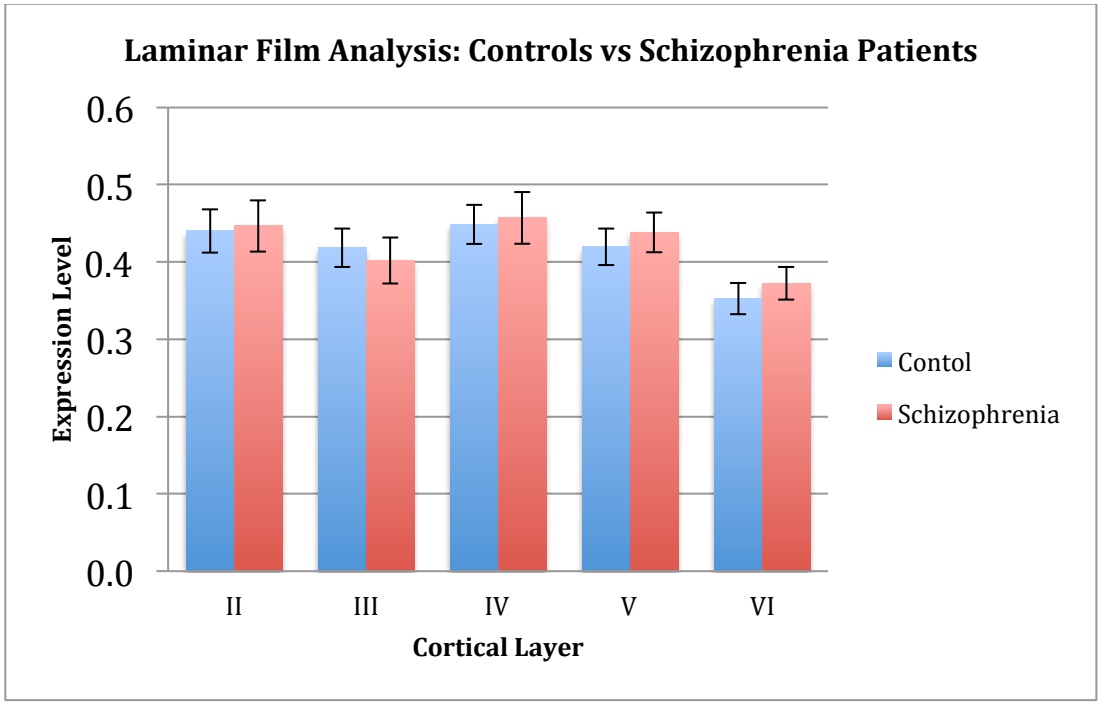

Figure 5.3: Mean comparison between schizophrenia patients and controls for NMDAR NR1 mRNA in the expression across laminar layers II, III, IV, V, and VI. Error bars indicate the standard error.

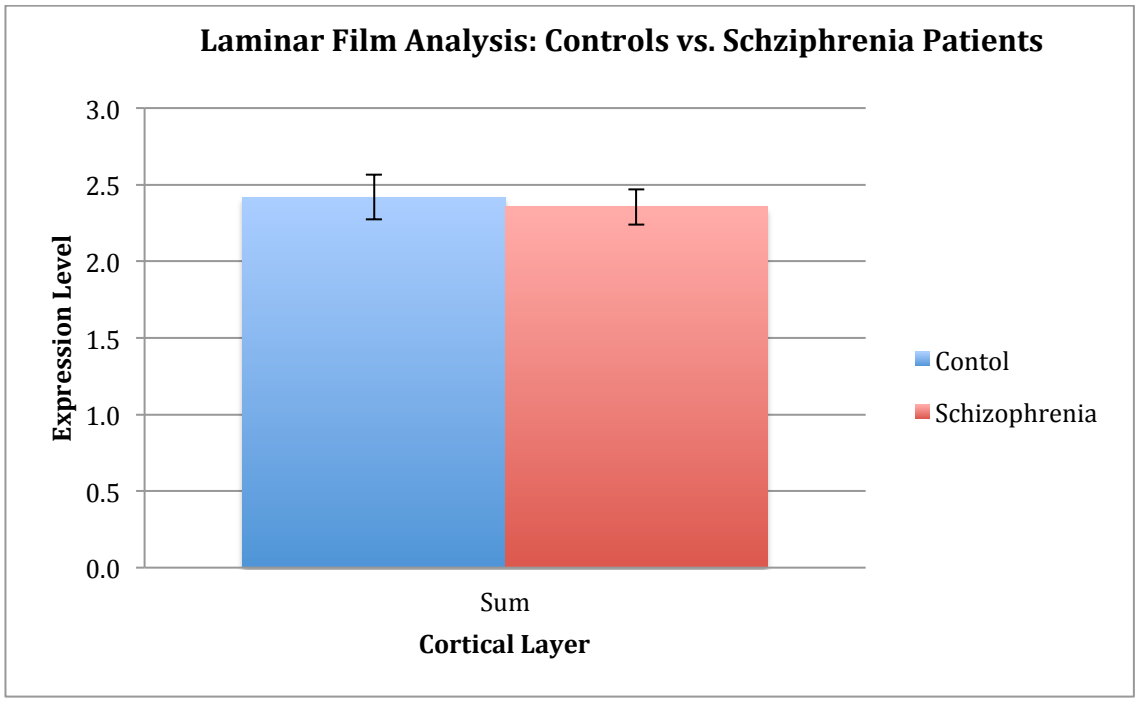

Figure 5.4: Comparison between schizophrenia patients and controls for NMDAR NR1 mRNA in the expression for the sum of all laminar layers. Error bars indicate the standard error.

To confirm that there was no significant diagnostic difference in the level of NMDAR NR1 mRNA, I used separate 1-way ANCOVAs to examine the expression level on a layer-to-layer basis between schizophrenia patients and controls, co-varying for age and pH. Again, there was no difference found in the NMDAR NR1 mRNA levels in any cortical layer examined: for layer II ($F=0.026$, $df=1, 72$, $p=0.872$), layer III ($F=0.076$, $df=1, 72$, $p=0.784$), layer IV ($F=0.542$, $df=1, 72$, $p=0.464$), layer V ($F=0.691$, $df=1, 72$, $p=0.409$), and VI ($F=1.671$, $df=1, 72$, $p=0.201$). This is shown in Figure 5.5.

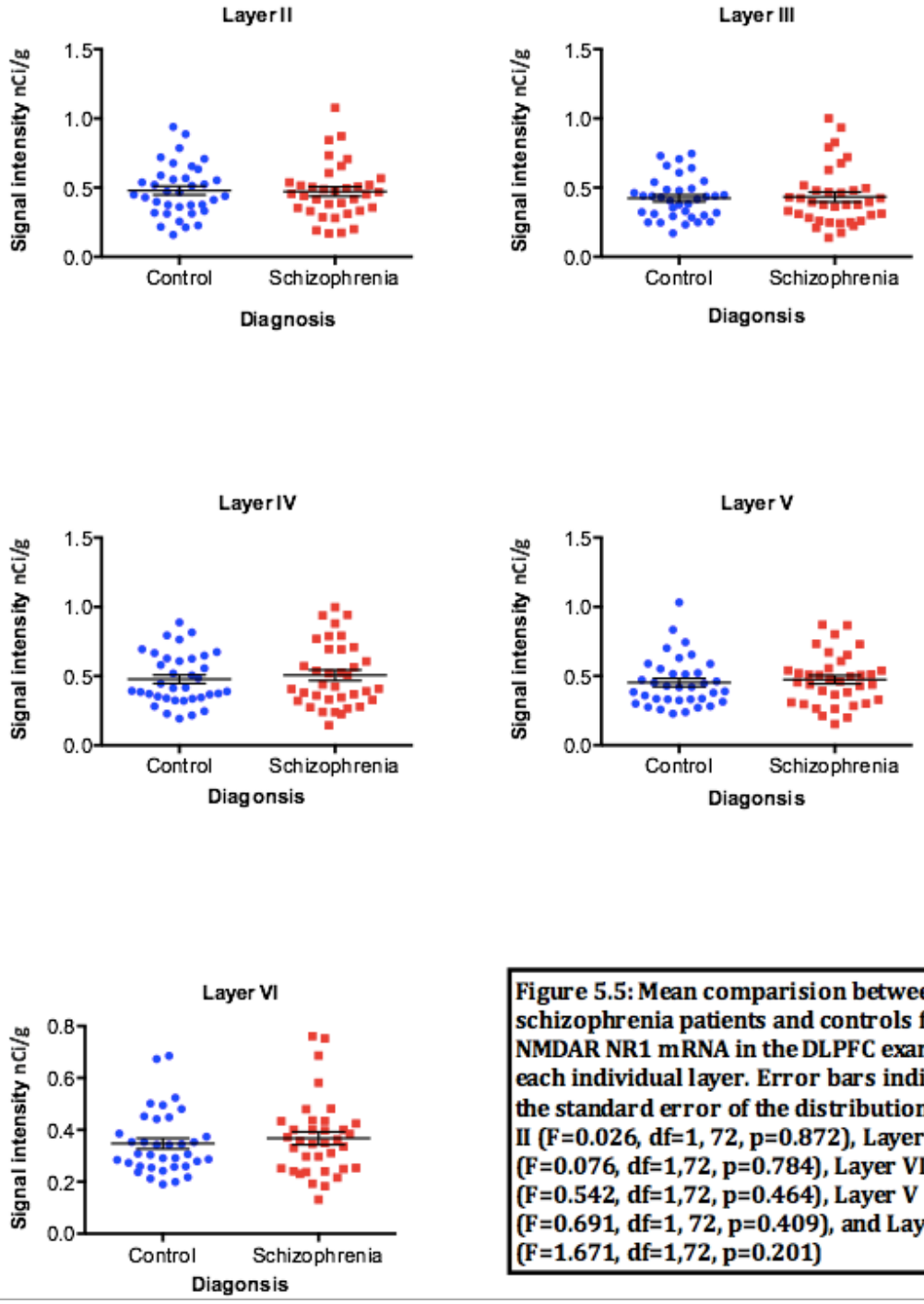

Figure 5.5: Mean comparision between schizophrenia patients and controls for NMDAR NR1 mRNA in the DLPFC examining each individual layer. Error bars indicate the standard error of the distribution. Layer II (F=0.026, df=1, 72, p=0.872), Layer III (F=0.076, df=1,72, p=0.784), Layer VI (F=0.542, df=1,72, p=0.464), Layer V (F=0.691, df=1, 72, p=0.409), and Layer VI (F=1.671, df=1,72, p=0.201)

The averages for control individuals when looking at specific layers examining the signal intensity are as follows: layer II- 0.480±0.031, layer III- 0.423±0.025, layer IV- 0.478±0.031, layer V- 0.453±0.030, and layer VI- 0.347±0.020 (Seen in Figure 5.5). The averages for schizophrenia patients when

looking at specific layers examining the signal intensity are as follows: layer II- 0.471±0.034, layer III- 0.433±0.0352, layer IV- 0.507±0.038, layer V- 0.474±0.031, and layer VI- 0.368±0.025 (Seen in Figure 5.5). Standard error is noted. There was not a statistically significant difference between NR1 mRNA expression in males and females (F=0.071, df=1, 72, p=0.791; nor was there an interaction effect between gender and diagnosis F=2.632, df=1, 72, p=0.110) for the entire cohort. When I took closer look at 2-way ANCOVAs with gender and diagnosis taken into account, I saw that there was a trend towards an interaction in layer IV (film based)(F=3.566, df=1, 72, p=0.064), and VI (F=3.369, df=1, 72, p=0.071). Upon exploring further by looking at graph and running the analysis on the gender split cohort, males with schizophrenia were shown to have trends towards having significantly higher NMDAR NR1 mRNA levels compared to males without schizophrenia in layer IV (F=3.069, df=1, 72, p=0.087), and layer VI (F=3.978, df=1, 72, p=0.052). This is against my hypothesis; however, the schizophrenia females had lower mRNA levels compared to female controls in layer IV (F=2.860, df=1, 72, p=0.110), and layer VI (F=1.105, df=1, 72, p=0.309), though the results did not reach statistical significance. This is possibly due to a power issue, as there relatively few female controls (n=7) and patients (n=13). Calculation of effect sizes based on the F-values indicate that the decrease in NR1 mRNA is of a medium (d=0.47) to large (d=0.76) effect size, depending on which layer is analysed. Power calculations indicate that samples sizes of 23 (layer IV) to 57 (layer VI) women per group would be required to have 80% power to reach statistical significance. This finding is potentially important and it should be considered that I needed to examine NMDAR NR1 mRNA tissue from more women.

There was not a statistically significant difference between NR1 mRNA expression across left and right hemisphere using a 2-way ANCOVA for the sum of all layers (F=0.0.494, df=1, 72, p=0.485), but there was a trend for an interaction effect (F=3.034, df=1, 72, p=0.086) for the entire cohort, with non-significant increased expression in schizophrenia patients relative to controls in the left hemisphere (F=2.770, df=1, 72, p=0.107) and decreased expression in schizophrenia patients relative to controls in the right hemisphere (F=0.807, df=1, 72, p=0.375). This was between hemisphere diagnosis in a significant interaction of NMDAR NR1 mRNA levels effect for layer II (F=4.319, df=1, 72, p=0.042), layer V (F=4.512, df=1, 72, p=0.038) and layer VI (F=4.102, df=1, 72, p=0.047), as well as trends for interaction in layer III (F=2.826, df=1, 72, p=0.098) and layer IV (F=3.759, df=1, 72, p=0.057). In layer V of the left hemisphere, patients with schizophrenia had significantly higher levels of NR1 than controls (F=4.610, df=1, 72, p=0.040) and in layer VI (F4.679, df=1, 72, p=0.039). All other post-hoc tests for diagnostic changes within hemisphere did not reach statistical significance.

There was not a statistically significant effect of being a smoker, non-smoker and never-smoker, unlike in protein, on NR1 expression in a 2-way ANCOVA (Smoking status: F=0.207, df=2, p=0.814; Diagnostic status: F=0.636, df=1, p=0.429; Interaction effect: F=0.340, df=1, p=0.563). Similar absence of effect was observed in individual cortical layers (data not shown).

There was no significant difference in the sum of NR1 expression levels across cortical layers between schizophrenia patients who died by suicide and those who did not (F=1.054 df=1, p=0.308).

In the total cohort, it was found that pH in the DLPFC correlated positively with the sum of the overall mRNA expression in μCi/g in BA46 (r=.337, p=0.004,

n=73). This was replicated in the control group (r=.437, p=0.007, n=37) and the schizophrenia group (r=0.377, p=0.023, n=36) when analysed separately.

There was a positive correlation with brain weight and overall NR1 mRNA expression (r=.231, p=0.049, n=73), and a positive trend for the correlation between brain volume and NR1 mRNA levels was found (r=.212, p=0.072, n=73) in the total cohort. In the schizophrenia group, there was a positive correlation between NR1 mRNA expression and brain volume (r=.362, p=0.030, n=36) and a trend towards a positive correlation of NR1 mRNA with brain weight (r=.319, p=0.056, n=36). Also, correlations between each layer and age, pH, and brain weight were analysed for the full cohort, seen in Table 5.2. Statistically significantly negative correlations were found between age and NMDAR NR1 mRNA in cortical layer II (r= -0.295, p=0.011, n=73), layer III (r=-0.279, p=0.017, n=73), and layer IV (r=-.236, p=0.044, n=73). For pH, significant positive correlations were seen in layer III (r=0.353, p=0.002, n=73), layer IV (r=0.383, p=0.001, n=73), layer V (r=0.388, p=0.001, n=73), and layer VI (r=0.316, p=0.007, n=73), as well as a positive trend for layer II (r=0.215, p=0.068, n=73). Finally, for brain weight, significant positive correlations were seen for layer III (r=0.206, p=0.027, n=73) and layer IV (r=0.287, p=0.014, n=73), along with a positive trend for layer II (r=0.209, p=0.068, n=73) and layer V (r=0.204, p=0.082, n=73).

Table 5.2: Demographics (age, pH, and brain weight) correlated with NR1 mRNA in layers II, III, IV, V, and VI in the total cohort. ***p<0.001,**p<0.01, *p<0.05, #p<0.10, which statistically significant correlations are bolded.

Full Cohort	Layer II	Layer III	Layer IV	Layer V	Layer VI
Age	**r= -0.295* p= 0.011 n= 73**	**r= -0.279* p= 0.017 n= 73**	**r= -0.236* p= 0.044 n= 73**	r= -0.184 p= 0.119 n= 73	r= -0.105 p= 0.377 n= 73
Brain pH	r= 0.215# p= 0.068 n= 73	r= 0.353** p= 0.002 n= 73	r= 0.383*** p = 0.001 n= 73	**r= 0.388*** p= 0.001 n= 73**	**r= 0.316** p= 0.007 n= 73**
Brain Weight	r= 0.209# p= 0.079 n= 73	**r= 0.206* p= 0.027 n= 73**	**r= 0.287* p= 0.014 n= 73**	r= 0.204# p= 0.083 n= 73	r= 0.172 p= 0.146 n= 73

When splitting up the correlation by diagnosis, statistical significance was still seen in pH and brain weight for schizophrenia patients, and for age in the control group, shown in Tables 5.3 and 5.4 respectively. For the schizophrenia group, it was seen that there was a positive correlation with pH in layer IV (r=0.350, p=0.034, n=37) and layer V (r=0.413, p=0.011, n=37), along with a positive trend in layer III (r=0.285, p=0.087, n=37). For brain weight in the schizophrenia group, there was a positive significant correlation in layer IV (r=0.358, p=0.030, n=37) and layer V (r=0.338, p=0.041, n=37), and a positive trend for layer III (r=0.277, p=0.097, n=37) and layer VI (r=0.295, p=0.076, n=37).

Table 5.3: Demographics (pH, and brain weight) correlated with NR1 mRNA in layers II, III, IV, V, and VI in the schizophrenia diagnostic group. *p<0.05, #p<0.10, which statistically significant correlations are bolded.

Schizophrenia	Layer II	Layer III	Layer IV	Layer V	Layer VI
Brain pH	r= 0.112 p= 0.510 n= 37	r= 0.285# p= 0.087 n= 37	**r= 0.350* p= 0.034 n= 37**	**r= 0.413* p= 0.011 n= 37**	r= 0.230 p= 0.171 n= 37
Brain Weight	r= 0.197 p= 0.242 n= 37	r= 0.277# p= 0.097 n= 37	**r= 0.358* p= 0.030 n= 37**	**r= 0.338* p= 0.041 n= 37**	r= 0.295# p= 0.076 n= 37

In the control group alone, there was a negative correlation between age and NR1 mRNA in layer II (r=-0.497, p=0.002, n=36) and layer III (r=-0.361, p=0.026, n=36). For pH, there was a positive correlation in all five layers: layer II (r=0.438, p=0.008, n=36), layer III (r=0.468, p=0.004, n=36), layer IV (r=0.453, p=0.006, n=36), layer V (r=0.370, p=0.026, n=36), and layer VI (r=0.415, p=0.012, n=36).

Table 5.4: Demographics (age, pH, and brain weight) correlated with NR1 mRNA in layers II, III, IV, V, and VI in the control group. **p<0.01, *p<0.05, #p<0.10

Control	Layer II	Layer III	Layer IV	Layer V	Layer VI
Age	**r=-0.497 ** p= 0.002 n= 36**	**r= -0.361* p= 0.026 n= 36**	r= -.216 p= 0.125 n= 36	r= -0.204 p= 0.233 n= 36	r= -.115 p= 0.367 n= 36
Brain pH	**r= 0.438 ** p= 0.008 n= 36**	**r= 0.468 ** p= 0.004 n= 36**	**r= 0.453 ** p= 0.006 n= 36**	**r= 0.370 * p= 0.026 n= 36**	**r= 0.415 * p= 0.012 n= 36**
Brain Weight	r= 0.283 # p= 0.094 n= 36	r= 0.287 # p= 0.090 n= 36	r= 0.208 p= 0.224 n= 36	r= 0.061 p= 0.724 n= 36	r= 0.031 p= 0.860 n= 36

Next, correlations were completed looking at NR1 mRNA with age of onset, duration of illness, and antipsychotic drug history (lifetime and mean dosage). The correlations are in Table 5.5 below. The only significant data that was found was for the duration of illness in layer II. (r= -0.344, p=0.037, n=37).

Table 5.5: Correlations examining age of onset, duration of illness, and lifetime, low, high, and mean dosage of antipsychotic medication was correlated with NR1 mRNA in layers II, III, IV, V, and VI in the schizophrenia patients group. *p<0.05

Schizophrenia	Layer II	Layer III	Layer IV	Layer V	Layer VI
Age of onset	r=0.111 p= 0.513 n= 37	r=0.179 p= 0.288 n= 37	r= .211 p= 0.210 n= 37	r= .189 p= 0.262 n= 37	r= .177 p= 0.106 n= 37
Duration of Illness	**r= -0.344*** **p= 0.037** **n= 37**	r=-0.272 p= 0.103 n= 37	r= -0.291 p= 0.081 n= 37	r= -0.164 p= 0.333 n= 37	r= -0.074 p= 0.188 n= 37
CPZ Lifetime	r= -0.059 p= 0.730 n= 37	r= -0.099 p= 0.560 n= 37	r= -0.126 p= 0.456 n= 37	r= 0.003 p= 0.988 n= 37	r= 0.054 p= 0.750 n= 37
CPZ Low	r= -0.055 p= 0.745 n= 37	r= 0.017 p= 0.920 n= 37	r= 0.106 p= 0.533 n= 37	r= 0.116 p= 0.494 n= 37	r= -0.031 p= 0.919 n= 37
CPZ High	r= 0.129 p= 0.455 n= 37	r= 0.040 p= 0.815 n= 37	r= 0.024 p= 0.886 n= 37	r= 0.089 p= 0.599 n= 37	r= 0.145 p= 0.393 n= 37
CPZ Mean	r= 0.185 p= 0.272 n= 37	r= 0.090 p= 0.596 n= 37	r= 0.077 p= 0.659 n= 37	r= 0.155 p= 0.259 n= 37	r= 0.152 p= 0.368 n= 37

Discussion

Lamina-specific abnormalities in ionotropic receptors have been examined in previous studies [91,232]. From this study, I showed that there are significant changes in the expression of the NMDAR subunits in the DLPFC in mRNA between schizophrenia and control groups.

From the above data, it can be seen that the lower level NR1 mRNA appears to be related to smaller brain weight particularly in people with schizophrenia and particularly in layers IV and V. This could be due to tissue damage over time because of neurological malfunctions. When just focusing on neurons and the NMDAR, seen in Figure 5.6, I believe something interesting could be occurring.

Contrary to my hypothesis, I found no overall change in the amount of NMDAR NR1 mRNA in the lamina analysis seen in the total group. However, when looking at the PSD proteins in the total group, tying in previous chapters, a decrease was seen. I believe the while similar amount of NMDAR NR1 mRNA is being made overall, something posttranscriptional may be malfunctioning, not allowing the receptors to be brought from areas of synthesis within the neurons to the PSD. There are three ways of looking at this data: 1) there could be problems with RNA translation, 2) difficulties with NMDA receptor complex assembly, glycosylation and trafficking from the Golgi apparatus and endoplasmic reticulum, or 3) decreased insertion of NMDAR into the PSD via vesicles or increased endocytosis or decreased lateral diffusion from extra-synaptic membrane to the PSD. Data previously published suggest total NMDA NR1 protein and mRNA is slightly but significantly decreased in homogenate[117], this supports that issues with mRNA synthesis may exist overall but can also combine with alterations at other steps of NMDAR production, such as trafficking and localisation, to produce abnormalities.

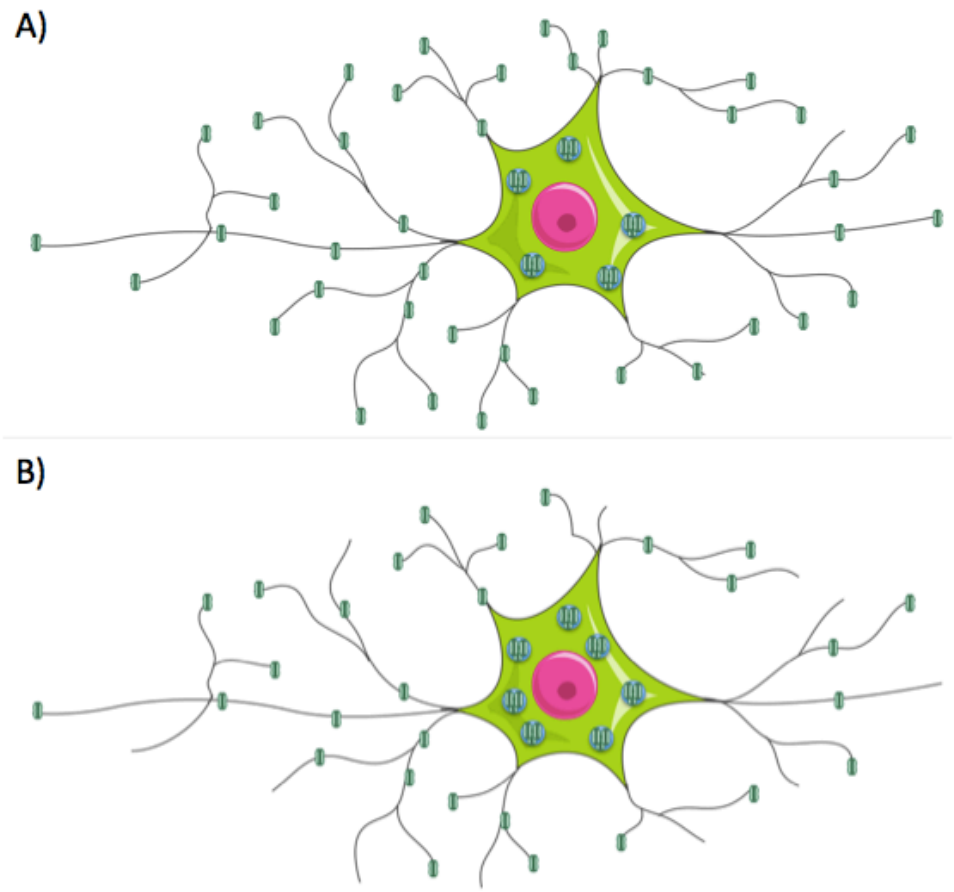

Figure 5.6: Two neurons are seen with the NMDARs, teal receptors. A) A neuron in a normal healthy control. B) A neuron in schizophrenia patients. Functional NMDARs are thought to be limited to outer regions of the neuron, the PSD. But, NMDAR can actually be found within neurons as well. It is possible that overall there is no change in the amount of NMDARs, but fewer where it is usable, at the synapse. The extras are in the soma and are not being trafficked out to the synapse to be used.

Also, there are two possible explanations for the smaller brain size relating to lower NMDAR mRNA in schizophrenia patients, which can be seen in a previous meta-analysis study[233]. Firstly, there may be lower NMDAR levels, particular in the interneuronally enriched layer IV, which could result in less glutamate excitability of interneurons and thus the inhibitory neurons would fire less. Also, perhaps the NMDARs are firing for less time leading to a decrease in the release of GABA, the

main inhibitory neurotransmitter, in the cortex. This would relate to more cortical excitation, or hyperfunction, which has been studied recently by Moghaddam[220]. It has been shown that NMDAR blockade causes increased glutamate, not decreased glutamate as once thought. One hypothesis is that NMDAR blockade could cause transient increases in cortical glutamate and perhaps increases in NMDAR in some patients, however this increased glutamate could cause excitotoxcity and tissue damage over time, leading to less brain weight. Secondly, my finding of decreased brain size could be due to the fact that females with schizophrenia tended to have less NMDAR NR1 mRNA particularly in layer IV, as seen in a prior study. [234] Maybe this decrease, along with other potential differences between schizophrenia and controls, could be due to specific neuron types malfunctioning in some way.

To potentially clear up changes in gender and hemisphere, along with figuring out if a specific layer has more to do with a diagnosis of schizophrenia, I next examined individual neurons of specific types: interneurons and pyramidal neurons. Silver grain analysis looks at individual cells' mRNA to observe what is occurring at a cellular level. I tested this because the failure to find a clear decrease in NMDAR NR1 mRNA in my laminar film analysis could be caused by a higher density of NMDAR NR1 expressing cells in schizophrenia patients due to cortical thinning even though there may still be less NMDAR NR1/cell. Indeed, it has been reported in a different cohort that there is an increase in neuronal density in the PFC of people with schizophrenia thought to result from a cortical thinning as detected by structural MRI scan and/or loss of neuropil[60]. The interneurons and pyramidal neurons were analysed as discussed in chapter six.

Chapter 6: Silver Grain Assessment of NMDAR NR1 mRNA in Interneurons and Pyramidal Neurons

Introduction:

Silver grain analysis involves examining mRNA being produced by specific cells, in this case specifically interneurons and pyramidal neurons. The more silver grains, or positive hybridisation signal, there is the more mRNA is being expressed by that particular cell [235]. So, simplistically, the more silver grains seen, the more mRNA is available within that cell. Interneurons and pyramidal neurons both transcribe GRIN1 producing GRIN1 or NMDAR mRNA.

In schizophrenia, I postulate there is a problem with either hypofunction or hyperfunction of the glutamatergic receptor NMDAR. Reduced NMDAR in the interneurons would suggest that schizophrenia is caused by a hyperglutamatergic system, whereas if the pyramidal neurons were a source of reduced NMDAR in schizophrenia, the system that is being examined may be a hypoglutamatergic system or underactive pyramidal neurons. By doing silver grain analysis, individual cells can be studied and analysed to see whether interneurons or pyramidal neurons or both play a role in the glutamatergic functioning in the NMDAR NR1 subunit mRNA.

The next logical step of studying specific mRNA expression levels in both interneurons and pyramidal neurons in my thesis work was done to determine if there is a cellular source causing the NMDAR NR1 change. Although silver grain analysis is not specifically examining what is occurring to NMDAR subunit at the PSD, this could provide unambiguous details of what is occurring in specific types of cortical neurons themselves. I wanted to confirm the deficit in mRNA expression that our laboratory found previously[194] by more thoroughly investigating the

cortical laminar and cellular expression of NR1 mRNA using in situ hybridisation seeing which neuron type causes this deficit. In a Molecular Psychiatry paper from 2003, it was noted that examining both film analysis and cell specific analysis, as I did, differences between the control group and the schizophrenia group that were not detectable from film-based analysis were found by carefully observing specific neurons at the cellular level[236]. This may be because the film-based measures relies on density and since neuronal density can be increased in the brains of patients with schizophrenia deficits on a per neuron basis are harder to detect with analysis of film.

The aim of this chapter is to examine if the amount of mRNA for the NMDAR NR1 subunit differs between schizophrenia patients and controls. To do this, in situ hybridisation was completed to look at the density of silver grains being produced by pyramidal neurons and interneurons in BA46. It is hypothesised that the GRIN1 mRNA in the pyramidal neurons or interneurons in schizophrenia patients will be changed causing an imbalance between inhibitory and excitatory neurons.

Methods

The in situ hybridisation was completed prior to my arrival in the laboratory by Dr Samantha Fung and Ms Shan Yuan-Tsai. Appendix 2 discusses the method that was used.

In situ hybridisation silver grain analysis:

Stereo Investigator:

Silver grain analysis was completed using Stereo Investigator version 8.27, 32-bit program. Under low power, the slide was scanned to find the area of interest, which was indicated by pre-marked boxes. The boxes were drawn on the slides based on Nissl-stained images, in BA46 was located using the

cytoarchitecture of the brain, completed by Professor Cyndi Shannon Weickert and Ms Alice Rothwell prior to my thesis work.

A measurement of the width of the cortex was performed, to determine if there is an increase or decrease in cortex thickness between schizophrenia patients and controls and to confirm that the correct layer was being sampled from. The cortical distance varied greatly between slides and parts of individual brain sections. The cortical width was measured three times and averaged and then the approximate position of the cortical layer of interest was calculated: layer II- 10-20% from the pial surface, layer III- 20-46% from the pial surface, and layer V- 54-70% from the pial surface [58]. From these estimates, and after confirming the appropriateness of the cytoarchitecture within each layer, photos were taken at 200x, generally three photos for each layer.

ImageJ:

Photos were opened using Image J (version 1.44o, 32-bit) with the Lipschitz filter plug-in installed from the internet: <http://rsbweb.nih.gov/ij/plugins/lipschitz/index.html>.

The Lipschitz filter allows the coloured picture to be converted into black and white with only the silver grains being shown in black. This is completed by turning the photo of interest in to the equivalent photo in a grayscale image, then uses an algorithm programed into this plugin to allow the black and white image to be made.This allows each silver grain, in the image, to be measured and calculated with no interference of background colour.

Cell counts and nuclear diameter measurements

Next, I measured the scale bar to enable measurement of the size of the nuclei of cells that were being analysed. Since the pyramidal neuron nuclei were

larger than interneuron nuclei, and the interneuron nuclei were larger than glia nuclei, this was one way to differentiate between the cell types. The density of glial cells, interneurons and pyramidal cells were counted in each analysed image. All cells in the image were counted excluding those whose nuclei touched the top and left boundary. This was done to correct for over-counting cells in two dementsionswhen taking density measurements, consistantly capture only half of the cells which were going off the image. Next, nuclear diameters of 10 glial cells, 10 interneurons, and 10 pyramidal neurons were measured to ensure that the correct cells were being counted within each grouping of cells[237].

Silver grain counts

An analysis of silver grains was completed on a subset of slides selected using our laboratory's previous qPCR data on NMDAR NR1 mRNA levels. I choose 10 slides from schizophrenia patients with the lowest expression of NR1 and their matched controls to analyse layer III. The full cohort was included while examining layers II and V. When counting the number of silver grains per cell for pyramidal cells and interneurons, all neurons in the field of view were encircled and measured. The measurement circles were corrected for size of the neuron of interest (either 15μm for interneurons or 35μm for pyramidal cells). These sizes were chosen based on known human neuron sizes[224]. A background count of five circles of each size was performed. The Lipschitz filter was used, along with the "Top down" and "Top hat" options with the slope set to 10.00, and the image then changed into "Binary". These changes to the image adjusted the contrast to a black and white image showing only the silver grains. Next, five individual silver grains were measured by drawing a circle 5μm x 5μm around a single silver grain in order to determine the number of pixels a single silver grain comprised for each slide. By

determining the number of pixels each silver grain was comprised of, it was possible to then extrapolate how many pixels or silver grains were contained within one specific neuron.

Excel:

In the excel file, the lengths of each nuclei type were averaged per sample to give an overall average, along with the how many glia, interneurons and pyramidal neurons per slide there were. Also, the background and silver grain size for each image were averaged. Then the "Cell-Background" for each neuron was calculated, along with the "Area covered", and "Number of silver grains".

Data analysis

Data analysis was completed using IBM SPSS Statistics version 21. Figures were made using Excel for Mac 2011, version 14.3.8, along with Graph Pad Prism 6.0c for Mac OS X. I tested the data for normal distribution, homogeneity of variance, performed correlations between demographics of schizophrenia patients and controls, and ran cell counts and mRNA ANOVAs or ANCOVAs to test for effect of diagnosis, gender, brain weight, and hemisphere, and explored potential confounders like medication. I examined the total amount of expressing interneurons and pyramidal neurons, along with examining grains per interneurons and grains per pyramidal neurons. Correlations were completed to examine the relationship between demographic data and silver grains in pyramidal neurons and interneurons.

Results

Cortical width of BA46

The width of the DLPFC cortex was measured for each individual in the cohort on microscopic Nissl stained slides. The cortical width between the start of

layer I and outer edge of layer VIb in schizophrenia patients (3294.7±477.9μm) and controls (3446.0±840.7μm) were not statistically different (t(69)=-0.772, p=0.447, unpaired independent sample Student's t-tests).

Silver grain analysis of Layer III in BA46

I was not able to detect statistically significant differences in NMDAR NR1 mRNA expression level between schizophrenia patients and controls in layer III neurons based on this pilot experiment. However, based on the experience from analysing this layer, the background and silver grain size measurements were optimised and this modified methodology was then used throughout analysis of layer II and V.

Silver grain analysis of Layer II in BA46

The small difference in size between interneurons and pyramidal neurons in layer II made the two cell types extremely difficult to differentiate using the Nissl stain, but is consistent with layer II being known to have small pyramidal cells. This layer was not further examined.

Silver grain analysis of Layer V in BA46

I chose to focus my analysis on Layer V was of interest because of previous work by Beneyto and Meador-Woodruff[91] who found the greatest decrease in NR1 mRNA expression in layer V of the DLPFC.

Number of cells counted in layer V for schizophrenia patients and controls

I determined the number of cells counted per individual in order to check if there was more cells counted in either diagnostic group. The control group had an average of 186.4±58.9 cells per individual person in total, whereas schizophrenia patients had 202.6±31.4 cells counted per individual in total, shown in Figure 6.1. There was no significant difference between groups in the total number of cells

counted (t(48.48)=1.398, p=0.1685, two-tailed independent sample Student's t-tests). Outliers removed if more than two standard deviations from mean. Although, I noted that there was less variability in the number of cells counted for people with schizophrenia compared to controls.

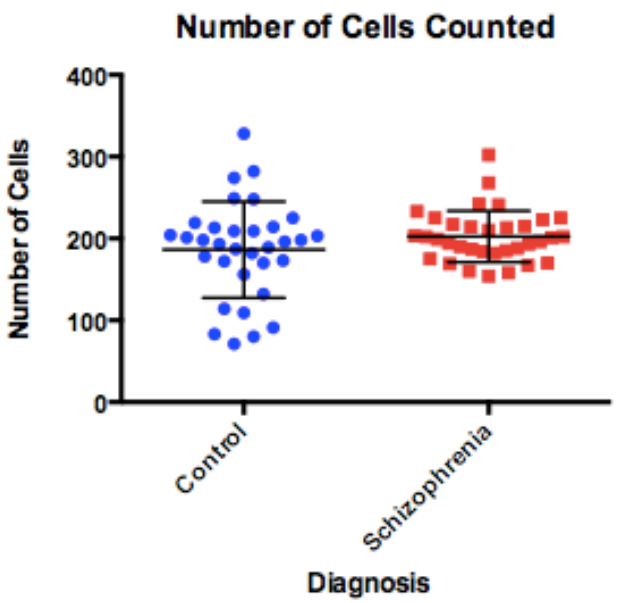

Figure 6.1: Comparing total number of cells per 200x viewing area were counted for individual controls and schizophrenia patients in five separate views. One standard deviation noted by error bars. Outliers removed if more than two standard deviations from mean.

Density of glial cells

The glial cell density was determined to see if there was a difference between diagnostic groups. The glial cell density in the control group was $2.43 \times 10^{-5} \pm 7.04 \times 10^{-6}$ cells/μm^3, whereas schizophrenia patients had a glial cell density of $2.24 \times 10^{-5} \pm 8.60 \times 10^{-6}$ cells/μm^3, seen in Figure 6.2. These densities were not significantly different (t(64.25)=0.976, p=0.3327, two tailed independent sample Student's t-tests). Outliers removed if more than two standard deviations from mean.

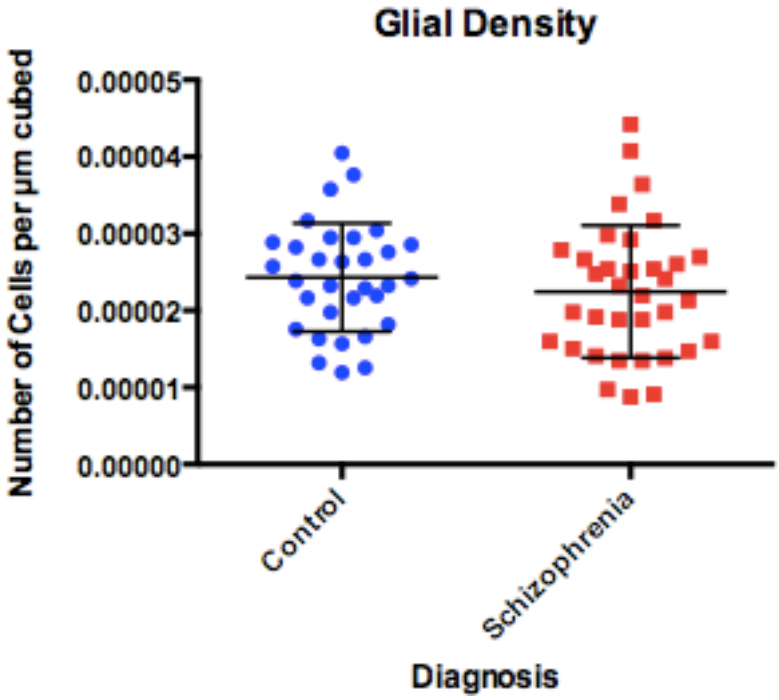

Figure 6.2: Density of glial cells in layer V per µm³. One standard deviation noted by error bars. Outliers removed if more than two standard deviations from mean.

Density of interneurons-like cells

The density of interneurons was next calculated. Controls were found to have an interneuron density of $1.71 \times 10^{-4} \pm 5.14 \times 10^{-5}$ cells/µm³, whereas schizophrenia patients had a density of $1.94 \times 10^{-4} \pm 5.52 \times 10^{-5}$ cells/µm³. This was found to account for approximately 30% of neurons in the cortex. While doing the analysis, seen in Figure 6.3, I noted that schizophrenia patients seem to have a subgroup with a higher density than the groups as a whole. Although not significantly different, there was a trend for schizophrenia patients to have a higher density of small inhibitory–like interneurons ($t(68)=1.728$, $p=0.0887$, two tailed independent sample Student's t-tests). Outliers removed if more than two standard deviations from mean.

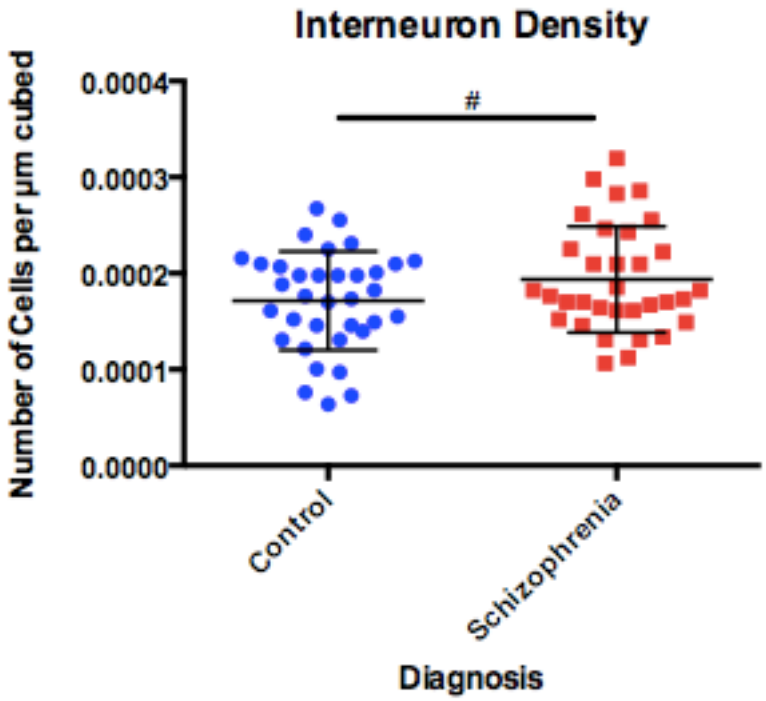

Figure 6.3: Number of interneurons in layer V comparing schizophrenia patients and controls. One standard deviation noted by error bars. Outliers removed if more than two standard deviations from mean. # indicates trend towards significance

Density of pyramidal cells

Pyramidal cell density was also analysed. Control individuals had a mean value of $3.82 \times 10^{-4} \pm 1.10 \times 10^{-4}$ cells/µm^3, whereas schizophrenia patients had $4.08 \times 10^{-4} \pm 5.94 \times 10^{-5}$ cells/µm^3. This was not statistically significant ($t(65)1.203$, $p=0.234$, two tailed independent sample Student's t-tests), shown in Figure 6.4. Outliers removed if more than two standard deviations from mean.

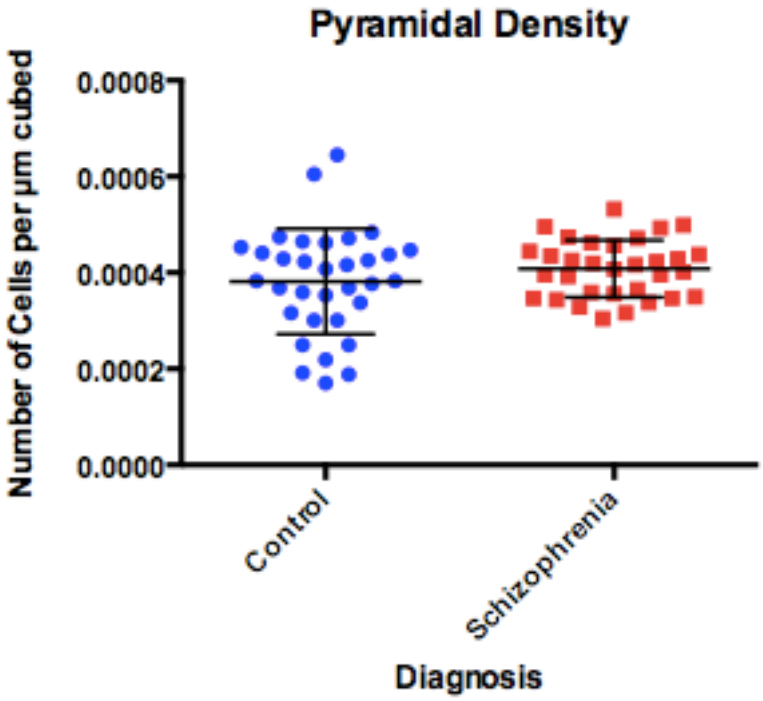

Figure 6.4: The density of pyramidal cells per µm^3 comparing schizophrenia patients and controls. One standard deviation noted by error bars. Outliers removed if more than two standard deviations from mean.

Nuclei size of glial cells, interneurons, and pyramidal neurons

I sought to confirm that the correct nuclei were chosen for each cell type by calculating the average nuclei diameter for each cell type. Each cell type group was distinctly different from one another ($F(2)945.4$, $p<0.0001$) as is clearly evident in Figure 6.5. Post-hoc tests show that glial nuclei were significant smaller than both interneurons and pyramidal cell nuclei ($p<0.0001$) and pyramidal cell nuclei were significantly larger than interneuron nuclei ($p<0.0001$). Outliers removed if more than two standard deviations from mean.

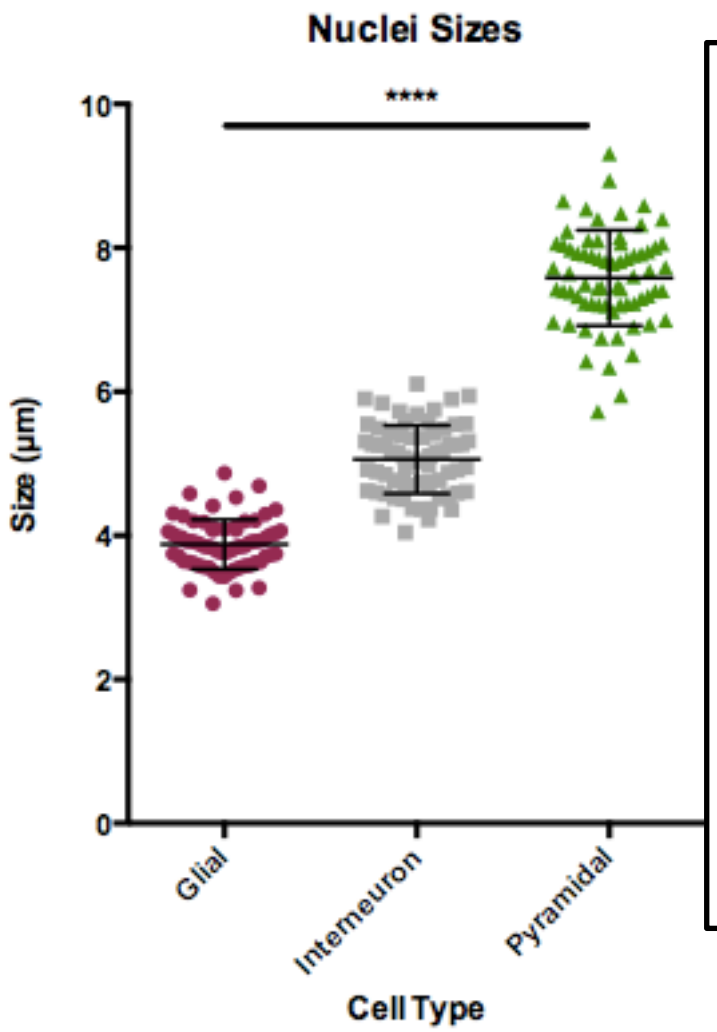

Figure 6.5: Comparing the nuclei sizes of glial cells, interneurons, and pyramidal neurons to see if the correct cells were chosen for each group. One standard deviation noted by error bars. Outliers removed if more than two standard deviations from mean. ****Post-hoc tests indicated glial nuclei were significant smaller than both interneurons and pyramidal cell nuclei ($p<0.0001$) and pyramidal cell nuclei were significantly larger than interneuron nuclei ($p<0.0001$).

Binning for interneurons and pyramidal neurons analysis:

Original binning for interneurons and pyramidal neurons

From my initial inspection of the silver grain data it was clear that the majority of the interneurons had between 0 to 10 silver grains per cell with background levels not exceeding 2 silver grains/circle. So, the interneurons were grouped into 0 to 5, 5 to 10, 10 to 20, 20 to 30, 30 to 40, 40 to 50, 50 to 60, 60 to 70, 70 to 80, 80 to 90, and above 90 silver grains/cell bins. Figure 6.6 shows the original binning of interneurons comparing schizophrenia patients and controls. No statistical difference was seen between patients and controls ($F(1)=0.2552$, $p=0.6482$, column factor).

Pyramidal cells, on the other hand, had mainly between 10 and 80 silver grains per cell and background levels were not more than ten silver grains/circle. Therefore the initial bins were set up as follows: 0 to 5, 5 to 10, 10 to 20, 20 to 30, 30 to 40, 40 to 50, 50 to 60, 60 to 70, 70 to 80, 80 to 90, 90 and above silver grains per cell. Although no statistical difference was seen between patients and controls F=(1)=0.0094, p=0.9229), breaking the groups like this revealed an interesting pattern (see Figure 6.7). While bins between 0 to 10 had no apparent diagnostic difference, bins containing cells with between 10 and 60 silver grains (with a low level of expression) suggested schizophrenia patients had a higher percentage of cells with these levels of silver grains whereas bins containing cells between 60 or more silver grains (with a high level of expression) suggested schizophrenia patients had a lower percentage of cells with these higher levels of silver grains per cells.

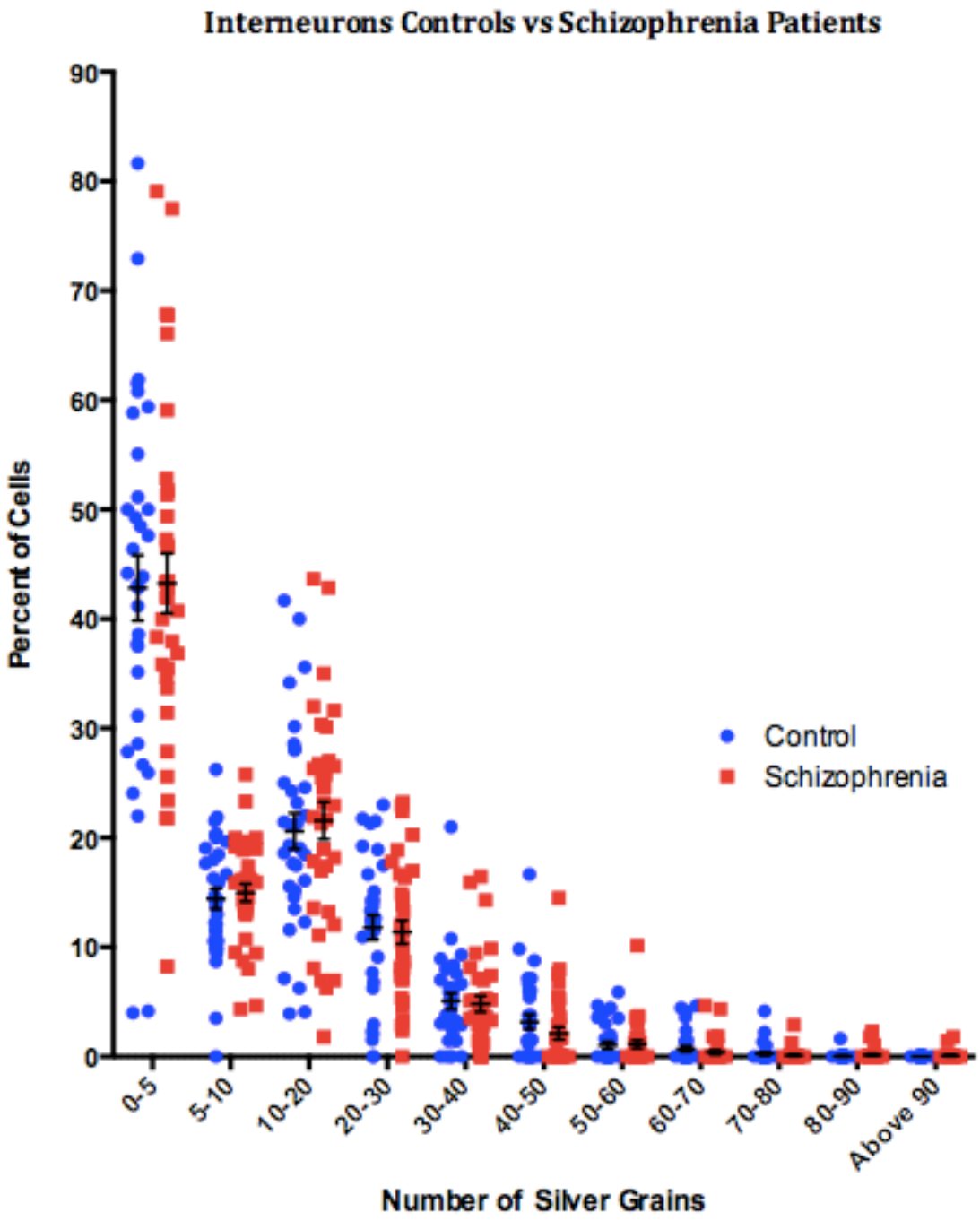

Figure 6.6: Shows the original binning comparing schizophrenia patients and controls. The bins were grouped as follows: 0 to 5, 5 to 10, 10 to 20, 20 to 30, 30 to 40, 40 to 50, 50 to 60, 60 to 70, 70 to 80, 80 to 90, and above 90 silver grains/cell bins. No statistical difference was seen. SEM is noted.

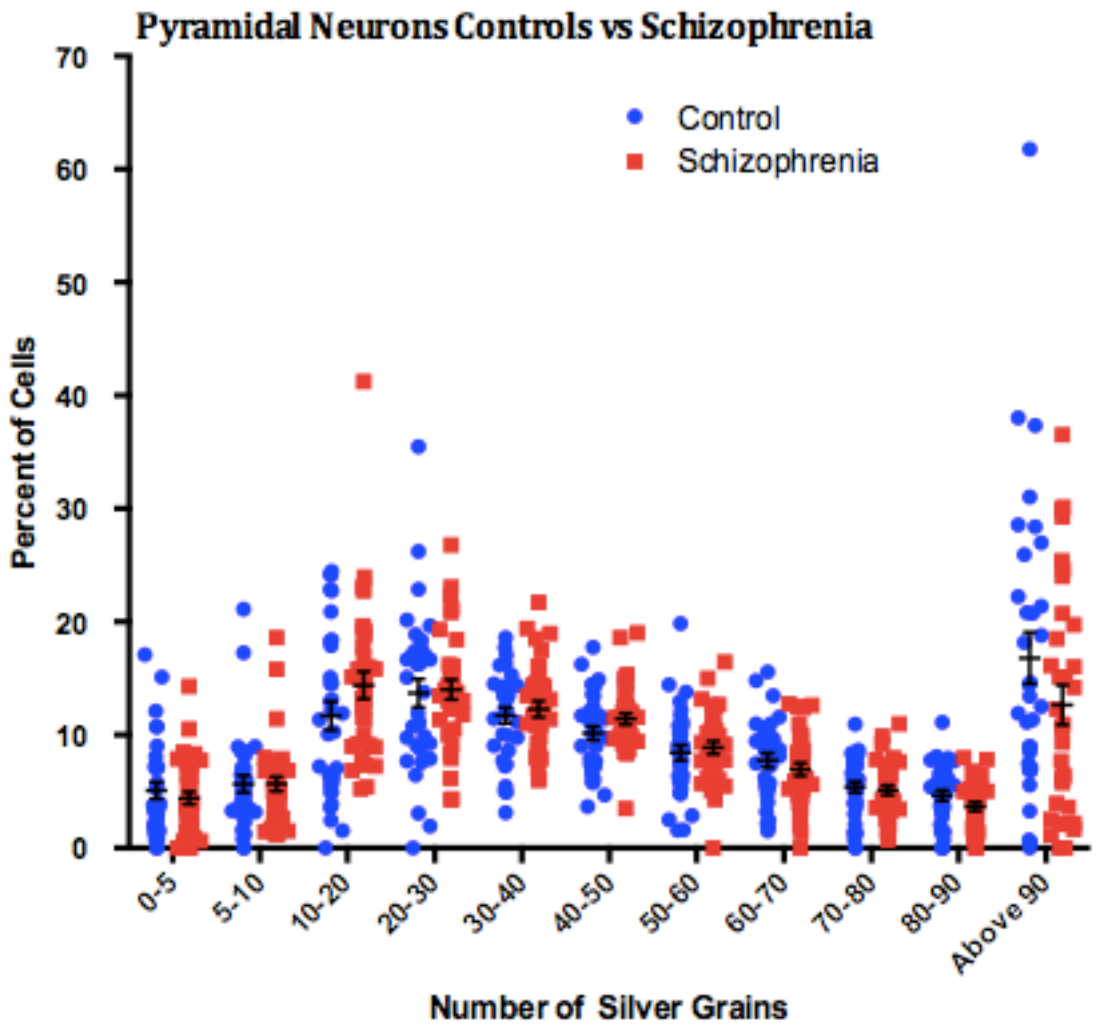

Figure 6.7: The original bins comparing schizophrenia patients and controls were as follows: 0 to 5, 5 to 10, 10 to 20, 20 to 30, 30 to 40, 40 to 50, 50 to 60, 60 to 70, 70 to 80, 80 to 90, 90 and above. No statistical difference was seen. SEM is noted.

Bins separated into no, low, medium, and high expression for interneurons and pyramidal neurons

From the previous data with many bins, the expression level of silver grains were separated into four groups, no, low, medium, and high expressing for both interneurons and pyramidal neurons. Interneurons were separated into 0 to 5 silver grains per cell (no expression), 5 to 10 silver grains per cell (low expression), 10 to 40 silver grains per cell (medium expression), and 40 and above silver grains per cell (high expression).

Correlations for interneurons when looking at grains/cell/expression level and age, pH, RIN, and brain weight in the total cohort are shown in Table 6.1. Note, all tables in this chapter show the r-value, p-value, and n value, respectively from top to bottom in each box, unless otherwise specified. For age, there was a positive correlation and percent of low expressing (r=0.348, p=0.003, n=69) and a negative correlation with percent of high expressing (r=-0.347, p=0.004, n=69) interneurons in schizophrenia patients. For pH, there was a positive correlation with percent of high expressing interneurons (r=0.375, p=0.002, n=67), as well as negative trends for both no expressing (r=-0.237, p=0.057, n=65) and percent of low expressing (r=-0.204, p=0.092, n=69) interneurons. For RIN, there was a positive correlation with percent of high expressing interneurons (0.375, p=0.031, n=67), along with a negative trend with percent of medium expressing interneurons (r=-0.214, p=0.080, n=68).

Table 6.1: Demographics (age, pH, RIN, and brain weight) correlated with the percent of neurons in the no, low, medium (med), and high expressing interneuron category in the total cohort.**p<0.01, *p<0.05, #p<0.1 The data that are significant are bolded.

Full Cohort	No	Low	Med	High
Age	r= 0.071 p= 0.576 n= 65	**r= 0.348 **** **p= 0.003** **n= 69**	r= -0.091 p= 0.462 n= 68	**r= -0.347**** **p= 0.004** **n= 67**
pH	r= -0.237# p= 0.057 n= 65	r= -0.204# p= 0.092 n= 69	r= -0.076 p= 0.536 n= 68	**r= 0.375**** **p= 0.002** **n= 67**
RIN	r= -0.139 p= 0.268 n= 65	r= -0.052 p= 0.673 n= 69	r= -0.214# p= 0.080 n= 68	**r= 0.264*** **p= 0.031** **n= 67**
Brain Weight	r= 0.028 p= 0.824 n= 65	r= -0.143 p= 0.243 n= 69	r= -0.045 p= 0.718 n= 68	r= 0.232# p= 0.059 n=67

For schizophrenia patients, there was a positive correlation with age and number of cells in the low expressing interneurons category (r=0.387, p=0.018, n=37), seen in Table 6.2. For controls only, (Table 6.3) there was a positive correlation with age and percent of low expressing interneurons (r=0.372, p=0.025, n=36) and a negative correlation with age seen in high expressing interneurons (r=-0.422, p=0.015, n=33). For pH, there was positive correlation with high expressing interneurons (r=0.610, p=0.000, n=33), along with a negative trend in both no expressing (r=-0.310, p=0.079, n=33) and low expressing (r=-0.306, p=0.069, n=36) interneurons. For PMI, there was a positive correlation with percent of medium expressing interneurons (r=0.389, p=0.023, n=34), as well as a positive trend for high expressing interneurons (r=0.326, p=0.064, n=33).

Table 6.2: Demographics (age) correlated with no, low, medium (med), and high expressing interneurons in the schizophrenia group. *p<0.05, which statistically significant are bolded.

Schizophrenia	No	Low	Med	High
Age	r= 0.021 p= 0.907 n= 32	**r= 0.387*** **p= 0.018** **n= 37**	r= -0.006 p= 0.975 n= 34	r= -0.236 p= 0.178 n= 34

Table 6.3: Demographics (age, pH, and PMI) correlated with no, low, medium (med), and high expressing interneurons in the control group.***p<0.001, *p<0.05, #p<0.1, which statistically significant are bolded.

Control	No	Low	Med	High
Age	r= 0.120 p= 0.506 n=33	**r= 0.372*** **p= 0.025** **n= 36**	r= -0.176 p= 0.320 n= 34	**r= -0.422*** **p= 0.015** **n= 33**
pH	r= -0.310# p= 0.079 n= 33	r= -0.306# p= 0.069 n=36	r= -0.032 p= 0.856 n= 34	**r= 0.610***** **p= 0.000** **n= 33**
PMI	r= -0.044 p= 0.809 n= 33	r= -0.187 p= 0.282 n= 35	**r= 0.389*** **p= 0.023** **n= 34**	r= 0.326# p= 0.064 n= 33

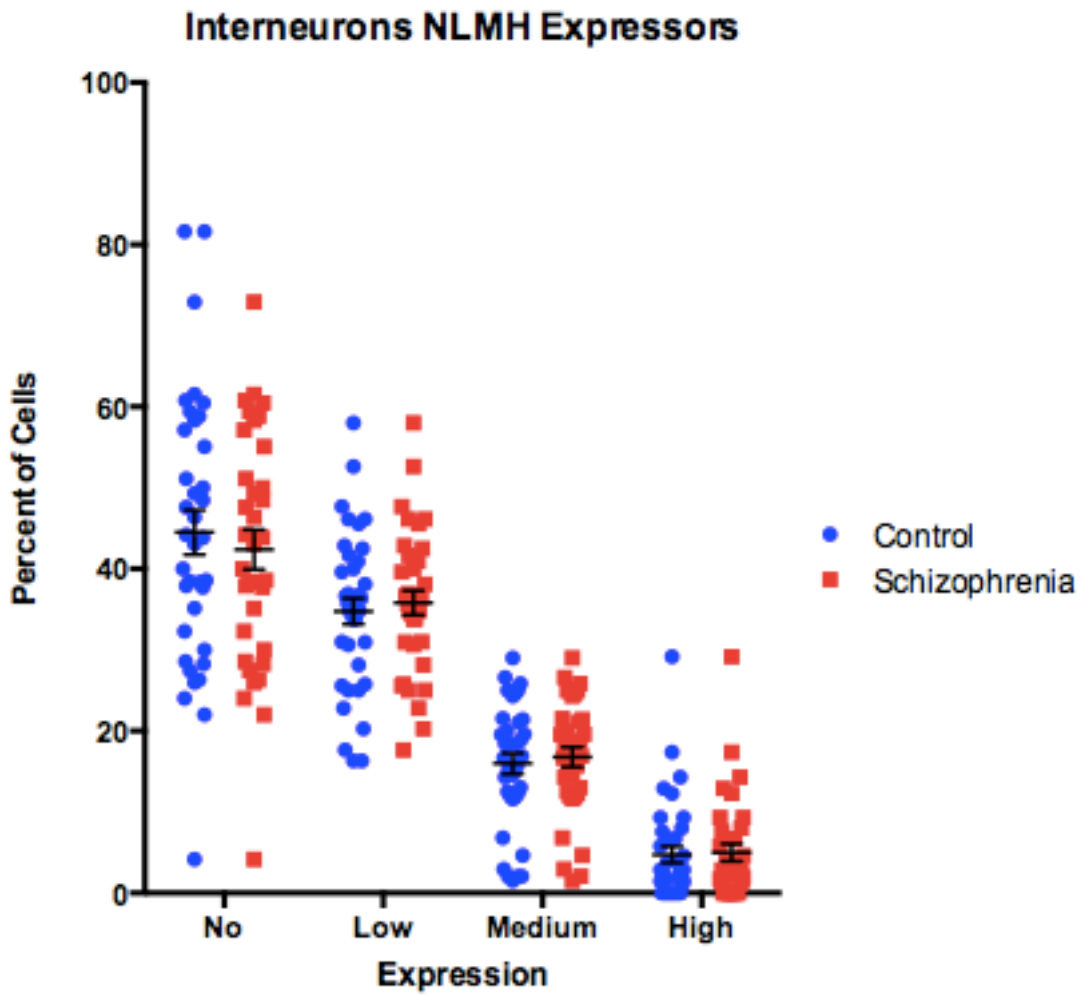

Figure 6.8: Expression bins were created looking at no expression, low expression, medium expression, and high expressing cells. No statistical difference between patients with schizophrenia and controls was seen.
Blue: Schizophrenia, Red: Controls
NLMH in the title stands for No, Low, Medium, and High expressers.

Looking at the interneurons specifically, there were no statistically significant difference between patients with schizophrenia and controls for any of the four expression levels (no, low, medium, or high: $F(1)=-1.352\times10^{-13}$, $p>0.9999$), seen in Figure 6.8.

Pyramidal neuron bins were separated into 0 to 10 (no expression), 10 to 40 (low expression), 40 to 60 (medium expressions), and 60 and above (high expression) silver grains per cell. For pyramidal neurons for the total cohort, it was seen that pH, and PMI correlated with percent of cells in each bin seen in Table 6.4. For age, there was a negative correlation with high expressing pyramidal neurons (r=0.250, p=0.042, n=67), suggesting that the older humans become, the less NR1 the pyramidal neurons express, following data previously published [238]. There was also a positive correlation between PMI and percent of high expressing pyramidal neurons (r=0.326, p=0.007, n=67).

Table 6.4: Demographics (age, pH, and PMI) correlated with no, low, medium (med), and high expressing pyramidal neurons in the total cohort.**p<0.01, *p<0.05, #p<0.1, which statistically significant are bolded.

All	No	Low	Med	High
Age	r= 0.034 p= 0.790 n= 65	r= 0.165 p= 0.168 n= 71	r= -0.159 p= 0.195 n= 68	r= -0.205# p= 0.096 n= 67
pH	r= 0.053 p= 0.676 n= 65	r= -0.034 p= 0.778 n= 71	r= 0.157 p= 0.201 n= 68	**r= 0.250*** **p= 0.042** **n= 67**
PMI	r=-0.072 p= 0.570 n= 65	r= 0.036 p= 0.766 n= 71	r= 0.151 p= 0.218 n= 68	**r= 0.326**** **p= 0.007** **n= 67**

When examining hemisphere differences in NMDAR NR1 mRNA silver grains in interneurons and pyramidal neurons in BA46, there were no statistically significant differences between the right and left hemisphere. Data shown in Table 6.5.

Table 6.5: Hemispherical differences in no, low, medium (med), and high expressing interneurons and pyramidal neurons in the total cohort using independent sample two tailed t-test. Two standard deviation outliers were removed.

	No	Low	Med	High
Interneurons	t(54)=-.463 p=.645	t(54)=1.122 p=.267	t(54)=-.376 p=.709	t(54)=-.197 p=.844
Pyramidal Neurons	t(54)=-.821 p=.415	t(54)=.376 p=.708	t(54)=.216 p=.830	t(54)=-.039 p=.969

In schizophrenia patients alone (Table 6.6), a positive correlation with age was seen in percent of low expressing pyramidal neurons (r=0.399, p=0.016, n=36), whereas age had a negative correlation for percent of high expressing pyramidal neurons (r=-0.359, p=0.040, n=33). No significant correlation for age was seen in the normal individuals (Table 6.7).

Table 6.6: Demographics (age) correlated with no, low, medium (med), and high expressing pyramidal neurons in the schizophrenia group. *p<0.05, which statistically significant are bolded.

Sch	No	Low	Med	High
Age	r= -0.301 p= 0.100 n= 31	**r= 0.399*** **p= 0.016** **n= 36**	r= -0.112 p= 0.535 n= 33	**r= -0.359*** **p= 0.040** **n= 33**

Table 6.7: Demographics (age) correlated with no, low, medium (med), and high expressing pyramidal neurons in the control group.

Control	No	Low	Med	High
Age	r= 0.254 p= 0.146 n= 34	r= -0.131 p= 0.445 n= 35	r= -0.193 p= 0.267 n= 36	r= -0.090 p= 0.613 n= 34

When examining correlations between the four different expressing interneurons and age of onset, illness duration, and antipsychotic medication, there were some statistically significant data noted. For age of onset, low expressing interneurons had a positive correlation (r=0.396, p=0.020, n=34). But, also for pyramidal neurons, age of onset negatively correlated with percent high expressers. So, it seems that the earlier the onset of the illness, the higher the percentage of high NMDAR mRNA expressing cells. There was no sign of correlation between percent of expression type and lifetime CPZ levels. When correlating high expressing interneurons with low dosage of CPZ given to the patients over the course of the illness, there was a positive trend seen (r=0.319, p=0.066, n=34). The rest of the data is in table 6.8.

When inspecting correlations between the four different expressing pyramidal neurons and age of onset, illness duration, and antipsychotic medication, it was noted that age of onset negatively correlated with high expressing pyramidal neurons (r=-0.388, p=0.025, n=33). The rest of the data is in table 6.9.

Table 6.8: Correlations with no, low, medium (med), and high expressing interneurons in the schizophrenia group examined age of onset, duration of illness, and antipsychotic medications (lifetime and mean dosage).*p<0.05, #p<0.1, which statistically significant are bolded.

Schizophrenia	No	Low	Med	High
Age of onset	r=0.131 p= 0.473 n= 32	**r=0.396*** **p= 0.020** **n= 34**	r= -0.010 p= 0.957 n= 34	r= -0.171 p= 0.333 n= 34
Duration of Illness	r= -0.073 p= 0.692 n= 32	r=0.200 p= 0.256 n= 34	r= -0.073 p= 0.683 n= 34	r= -0.162 p= 0.360 n= 34
CPZ Lifetime	r= -0.160 p= 0.382 n= 32	r= 0.066 p= 0.711 n= 34	r= -0.039 p= 0.825 n= 34	r= 0.087 p= 0.624 n= 34
CPZ Mean	r= -0.174 p= 0.342 n= 32	r= 0.021 p= 0.906 n= 34	r= -0.058 p= 0.744 n= 34	r= 0.223 p= 0.205 n= 34

Table 6.9: Correlations with no, low, medium (med), and high expressing pyramidal neurons in the schizophrenia group examined age of onset, duration of illness, and antipsychotic medications (lifetime and mean dosage).***p<0.001, *p<0.05, #p<0.1, which statistically significant are bolded.

Schizophrenia	No	Low	Med	High
Age of onset	r=-0.243 p= 0.188 n= 31	r=0.180 p= 0.292 n= 36	r= -0.006 p= 0.975 n= 33	**r= -0.388*** **p= 0.025** **n= 33**
Duration of Illness	r= -0.121 p= 0.515 n= 31	r=0.229 p= 0.180 n= 36	r= -0.159 p= 0.379 n= 33	r= -0.171 p= 0.341 n= 33
CPZ Lifetime	r= 0.052 p= 0.781 n= 31	r= 0.176 p= 0.304 n= 36	r= 0.043 p= 0.810 n= 33	r= 0.024 p= 0.895 n= 33
CPZ Mean	r= 0.032 p= 0.864 n= 31	r= 0.055 p= 0.751 n= 36	r= 0.221 p= 0.216 n= 33	r= 0.128 p= 0.478 n= 33

Comparing controls versus schizophrenia patients for NMDAR NR1 mRNA levels as measured by silver grains for pyramidal neurons, no expressers (t(68)=-0.161, p=0.873, two tailed independent sample Student's t-tests), low expressers (t(68)=1.632, p=0.107, two tailed independent sample Student's t-tests), medium expressers (t(68)=0.853, p=0.397, two tailed independent sample Student's t-tests), and high expressers (t(68)=-1.529, p=0.131, two tailed independent sample Student's t-tests) were not significantly different. Again, although not statistically significant, there seems to be fewer high expressers and more low expressers in the schizophrenia patient group, as seen in Figure 6.9.

Pyramidal NLMH Expressing Categories

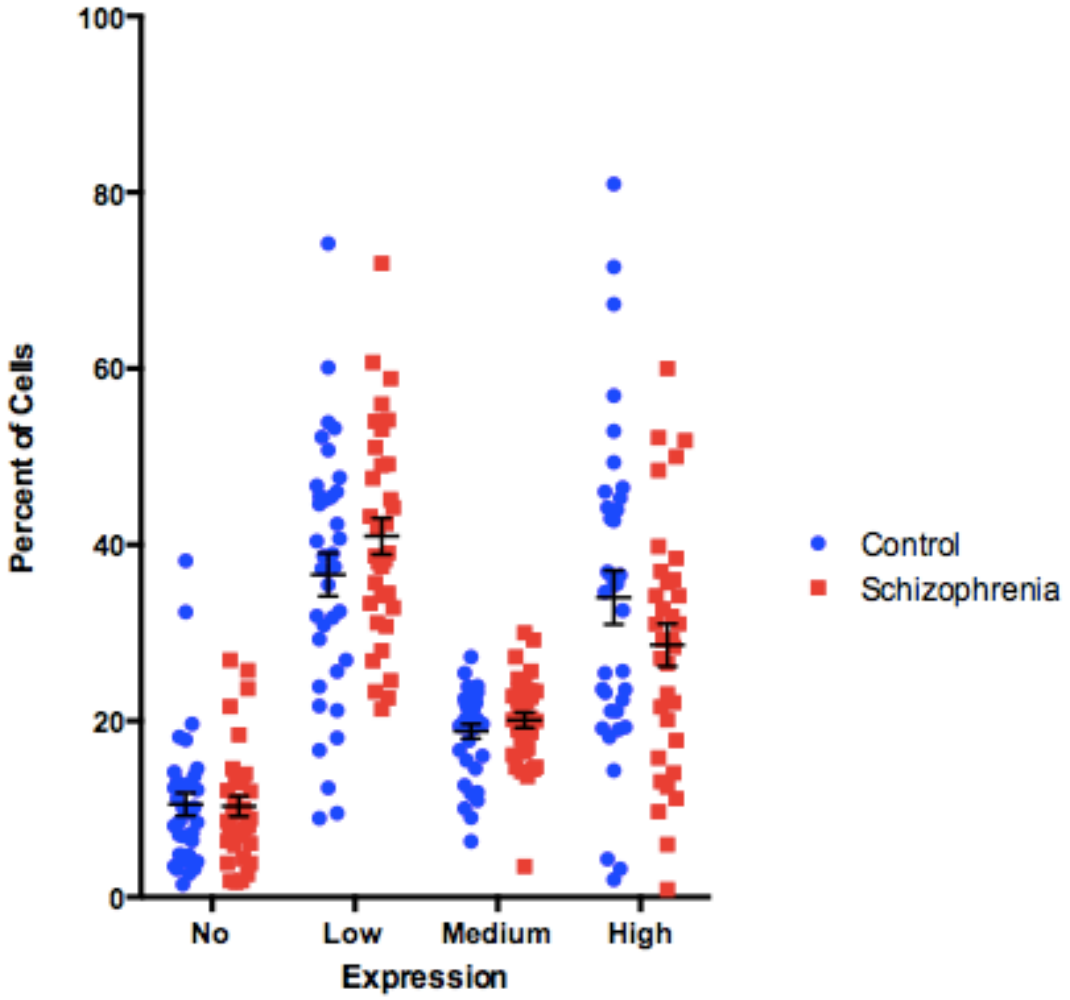

Figure 6.9: Expression bins were created for pyramidal cells looking at no expression, low expression, medium expression, and high expressing cells. It is apparent that there are slightly more low expressers and slightly less high expressers in schizophrenia patients compared to controls, but it does not reach statistical significance. Two standard deviations noted. NLMH in the title stands for No, Low, Medium, and High expressers.

Total percent of interneurons and pyramidal neurons that were considered expressers correlations

The total percent expressers for interneurons were calculated by first considering the cut off for being classified as an "expresser" of mRNA using

classical standards of being four times above background levels. I first took the maximum background levels (also used to define the highest "non-expresser"), which was five silver grains per cell, and multiplied that by four. Those neurons that had, at minimum, 20 silver grains per cell were considered expressers. The total percent expressers for pyramidal neurons, on the other hand, was calculated by taking the highest background measurement (also used to define the cut off for "non-expresser"), which was ten silver grains per cell, and multiplied that by four. Those neurons that had, at minimum, 40 silver grains per cell were considered expressers. Table 6.10 shows the correlations between the total percent expressers for both interneurons and pyramidal neurons for the total cohort. Looking at interneurons, the percent expressing NR1 mRNA was found to negatively correlate with age ($r=-0.280$, $p=0.020$, $n=69$), positively correlate with pH ($r=0.271$, $p=0.024$, $n=69$), and showed a positive trend for brain weight ($r=0.207$, $p=0.089$, $n=69$). For the pyramidal neurons, there was a positive correlation of NR1 percent expressing and PMI ($r=0.272$, $p=0.023$, $n=70$) and a positive trend for pH ($r=0.211$, $p=0.079$, $n=70$).

Table 6.10: Demographics (age, pH, PMI, RIN, and brain weight) correlated with total percent expressing interneurons and pyramidal neurons in the total cohort.*p<0.05, #p<0.1, which statistically significant are bolded.

Total cohort	Total Percent Expression of Interneurons	Total Percent Expression of Pyramidal Neurons
Age	**r= -0.280*** **p= 0.020** **n= 69**	r= -0.167 p= 0.167 n= 70
pH	**r= 0.271*** **p= 0.024** **n= 69**	r= 0.211# p= 0.079 n= 70
PMI	r= 0.116 p= 0.341 n= 69	**r= 0.272*** **p= 0.023** **n= 70**
RIN	r= 0.145 p= 0.235 n= 69	r= 0.083 p= 0.496 n= 70
Brain Weight	r= 0.207# p= 0.089 n= 69	r= 0.134 p= 0.267 n= 70

Table 6.11 shows the correlations between the total percent expressers for both interneurons and pyramidal neurons for schizophrenia patients alone. For interneurons and pyramidal neurons, no significant correlations were seen.

Table 6.11: Demographics (age, RIN, and brain weight) correlated with total percent expressing interneurons and pyramidal neurons in the schizophrenia group.

Schizophrenia	Total Percent Expression of Interneurons	Total Percent Expression of Pyramidal Neurons
Age	r= -0.127 p= 0.462 n= 35	r= -0.132 p= 0.449 n= 35
RIN	r= 0.116 p= 0.507 n= 35	r= 0.178 p= 0.306 n= 35
Brain Weight	r= 0.169 p= 0.332 n= 35	r= 0.125 p= 0.473 n= 35

Table 6.12 shows the correlations between the total percent expressers for both interneurons and pyramidal neurons for control individuals alone. Looking at

interneurons, a negative correlation with age (r=-0.403, p=0.018, n=34), along with a positive correlation for pH (r=0.508, p=0.002, n=34) and PMI (r=0.361, p=0.036, n=34), show that the control group is driving the total cohort correlations. For the pyramidal neurons, there was a positive correlation for pH (r=0.399, p=0.010, n=35) and PMI (r=0.402, p=0.017, n=35) and shows that the control group is again driving the total cohort's correlations. But there is no statistically significant correlation with age and pyramidal neurons (r=0.194, p=0.263, n=35)

Table 6.12: Demographics (age, pH, and PMI) correlated with total percent expressing interneurons and pyramidal neurons in the control group.**p<0.01,*p<0.05, #p<0.1, statistically significant correlations are bolded.

Control	Total Percent Expression of Interneurons	Total Percent Expression of Pyramidal Neurons
Age	**r= -0.403*** **p= 0.018** **n= 34**	r= -0.194 p= 0.263 n= 35
pH	**r= 0.508**** **p= 0.002** **n= 34**	**r= 0.399*** **p= 0.010** **n= 35**
PMI	**r= 0.361*** **p= 0.036** **n= 34**	**r= 0.402*** **p= 0.017** **n= 35**

Average silver grains per cell type per expression group

Next, the average number of silver grains per cell type per bin expression group was calculated. The calculation was completed to see if within each bin, there was a difference in how many silver grains were seen between diagnoses. For both interneurons and pyramidal neurons, no difference was seen when co-varying with pH, PMI, and RIN (interneurons: F(1,136)=0.8531, p=0.3573, pyramidal neurons: F(1,136)=0.3372, p=0.5624), Figures 6.10 and 6.11, respectively.

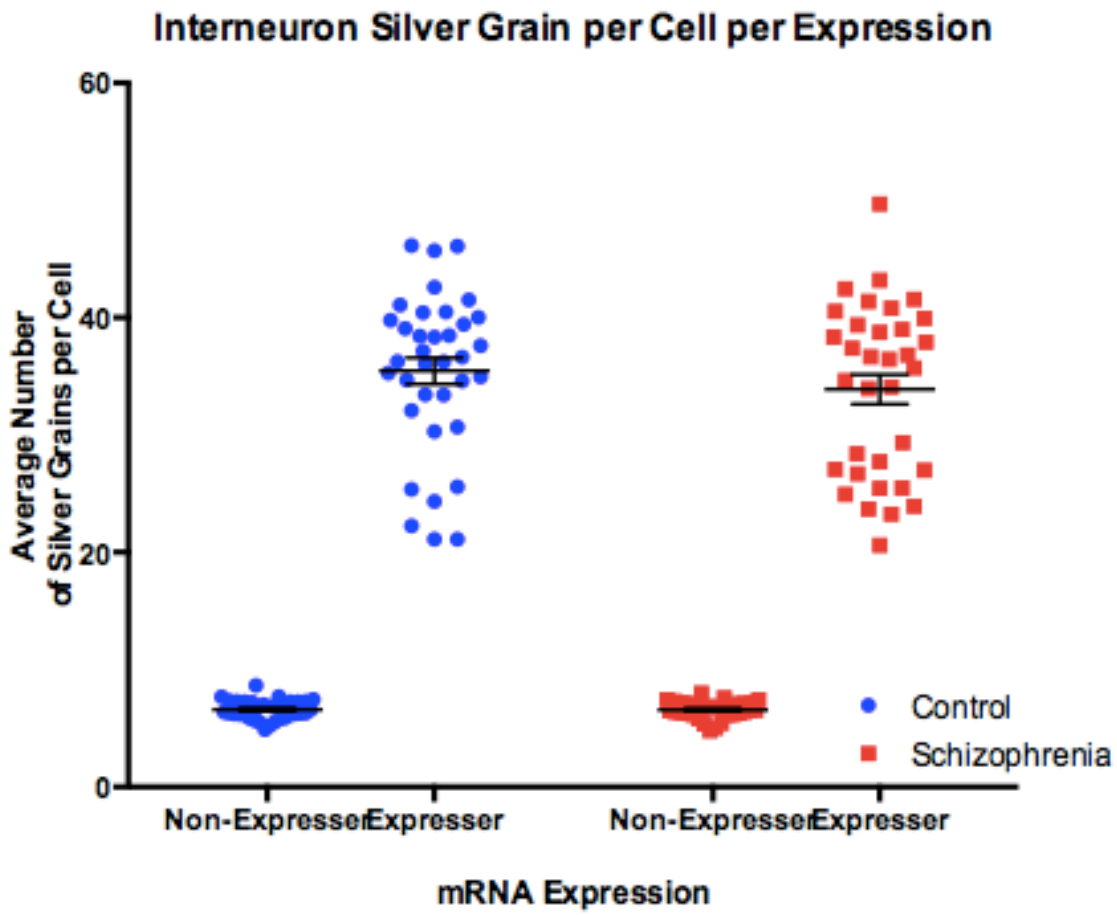

Figure 6.10: The average number of silver grains per interneuron per bin expression group was calculated. No statistically significant difference noted between diagnostic groups. SEM was noted.

Percent expression in the interneurons and pyramidal neurons by diagnosis

As the data on percent expression in the interneurons and pyramidal neurons were not normally distributed I proceeded with analysis using the non-parametric two-sample Kolmogorov-Smirnov test, which compared the cumulative distribution of two data sets and does not assume a Gaussian distribution. I found that there was a significant decrease in percentage of pyramidal neurons expressing NMDAR NR1 in schizophrenia in layer V by Kolmogorov-Smirnov directional test (p=0.032), with a 16% decrease in the percentage of excitatory neurons expressing NR1 in layer V of the DLPFC from people with schizophrenia

compared to controls. Data are seen in Figures 6.12 and 6.13. There were no statistically significant changes with diagnosis in the interneurons for this analysis. There was a significant effect of sex in the schizophrenia group on the percentage of interneurons expressing NR1 (directional test, p=0.043), but no effect of sex on the percentage of pyramidal cell expressing NR1.

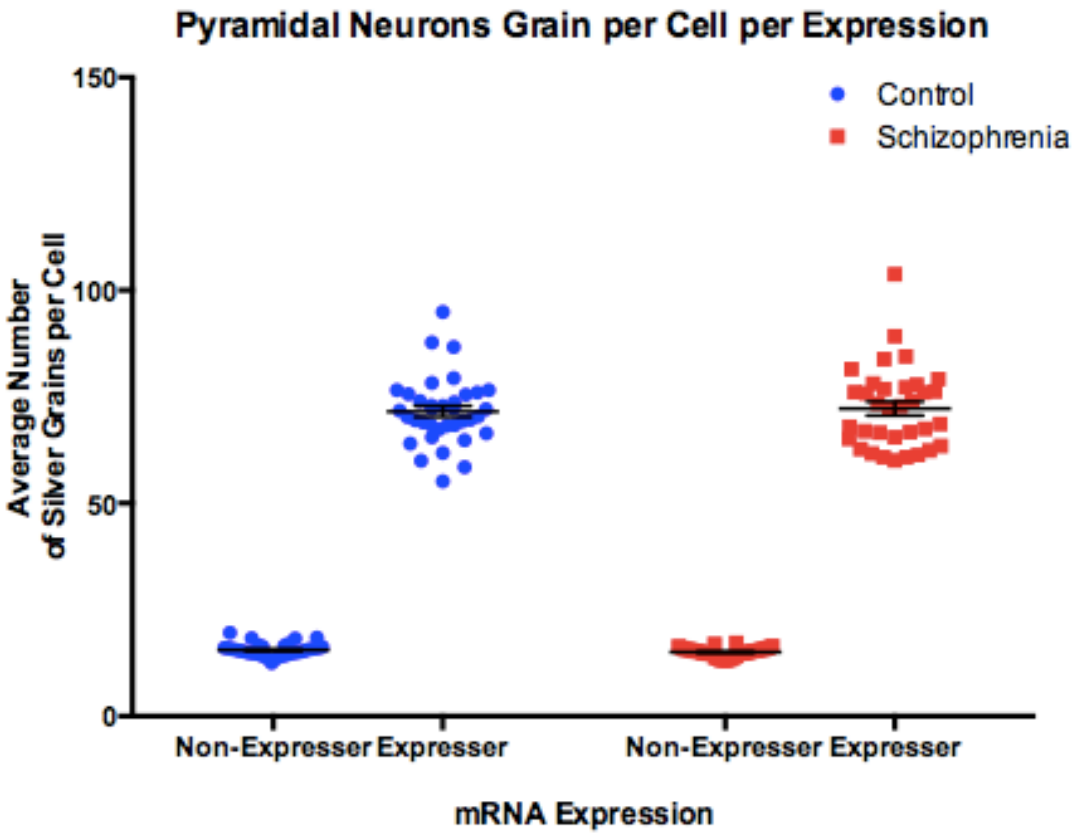

Figure 6.11: The average number of silver grains per pyramidal neuron per bin expression group was calculated. No statistically significant difference was noted between diagnostic groups. SEM was noted.

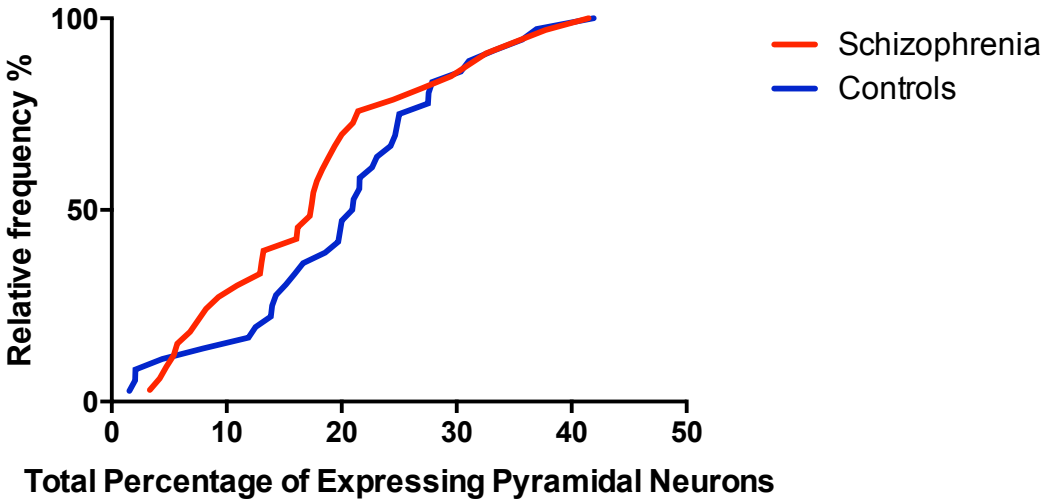

Figure 6.12: The relative frequency of the percentage of total expressing pyramidal neurons comparing schizophrenia patients vs controls.

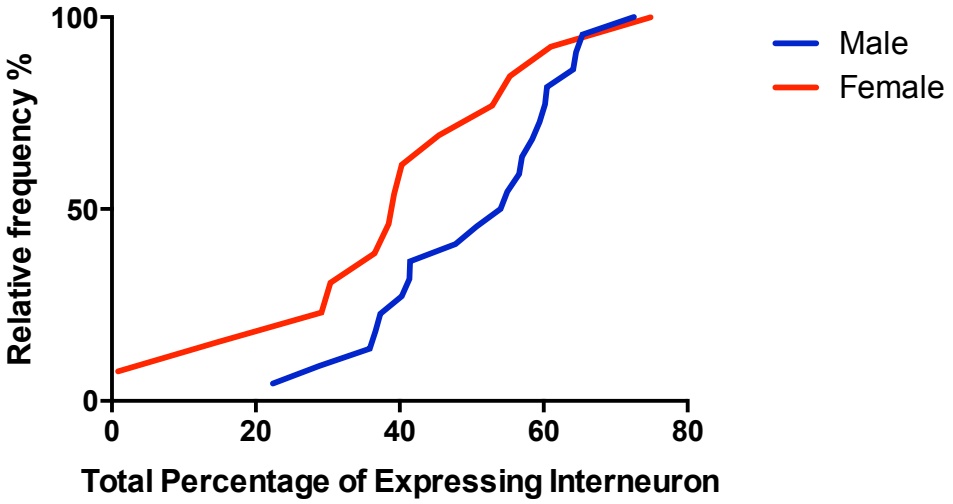

Figure 6.13: The relative frequency of total percentage of expressing interneurons comparing males and females.

Tables 6.13, 6.14, and 6.15 shows the correlations between the average number of silver grains per neurons (interneurons or pyramidal neurons) deemed to be expressing NR1 mRNA. In the total cohort (Table 6.13), it was seen that the average number of silver grains per interneuron positively correlated with pH

(r=0.401, p=0.001, n=70), PMI (r=0.283, p=0.017, n=70), RIN (r=0.249, p=0.038, n=70), and brain weight (r=0.333, p=0.005, n=70); and pyramidal neurons NR1 grains/cell negatively correlated with age (r-0.362, p=0.002, n=70), positively correlated with PMI (r=0.252, p=0.035, n=70), and had a trend for a statistically significant positive correlation with both RIN (r=0.225, p=0.067, n=70) and brain weight (r=0.223, p=0.068, n=70).

Table 6.13: Demographics (age, pH, PMI, RIN, and brain weight) correlated with average number of silver grains per cell (interneurons or pyramidal neurons) with NR1 expression in the total cohort. **p<0.01*p<0.05, #p<0.1, which statistically significant are bolded.

All	Average Number of Silver Grains per Interneuron with NR1 Expression	Average Number of Silver Grains per Pyramidal Neuron with NR1 Expression
Age	r= -0.146 p= 0.228 n= 70	**r= -0.362**** **p= 0.002** **n= 70**
pH	**r= 0.401**** **p= 0.001** **n= 70**	r= 0.142 p= 0.282 n= 70
PMI	**r= 0.283*** **p= 0.017** **n= 70**	**r= 0.252*** **p= 0.035** **n= 70**
RIN	**r= 0.249*** **p= 0.038** **n= 70**	r= 0.225# p= 0.067 n= 70
Brain Weight	**r= 0.333**** **p= 0.005** **n= 70**	r= 0.223# p= 0.068 n= 70

Table 6.14 shows the correlations between the average number of silver grains per interneuron or pyramidal neuron with NR1 expression in only the schizophrenia patients. It was seen that the average number of silver grains per interneuron with NR1 expression positively correlated with brain weight (r=-0.426, p=0.011, n=35). Also, it was seen that the average number of silver grains

per pyramidal neuron with NR1 expression positively correlated with RIN (r=0.339, p=0.046, n=35).

Table 6.14: Demographics (age, RIN, and brain weight) correlated with average number of silver grains per cell per expression group in interneurons and pyramidal neurons in the schizophrenia diagnostic group.*p<0.05

Schizophrenia	Average Number of Silver Grains per Interneuron with NR1 Expression	Average Number of Silver Grains per Pyramidal Neuron with NR1 Expression
Age	r= -0.125 p= 0.474 n= 35	r= -0.257 p= 0.136 n= 35
RIN	r= 0.281 p= 0.102 n= 35	**r= 0.339*** **p= 0.046** **n= 35**
Brain Weight	**r= 0.426*** **p= 0.011** **n= 35**	r=0.198 p= 0.255 n= 35

Table 6.15 shows the correlations between the average number of silver grains per cell (interneuron or pyramidal neuron) with NR1 expression in the control individuals. The average number of silver grains per cell per interneuron correlated positively with pH (r=0.628, p<0.001, n=35) and PMI (r=0.365, p=0.031, n=35). In the pyramidal neurons, it was seen that the average number of silver grains per cell per expression group correlated negatively with age (r=0.402, p=0.005, n=35) and positively correlated with PMI (r=0.415, p=0.013, n=35).

Table 6.15 Demographics (age, RIN, and brain weight) correlated with average number of silver grains per cell per expression group in interneurons and pyramidal neurons in the control group. ***p<0.001, **p<0.01, *p<0.05

Control	Average Number of Silver Grains per Interneuron with NR1 Expression	Average Number of Silver Grains per Pyramidal Neuron with NR1 Expression
Age	r= 0.174 p= 0.318 n= 35	**r= -0.402**** **p= 0.005** **n= 35**
pH	**r= 0.628***** **p= 0.000** **n= 35**	**r= 0.415*** **p= 0.013** **n= 35**
PMI	**r= 0.365*** **p= 0.031** **n= 35**	r= 0.241 p= 0.163 n= 35

Grains/cell in the expressers in interneurons and pyramidal neurons by diagnosis

It was found there was no significant effect of diagnosis on grains/interneurons by the nonparametric test Kolmogorov-Smirnov (p=0.355). Similarly, grains/pyramidal neuron was also not significant by test Kolmogorov-Smirnov (p=0.063).

Gender differences between no, low, medium, and high expressing interneurons and pyramidal neurons

Gender was also analysed to determine if there were any differences in the number of silver grains/cell for non-, low, medium, and high expressers of pyramidal and interneurons. In Table 6.16 the total cohort, schizophrenia diagnostic group, and controls, respectively, are seen. There was no statistically significance seen for any of the mean comparisons.

Smoking effects on no, low, medium, and high expressing interneurons and pyramidal neurons

When looking at smoking effects for interneurons and pyramidal neurons, there were no significant differences seen for no, low, medium, or high expressing neurons. Data are not shown.

Suicide effects on no, low, medium, and high expressing interneurons and pyramidal neurons-combine with above into confounds section

There were no statistical significances between the NR1 silver grain/cell in interneurons or pyramidal neurons based on whether a schizophrenia patient had died by suicide or by other cause. Data are not shown.

Table 6.16: The means of NR1 silver grains/cell for interneurons and pyramidal neurons for no, low, medium, and high expressers in the total cohort were compared by two-way ANOVA between males and females, patients and controls.

	Effect of diagnosis	Effect of sex	Interaction effect
Interneuron no expression	F(1,61)0.184, p=0.669	F(1,61)0.356, p=0.553	F(1,61)0.153, p=0.697
Interneuron low expression	F(1,65)2.758, p=0.102	F(1,65)0.985, p=0.325	F(1,65)0.000, p=0.991
Interneuron medium expression	F(1,64)2.864, p=0.095	F(1,64)0.212, p=0.646	F(1,64)2.461, p=0.122
Interneuron high expression	F(1,63)1.964, p=0.166	F(1,63)1.217, p=0.274	F(1,63)1.104, p=0.298
Pyramidal neuron no expression	F(1,61)0.022, p=0.882	F(1,61)0.233, p=0.631	F(1,61)0.206, p=0.651
Pyramidal neuron low expression	F(1,67)0.118, p=0.732	F(1,67)0.009, p=0.924	F(1,67)1.449, p=0.233
Pyramidal neuron medium expression	F(1,64)1.103, p=0.297	F(1,64)0.130, p=0.720	F(1,64)1.025, p=0.315
Pyramidal neuron high expression	F(1,63)0.180, p=0.673	F(1,63)0.040, p=0.842	F(1,63)0.107, p=0.745

Antipsychotics (CPZ equivalent) effect on no, low, medium, and high expressing interneurons and pyramidal neurons combine with above

When looking at the quantity of antipsychotic medication a schizophrenia patient was on, there were no effects on NR1 silver grains/cell for interneurons looking at the CPZ equivalent lifetime dosage (r=0.044, p=0.802), and average dosage throughout the course of their lifetime (r=0.231, p=0.182). There were also no effects on NR1 silver grains/cell for interneurons looking at the CPZ equivalent lifetime dosage (r=0.279, p=0.111), though there was an effect of average dosage throughout the course of their lifetime (r=0.418, p=0.014).

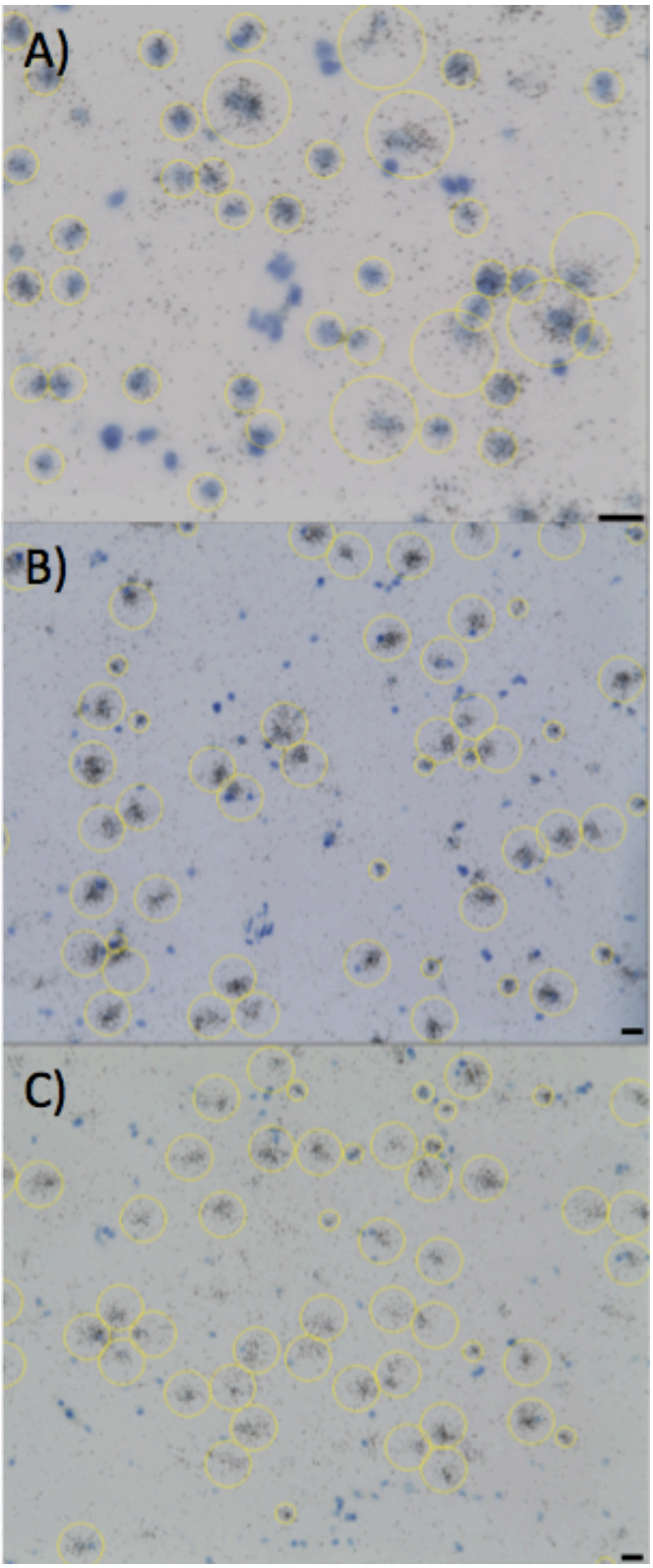

Figure 6.14: A) Layer II is seen with many small pyramidal cells and there are a fewer number of interneurons. 400x. B) Layer III is seen with medium sized pyramidal cells and there are a fewer number of interneurons. 200x. C) Layer V is seen with many medium to large pyramidal neurons with few interneurons. 200x. Scale bar = 20 µm.

Discussion

It is known that there is a link between human NMDAR expression and cognition where individuals who have increased NMDARs tend to be younger and

learn better and individuals who have NMDAR blockade tend to lose focus, concentration and memory[239]. From this prior knowledge, delving deeper into the expression of NMDAR at a cellular level may help to identify the molecular basis for differences in cognitive ability between schizophrenia patients and healthy controls. I started by examining the expression of mRNA by analysing the laminar film that expressed NMDAR NR1 mRNA, discussed in chapter 5. It was previously found that NMDAR NR1 mRNA was significantly changed in schizophrenia including a reduction in NR1 in cortical layer V[91]. Also, consistent with this, a previous study found that there was a significant increase in small to medium size neurons in layer V of the PFC[240]. I add to this knowledge, in this chapter, by demonstrating that this reduction in NMDAR mRNA likely stems from a reduction in the percent of pyramidal neurons expressing moderate to high levels of the NMDAR NR1 mRNA, not the inhibitory interneurons. This is important as many prior theories assume that the NMDAR deficiency in the brains of patients with schizophrenia is localized to the interneurons, but this data challenge this theory as I did not find any significant change in either the percentage of interneurons expression NMDAR NR1 mRNA or the average amount of expression of NMDAR NR1 mRNA per interneuron in the disease.

There has been a debate over whether schizophrenia is a hypoglutamatergic system or a hyperglutamatergic system. Since I found the pyramidal neurons to have a deficit in the NMDAR NR1 mRNA, it would suggest that schizophrenia patients' brains have a hypoglutamatergic system occurring, at least seen here at the time of death. Cortical GABAergic neuron deficiency is one of the most consistently reported findings in people with schizophrenia. Over the past 30 years, schizophrenia has been thought to be caused by some damage to

connectivity between different regions of the brain[241]. Looking at the NMDAR hypofunction in schizophrenia, it can be thought that by blocking the excitatory glutamatergic receptors, this would result in disruptions of cortical inhibition, which would result in clinical symptoms[241], as well as what has been seen in ketamine studies[100].

Figure 6.15 shows the structure of how pyramidal neurons and interneurons work together. Pyramidal neurons are more numerous than NMDAR mRNA levels in interneurons in the brain.

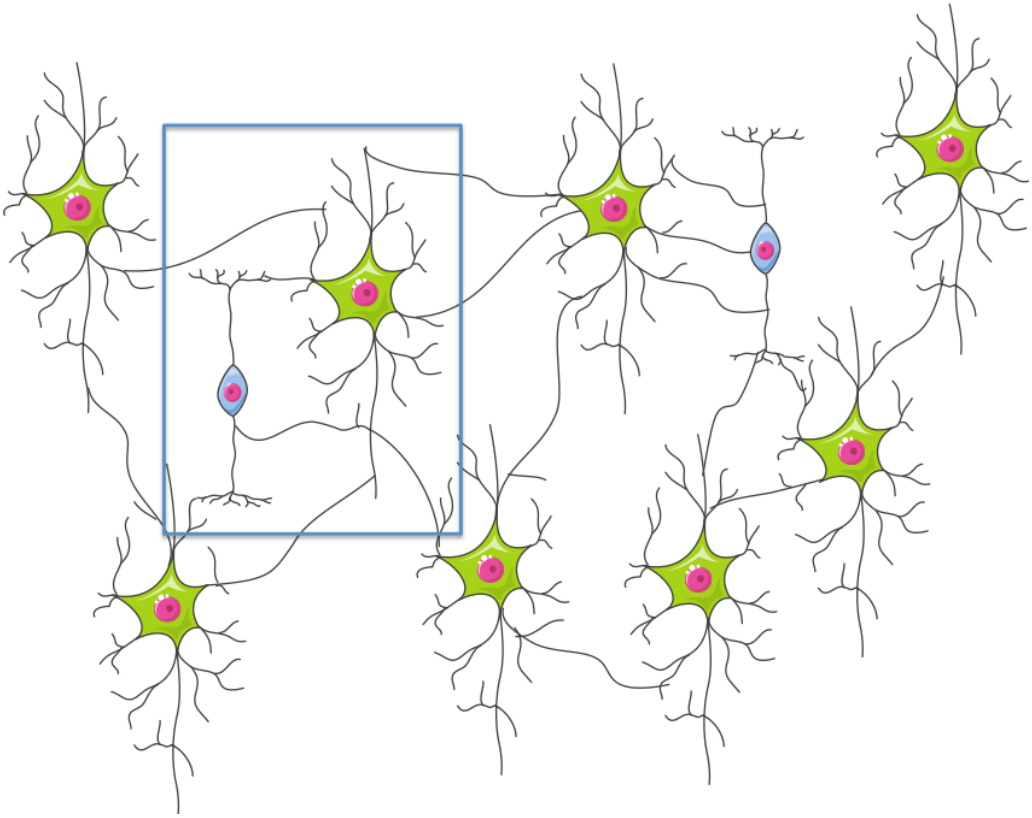

Figure 6.15: An example of the interconnections between pyramidal neurons and interneurons. Key: Pyramidal neurons are green, interneurons are blue. Blue box represents zoomed in view on Figure 6.16.

When focusing on just an interaction between one pyramidal neuron and one interneuron, it can be seen that both neuron types have NMDARs; this can been seen by silver grains on thesis specific neuron types. From what I found in my thesis, Figure 6.16 shows an overview of what I believe is occurring on both neuron types. The number of receptors represents how much NMDAR NR1 mRNA is being produced by the average neuron. On interneurons (blue), the mRNA amount does not appear to change, but the change is occurring in the pyramidal neurons (green). This would signify a hypoglutamatergic system. There are likely fewer excitatory neurons firing, whereas the NMDAR mRNA levels in inhibitory interneurons appear to be normal, suggesting they may have a normal response to glutamate.

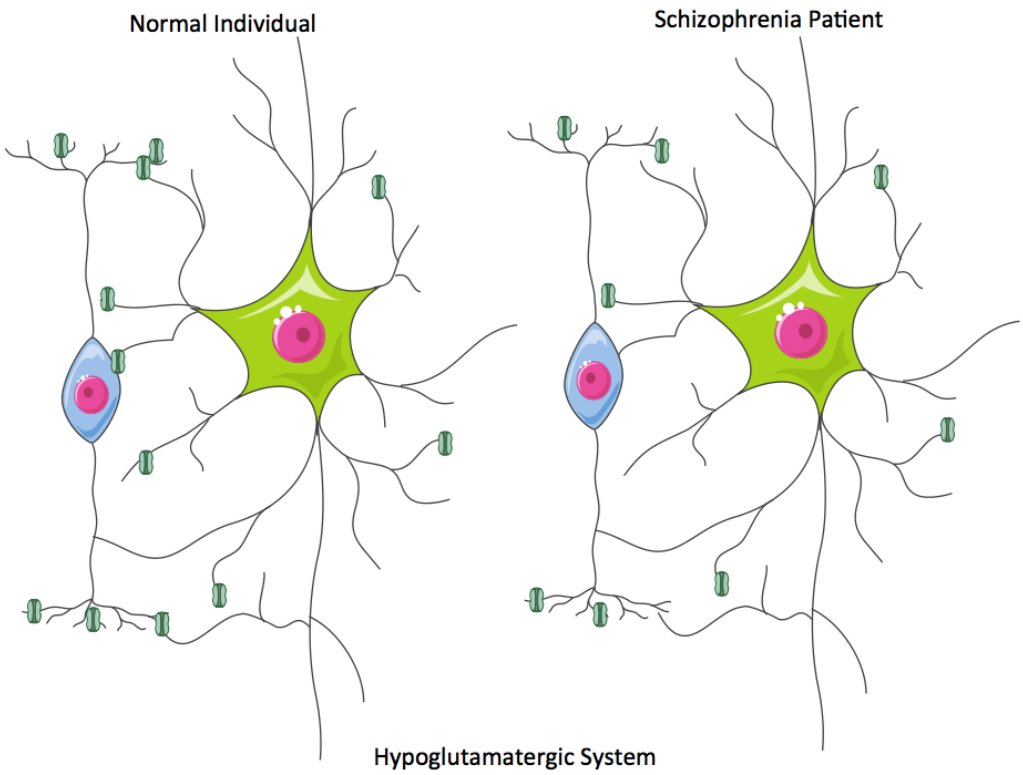

Figure 6.16: This figure represents interneurons, in blue, and pyramidal neurons, in green, in both normal individuals and schizophrenia patients. It can be seen that both groups have the same number of interneurons NMDARs (teal receptors), however, the pyramidal neurons have a deficit of NMDARs.

Looking at prior research in the field, it was found that acute administration of MK-801, a synthetic compound that is a non-competitive antagonist to the NMDAR, would cause immediate hyperactivity of pyramidal neurons[242], leading to the assumption that in schizophrenia the brain is in a hyperglutamatergic state. However, with these findings here, I know that there are less NMDAR NR1 subunits in pyramidal neurons in schizophrenia. Being able to look at individual neurons, I found that there was a deficit of NMDAR NR1 subunits, which does not appear to readily relate to an increased glutamate signalling or hyperactivity state because of the decrease in NMDAR NR1 mRNA on excitatory neurons. I found that not only were the pyramidal neurons the putative source of decrease glutamate NMDAR NR1 mRNA, but the interneurons may have no change in mRNA amount between schizophrenia patients and control individuals. This would lead to the assumption that there may be less excitatory signalling occurring in the cortex of individuals with schizophrenia. The reason why other researchers could have found a glutamate increase by MRI is possibly because glutamate still is being released into the system correctly [243], but it appears there may be fewer receptors available for the glutamate to bind to or another hypothesis could be that our results suggest different processes could be occurring when researchers examine individuals at different stages of illness or not at time of death. Also, since there are less NDMARs, this may lead to a decrease in GAD67 and GABA synthesis because the pyramidal neurons are malfunctioning and leading to decreased excitatory drive on the interneurons. Integrating my finding with previous work completed in the field and tying it all together will require future animal model work by looking at rats with decreased amount of NMDAR on pyramidal neurons in the cortex.

It is known that the NMDAR NR1 mRNA is enriched in areas responsible for learning including the entire cortex and hippocampus and is expressed from birth to adulthood and the elderly[244]. Using in situ hybridisation with riboprobes, the NR1 mRNA was found throughout all five layers in cortical human brain tissue and more precisely, in the PFC, layers II, III, IV, V, and VI all appeared heavily labelled and while the signal appeared higher in layer II and mid-cortical, there was not a significant different across layers[122]. Another study showed that there was a mean decrease of about 4% or about 150μm on average in cortical width in the brains of people with schizophrenia compared to controls[245], the same difference that my study found.

Age is a factor in how much of specific NMDAR subunits are expressed[106]. I found that NMDAR mRNA (like protein) decreases with increasing age in the normal healthy brain. So, specifically we are seeing a negative correlation in high NR1 expressing interneurons increasing with age, whereas we detect a positive correlation with age in the low expression interneurons. From this, I could potentially conclude that as a person ages, less NR1 could be produced/cell. However, more research needs to be completed to see if this hypothesis is true. This has also been demonstrated in previous studies animals[123,238,246]. Since a previous study finding higher expression of mRNA for NR1 subunits schizophrenia patients as compared to controls were conducted in an aged group (average age=80 years), it may be that the control group had artificially lower NMDAR NR1 as compared to the control group[106]. However, since schizophrenia patients already have a deficit in the NMDARs, it is possible that they are in a state where they may not lose more NMDARs over time. So it is possible that around the age of 70, the trajectories intersect and at that point the schizophrenia patients may have

more NDMAR mRNA than normal, healthy aging controls. So this means humans might be losing NDMAR NR1 mRNA in interneurons as we age.

In one study, it was determined that females have lower amounts of mRNA of NR1 than males[247], but in our laboratory cohort, this could be a result of females being significantly older than males overall in the study. In the cohort that I used, a previous study by our laboratory found no differences in NR1 mRNA expression looking at gender[117], which is not consistent with my results, where I found that females may have less NR1 mRNA expressing interneurons. This observation may suggest that this could be one of the biases why males tend to get schizophrenia more often than females. If there are less inhibitory interneurons expressing NR1 mRNA in females, the lack of NMDAR NR1 mRNA being produced in females may not always have as big of an effect.

I also do not think that the difference I detected in NMDAR NR1 mRNA was due to confounding factors. Previously, it was found that there was a weak positive trend for a significant correlation between PMI and mRNA[247]. This study of NR1 expression in interneurons and pyramidal neurons in controls only showed a positive correlation between PMI and pH. With age, it was seen that there is less NMDAR NR1 mRNA the older people become. So, it seems that less NR1, specifically in the pyramidal neurons, is being produced with advancing age, following data previously published [238]. I did not detect any relationship between pH and PMI with NMDAR NR1 mRNA levels in schizophrenia patients in this study. However, when looking at brain pH and NR1 mRNA in controls, I found a positive correlation consistent with previous work[247]. This would suggest that there is more NR1 mRNA present with high pH and a longer PMI. For pH, it has been found that low pH can cause mRNA degradation[181], which my study supports. In a couple of

studies, it was suggested that there was no statistical significance with PMI and NMDAR mRNA[248,249], while my study shows differently. It shows that the longer PMI a control individual has, the more mRNA is present but this was only in NRI mRNA positive pyramidal neurons in the unaffected control group. But this is not seen in the schizophrenia group. This could indicate that more research on this topic should be completed in order to see if other cohorts could find the same changes in schizophrenia patients compared to healthy controls.

When looking at smoking, suicide, and dosage of antipsychotics, there were no significant correlations with the amount of NR1 mRNA seen in the NMDAR NR1 positive cells in my analysis. I also did not find any correlations with antipsychotic and the amount of NDMAR NR1 mRNA seen in a previous study[117]. Another study also showed that antipsychotics did not alter the levels of mRNA for the NR1 subunit[212]. However, when looking at antipsychotics over time, it was seen that antipsychotics could be protective or stop the loss of NMDAR NR1 mRNA over time. This was also seen in a previous study looking at elderly patients with schizophrenia on and off of antipsychotics[121]. They found that NMDAR NR1 mRNA did not differ in patients with schizophrenia and controls if the patients were on antipsychotics, unlike the others not taking medication at the time of death[121]. Since the majority of this cohort is on some type of antipsychotic, I might also have a greater difficulty of finding differences between diagnostic groups.

The data from this thesis presents evidence that brain weight can be related to the NMDAR NR1 mRNA levels. Another article presents similar results[250]. According to their paper, brain weight is another potential variable, not just PMI, pH, and other common variables, that might influence the level of mRNA[250]. Prior to this 2010 article, there was no known evidence of brain weight affecting the

amount of mRNA in the brain[250]. However, a possible list of reasons why brain weight could be a contributing factor include the size of the brain could be a heritable trait[251], bigger brains require an increase in gene regulation[250], and how increased synaptic plasticity could allow for larger brain development[252]. It was also stated that the relationship between mRNA and brain weight was not simply a result of differences in age, gender, RIN or other possible confounders[250]. Besides those couple of possibilities causing the differences, it is also known that the spine is plastic[253]. With this plasticity, schizophrenia patients may at times have a normal amount of spines and NMDAR mRNA being produced while they are not experiencing an acute episode. My data suggest that some cortical neurons may in fact have a normal level of NMDAR NR1 mRNA and that only a subset of pyramidal neurons seems to have reduced levels of NMDAR NR1 such that they fall below the threshold to be considered NMDAR NR1 expressing.

I found that normal individuals have a large amount of variability in the percentage of cells that have high levels of NMDAR NR1, with some people having less than 10% and others having more than 50%. Thus, having a lower percentage of NMDAR expressing pyramidal neurons alone is not likely to result in schizophrenia. This results raises several interesting questions, for example 1) why do human pyramidal neurons have such variable amounts of NMDAR NR1 mRNA?, 2) is there a particular function or role for the neurons making more NMDAR NR1?, 3) are the neurons that appear to not express NMDAR not involved in learning and memory?, and 4) how stable is the NMDAR expression grouping of pyramidal neuron over time?

Looking at data from large cells from another paper, it was noted that most likely pyramidal cells in the DLPFC were causing most of the NMDAR NR1 mRNA

changes in schizophrenia[91]. The majority of cells where differences were seen were in layers III and V[91]. The majority of cells where differences were seen were in layers III and V[91]. In my study, I uncovered mRNA changes in pyramidal neurons in layer V.

No differences in the interneurons in the cohort in layer V were found. The glutamate hypothesis revolves around the idea of an imbalance between inhibition and excitation on interneurons eventually leading to psychosis and cognitive deficits[108]. My findings suggest that schizophrenia patients brains are in a hypoglutamatergic state, which means less glutamate overall is being produced or responding to. Since there is less NR1 mRNA being produced on pyramidal neurons, and there is less NMDAR NR1 protein at the PSD, a hypothesis can be advanced that there are fewer functional NMDARs in schizophrenia patients compared to healthy controls. Since I now know the deficit in protein is most likely from the pyramidal neurons, a secondary consequence of a decrease of GAD67 could occur. Reductions in GAD67, an interneuron specific enzyme, have been seen in other schizophrenia studies[254,255]. It has not been tested, to my knowledge, whether or not enhancing the function of interneurons would help or hinder in schizophrenia. A knockout mouse has been made to see if decreasing NMDAR NR1 subunit expression in interneurons would cause increase in positive, negative, and/or cognitive schizophrenia-like symptoms[256]. But according to my findings, this knockout mouse would not be showing an accurate model of schizophrenia since the pyramidal cells are where the NMDAR NR1 deficit is found. In one study, it was found that removing NMDAR expressing interneurons before maturity in mice causes schizophrenia-like symptoms to occur[193], signifying less NMDAR NR1 obligatory subunits might interfere with proper brain development. One of the

limitations could be that there is a low level of expression in interneurons. With this low natural level of expression, finding minute changes between schizophrenia patients and controls could be more difficult if there is indeed something occurring with the NMDAR in interneurons.

It is known that pyramidal neurons, interneurons, and glial cells all work together as one unit. It can be taken away from this chapter that an overall decrease in the percentage of pyramidal neurons expressing NMDAR NR1 subunit mRNA is found in schizophrenia. Since interneurons are inhibitory and stop the excitatory pyramidal neurons from carrying information away from the cortex to facilitate cognition and action, a negative feedback cycle could be in place. The lower levels of NMDAR mRNA may make the pyramidal neurons less able to fire action potentials that would result in less glutamate being released. Since excitatory pyramidal neurons synapse onto the inhibitory interneurons, the interneurons may be less likely to be stimulated and thus, could be underactive and synthesize less GAD-67 and calcium binding protein mRNAs as a consequence of pyramidal neuron dysfunction. It is currently unknown which of the neuron types could be the cause of such a negative feedback cycle, which could potentially lead to a cognitive decline over time. The next step forward could be to look at subpopulations of interneurons and pyramidal neuron types to see if any of the specific subclasses are either more less likely to show NMDAR NR1 decrease. More research is needed on this topic to understand the specific increases, decreases, and no changes found in these neuron types.

Limitations of this study

One experiment that would greatly help in the efforts of distinguishing between different neuron types would be to double label the neurons with GAD.

This discussion was brought up during this experiment, but our laboratory does not have this technique working at the moment. Previously, Dr. Samantha Fung and Dr. Dipesh Joshi were working on double labeling, and currently Dr. Vibeke Catts is still working on this technique.

Another limitation was when looking at layer II. Figure 6.16 shows an example of the difference in size between the "small" interneurons and the "large" pyramidal cells. In green, there is a clear pyramidal neuron, in grey, there is a clear interneuron, but in red, it is near impossible to tell which type of neuron it is due to the fact the nucleus is hidden behind the silver grains. The diameter size conventionally used to sample silver grains for pyramidal neurons (35μm) is larger by design than the outline of the cell in order to capture all the radioactivity that radiates and silver grans that can scatter in a radius outside the border of the cell body. With the NR1 silver grain and Nissl stain, there is no distinct cell border outline evident to indicate an approximate size of the cells being examined. Because of these difficulties I chose not to analyse NMDAR NR1 mRNA levels in layer II further and instead focused my efforts on examining layer V where larger pyramidal neurons are more easily distinguishable from the smaller interneurons.

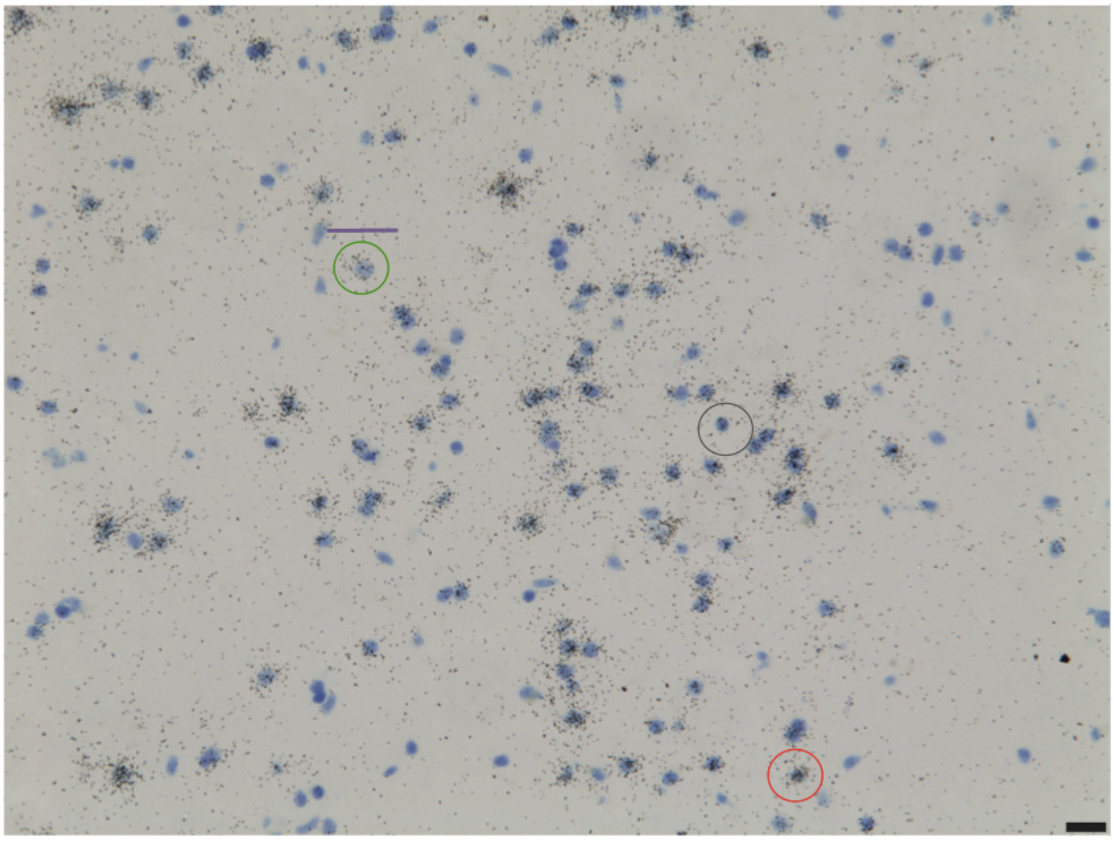

Figure 6.16: Illustration of the small difference in the size of "small" interneurons (grey circle) and "large" pyramidal cells (green circle) in layer II. A intermediate sized neuron of unknown identify is denoted by a red circle. The black scale bar equals 20 um.

Chapter 7- Overall Discussion: What does this mean to schizophrenia?

Throughout this thesis, it has been suggested that not every person with schizophrenia has the same aetiology. NDMAR exists throughout the brain and can be identified at the mRNA and protein levels, and the level of NMDAR synthesis is controlled at many levels[257]. Also, schizophrenia is thought to be a neurodevelopmental disorder typically occurring in teens, that may involve certain brain areas more than others, one area particularly impacted includes the cerebral cortex, and I have shown that the cortical pathology involves cellular and subcellular deficits in the NMDAR, which has also been seen in a prior study.[258] The pathology of neurodevelopmental illnesses could sometimes be caused by an altered glutamate-signalling pathway that reduces NMDAR signalling, previously seen. [108,220] Some other studies proposed the idea that by improving functions of the NMDAR, neuropsychiatric disorders could be improved[108]. From what was found in this thesis; a lower amount of NMDAR NR1 protein, specifically at the PSD, and lower amounts of NMDAR NR1 mRNA in excitatory pyramidal neurons, it seems the idea of improving schizophrenia patients' functioning by focusing on the NMDAR seems well justified.

The evidence that has accumulated in this thesis will be summarised. Firstly, as reviewed in Chapter 1, the NMDAR protein expression in the PFC (BA10) in schizophrenia has been studied with mixed results. In my findings, the NMDAR NR1 protein in the PSD in the PFC was significantly decreased. This decrease in protein at the PSD corresponds to changes that our group has previously found in the total homogenate, in a similar region (BA46). [117] But, my findings in the PSD, in fact, are larger in magnitude as compared to the total homogenate. Finding a decrease at the PSD is important because this is where functional receptors

lie.[259,265] If something is going wrong during trafficking, there could be the correct amount of NMDARs being created, but no way for these receptors to work efficiently. This information about the PSD proteins, coupled with the fact that there was less mRNA found and fewer large neurons expressing NMDAR NR1 mRNA could mean that there are fewer NR1 subunits being made in schizophrenia patients, and that fewer receptors are being moved to the PSD where they are needed. One reason why our laboratory finds differences in protein levels, while others have not, could be due to different cohorts being used, as well as slightly different brain regions being studied. Since there are so many different subgroups of schizophrenia, and it is convention to group these subgroups together for research in order to include the largest number of subjects in the analysis, it is not known if the different cohorts contain more or less of one subgroup compared to others. Looking at the NMDAR NR1, total protein gives a good idea of what is happening to an overall level, but looking at the receptor on a specific region of the neurons, the PSD, where ethological changes for schizophrenia are thought to be occurring can help bring new knowledge to a very difficult field. With new methods of tissue fractionation, more can be discovered about proteins on specific regions of the neuron.

BA10 and BA46, as stated in chapter one, are both apart of the PFC, frontal pole[66] and middle frontal gyrus[58], respectively. BA46 was used because a previous study in our laboratory looked at this region and found changes in mRNA based on homogenate studies.[117] Because the techniques differ between that article, protein homogenate, and my work, cellular and laminar analysis, this is where these differences could be seen. Since there were differences in my BA10 protein work, and this is extending from the DLPFC protein finding (BA46) from Professor

Shannon Weickert's paper, this suggests that the pathology of schizophrenia could pertain not only to BA46, but may be prefrontal cortex wide, ie changes observed in BA46 may also extend to BA10.

Secondly, I move from protein analysis at the PSD to looking at individual neuron types and how NMDAR NR1 mRNA may be changed specifically in those neurons. It is known that pyramidal neurons, interneurons, and glial cells all work together to keep a healthy brain functioning properly. It could be inferred from animal models using electrophysiology that the NMDAR on inhibitory interneurons would be expected to be decreased in schizophrenia patients [260], even though that is not what my research has found. I did however find pyramidal neurons, although not decreased in total numbers, had a decrease in the amount of NMDAR NR1 being produced. These two points can help the field of schizophrenia research understand what is possibly occurring in brain tissue of schizophrenia patients that differ from control individuals. Furthermore, exploring the normative changes in NMDAR NR1 expression on a per neuron basis during normal aging may provide some mechanistic insights into normative age-related cognitive decline. [261,262]

Glycine modulation was proposed in the 1990's to look at one way schizophrenia may transpire. [87] Blocking glycine transporter 1 was found to increase glycine levels, which would allow more binding of glycine to NMDARs and stimulating them[87,263-265]. In this thesis, I seem to have found that it is the pyramidal neurons are most being affected, thus, they may receive the most benefit from glycine transporter inhibitors.

Subsequently, I have speculated that schizophrenia may be a hypoglutamatergic system, meaning that the system in schizophrenia has less glutamate activity in the pyramidal cells in layer V of the DLPFC. This hypothesis

suggests that a secondary consequence is a decrease in GAD67 in inhibitory interneurons, which this has been the most widely replicated and agreed upon finding in schizophrenia [254,255]. When this was found, it was initially thought that interneuron malfunctions were the cause of this issue, consequently causing the pyramidal cells to be overactive or to actively fire when they should not[256]. But, from this thesis, there is an indication that pyramidal neurons, being the predominant neuron in the cortex, are the initial cause of the problem, leading to a decreased amount of mRNA and protein for the NMDAR NR1 subunit.

When looking at everything together in this thesis, it has been observed that although NMDAR NR1 protein levels are reduced in adult schizophrenia patients, mRNA levels in some interneurons may be preserved. Observations from this, along with other, post-mortem studies researching the pathophysiology of schizophrenia have shown the complexity of this illness. At the molecular level, abnormalities with the NMDAR NR1 subunit have been seen. Through the current data from my research, the NMDAR knowledge should help in understanding more of this complicated illness. Knowing that there is less NMDAR NR1 protein in the PFC, along with less mRNA being produced by excitatory pyramidal neurons, pharmaceutical companies, in the future, could target these specific neurons.

Experimental Limitations and Future Directions

There were a few limitations throughout the research done for this thesis. When working with protein homogenate, it is impossible to tell whether NR1 protein is mainly from pyramidal or interneurons. Doing cell culture and separating interneurons and pyramidal neurons from schizophrenia patients and controls could help with the understanding of where the majority of the protein is from. Isolated hippocampal pyramidal neurons have been cultured to examine

GABA receptors [266]. To complete this research, growing enough pyramidal cells and interneurons in cell culture to run a Western blots or to do immunohistochemistries may be challenging, but seeing how NMDAR levels differ between the two neuron types would be another step forward in schizophrenia research. Another putative method to understanding which neuron type could be malfunctioning at the protein level would be to determine a way to separate pyramidal and interneurons from the human post-mortem brain via cell fractionation so one could see how much protein in being made within each individual cell type. Being able to complete this could allow researchers to understand if mRNA changes directly correlate with changes in protein level.

Another limitation is the use of two different brain regions throughout my thesis. It would have been better to work solely in BA10 or BA46, but due to limited tissue this was not possible. These areas are both part of the frontal cortex and these regions are similar and adjacent to one another, but because they are not the same region, what occurs in one region may not be occurring in the other. There are, indeed, differences in their cytoarchitecture which could potentially cause differences in NMDAR at the protein and mRNA levels. This would impact on the interpretation of results for the protein work and the mRNA work.

Finally, NR1 mRNA and protein levels were found to be altered based on age in a sample of 0 to 25 year old control subjects[77]. Since this cohort ranges over a half century in age difference, the number of subjects for each decade of life is small making it challenging to identify specific changes in NMDAR occurring at different stages of schizophrenia. In science, we are always looking for a larger n to help solidify these findings. There are many factors that could contribute to lack of a clear and dramatic change of molecules in post-mortem brain research. One theory

behind dissociative psychiatric disorders, like schizophrenia, is that there is a waxing and waning of symptoms, and those of NMDAR function, throughout the course of the illnesses[267], and this could be occurring in schizophrenia as well between episodes. This cohort did not provide which stage of illness the person is in at the time of death. If more information could be obtained, it could greatly increase the knowledge base of schizophrenia.

Future Directions and overall conclusions

Throughout this thesis, the NMDAR NR1 subunit has been discussed from the protein and mRNA viewpoints. Further work should be aimed at understanding other subunits that form the NMDAR complex, like NR2A-D and NR3/B. Looking at schizophrenia from the view point of NR1 alone, it has been found that there is a decrease in both protein and mRNA and in this thesis, I support these finding and take an important step forward by having an up close look via subcellular tissue fractionation and cellular histology. This work has helped to illuminate where NR1 is disrupted, the NR1 protein at the PSD and the NR1 mRNA in individual pyramidal neurons. From this, it can be extrapolated that schizophrenia could have a glutamatergic hypofunction cause for some patients. The work in this thesis is important as may cause the schizophrenia research field to reconsider the primacy of NMDAR deficits in interneurons by suggesting that NMDAR deficiency in pyramidal neurons cannot, at least at this stage, be ruled out.

References:

1. Demyttenaere, K. *et al.* Prevalence, severity, and unmet need for treatment of mental disorders in the World Health Organization World Mental Health Surveys. *JAMA* **291,** 2581 (2004).
2. Konradi, C. & Heckers, S. Molecular aspects of glutamate dysregulation: implications for schizophrenia and its treatment. *Pharmacol Ther* **97,** 153–179 (2003).
3. Wyatt, R. J., Alexander, R. C., Egan, M. F. & Kirch, D. G. Schizophrenia, just the facts: What do we know, how well do we know it? *Schizophr Res* **1,** 3–18 (1988).
4. Saha, S. A Systematic Review of Mortality in SchizophreniaIs the Differential Mortality Gap Worsening Over Time? *Arch Gen Psychiatry* **64,** 1123 (2007).
5. Mathers, C. D., Vos, E. T., Stevenson, C. E. & Begg, S. J. The burden of disease and injury in Australia. *Bull World Health Organ* **79,** 1076–1084 (2001).
6. Harkavy-Friedman, J. M. *et al.* Suicidal Behavior in Schizophrenia: Characteristics of Individuals Who Had and Had Not Attempted Suicide. *Am J Psychiatry* **156,** 1276–1278 (1999).
7. Picchioni, M. M. & Murray, R. M. Schizophrenia. *BMJ* **335,** 91–95 (2007).
8. van Os, J. & Kapur, S. Schizophrenia. *Lancet* **374,** 635–645 (2009).
9. Mueser, K. T. & McGurk, S. R. Schizophrenia. *The Lancet* **363,** 2063–2072 (2004).
10. Hanssen, M., Bak, M., Bijl, R., Vollebergh, W. & Os, J. The incidence and outcome of subclinical psychotic experiences in the general population. *Br J Clin Psychol* **44,** 181–191 (2005).

11. Pogue-Geile, M. F. & Harrow, M. Negative and Positive Symptoms in Schizophrenia and Depression: A Followup. *Schizophr Bull* **10,** 371–387 (1984).

12. Andreasen, N. C. Negative Symptoms in SchizophreniaDefinition and Reliability. *Arch Gen Psychiatry* **39,** 784–788 (1982).

13. Association, A. P. *Diagnostic and Statistical Manual of Mental Disorders, Fourth Edition*. (American Psychiatric Pub, 2000).

14. Wang, M. *et al.* Alpha2A-adrenoceptors strengthen working memory networks by inhibiting cAMP-HCN channel signaling in prefrontal cortex. *Cell* **129,** 397–410 (2007).

15. Adler, C., Goldberg, T., Malhotra, A., Pickar, D. & Breier, A. Effects of Ketamine on Thought Disorder, Working Memory, and Semantic Memory in Healthy Volunteers. *Biol Psychiatry* **43,** 811–816 (1998).

16. Moghaddam, B. Targeting metabotropic glutamate receptors for treatment of the cognitive symptoms of schizophrenia. *Psychopharmacology* **174,** 39–44 (2004).

17. Krystal, J. H. *et al.* Subanesthetic Effects of the Noncompetitive NMDA Antagonist, Ketamine, in Humans. *Arch Gen Psychiatry* **51,** 199–214 (1994).

18. Buckley, P. F., Miller, B. J., Lehrer, D. S. & Castle, D. J. Psychiatric comorbidities and schizophrenia. *Schizophr Bull* **35,** 383–402 (2009).

19. Kendler, K. S. & Diehl, S. R. The genetics of schizophrenia. *Schizophr Bull* **19,** 261–285 (1993).

20. Boydell, J., Os, J., McKenzie, K. & Murray, R. M. The association of inequality with the incidence of schizophrenia. *Soc Psychiatry Psychiatr Epidemiol* **39,** 597–599 (2004).

21. Kathleen A Hodgkinson, J. M. S. O. L. B. A. S. B. Genetic Counselling for Schizophrenia in the Era of Molecular Genetics. *Can J Psychiatry* **46,** 123 (2001).

22. Boutros, N. N. *et al.* The status of spectral EEG abnormality as a diagnostic test for schizophrenia. *Schizophr Res* **99,** 225–237 (2008).

23. Ruhrmann, S. S., Schultze-Lutter, F. F. & Klosterkötter, J. J. Early detection and intervention in the initial prodromal phase of schizophrenia. *Pharmacopsychiatry* **36 Suppl 3,** S162–S167 (2003).

24. Tandon, R. Getting ready for DSM-5: Psychotic disorders. *Current Psychiatry* **11,** E1 (2012).

25. Gureje, O. Gender and schizophrenia: age at onset and sociodemographic attributes. *Acta Psychiatr Scand* **83,** 402–405 (1991).

26. McCabe, M. Demographic differences in functional psychoses. *Br J Psychiatry* **127,** 320–320 (1975).

27. Angermeyer, M. C. & K hnz, L. Gender differences in age at onset of Schizophrenia. *Eur Arch Psychiatr Neurol Sci* **237,** 351–364 (1988).

28. Jablensky, A. Prevalence and incidence of schizophrenia spectrum disorders: Implications for prevention. *Aust N Z J Psychiatry* 34 (2000).

29. McGrath, J., Saha, S., Chant, D. & Welham, J. Schizophrenia: A Concise Overview of Incidence, Prevalence, and Mortality. *Epidemiol. Rev.* **30,** 67–76 (2008).

30. Deckmann, M., Mamillapalli, R., Schechtman, L. & Shinitzky, M. A conformational epitope which detects autoantibodies from schizophrenic patients. *Clin Chim Acta* **322,** 91–98 (2002).

31. Pfefferbaum, A. *et al.* A Quantitative Magnetic Resonance Imaging Study of

Changes in Brain Morphology From Infancy to Late Adulthood. *Arch Neurol* **51,** 874–887 (1994).

32. Krubitzer, L. & Kahn, D. M. Nature versus nurture revisited: an old idea with a new twist. *Prog. Neurobiol.* **70,** 33–52 (2003).

33. Jellinger, K. A. Measuring the Mind: Speed, Control and Age. *Eur J Neurol* (2006). doi:10.1111/j.1460-9568.2005.04074.x

34. Benros, M. E. *et al.* Autoimmune Diseases and Severe Infections as Risk Factors for Schizophrenia: A 30-Year Population-Based Register Study. *Am J Psychiatry* **168,** 1303–1310 (2011).

35. Raine, A. & Yang, Y. Neural foundations to moral reasoning and antisocial behavior. *Soc Cognit Affecte Neurosci* **1,** 203–213 (2006).

36. Highley, J. R. *et al.* The size and fibre composition of the corpus callosum with respect to gender and schizophrenia: a post-mortem study. *Brain* **122 (Pt 1),** 99–110 (1999).

37. Honea, R., Crow, T. J., Passingham, D. & Mackay, C. E. Regional Deficits in Brain Volume in Schizophrenia: A Meta-Analysis of Voxel-Based Morphometry Studies. *Am J Psychiatry* **162,** 2233–2245 (2005).

38. Callicott, J. H. *et al.* Physiological dysfunction of the dorsolateral prefrontal cortex in schizophrenia revisited. *Cerebral Cortex* **10,** 1078–1092 (2000).

39. Callicott, J. H. *et al.* Complexity of prefrontal cortical dysfunction in schizophrenia: more than up or down. *Am J Psychiatry* **160,** 2209–2215 (2003).

40. DeYoung, C. G. *et al.* Testing Predictions From Personality Neuroscience: Brain Structure and the Big Five. *Psychological science* **21,** 820–828 (2010).

41. Manoach, D. S. Prefrontal cortex dysfunction during working memory

performance in schizophrenia: reconciling discrepant findings. *Schizophr Res* **60,** 285–298 (2003).

42. Pomarol-Clotet, E. *et al.* Medial prefrontal cortex pathology in schizophrenia as revealed by convergent findings from multimodal imaging. *Mol Psychiatr* **15,** 823–830 (2010).

43. Yang, Y. & Raine, A. Prefrontal structural and functional brain imaging findings in antisocial, violent, and psychopathic individuals: a meta-analysis. *Psychiat Res* **174,** 81–88 (2009).

44. Breier, A. Brain Morphology and SchizophreniaA Magnetic Resonance Imaging Study of Limbic, Prefrontal Cortex, and Caudate Structures. *Arch Gen Psychiatry* **49,** 921 (1992).

45. Miller, E. K., Freedman, D. J. & Wallis, J. D. The prefrontal cortex: categories, concepts and cognition. *Phil. Trans. R. Soc of London Series B, Bio. Sci.* **357,** 1123–1136 (2002).

46. Badre, D. Cognitive control, hierarchy, and the rostro-caudal organization of the frontal lobes. *Trends Cogn Sci* **12,** 193–200 (2008).

47. Garey, L. J. Brodmann's localisation in the cerebral cortex. *London: Smith-Gordon* 109–129 (1994).

48. Nolte, J. *The Human Brain*. (2002).

49. Caspers, S. *et al.* The human inferior parietal cortex: Cytoarchitectonic parcellation and interindividual variability. *NeuroImage* **33,** 430–448 (2006).

50. Zubin, J. *et al.* Biometric Approach to Psychopathology: Abnormal and Clinical Psychology—Statistical, Epidemological, and Diagnostic Approaches. *Annu Rev Psychol* **26,** 621–671 (1975).

51. Wynne, L. C., Cromwell, R. L. & Matthysse, S. The Nature of Schizophrenia. *John Wiley and Sons* 726 (1978). doi:10.1017/S0033291700021826

52. Weinberger, D. R. Physiologic Dysfunction of Dorsolateral Prefrontal Cortex in SchizophreniaI. Regional Cerebral Blood Flow Evidence. *Arch Gen Psychiatry* **43,** 114 (1986).

53. Cohen, J. D., Braver, T. S. & O'Reilly, R. C. A Computational Approach to Prefrontal Cortex, Cognitive Control and Schizophrenia: Recent Developments and Current Challenges. *Phil. Trans. R. Soc of London Series B, Bio. Sci.* **351,** 1515–1527 (1996).

54. Cohen, J. D. *et al.* Temporal dynamics of brain activation during a working memory task. *Nature* **386,** 604–608 (1997).

55. Catts, V., Fung, S., Long, L. & Joshi, D. Rethinking schizophrenia in the context of normal neurodevelopment. *Front Cell Neurosci* (2013).

56. Bekkers, J. M. Pyramidal neurons. *Curr Biol* **21,** R975 (2011).

57. Burgess, P. W., Scott, S. K. & Frith, C. D. The role of the rostral frontal cortex (area 10) in prospective memory: a lateral versus medial dissociation. *Neuropsychologia* **41,** 906–918 (2003).

58. Rajkowska, G. & Goldman-Rakic, P. S. Cytoarchitectonic definition of prefrontal areas in the normal human cortex: I. Remapping of areas 9 and 46 using quantitative criteria. *Cerebral Cortex* **5,** 307–322 (1995).

59. Christoff, K. *et al.* Rostrolateral Prefrontal Cortex Involvement in Relational Integration during Reasoning. *NeuroImage* **14,** 1136–1149 (2001).

60. Selemon, L. D., Rajkowska, G. & Goldman-Rakic, P. S. Elevated neuronal density in prefrontal area 46 in brains from schizophrenic patients: Application of a three-dimensional, stereologic counting method. *J Comp*

Neurol **392,** 402–412 (1998).

61. *The Human Nervous System*. 997–1007 (Elsevier, 2012).

62. Semendeferi, K., Armstrong, E., Schleicher, A., Zilles, K. & Van Hoesen, G. W. Prefrontal cortex in humans and apes: a comparative study of area 10. *Am J Phys Anthropol* **114,** 224–241 (2001).

63. Raichle, M. E. *et al.* A default mode of brain function. *PNAS* **98,** 676–682 (2001).

64. Koechlin, E. & Hyafil, A. Anterior Prefrontal Function and the Limits of Human Decision-Making. *Science* **318,** 594–598 (2007).

65. Rajkowska, G. & Goldman-Rakic, P. S. Cytoarchitectonic definition of prefrontal areas in the normal human cortex: II. Variability in locations of areas 9 and 46 and relationship to the Talairach coordinate system. *Cerebral Cortex* **5,** 323–337 (1995).

66. Burgess, P. W., Gilbert, S. J. & Dumontheil, I. Function and localization within rostral prefrontal cortex (area 10). *Philosophical transactions of the Royal Society of London. Series B, Biological sciences* **362,** 887–899 (2007).

67. Khadka, S., Chityala, S. R., Tian, F. & Liu, H. Photonic Therapeutics and Diagnostics VII. in *SPIE BiOS* (Kollias, N. et al.) **7883,** 78834B–78834B–9 (SPIE, 2011).

68. Luders, E. & Toga, A. W. Sex differences in brain anatomy. *Sex Differences in the Human Brain, Their Underpinnings and Implications* 1 (2011).

69. Eileen Luders, A. W. T. N. L. C. G. The underlying anatomical correlates of long-term meditation: Larger hippocampal and frontal volumes of gray matter. *NeuroImage* **45,** 672 (2009).

70. Damasio, A. R., Graff-Radford, N. R., Eslinger, P. J., Damasio, H. & Kassell, N.

Amnesia Following Basal Forebrain Lesions. *Arch Neurol* **42,** 263–271 (1985).

71. Petrides, M. & Pandya, D. N. Dorsolateral prefrontal cortex: comparative cytoarchitectonic analysis in the human and the macaque brain and corticocortical connection patterns. *Eur J Neuros* **11,** 1011–1036 (1999).

72. Henson, R., Rugg, M. D., Shallice, T. & Dolan, R. J. Confidence in recognition memory for words: Dissociating right prefrontal roles in episodic retrieval. *J. of Cogn. Neurosci.* **12,** 913–923 (2000).

73. Dobbins, I. G., Rice, H. J., Wagner, A. D. & Schacter, D. L. Memory orientation and success: Separable neurocognitive components underlying episodic recognition. *Neuropsychologia* **41,** 318–333 (2003).

74. Coyle, J. T. Glutamate and Schizophrenia: Beyond the Dopamine Hypothesis. *Cell Mol Neurobiol* **26,** 363–382 (2006).

75. Marín, O. Interneuron dysfunction in psychiatric disorders. *Nat Rev Neurosci* (2012). doi:10.1038/nrn3155

76. Benes, F. M. & Berretta, S. GABAergic interneurons: implications for understanding schizophrenia and bipolar disorder. *Neuropsychopharmacol* **25,** 1–27 (2001).

77. Henson, M. A. *et al.* Developmental Regulation of the NMDA Receptor Subunits, NR3A and NR1, in Human Prefrontal Cortex. *Cerebral Cortex* **18,** 2560–2573 (2008).

78. Cull-Candy, S., Brickley, S. & Farrant, M. NMDA receptor subunits: diversity, development and disease. *Curr Opin Neurobiol* **11,** 327–335 (2001).

79. Glausier, J. R. & Lewis, D. A. Selective Pyramidal Cell Reduction of GABAA Receptor α1 Subunit Messenger RNA Expression in Schizophrenia.

Neuropsychopharmacol **36,** 2103–2110 (2011).

80. Dr Stephen M Eggan, D. T. H. D. D. A. L. Reduced Cortical Cannabinoid 1 Receptor Messenger RNA and Protein Expression in Schizophrenia. *Arch Gen Psychiatry* **65,** 772 (2008).

81. Hashimoto, T. *et al.* Alterations in GABA-related transcriptome in the dorsolateral prefrontal cortex of subjects with schizophrenia. *Mol Psychiatr* **13,** 147–161 (2007).

82. Lewis, D. A., Hashimoto, T. & Volk, D. W. Cortical inhibitory neurons and schizophrenia. *Nat Rev Neurosci* **6,** 312–324 (2005).

83. Gonzalez-Burgos, G., Hashimoto, T. & Lewis, D. A. Alterations of Cortical GABA Neurons and Network Oscillations in Schizophrenia. *Curr Psychiatry Rep* **12,** 335–344 (2010).

84. Belsham, B. Glutamate and its role in psychiatric illness. *Hum Psychopharmacol Clin Exp* **16,** 139–146 (2001).

85. Ozawa, S., Kamiya, H. & Tsuzuki, K. Glutamate receptors in the mammalian central nervous system. *Prog. Neurobiol.* **54,** 581–618 (1998).

86. Petralia, R. S., Wang, Y. X. & Wenthold, R. J. The NMDA receptor subunits NR2A and NR2B show histological and ultrastructural localization patterns similar to those of NR1. *J Neurosci* **14,** 6102–6120 (1994).

87. Danysz, W. & Parsons, C. G. Glycine and N-methyl-D-aspartate receptors: physiological significance and possible therapeutic applications. *Pharma. Review* **50,** 597–664 (1998).

88. DeBiasi, S., Minelli, A., Melone, M. & Conti, F. Presynaptic NMDA receptors in the neocortex are both auto- and heteroreceptors. *Neuroreport* **7,** 2773–2776 (1996).

89. Carroll, R. C. & Zukin, R. S. NMDA-receptor trafficking and targeting: implications for synaptic transmission and plasticity. *Trends Neurosci* **25,** 571–577 (2002).

90. Heresco-Levy, U. & Javitt, D. The role of N-methyl-D-aspartate (NMDA) receptor-mediated neurotransmission in the pathophysiology and therapeutics of psychiatric syndromes. *Eur Neuropsychopharm* **8,** 141–152 (1998).

91. Beneyto, M. & Meador-Woodruff, J. H. Lamina-specific abnormalities of NMDA receptor-associated postsynaptic protein transcripts in the prefrontal cortex in schizophrenia and bipolar disorder. *Neuropsychopharmacol* **33,** 2175–2186 (2008).

92. Dingledine, R., Borges, K., Bowie, D. & Traynelis, S. F. The glutamate receptor ion channels. *Pharma. Review* **51,** 7–62 (1999).

93. Emptage, N., Bliss, T. V. & Fine, A. Single synaptic events evoke NMDA receptor-mediated release of calcium from internal stores in hippocampal dendritic spines. *Neuron* **22,** 115–124 (1999).

94. Zandi, M. S. *et al.* Disease-relevant autoantibodies in first episode schizophrenia. *J Neurol* **258,** 686–688 (2011).

95. Kim, J. S., Kornhuber, H. H., Schmid-Burgk, W. & Holzmüller, B. Low cerebrospinal fluid glutamate in schizophrenic patients and a new hypothesis on schizophrenia. *Neurosci Lett* **20,** 379–382 (1980).

96. Jahr, C. E. & Stevens, C. F. Calcium permeability of the N-methyl-D-aspartate receptor channel in hippocampal neurons in culture. *PNAS* **90,** 11573–11577 (1993).

97. Rhoads, J., Guirgis, H., McKnight, C. & Duchemin, A.-M. Lack of anti-NMDA

receptor autoantibodies in the serum of subjects with schizophrenia. *Schizophr Res* **129,** 213–214 (2011).

98. Paoletti, P. & Neyton, J. NMDA receptor subunits: function and pharmacology. *Curr Opin Pharma* **7,** 39–47 (2007).

99. Bodarky, C. L. *et al.* Novel Environment and GABA Agonists Alter Event-Related Potentials in N-Methyl-D-aspartate NR1 Hypomorphic and Wild-Type Mice. *J Pharmacol Exp Ther* **331,** 308–318 (2009).

100. Lahti, A. C., Weiler, M. A., Tamara Michaelidis, B. A., Parwani, A. & Tamminga, C. A. Effects of ketamine in normal and schizophrenic volunteers. *Neuropsychopharmacol* **25,** 455–467 (2001).

101. Kornhuber, J. *et al.* (3H]MK-801 binding sites in postmortem brain regions of schizophrenic patients. *J Neural Transm* **77,** 231–236 (1989).

102. Huettner, J. E. J. & Bean, B. P. B. Block of N-methyl-D-aspartate-activated current by the anticonvulsant MK-801: selective binding to open channels. *PNAS* **85,** 1307–1311 (1988).

103. Catts, V. & Catts, S. in *Secondary Schizophrenia* (Sachdev, P. & Keshavan, M.) 1–69 (Critical University Press, 2010).

104. Javitt, D. C. & Zukin, S. R. Recent advances in the phencyclidine model of schizophrenia. *Am J Psychiatry* **148,** 1301–1308 (1991).

105. Nudmamud-Thanoi, S. & Reynolds, G. P. The NR1 subunit of the glutamate/NMDA receptor in the superior temporal cortex in schizophrenia and affective disorders. *Neurosci Lett* **372,** 173–177 (2004).

106. Dracheva, S. *et al.* N-methyl-D-aspartic acid receptor expression in the dorsolateral prefrontal cortex of elderly patients with schizophrenia. *Am J Psychiatry* **158,** 1400–1410 (2001).

107. Beneyto, M., Kristiansen, L. V., Oni-Orisan, A., McCullumsmith, R. E. & Meador-Woodruff, J. H. Abnormal glutamate receptor expression in the medial temporal lobe in schizophrenia and mood disorders. *Neuropsychopharmacol* **32,** 1888–1902 (2007).

108. Paoletti, P., Bellone, C. & Zhou, Q. NMDA receptor subunit diversity: impact on receptor properties, synaptic plasticity and disease. *Nat Rev Neurosci* **14,** 383–400 (2013).

109. Grimwood, S., Slater, P., Deakin, J. F. & Hutson, P. H. NR2B-containing NMDA receptors are up-regulated in temporal cortex in schizophrenia. *Neuroreport* **10,** 461–465 (1999).

110. Carlsson, A. *et al.* Interactions between monoamines, glutamate, and GABA in schizophrenia: new evidence. *Annu Rev Pharmacol Toxicol* **41,** 237–260 (2001).

111. Traynelis, S. F. S. *et al.* Glutamate receptor ion channels: structure, regulation, and function. *Pharma. Review* **62,** 405–496 (2010).

112. Blahos, J., II & Wenthold, R. J. Relationship between N-methyl-D-aspartate receptor NR1 splice variants and NR2 subunits. *J Biol Chem* **271,** 15669–15674 (1996).

113. Das, S. *et al.* Increased NMDA current and spine density in mice lacking the NMDA receptor subunit NR3A. *Nature* **393,** 377–381 (1998).

114. Perez-Otano, I. *et al.* Assembly with the NR1 subunit is required for surface expression of NR3A-containing NMDA receptors. *J Neurosci* **21,** 1228–1237 (2001).

115. Hahn, C. G. *et al.* The Post-Synaptic Density of Human Postmortem Brain Tissues: An Experimental Study Paradigm for Neuropsychiatric Illnesses.

PLoS ONE **4,** e5251 (2009).

116. Hahn, C.-G. *et al.* Altered neuregulin 1–erbB4 signaling contributes to NMDA receptor hypofunction in schizophrenia. *Nat Med* **12,** 824–828 (2006).

117. Weickert, C. S. *et al.* Molecular evidence of N-methyl-D-aspartate receptor hypofunction in schizophrenia. *Mol Psychiatr* **18,** 1185–1192 (2013).

118. Gao, X. M. *et al.* Ionotropic glutamate receptors and expression of N-methyl-D-aspartate receptor subunits in subregions of human hippocampus: effects of schizophrenia. *Am J Psychiatry* **157,** 1141–1149 (2000).

119. Law, A. J. & Deakin, J. F. W. Asymmetrical reductions of hippocampal NMDAR1 glutamate receptor mRNA in the psychoses. *Neuroreport* **12,** 2971–2974 (2001).

120. Humphries, C., Mortimer, A., Hirsch, S. & de Belleroche, J. NMDA receptor mRNA correlation with antemortem cognitive impairment in schizophrenia. *Neuroreport* **7,** 2051–2055 (1996).

121. Sokolov, B. P. Expression of NMDAR1, GluR1, GluR7, and KA1 glutamate receptor mRNAs is decreased in frontal cortex of 'neuroleptic-free' schizophrenics: evidence on reversible up-regulation by typical neuroleptics. *J Neurochem* **71,** 2454–2464 (1998).

122. Akbarian, S. *et al.* Maldistribution of interstitial neurons in prefrontal white matter of the brains of schizophrenic patients. *Arch Gen Psychiatry* **53,** 425–436 (1996).

123. McCullumsmith, R. E. *et al.* Decreased NR1, NR2A, and SAP102 transcript expression in the hippocampus in bipolar disorder. *Brain Res* **1127,** 108–118 (2007).

124. Vrajová, M. *et al.* Expression of the Hippocampal NMDA Receptor GluN1 Subunit and Its Splicing Isoforms in Schizophrenia: Postmortem Study. *Neurochemical Research* **35,** 994–1002 (2010).

125. Le Corre, S., Harper, C., Lopez, P., Ward, P. & Catts, S. V. Increased levels of expression of an NMDARI splice variant in the superior temporal gyrus in schizophrenia. *Neuroreport* **11,** 983–986 (2000).

126. Beckwith, J. P., Stefanis, N. C., McLaughlin, D. P. & Kerwin, R. W. The expression of NMDA receptor subunits in schizophrenic post-mortem human hippocampus. *Schizophr Res* **15,** 54 (1995).

127. Gonzalez, R. A. *et al.* N-methyl-D-aspartate mediated responses decrease with age in Fischer 344 rat brain. *Neurobiol Aging* **12,** 219–225 (1991).

128. Wenk, G. L., Walker, L. C., Price, D. L. & Cork, L. C. Loss of NMDA, but not GABA-A, binding in the brains of aged rats and monkeys. *Neurobiology of Aging* **12,** 93–98 (1991).

129. Magnusson, K. R. & Cotman, C. W. Age-related changes in excitatory amino acid receptors in two mouse strains. *Neurobiology of Aging* **14,** 197–206 (1993).

130. Saransaari, P. & Oja, S. S. Dizocilpine binding to cerebral cortical membranes from developing and ageing mice. *Mechanisms of Ageing and Development* **85,** 171–181 (1995).

131. Magnusson, K. R. Aging of the NMDA receptor: from a mouse's point of view. *Future neurology* **7,** 627–637 (2012).

132. Errico, F. *et al.* Decreased levels of d-aspartate and NMDA in the prefrontal cortex and striatum of patients with schizophrenia. *J Psychiatr Res* (2013). doi:10.1016/j.jpsychires.2013.06.013

133. Kristiansen, L. V., Beneyto, M., Haroutunian, V. & Meador-Woodruff, J. H. Changes in NMDA receptor subunits and interacting PSD proteins in dorsolateral prefrontal and anterior cingulate cortex indicate abnormal regional expression in schizophrenia. *Mol Psychiatr* **11,** 737–747 (2006).

134. Emamian, E. S., Karayiorgou, M. & Gogos, J. A. Decreased Phosphorylation of NMDA Receptor Type 1 at Serine 897 in Brains of Patients with Schizophrenia. *jneurosci.org*

135. Toro, C. & Deakin, J. F. W. NMDA receptor subunit NRI and postsynaptic protein PSD-95 in hippocampus and orbitofrontal cortex in schizophrenia and mood disorder. *Schizophr Res* **80,** 323–330 (2005).

136. Kristiansen, L. V., Patel, S. A., Haroutunian, V. & Meador-Woodruff, J. H. Expression of the NR2B-NMDA receptor subunit and its Tbr-1/CINAP regulatory proteins in postmortem brain suggest altered receptor processing in schizophrenia. *Synapse* **64,** 495–502 (2010).

137. Kennedy, M. J. & Ehlers, M. D. Organelles and trafficking machinery for postsynaptic plasticity. *NSC* **29,** 325–362 (2005).

138. Scannevin, R. H. & Huganir, R. L. Postsynaptic organization and regulation of excitatory synapses. *Nat Rev Neurosci* **1,** 133–142 (2000).

139. Kalantzis, G. & Shouval, H. Z. Structural Plasticity Can Produce Metaplasticity. *PLoS ONE* **4,** e8062 (2009).

140. Seagar, M. & Takahashi, M. Interactions between presynaptic calcium channels and proteins implicated in synaptic vesicle trafficking and exocytosis. *J Bioenerg Biomembr* **30,** 347–356 (1998).

141. Seagar, M. *et al.* Interactions between proteins implicated in exocytosis and voltage-gated calcium channels. *Phil. Trans. R. Soc. B* **354,** 289–297 (1999).

142. Sheng, M. & Hoogenraad, C. C. The postsynaptic architecture of excitatory synapses: a more quantitative view. *Annu Rev Biochem* **76,** 823–847 (2007).

143. Kim, E. & Sheng, M. PDZ domain proteins of synapses. *Nat Rev Neurosci* **5,** 771–781 (2004).

144. Lewis, D. A. Cognitive Dysfunction in SchizophreniaConvergence of γ-Aminobutyric Acid and Glutamate Alterations. *Arch Neurol* **63,** 1372 (2006).

145. Talbot, K. K. *et al.* Dysbindin-1 is a synaptic and microtubular protein that binds brain snapin. *Hum Mol Genet* **15,** 3041–3054 (2006).

146. Harrison, P. J. & Weinberger, D. R. Schizophrenia genes, gene expression, and neuropathology: on the matter of their convergence. *Mol Psychiatr* **10,** 40–68– image 5 (2005).

147. Behan, Á., Byrne, C., Dunn, M. J., Cagney, G. & Cotter, D. R. Proteomic analysis of membrane microdomain-associated proteins in the dorsolateral prefrontal cortex in schizophrenia and bipolar disorder reveals alterations in LAMP, STXBP1 and BASP1 protein expression. *Mol Psychiatr* **14,** 601–613 (2008).

148. Lewis, D. A. The Human Brain Revisited: Opportunities and Challenges in Postmortem Studies of Psychiatric Disorders. *Neuropsychopharmacol* **26,** 143–154 (2002).

149. Crecelius, A. *et al.* Assessing quantitative post-mortem changes in the gray matter of the human frontal cortex proteome by 2-D DIGE. *Proteomics* **8,** 1276–1291 (2008).

150. Blanpied, T. A. & Ehlers, M. D. Microanatomy of dendritic spines: Emerging

principles of synaptic pathology in psychiatric and neurological disease. *Biol Psychiatry* **55,** 1121–1127 (2004).

151. Groc, L. & Choquet, D. AMPA and NMDA glutamate receptor trafficking: multiple roads for reaching and leaving the synapse. *Cell Tissue Res* **326,** 423–438 (2006).

152. Ehlers, M. D. Activity level controls postsynaptic composition and signaling via the ubiquitin-proteasome system. *Nat Neurosci* **6,** 231–242 (2003).

153. Blanke, M. L. & VanDongen, A. M. J. Activation Mechanisms of the NMDA Receptor. (2009).

154. Tabone, C. J. & Ramaswami, M. Is NMDA Receptor-Coincidence Detection Required for Learning and Memory? *Neuron* **74,** 767–769 (2012).

155. Matsuzaki, M. *et al.* Dendritic spine geometry is critical for AMPA receptor expression in hippocampal CA1 pyramidal neurons. *Nat Neurosci* **4,** 1086–1092 (2001).

156. Siekevitz, P. The postsynaptic density: a possible role in long-lasting effects in the central nervous system. *PNAS* **82,** 3494–3498 (1985).

157. Malenka, R. C. & Nicoll, R. A. Long-term potentiation--a decade of progress? *Science* **285,** 1870–1874 (1999).

158. Lan, J. Y. *et al.* Protein kinase C modulates NMDA receptor trafficking and gating. *Nat Neurosci* **4,** 382–390 (2001).

159. Nusser, Z. *et al.* Cell Type and Pathway Dependence of Synaptic AMPA Receptor Number and Variability in the Hippocampus. *Neuron* **21,** 545–559 (1998).

160. Wong, J. *et al.* Promoter specific alterations of brain-derived neurotrophic factor mRNA in schizophrenia. *NSC* **169,** 1071–1084 (2010).

161. Hall, R. A. & Soderling, T. R. Differential surface expression and phosphorylation of the N-methyl-D-aspartate receptor subunits NR1 and NR2 in cultured hippocampal neurons. *J Biol Chem* **272,** 4135–4140 (1997).

162. Horak, M. & Wenthold, R. J. Different Roles of C-terminal Cassettes in the Trafficking of Full-length NR1 Subunits to the Cell Surface. *J Biol Chem* **284,** 9683–9691 (2009).

163. Dalmau, J. *et al.* Anti-NMDA-receptor encephalitis: case series and analysis of the effects of antibodies. *Lancet Neurol* **7,** 1091–1098 (2008).

164. Kantrowitz, J. T. & Javitt, D. C. N-methyl-d-aspartate (NMDA) receptor dysfunction or dysregulation: The final common pathway on the road to schizophrenia? *Brain Res Bull* **83,** 108–121 (2010).

165. Murray, F. *et al.* Modulation of [3H]MK-801 binding to NMDA receptors in vivo and in vitro. *Eur J Pharmacol* **397,** 263–270 (2000).

166. Lynch, D. R. & Guttmann, R. P. Excitotoxicity: perspectives based on N-methyl-D-aspartate receptor subtypes. *J Pharmacol Exp Ther* **300,** 717–723 (2002).

167. Lau, C. G. & Zukin, R. S. NMDA receptor trafficking in synaptic plasticity and neuropsychiatric disorders. *Nat Rev Neurosci* **8,** 413–426 (2007).

168. Kristiansen, L. V., Bakir, B., Haroutunian, V. & Meador-Woodruff, J. H. Expression of the NR2B-NMDA receptor trafficking complex in prefrontal cortex from a group of elderly patients with schizophrenia. *Schizophr Res* **119,** 198–209 (2010).

169. Cuthbert, P. C. *et al.* Synapse-Associated Protein 102/dlgh3 Couples the NMDA Receptor to Specific Plasticity Pathways and Learning Strategies. *J Neurosci* **27,** 2673–2682 (2007).

170. Coyle, J. T. NMDA Receptor and Schizophrenia: A Brief History. *Schizophr Bull* **38,** 920–926 (2012).

171. Anderson, G. & Maes, M. Schizophrenia: Linking prenatal infection to cytokines, the tryptophan catabolite (TRYCAT) pathway, NMDA receptor hypofunction, neurodevelopment and neuroprogression. *Prog. Neuropsychopharmacol. Biol. Psychiatry* (2012). doi:10.1016/j.pnpbp.2012.06.014

172. López-Gil, X. *et al.* Importance of inter-hemispheric prefrontal connection in the effects of non-competitive NMDA receptor antagonists. *Int J Neuropsychopharmacol* **15,** 945–956 (2012).

173. Dzirasa, K. *et al.* Hyperdopaminergia and NMDA receptor hypofunction disrupt neural phase signaling. *J Neurosci* **29,** 8215–8224 (2009).

174. Meador-Woodruff, J. H., Clinton, S. M., Beneyto, M. & McCullumsmith, R. E. Molecular abnormalities of the glutamate synapse in the thalamus in schizophrenia. *Ann N Y Acad Sci* **1003,** 75–93 (2003).

175. Gandal, M. J. *et al.* Mice with reduced NMDA receptor expression: more consistent with autism than schizophrenia? *Genes Brain Behav.* **11,** 740–750 (2012).

176. Kristiansen, L. V. & Meador-Woodruff, J. H. Abnormal striatal expression of transcripts encoding NMDA interacting PSD proteins in schizophrenia, bipolar disorder and major depression. *Schizophr Res* **78,** 87–93 (2005).

177. Halene, T. B. *et al.* Assessment of NMDA receptor NR1 subunit hypofunction in mice as a model for schizophrenia. *Genes Brain Behav.* **8,** 661–675 (2009).

178. Miyamoto, Y. *et al.* Hyperfunction of dopaminergic and serotonergic

neuronal systems in mice lacking the NMDA receptor epsilon1 subunit. *J Neurosci* **21,** 750–757 (2001).

179. Harlow, E. & Lane, D. *Using Antibodies*. (Cold Spring Harbor Laboratory Press, 1998).

180. Catts, V. S. *et al.* A microarray study of post-mortem mRNA degradation in mouse brain tissue. *Mol Brain Res* **138,** 164–177 (2005).

181. Li, J. Z. *et al.* Systematic changes in gene expression in postmortem human brains associated with tissue pH and terminal medical conditions. *Hum Mol Genet* **13,** 609–616 (2004).

182. Hynd, M. R., Lewohl, J. M., Scott, H. L. & Dodd, P. R. Biochemical and molecular studies using human autopsy brain tissue. *J Neurochem* **85,** 543–562 (2003).

183. Wetmur, J. G., Ruyechan, W. T. & Douthart, R. J. Denaturation and renaturation of Penicillium chrysogenum mycophage double-stranded ribonucleic acid in tetraalkylammonium salt solutions. *Biochemistry* **20,** 2999–3002 (1981).

184. Wilcox, J. N. Fundamental principles of in situ hybridization. *J Histochem Cytochem* **41,** 1725–1733 (1993).

185. Pardue, M. L. & Gall, J. G. Molecular hybridization of radioactive DNA to the DNA of cytological preparations. *PNAS* **64,** 600–604 (1969).

186. *DIG Application Manual*. (Roche Diagnostics GmbH, 2002).

187. Harper, M. E., Marselle, L. M., Gallo, R. C. & Wong-Staal, F. Detection of lymphocytes expressing human T-lymphotropic virus type III in lymph nodes and peripheral blood from infected individuals by in situ hybridization. *PNAS* **83,** 772–776 (1986).

188. Cotter, D. *et al.* Reduced neuronal size and glial cell density in area 9 of the dorsolateral prefrontal cortex in subjects with major depressive disorder. *Cerebral Cortex* **12,** 386–394 (2002).

189. Hoftman, G. D. & Lewis, D. A. Lamina-Specific Alterations in Cortical GABAA Receptor Subunit Expression in Schizophrenia. *Cerebral Cortex* **21,** 999–1011 (2011).

190. Noguchi, I., Arai, H. & Iizuka, R. A study on postmortem stability of vasopressin messenger RNA in rat brain compared with those in total RNA and ribosomal RNA. *J Neural Transm* **83,** 171–178 (1991).

191. Kepecs, A. & Fishell, G. Interneuron cell types are fit to function. *Nature* **505,** 318–326 (2014).

192. McBain, C. J. & Fisahn, A. Interneurons unbound. *Nat Rev Neurosci* **2,** 11–23 (2001).

193. Belforte, J. E. *et al.* Postnatal NMDA receptor ablation in corticolimbic interneurons confers schizophrenia-like phenotypes. *Nat Neurosci* **13,** 76–83 (2010).

194. Weickert, C. S. *et al.* Selection of reference gene expression in a schizophrenia brain cohort. *Aust N Z J Psychiatry* **44,** 59–U21 (2010).

195. Weickert, C. S. *et al.* Selection of reference gene expression in a schizophrenia brain cohort. *Aust N Z J Psychiatry* **44,** 59–70 (2010).

196. Hardy, J. A. *et al.* The patients dying after long terminal phase have acidotic brains; implications for biochemical measurements on autopsy tissue. *J Neural Transm* **61,** 253–264 (1985).

197. Tomita, H. *et al.* Effect of agonal and postmortem factors on gene expression profile: quality control in microarray analyses of postmortem

human brain. *Biol Psychiatry* **55,** 346–352 (2004).

198. Mexal, S. *et al.* Brain pH has a significant impact on human postmortem hippocampal gene expression profiles. *Brain Res* **1106,** 1–11 (2006).

199. Levin, E. D. & Simon, B. B. Nicotinic acetylcholine involvement in cognitive function in animals. *Psychopharmacology* **138,** 217–230 (1998).

200. Leonard, S. Consequences of low levels of nicotinic acetylcholine receptors in schizophrenia for drug development. *Drug Development Research* **60,** 127–136 (2003).

201. Cotman, C. W., Banker, G., Churchill, L. & Taylor, D. Isolation of postsynaptic densities from rat brain. *J Cell Biol* **63,** 441–455 (1974).

202. Phillips, G. R. *et al.* The presynaptic particle web: Ultrastructure, composition, dissolution, and reconstitution. *Neuron* **32,** 63–77 (2001).

203. Chong, V. Z. *et al.* Elevated neuregulin-1 and ErbB4 protein in the prefrontal cortex of schizophrenic patients. *Schizophr Res* **100,** 270–280 (2008).

204. Calhoun, M. E. *et al.* Comparative evaluation of synaptophysin-based methods for quantification of synapses. *J Neurocytol* **25,** 821–828 (1996).

205. Kim, K. K., Adelstein, R. S. & Kawamoto, S. Identification of Neuronal Nuclei (NeuN) as Fox-3, a New Member of the Fox-1 Gene Family of Splicing Factors. *J Biol Chem* **284,** 31052–31061 (2009).

206. Ugwu, S. O. & Apte, S. P. The effect of buffers on protein conformational stability. *Pharm.Tech.* **28,** 86–109 (2004).

207. Hara, Y. & Pickel, V. M. Preferential relocation of the N-methyl-d-aspartate receptor NR1 subunit in nucleus accumbens neurons that contain dopamine D1 receptors in rats showing an apomorphine-induced sensorimotor gating deficit. *Neuroscience* **154,** 965–977 (2008).

208. Sans, N. *et al.* NMDA receptor trafficking through an interaction between PDZ proteins and the exocyst complex. *Nat Cell Biol* **5,** 520–530 (2003).

209. Mullen, R. J., Buck, C. R. & Smith, A. M. NeuN, a neuronal specific nuclear protein in vertebrates. *Development* **116,** 201–211 (1992).

210. Lind, D., Franken, S., Kappler, J., Jankowski, J. & Schilling, K. Characterization of the neuronal marker NeuN as a multiply phosphorylated antigen with discrete subcellular localization. *J Neurosci Res* **79,** 295–302 (2005).

211. Wickstead, B. & Gull, K. Evolution: The evolution of the cytoskeleton. *The Journal of Cell Biology* **194,** 513 (2011).

212. Kristiansen, L. V., Huerta, I., Beneyto, M. & Meador-Woodruff, J. H. NMDA receptors and schizophrenia. *Curr Opin Pharma* **7,** 48–55 (2007).

213. Karolewicz, B. *et al.* Elevated levels of NR2A and PSD-95 in the lateral amygdala in depression. *Int J Neuropsychopharmacol* **12,** 143–153 (2009).

214. Sifonios, L. *et al.* An enriched environment restores normal behavior while providing cytoskeletal restoration and synaptic changes in the hippocampus of rats exposed to an experimental model of depression. *Neuroscience* **164,** 929–940 (2009).

215. Niciu, M. J., Kelmendi, B. & Sanacora, G. Overview of glutamatergic neurotransmission in the nervous system. *Pharmacol. Biochem. Behav.* **100,** 656–664 (2012).

216. Toyooka, K. *et al.* Selective reduction of a PDZ protein, SAP-97, in the prefrontal cortex of patients with chronic schizophrenia. *J Neurochem* **83,** 797–806 (2002).

217. Forrest, D. *et al.* Targeted disruption of NMDA receptor 1 gene abolishes NMDA response and results in neonatal death. *Neuron* **13,** 325–338 (1994).

218. Kutsuwada, T. *et al.* Impairment of suckling response, trigeminal neuronal pattern formation, and hippocampal LTD in NMDA receptor epsilon 2 subunit mutant mice. *Neuron* **16,** 333–344 (1996).

219. Mohn, A. R., Gainetdinov, R. R., Caron, M. G. & Koller, B. H. Mice with reduced NMDA receptor expression display behaviors related to schizophrenia. *Cell* **98,** 427–436 (1999).

220. Moghaddam, B. & Javitt, D. From revolution to evolution: the glutamate hypothesis of schizophrenia and its implication for treatment. *Neuropsychopharmacol* **37,** 4–15 (2012).

221. Itokawa, M. *et al.* A microsatellite repeat in the promoter of the N-methyl-D-aspartate receptor 2A subunit (GRIN2A) gene suppresses transcriptional activity and correlates with chronic outcome in schizophrenia. *Pharmacogenetics* **13,** 271–278 (2003).

222. Koutsouleris, N. *et al.* Accelerated Brain Aging in Schizophrenia and Beyond: A Neuroanatomical Marker of Psychiatric Disorders. *Schizophr Bull* **40,** 1140–1153 (2014).

223. Schmitt, A. *et al.* Effects of long-term antipsychotic treatment on NMDA receptor binding and gene expression of subunits. *Neurochemical Research* **23,** 235–241 (2003).

224. Weickert, C. S. *et al.* Reductions in neurotrophin receptor mRNAs in the prefrontal cortex of patients with schizophrenia. *Mol Psychiatr* **10,** 637–650 (2005).

225. Pierri, J. N., Volk, C. L. E., Auh, S., Sampson, A. & Lewis, D. A. Decreased Somal Size of Deep Layer 3 Pyramidal Neurons in the Prefrontal Cortex of Subjects With Schizophrenia. *Arch Gen Psychiatry* **58,** 466–473 (2001).

226. Glantz, L. A. & Lewis, D. A. Decreased dendritic spine density on prefrontal cortical pyramidal neurons in schizophrenia. *Arch Gen Psychiatry* **57,** 65–73 (2000).

227. Keshavan, M. S., Tandon, R., Boutros, N. N. & Nasrallah, H. A. Schizophrenia, 'just the facts': what we know in 2008 Part 3: neurobiology. *Schizophr Res* **106,** 89–107 (2008).

228. Fung, S. J. *et al.* Expression of interneuron markers in the dorsolateral prefrontal cortex of the developing human and in schizophrenia. *Am J Psychiatry* **167,** 1479–1488 (2010).

229. Gassmann, M., Grenacher, B., Rohde, B. & Vogel, J. Quantifying Western blots: Pitfalls of densitometry. *Electrophoresis* **30,** 1845–1855 (2009).

230. Sinclair, D., Webster, M. J., Fullerton, J. M. & Weickert, C. Glucocorticoid receptor mRNA and protein isoform alterations in the orbitofrontal cortex in schizophrenia and bipolar disorder. *BMC Psychiatry* **12,** 84 (2012).

231. Weickert, C. S. *et al.* Reduced GAP-43 mRNA in dorsolateral prefrontal cortex of patients with schizophrenia. *Cerebral Cortex* **11,** 136–147 (2001).

232. Meador-Woodruff, J. H., Davis, K. L. & Haroutunian, V. Abnormal kainate receptor expression in prefrontal cortex in schizophrenia. *Neuropsychopharmacol* **24,** 545–552 (2001).

233. Haijma, S. V. *et al.* Brain volumes in schizophrenia: a meta-analysis in over 18 000 subjects. *Schizophr Bull* **39,** 1129–1138 (2013).

234. Meoni, P., Bunnemann, B. H., Kingsbury, A. E., Trist, D. G. & Bowery, N. G. NMDA NR1 subunit mRNA and glutamate NMDA-sensitive binding are differentially affected in the striatum and pre-frontal cortex of Parkinson's disease patients. *Neuropharmacology* **38,** 625–633 (1999).

235. Gluhak-Heinrich, J., Yang, W., Harris, M. A. & Harris, S. E. Quantitative in situ hybridization with enhanced sensitivity in soft, bone and tooth tissue using digoxigenin tagged RNA probes. *Biochem Med* 59–80 (2008). doi:10.11613/BM.2008.008

236. Weickert, C. S. *et al.* Reduced brain-derived neurotrophic factor in prefrontal cortex of patients with schizophrenia. *Mol Psychiatr* **8,** 592–610 (2003).

237. Pearson, E. C., Bates, D. L., Prospero, T. D. & Thomas, J. O. Neuronal nuclei and glial nuclei from mammalian cerebral cortex. *European Journal of Biochemistry* **144,** 353–360 (1984).

238. Liu, P., Smith, P. F. & Darlington, C. L. Glutamate receptor subunits expression in memory-associated brain structures: Regional variations and effects of aging. *Synapse* **62,** 834–841 (2008).

239. Goldman-Rakic, P. S. Development of cortical circuitry and cognitive function. *Child Dev* 601–622 (1987).

240. Rajkowska, G., Selemon, L. D. & Goldman-Rakic, P. S. Neuronal and glial somal size in the prefrontal cortex: a postmortem morphometric study of schizophrenia and Huntington disease. *Arch Gen Psychiatry* **55,** 215 (1998).

241. Adell, A., Jiménez-Sánchez, L., López-Gil, X. & Romón, T. Is the acute NMDA receptor hypofunction a valid model of schizophrenia? *Schizophr Bull* **38,** 9–14 (2012).

242. Moghaddam, B., Adams, B., Verma, A. & Daly, D. Activation of glutamatergic neurotransmission by ketamine: a novel step in the pathway from NMDA receptor blockade to dopaminergic and cognitive disruptions associated with the prefrontal cortex. *J Neurosci* **17,** 2921–2927 (1997).

243. Stone, J. M. Glutamatergic antipsychotic drugs: a new dawn in the treatment of schizophrenia? *Therapeutic Advances in Psychopharmacology* **1,** 5–18 (2011).

244. Akazawa, C., Shigemoto, R., Bessho, Y., Nakanishi, S. & Mizuno, N. Differential expression of five N-methyl-D-aspartate receptor subunit mRNAs in the cerebellum of developing and adult rats. *J Comp Neurol* **347,** 150–160 (1994).

245. Andreasen, N. *et al.* Structural abnormalities in the frontal system in schizophrenia. A magnetic resonance imaging study. *Arch Gen Psychiatry* **43,** 136–144 (1986).

246. Mesches, M. H. *et al.* Sulindac improves memory and increases NMDA receptor subunits in aged Fischer 344 rats. *Neurobiology of Aging* **25,** 315–324 (2004).

247. Preece, P. & Cairns, N. J. Quantifying mRNA in postmortem human brain: influence of gender, age at death, postmortem interval, brain pH, agonal state and inter-lobe mRNA variance. *Mol Brain Res* **118,** 60–71 (2003).

248. Bitanihirwe, B. K., Lim, M. P. & Woo, T.-U. W. N-methyl-D-aspartate receptor expression in parvalbumin-containing inhibitory neurons in the prefrontal cortex in bipolar disorder. *Bipolar Disorders* **12,** 95–101 (2010).

249. Hynd, M. R., Scott, H. L. & Dodd, P. R. GlutamateNMDA receptor NR1 subunit mRNA expression in Alzheimer's disease. *J Neurochem* **78,** 175–182 (2001).

250. Harrison, P., Laatikainen, L., Tunbridge, E. & Eastwood, S. Human brain weight is correlated with expression of the 'housekeeping genes' beta-2-microglobulin (β2M) and TATA-binding protein (TBP). *Neuropath Appl Neuro* **36,** 498–504 (2010).

251. Peper, J. S. *et al.* Genetic influences on human brain structure: a review of brain imaging studies in twins. *Hum Brain Mapp* **28,** 464–473 (2007).

252. Boulanger, L. M. Immune Proteins in Brain Development and Synaptic Plasticity. *Neuron* **64,** 93–109 (2009).

253. Alvarez, V. A. & Sabatini, B. L. Anatomical and physiological plasticity of dendritic spines. *Annu Rev Neurosci* **30,** 79–97 (2007).

254. Guidotti, A. *et al.* Decrease in Reelin and Glutamic Acid Decarboxylase67 (GAD67) Expression in Schizophrenia and Bipolar Disorder: A Postmortem Brain Study. *Arch Gen Psychiatry* **57,** 1061–1069 (2000).

255. Huang, H.-S. & Akbarian, S. GAD1 mRNA expression and DNA methylation in prefrontal cortex of subjects with schizophrenia. *PLoS ONE* **2,** e809 (2007).

256. Nakazawa, K. *et al.* GABAergic interneuron origin of schizophrenia pathophysiology. *Neuropharmacology* **62,** 1574–1583 (2012).

257. Köpke, A. K. A., Bonk, I. I., Sydow, S. S., Menke, H. H. & Spiess, J. J. Characterization of the NR1, NR2A, and NR2C receptor proteins. *Protein Sci* **2,** 2066–2076 (1993).

258. Catts, S. V. *et al.* Molecular Biological Investigations into the Role of the NMDA Receptor in the Pathophysiology of Schizophrenia. *Aust N Z J Psychiatry* **31,** 17–26 (1997).

259. Owens, D. F. & Kriegstein, A. R. Developmental neurotransmitters? *Neuron* **36,** 989–991 (2002).

260. Wyneken, U., Marengo, J. & Orrego, F. Electrophysiology and plasticity in isolated postsynaptic densities. in *Brain Res Rev* **47,** 54–70 (2004).

261. Hara, Y., Rapp, P. R. & Morrison, J. H. Neuronal and morphological bases of

cognitive decline in aged rhesus monkeys. *Age* **34,** 1051 (2012).

262. Hara, Y. *et al.* Synaptic correlates of memory and menopause in the hippocampal dentate gyrus in rhesus monkeys. *Neurobiology of Aging* **33,** 421.e17–421.e28 (2012).

263. Javitt, D. C. *et al.* Reversal of phencyclidine-induced dopaminergic dysregulation by N-methyl-D-aspartate receptor/glycine-site agonists. *Neuropsychopharmacol* **29,** 300–307 (2004).

264. Thomas, J. W., Hood, W. F., Monahan, J. B., Contreras, P. C. & O'Donohue, T. L. Glycine modulation of the phencyclidine binding site in mammalian brain. *Brain Res* **442,** 396–398 (1988).

265. Ransom, R. W. & Deschenes, N. L. Glycine modulation of NMDA-evoked release of [3H]acetylcholine and [3H]dopamine from rat striatal slices. *Neurosci Lett* **96,** 323–328 (1989).

266. Mangan, P. S. Cultured Hippocampal Pyramidal Neurons Express Two Kinds of GABAA Receptors. *Mol Pharmacol* **67,** 775–788 (2004).

267. García-Campayo, J., Fayed, N., Serrano-Blanco, A. & Roca, M. Brain dysfunction behind functional symptoms: neuroimaging and somatoform, conversive, and dissociative disorders. *Curr Opin Psychiatry* **22,** 224–231 (2009).

Appendix 1: Solutions

ChemiDoc

Electrochemoluminescence (ECL)

- 500µL of lumin
- 500µL of perox

In situ hybridisation with riboprobes:

0.1M Triethanolamin-HCl

- 37.14g TEA 2L of DEP diH_2O
- Adjust pH to 8 with 10N NaOH
- Shake well

1x Hybridisation Buffer

- 5mL 2x Hybridisation Buffer
- 5mL Formamide
- 20µL 50% Sodium Thiosulfate
- 200µL 5M DTT (use 1mL if 1M DDT)
- 100µL 10% SDS (also known as Laural Sulfate)
- Vortex then allow bubbles to settle

2x Hybridisation Buffer

- 3mL 5M NaCl (1200mM final)
- 250µL 1M Tris-HCl (pH 7.5)
- 82.5µL 6% Ficoll (-20°C) (0.04% final)
- 82.5µL 6% BSA (-20°C) (0.04% final)
- 82.5µL 6% PVP (-20°C) (0.04% final)
- 50µL 0.5M EDTA pH 8 (2mM final)

- 250μL salmon sperm DNA (0.2% final)
- 625 μL total yeast RNA (0.10% final) if 20 mg/ml stock
- 125μL yeast tRNA (0.01% final), if 10 mg/ml stock
- 5mL 50% Dextran Sulfate
- 2.953 mL DEP diH_2O
- Mixture needs to then be vortexed

4xSSC/50% Formamide (for 1L)

- 500mL Formamide
- 200mL 20XSSC
- 300mL DEP ddH_20

50% EtOH 300mM ammonium acetate

- 46.24g ammonium acetate
- 1L 100%EtOH
- 1L DEP diH_2O

70% EtOH 300mM ammonium acetate

- 46.24g ammonium acetate
- 1400mL 100%EtOH
- 600mL DEP diH_2O

80% EtOH:

- 1600mLs of 100% EtOH
- 400mLs of diH_2O

80% EtOH 300mM ammonium acetate

- 46.24g ammonium acetate
- 1600mL 100%EtOH

- 400mL DEP diH_2O

90% EtOH:

- 1900mLs of 100% EtOH
- 100mLs of diH_2O

95% EtOH 300mM ammonium acetate

- 46.24g ammonium acetate
- 1900mL 100%EtOH
- 100mL DEP diH_2O

100% EtOH

100% EtOH 300mM ammonium acetate

- 46.24g ammonium acetate
- 2000mL 100%EtOH

Riboprobe kit:

- 1μL DEP diH_2O (nuclease free water)
- 2μL 5X Transcription Buffer
- 1μL 100mM DTT
- 1μL RNasin
- 1μL 10mM rATP
- 1μL 10mM rCTP
- 1μL 10mM rGTP
- 1μL linearized DNA template (200ng/μL)
- 1μL RNA polymerase:
  - ____ SP6
  - ____ T3

- ____ T7

RNase A Solution:

- 200mL 5M NaCl
- 20mL 1M Tris pH8.0
- 4mL 0.5M EDTA
- 1776mL of DEP diH_2O

RNase Buffer with RNase A

- 1L RNase A solution
- 2mL of 10mg/mL stock (20µg/mL) RNase A (-20°C)

SSC's

- 0.2xSSC
  - 20mL 20xSSC
  - 1980mL DEP diH_2O

Wash Buffer (0.5M $NaPO_4$):

- 69g $NaPO_4$
- 1L diH_2O

<u>Subcellular Tissue Fractionation:</u>

0.1mM $CaCl_2$:

- 5µL 1 M $CaCl_2$
- 50mL milliQ H_2O

0.85M Sucrose + 1 mM $NaHCO_3$:

- 21.25mL 2 M Sucrose Stock
- 170mL 300 mM $NaHCO_3$ Stock
- 28.75mL 2 M milliQ H_2O

1x Triple Detergent

- 0.5% Digitonin
- 0.2% Sodium Cholate
- 0.5% NP-40

1.0M Sucrose + 1 mM $NaHCO_3$:

- 25mL 2 M Sucrose Stock
- 170mL 300 mM $NaHCO_3$ Stock
- 25mL 2 M milliQ H_2O

1.0M Tris, pH 6:

- 15.77g Trizma HCl
- 80mL milliQ H_2O
- Use HCl and NaOH to bring pH to 6, then bring total amount of solution to 100mL of milliQH_2O

1.0M Tris, pH 8:

- 15.77g Trizma HCl
- 80mL milliQ H_2O
- Use HCl and NaOH to bring pH to 6, then bring total amount of solution to 100mL of milliQH_2O

1.2M Sucrose + mM $NaHCO_3$:

- 30mL 2 M Sucrose Stock
- 170mL 300 mM $NaHCO_3$ Stock
- 20mL 2 M milliQ H_2O

2.0 Sucrose:

- 68.46g Sucrose

- Fill to 100mL milliQ H_2O

2.3M Sucrose:

- 15.7g Sucrose
- Fill to 20mL milliQ H_2O

20mM Tris, pH 7.4 with Triple Detergent:

- 800µL 25 mM Tris HCl, pH 7.4
- 200µL 5X Triple Deterge

20mM $CaCl_2$:

- 40µL 1M $CaCl_2$
- 100mL diH_2O

40mM Tris-HCl pH 6 + 2% Triton-X 100:

- 2mL 1 M Tris, pH 6
- 1mL Triton X-100
- 47mL milliQ H_2O
- Use HCl and NaOH to bring pH to 6

40mM Tris-HCl pH 8 + 2% Triton X-100:

- 2mL 1 M Tris, pH 6
- 1mL Triton X-100
- 47mL milliQ H_2O
- Use HCl and NaOH to bring pH to 6

NIM:

- 1.71g sucrose (0.25 M final)
- 0.037g KCl (25 mM final)
- 100µL 1M $MgCl_2$ (5 mM final)

- 200µL 1M Tris HCl (10 mM final)
- Adjust pH to 7.4 with HCl and NaOH

*Nuclear Lysis Buffer (NLB) with high NaCl:*1°

- 600µL 1M HEPES
- 10.5mL 1M NaCl
- 22.5µL 2M $MgCl_2$
- 60µL 0.1M EDTA
- 300µL 10% Triton X-100
- Use HCl and NaOH to adjust pH to 7.9
- Add milliQ H_2O to make up to 30 mL

Nuclear Lysis Buffer (NLB) with high NaCl with DDT:

- 1mL of NLB with high NaCl
- 1µL DDT

Nuclear Lysis Buffer (NLB) with no NaCl:

- 600µL 1M HEPES
- 22.5µL 2M $MgCl_2$
- 60µL 0.1M EDTA
- 300µL 10% Triton X-100
- Use HCl and NaOH to adjust pH to 7.9
- Add diH_2O to make up to 30mL

Nuclear Lysis Buffer (NLB) with no NaCl with DDT:

- 1mL of NLB with no NaCl
- 1µL DDT

SDB:

- 24mL 2.3M Sucrose
- 2.4mL KCl
- 1.20µL $MgCl_2$
- 240µL Tris pH 7.5

Solution A:

- 8mL 2M Sucrose
- 170µL 300mM $NaHCO_3$
- 25µL 2M $MgCl_2$
- 25µL 1M $CaCl_2$
- 42mL diH_2O

Solution B

- 8mL 2M Sucrose
- 170µL 300mM $NaHCO_3$
- 42mL diH_2O

<u>Western Blotting:</u>

8% Western Blot Gel:

- <u>Separating Gel</u>
  - 5.30mL H_2O
  - 2.0mL 40% Polyacrylamide
  - 2.5mL 1.5 M Tris pH 8.8
  - 100µL 10% SDS
  - 6.0µL TEMED
  - 100µL 10% Ammonium persulfate*
- <u>Stacking Gel</u>

- 2.1mL H_2O
- 0.5mL 40% Polyacrylamide
- 380µL 0.5 M Tris pH 6.8
- 30µL 10% SDS
- 3.0µL TEMED
- 30µL 10% Ammonium persulfate*

*Made with 0.1g Ammonium persulfate and 1000 µL milliQ H_2O

1x Running Buffer:

- 200mL 5x Running Buffer
- 800mL diH_2O

1x Transfer Buffer:

- 100mL 10x Transfer Buffer
- 900mL diH_2O

1x TBST

- 100mL 10x TBS Buffer
  - 8.7%NaCl
  - 0.1M Trizma Base
- 1mL Tween 20 (Sigma P2287)
- 900mL diH_2O

Block – 5% skim milk in TBST:

- 2.5g of skim milk
- 50ml TBST

Laemmli Loading Buffer

- 950µL Laemmli Buffer
- 50µL β-mercaptoethanol

Stripping Buffer

- 1.88g Glycine
- 15g SDS
- Make up to 950mL with diH_2O
- pH solution to 2.0 with approximately 3.5mL of 37% HCl
- Make solution up to 1L with diH_2O

Appendix 2: Methods related to thesis, carried out by others

All of these procedures were done prior to the start of my thesis work, completed by other researchers in the laboratory.

Pre-In Situ

Prior to experiment, the in situ checklist was checked to see if there was enough DEP-C treated supplies. Without the DEP-C treated supplies, in situ hybridisation could not be completed.

Day 1:

Riboprobes had to be made a day in advance of the actual in situ. NMDAR#52 (NR1) (-)cDNA linearised with BamH1 using the DNA template 165.45ng.µL was used. First, radioactively labelled nucleotides of ^{35}S-UTP 1250 (24µL) was dried down. From the Riboprobe Kit 1.79µL of solution had to be made, 0.79µL of DEP diH_2O (nuclease free water), 4µL of 5X transcription buffer, 2µL of 100mM DTT, 2µL RNasin, 2µL of 10mM rATP, 2µL of 10mM rCTP, 2µL of 10mM rGTP, 2.42µL of linearized DNA template (165.45ng/µL), and 2µL of RNA polymerase T3.

The Riboprobe kit mixture was then incubated at 37°C for 15 minutes in a water bath. Next, 6µL of 10U/µL DNAse stock was added. This was then incubated at 37°C for 37mins in a water bath. Then 10µL of 0.5M EDTA and 164µL of DEP treated diH_2O were added. This stopped the reaction of occurring. Then, 1µL aliquots drops of the sample were place onto Whatman's DE-81 paper. Two of these pieces of paper were washed in NaH_2PO_4, where the other two pieces of paper were not washed. This was to see the total CPM. Each piece of paper was then allowed to dry in a hybridisation oven. Once dried, they were placed into scintillation vials with 3-5mL of scintillation fluid. The CPMs were then determined

for each piece and the unwashed pieced and washed pieces of paper were then averaged. Using the SEE 35S probe calculator template, the specific activity and incorporation were calculated. The probes were then precipitated by adding 4μL of tRNA (10mg/ml), 44μL of 7.5M NH_4Ac, and 450μL of 100% EtOH (-20°C). This was then vortexed and left in the -20°C freezer for at least 1hr to overnight.

Next, NMDAR#52 (NR1) (-)cDNA linearised with HindIII using the DNA template 199.25ng/μL was used. First, radioactively labelled nucleotides of ^{35}S-UTP 1250 (6μL) was dried down. From the Riboprobe Kit 1.79μL of solution had to be made, 0.5μL of DEP diH_2O (nuclease free water), 1μL of 5X transcription buffer, 0.5μL of 100mM DTT, 0.5μL RNasin, 0.5μL of 10mM rATP, 0.5μL of 10mM rCTP, 0.5μL of 10mM rGTP, 0.15μL of linearized DNA template (199.25ng/μL), and 0.5μL of RNA polymerase T7.

The Riboprobe kit mixture was then incubated at 37°C for 15 minutes in a water bath. Next, 1.5μL of 10U/μL DNAse stock was added. This was then incubated at 37°C for 37mins in a water bath. Then 2.5μL of 0.5 M EDTA and 41μL of DEP treated diH_2O were added. This stopped the reaction of occurring. Afterwards, 1μL aliquots drops of the sample were place onto Whatman's DE-81 paper. Two of these pieces of paper were washed in NaH_2PO_4, where the other two pieces of paper were not washed. This was to see the total CPM. Each piece of paper was then allowed to dry in a hybridisation oven. Once dried, they were placed into scintillation vials with 3-5mL of scintillation fluid. The CPMs were then determined for each piece and the unwashed pieced and washed pieces of paper were then averaged. Using the SEE 35S probe calculator template, the specific activity and incorporation were calculated. The probes were then precipitated by adding 4μL of tRNA (10 mg/ml), 44μL of 7.5M NH_4Ac, and 450μL of 100% EtOH (-20°C). This was

then vortexed and left in the -20°C freezer for at least 1hr to overnight. Finally, 2x hybridisation buffer was made. This solution was kept at -80°C once it was dried using EtOH and retreated with 95% EtOH for 1min then allowed to air-dry before use.

Day 2:

The precipitating probe must be taken out of the -20°C freezer and purify. To do this, the riboprobe was spun for 20min at 4°C at 13,300RPM (Thermo Electron Corporation, Heraeus Fresco 21 Centrifuge). The supernatant must be poured off, then 1mL of cold 70% EtOH was added. Mix the tube by inverting it ~10 to 15 times to wash the pellet of salt. The tube was spun at max speed (13,300RPM) for five minutes at 4°C. The supernatant was poured off after the spin. Dry in speed vac for 3-5 minutes. The pellet was then resuspended in 50µL of DEPC-H_2O. On DS-81 paper, 1µL of solution was placed and then in a scintillation counter was used to calculate the concentration of the riboprobe by taking cpm/µL and dividing it by the previously calculated specific activity. The probes were then placed on ice.

To prepare the slides, all the slides were placed from an empty box on dry ice onto foil for 20min at RT to defrost and slides were labelled. The slides were then placed in a DEPC-treated, autoclaved slide rack. The slides were then fixed in 4% Formaldehyde in 1xPBS for 5min at RT. In 1xPBS, the slides were rinsed twice. Next, 0.1M triethanolamine-HCl (TEA-HCl) was made and shaken well. Slides were then rinsed in 1L of TEA-HCl. In a dry container, 2.5mL acetic anhydride was added. A fresh 1L 0.1 M TEA-HCl was poured into the dry container with acetic anhydride. This was then shaken vigorously and slides were immediately added to this solution and incubated for 10min at RT.

After 10min, the slides were rinsed twice in 2xSSC. Then the slides were rinsed in the following:

70% EtOH	1min
80% EtOH	1min
95% EtOH	2min
100% EtOH	1min
100% Chloroform	5min
100% EtOH	1min
95% EtOH	1min

The slides were then left to air dry at a tilt. While the slides are drying, 2x hybridisation buffer was made. This buffer was then heat denatured for 10min and probes for 5min at 85°C. Then the solutions were then placed directly on ice. 1x hybridisation buffer was then made. The concentration of the probe was adjusted to 5ng/mL using Hybridisation Cocktail mix. The counts can be checked at this point: 25µL of mix should be less than 3-5x10^5 cpm. The mixture was vortexed and the bubbles were allowed to settle. The incubation chambers were prepared by lining with sheets of Whitman 3MM filter paper saturated with 4xSSC/50% formamide. Two falcon tube tops were then added to each chamber with the 4xSSC/50% formamide solution so chambers will not dry out. Slides were then placed flat on the chamber, then 175-300µL of hybridisation mixture was added to each section. Bubbles should not be seen after solution was added to the slide. If there are bubbles, try to let them settle on top or pop them carefully. Cover slips were then added to each slide. In an incubator set to 55°C, place chambers in there overnight. Place 2 dishes with diH_2O in the incubator so it will be humid in the machine.

Day 3

In the morning, the water baths were turned on. One was set for 50°C (2xSCC) and the other was set for 55°C (0.2xSCC). The appropriate bottles were then placed in the baths to equilibrate. The chambers were then removed from the incubator and slides were placed in a rack in a dish of 2xSSC to soak at RT for at least 10min (20min would be preferable). (Note: Wherever this sign occurs, liquid was placed into the liquid radioactive waste.) Five 500mL plastic buckets were filled with 2xSSC and one additional dish and rack. Each slide was removed and dunked several times into each bucket to remove the coverslips. The slides were then rinsed twice in 2xSSC (first wash only). RNase A solution was then made. Half of the 2L solution was poured into the RNase Buffer with RNase A. The RNase Buffer with RNase A was then made. Slides were added to the RNase Buffer with RNase A for 30mins at RT. After the incubation, the RNase buffer with RNase A was poured off and the buffer without RNase A was added. This was then incubated for 30mins at RT. The slides were then rinsed twice with 2xSSC at RT. The pre-equilibrated 2xSSC at 50°C was added. The slides were then covered with foil and placed in a shaking water bath for 1hr. After the incubation, the slides were then rinsed twice in 0.2xSCC pre-equilibrated at 55°C. The water bath was then raised to 55°C. The slides were then washed in the 0.2xSSC pre-equilibrated at 55°C for 1hr. After 1hr, the water bath was then increased to 60°C.

Once that incubation was over, the slides were dehydrated. This was completed by placing the slide rack in 50% ETOH 300mM ammonium acetate for 1min, then into 70% ETOH 300mM ammonium acetate for 1min, then in 80% ETOH 300mM ammonium acetate for 1min, then in 95% ETOH 300mM ammonium

acetate for 1min, then finally into 100% ETOH for 1min. The slides were allowed to air-dry using tilt.

Once the slides were completely dry, the slides were taped into cassettes with standards. The cassette was then labelled with the probe used, date, and initials of the people who worked on the in situ. Then the slides were exposed to the film.

Appendix 3: Full Detailed Methods Completed in my Thesis

Tissue Fractionation

Proper personal protective equipment (PPE) was used throughout all procedures. For tissue fractionation, extra precautions were taken including completing experimental work in a PC2 laboratory. All chemical compositions of solutions are described in Appendix 1.

Tissue Pulverisation:

Protective paper booties, latex gloves, lab coat, and masks were worn for all human tissue pulverisation procedures in a Class I fume hood. When I received this tissue from the NSW TRC, tissue pulverisation was completed. In a fume hood, the walls and working surface were lined with bench cover since human tissue was being used. After that was done, dry ice was placed into a container with the tissue samples to be kept frozen. To prepare the tissue, a metal tray was placed into dry ice in the hood to keep the metal cold enough for the brain tissue to stay frozen. This was all placed on blue absorbent pads. Next, a hammer, a razor blade, forceps, freezer bags (medium), a separate small freezer bag used for dry ice pack that was placed on top of the sample to keep both sides frozen, and foil (cut to cover the hammer and the bottom of the metal tray) were retrieved. Paper towels and 100% ethanol (Sigma-Aldrich) were used for cleaning all materials between samples.

Outside of the hood, the samples were weighed by placing small pieces of dry ice under the balance plate on the scale (Mettle Toledo XS105 Dual Range scale). The samples that were in frozen 50mL Falcon tubes on dry ice were one by one briefly removed from the dry ice, the cap was removed, and the still frozen cap placed on the scale that was cooled from the dry ice underneath. The scale was then tared. Chunks of the frozen tissue were then tipped into the cap and the

sample was weighed. Approximately 400mg of frozen tissue chunks were then poured back into the 50mL Falcon tube until later pulverisation.

Right before the pulverisation process, the sample was poured from the original 50mL tube, into a medium plastic bag and it was placed on dry ice until it was ready for the pulverisation. While transferring the sample from one dry ice container to the pulverisation tray, the sample could have warmed slightly so the dry ice pack was placed on top of the sample for a couple of seconds to bring the sample back down close to -80°C. When the sample was clearly in a completely frozen state, the foiled hammer was used to smash the brain tissue into small, fine pieces inside the bag. When the pieces were fine, the bag was shaken down so all the pieces were in one corner. This corner was cut off using the razor blade and the sample was poured into a pre-frozen, coded and labelled 50mL Falcon tube. The tube was then transferred to another dry ice box and kept at -80°C. Next, the foil was thrown in the clinical waste and everything that was used was rinsed with 100% ethanol before the next sample was started. When complete, all of the bench coats and absorbent pads were placed into the clinical waste and everything was washed with 100% ethanol. All of the samples were placed into the -80°C freezers.

Subcellular Tissue Fractionation of Post-mortem Brain Tissue:

Throughout the entire tissue fractionation procedure, all centrifugation was done at 4°C and all of the samples and solutions, excluding the Protease inhibitor (Sigma P8340), were kept at 4°C. This procedure required four days to fully process one sample. Seven fractions were obtained for each sample. The seven samples included the total homogenate (T), cytosolic fraction (C), nuclear fraction (N), synaptic membrane fraction (SPM), PSD, synaptic vesicular fraction (SV), and

presynaptic membrane fraction (PPF). Details of all solutions used are in Appendix 1.

Day 1:

Day one required seven solutions: 2.0M sucrose, 2.3M sucrose, nuclear isolation media (NIM), sucrose density barrier (SDB), solution A (Sol. A), nuclear lysis buffer with no sodium chloride (NLB with no NaCl), and nuclear lysis buffer with high sodium chloride (NLB with high NaCl). Every sucrose solution had to be used within 24hrs of being made due to the high risk of bacteria contaminations in these solutions.

The next part of the procedure was completed in a Class 1 fume hood in a PC2 laboratory. Along with working in the fume hood, the PPE required for this part of the process was gloves, lab coat, face mask, and shoe covers. Using an Potter-Elvehjem homogeniser (Kontes Glass Co., Vineland, NJ, US), approximately 0.4g of post-mortem brain tissue was homogenised up and down approximately 12 times or until no chucks of tissue was seen in 5mL of solution A. Two tubes containing 200µL and 22µL aliquots (for BCA analysis) of this was labelled T (for total), along with the date, sample number, and my initials, and stored in a -80°C freezer.

In four microcentrifuge tubes, the remaining T fraction (1.2mL/tube) was centrifuged at 1400×g (RCF) for 15min at 4°C in the Eppendorf centrifuge (refrigerated microcentrifuge Eppendorf 5415R). After centrifugation, the ~5mL of supernatant (S1) from the tubes were combined and was saved in a 15mL Falcon tube and placed on ice. The pellets (P1) from each of the four tubes were then rehomogenised with small plastic pestles in a total amount of 1mL of solution A (250µl/tube) and the four tubes were combined into one 1.5mL microcentrifuge

tube. Next, the tubes containing the combined resuspended pellets were centrifuged at 710×g in the Eppendorf centrifuge for 10min at 4°C. The approximate 1.5mL of supernatant (S2) was then added to S1 in the 15mL Flacon tube. The pellet (P2) was placed on ice to be used later on in the procedure.

The pooled S2 samples (approximately 5mL) were then placed into four 1.5ml microcentrifuge tubes and centrifuged at 16000×g in the Eppendorf centrifuge for 20mins at 4°C. After centrifugation, supernatant (S3) was considered to be the cytosolic (C) fraction. The C fraction (approximately 4mL) was pipetted into three 1.5mL microcentrifuge tubes (about 1.3mL each) and placed into the -80°C freezer, along with a 22μL aliquot set aside for BCA quantification of the protein in the cytosolic homogenate. The pellets (P3) from this spin were also placed into the -80°C freezer and saved for the Day 2 procedure.

A crude suspension of the pellet P2 after the 710xg centrifugation was prepared using 500μL NIM and a plastic homogeniser to grind samples more finely. Each sample was split into two 1.5mL microcentrifuge tubes, and NIM was added until the total volume was 3mL. In a clean 15mL Falcon tube, 6mL of 2M SDB was added, along with the NIM/sample mixture and mixed thoroughly with a P1000 pipette. Four mL of 2.3M sucrose was added into 13.2mL ultracentrifuge tubes for the swinging bucket ultracentrifuge rotor (SW41Ti, 09E2800). Then the NIM/SDB mixture was carefully overlayed on top. This was spun for 1hr at 100,000xg (24,200RPM) at 4°C in order to separate the nuclei from the rest of the mixture.

After one hour, any material floating on the meniscus was removed with a spatula then the supernatant liquid was poured off to leave the nuclear pellet (P4) at the bottom. The tube was inverted a few minutes to drain and walls of the tube were wiped off with a Kimwipe to remove as much sucrose as possible. P4 was

resuspended in 150µL NLB with high NaCl using a P200 micropipette mixing five times. This step is completed because high salt solutions load the nucleus with ions to make them hypertonic and this later helps lyse the nuclear membranes (under low salt reconditions) and force the DNA, along with other nuclear contents, into solution. The P4 in solution was vortexed quickly to make sure the solution was mixed. This was then placed on a rotation wheel to incubate at 4°C for 20mins. Thereafter, 150µL NLB with no NaCl (low salt) was added and the solution allowed to precipitate on ice for 20mins causing the nuclei to lyse under hypertonic conditions. After 20mins, the samples were centrifuged at 14,000xg in the Eppendorf centrifuge for 10mins at 4°C. The supernatant (S4) was considered to be the N fraction. S4 was collected and saved for analysis and 22µL of the nuclear fractions was saved for BCA protein determination. The pellet (P5) received after the 14,000xg centrifugation contained DNA, lipids, and other nuclear contents, which was discarded in yellow clinical waste bin.

Day 2:

P3 from Day 1 were resuspended in total volume of 750µL of solution B. It was important to combine all pellets from the four tubes saved and to make sure that no clumps of the pellet remained in suspension. A three-layer sucrose gradient (5mLs of 1.2M, and 3mLs of each 1M and 0.85M sucrose) was pipetted into a 13.2mL ultracentrifuge tubes (99U4065), taking great care to not allow mixture of the layers. If these layers mixed, the band of interest would not be clearly visible following centrifugation. The solution B mixture was added on top, then centrifuged for 3hrs at 100,000×g (24,200RPM) in a SW41Ti rotor in Beckmann ultracentrifuge at 4°C.

After the 3hr centrifugation the white band (P6) between the 1.0M and 1.2M sucrose was removed using a 10mL syringe and needle (18GA 3.5in, Ref: 405248) and placed into 13.5mL ultraclear tubes for the Beckmann 70.1Ti. P6 contained synaptosomes. The synaptosome fraction was diluted with 5X volume of solution B and centrifuged in 13.5mL tubes in the ultracentrifuge for 30mins at 35,000×g (19,500RPM) at 4°C. The supernatant (S5) was removed and the pellet resuspended with 500µL of 0.1mM $CaCl_2$ and centrifuged at 15,000×g (RCF) in an Eppendorf centrifuge at 4°C for 20mins. $CaCl_2$ was used as a wash. The calcium binds around the protein preventing it from dissolving. After the $CaCl_2$ solution was removed, the pellet (P7) was resuspended in 200µL of 20mM Tris pH 7.4, triple detergent, made with 0.5% Digitonin, 0.2% Sodium Cholate and 0.5% NP-40, to dissolve the pellet. The pellet was dissolvable because the Tris solution is a polar salt solution and the salt in the Tris solution allows protein to become more polar and becomes water-soluble. The samples were then placed on the rotation wheel for 60mins in the 4°C refrigerator. This fraction was designated as the synaptic membrane fraction (SPM). Forty-five µL of this sample was set aside for the SPM fraction and 6µL was set aside for quantification in -80°C freezer. The remaining 150µL of sample was set aside for further processing on day 3.

Day 3:

The remaining 150µL aliquot of SPM was diluted with 850µL ice cold 0.1mM $CaCl_2$. The sample was then split into two tubes and 0.5mL of 40mM Tris-HCl pH 6 supplemented with 2% Triton-X 100 was added to each tube. The samples were then left on the rocker at 4°C for 30mins. During these 30 minutes, precipitation of the samples occurred. After the 30mins, the samples were transferred to 3mL

ultraclear ultracentrifuge tube with adaptors for the 70.1Ti rotor and centrifuged at 35,000×g (19,500 RPM) for 20mins at 4°C.

The supernatant (S6) was designated as the SV fraction. S6 was removed and protein was precipitated in 5X volume ice-cold acetone in a 15mL Falcon tube. The samples were vortexed for at least 30secs and left in a -20°C freezer overnight. The pellet (P8) from the prior centrifugation was allowed to air dry and then dissolved in 1mL 0.1mM $CaCl_2$. These samples were split into two tubes and 0.5mL of 40mM Tris pH 8, 2% Triton-X 100 was added to each tube. At pH 8, the presynaptic membrane separates from the PSD. These samples were agitated on a rocker for 60mins at 4°C. After 60 minutes, the samples were then quickly (5-10secs) centrifuged. The samples were pooled into one 3mL ultracentrifuge tube and centrifuged at 140,000×g (39,000RPM) in Beckmann type 70.1Ti rotor for 30mins at 4°C.

The supernatant (S7) contained the less dense synapse component and was designated as the presynaptic membrane fraction (PPF), leaving a pellet of the denser PSD protein (P9). S7, the PPF fraction, was precipitated in 5X volume ice-cold acetone in a 15mL Falcon tube by vortexing for at least 30secs and then left in a -20°C freezer overnight. The pelleted (P9) PSD fraction was allowed to air dry and it was dissolved in 100µL 20mM Tris pH 7.4 triple detergent. Six µL of the PSD fraction was set aside for BCA assay to determine how much protein was in the PSD fraction.

Day 4:

The acetone precipitated SV and PPF fractions that were left overnight in the -20°C freezer were centrifuged in 13.5mL polyallomer tubes (Thin wall 13.5mL polyallomer tubes for 70.1Ti Rotor, 41121703) at 24,000×g (11,800RPM) in

Beckmann type 41 Ti rotor for 30mins at 4°C. Once centrifuged, the acetone was placed into the acetone waste container and the centrifuge tubes were inverted on a paper towel to air dry for 30mins. If this were not done, the acetone would inhibit the pellet from being dissolved in the next step. The pellets were then dissolved in 200μL of 20mM Tris pH 7.4, triple detergent. Six μL of each fraction were set aside for BCA protein quantification.

BCA Protein Analysis:

The protein concentration was determined for T, C, N, SPM, SV, PPF and PSD fractions by BCA method (Pierce). NLB (175mM NaCl), Solution A and Tris pH 7.4, triple detergent with inhibitors was used as appropriate dilutes for standards.

For BCA analysis, 5μL of each standard at different concentrations (0.1 to 1.4mg/mL) was pipetted in triplicate into a 96-well plate. Five μL of each sample, in either singlet (SPM, PSD, PPF, or SV) or triplicate (T, C, N), were then loaded into the plate. To prepare the BCA solution, 50 parts Reagent A was mixed with one part Reagent B. Then, 200μL of the Reagent A/Reagent B mixture was added to each well. The plate was shaken for 30secs before it was covered with aluminium foil and placed in an incubator at 45°C for 30mins. The plate was then allowed to cool to room temperature. Using a plate reader, the absorbance was measured at 562nm.

Western Blotting Procedure:

All solution compositions used for Western blots can be found in Appendix 1.

Day 1:

An 8% polyacrylamide gel with the appropriate number of wells, generally 15, was made. Appendix 1 shows how to make the 8% Western Blot gel. The

heating block was turned on and allowed to heat to 95°C. The TRC cohort protein samples were removed from the -80°C freezer and placed on wet ice. For the total homogenate (T) samples, 10μg of protein (5μL) was used and for PSD samples 1μg of protein (10μL) were combined with an equal volume of Laemmli sample buffer that contains 5% β-mercaptoethanol (1:1) in a 1.5mL tube on ice, and mixed by vortexing. An internal control, a pooled sample of five control samples and five schizophrenia samples, was used to assure efficiency of the run. The samples were heated at 95°C for 5mins. Using an Eppendorf centrifuge, the samples were spun down for 5 to 10secs. After the centrifuge, the samples were not placed back on ice. The protein ladder was not heated.

Polyacrylamide gels were set up in the tank with 1x running buffer and the samples were loaded into gels. Ten μL of lane marker, the total volume of protein samples, and 10μL of Laemmli buffer into empty wells were added. If one or three gels were being run, a plastic mini cell buffer dam (BioRad #165-3130Edu) was used in place of running a blank gel. The tank was then filled up to the correct line, either the two or four gel line depending on how many gels were being run in that tank. For one gel being run, the tank was filled to the two-gel mark; for three gels being run, the tank was filled to the four gel mark. The gels were run at 150 V for 40mins to 1.25hrs, depending on how fast the visible blue bands (Laemmli buffer dye) ran down the gel. Once the blue band reached about 1cm from the bottom of the running gel, the gel was removed and placed in transfer buffer. The gel was carefully removed from between the glass plates and allowed to sit in the transfer buffer for 10mins to equilibrate. The gel had the stacking gel layer removed and discarded.

Transfer buffer, containing 10% 10x Transfer Buffer and 90% diH_2O, was prepared fresh. The nitrocellulose membrane was cut to the required (approximately 90 x 60mm) dimensions. Forceps were used while handling the membranes because membranes are sensitive to all proteins, including those one human hands and those that could be on the gloves. The membranes were labelled with a pencil so the labels would not smear or come off the nitrocellulose membrane. Membranes were placed into a plastic container with enough transfer buffer to cover the membrane. Filter paper was placed into another plastic container and transfer buffer was added. In the larger compartment of the transfer container, a cassette was placed with the black side face up and the red side facedown, and the compartment was filled about half way with transfer buffer. In the smaller compartment, two fibre pads were placed and covered in transfer buffer. The transfer tank was placed into an insulated container and ice was packed around it. An ice pack was placed into the transfer tank as well, underneath the white flap. This setup was placed on a stirring block with a magnetic stirrer placed inside the transfer tank.

In the cassette, a fibre pad was placed on top of the red side of the cassette. This had to be submerged in transfer buffer. Next, a wet filter paper was added onto of the fibre pad, then the wet nitrocellulose membrane was placed on top. The side of the membrane that had writing on it was face up. Next, the gel was added along with another filter paper and finally the second fibre pad. After each layer was added, a roller was carefully used to remove any bubbles that would have formed. The cassette was closed and the latch was then locked into position.

Once the cassette was locked, it was moved into the groove in the transfer tank and the tank was filled with transfer buffer, approximately 1L. The red side of

cassette was aligned with the red electrode. The lid was placed on and cables were attached to the power supply. The protein was transferred from the gel onto nitrocellulose membrane at 100 V for 3hrs.

During the three-hour transfer, Western blocking solution–5% skim milk in Tris-buffered saline with Tween 20 (TBST) was made. For small trays (5cmx7cm), a minimum amount of 5mL per membrane was required, plus 4 mL per membrane for primary antibody (1° Abs) incubation in small trays.

Once the transfer was complete, the membrane was stained with Ponceau S Solution (Sigma, P7170-1L) to confirm transfer. The stain was added to the membrane in a gel tray and was placed on a rotating rocker for approximately 30secs to one minute until the colour developed. The excess Ponceau stain was emptied back into the original container for reuse. Using TBST, the membrane was rinsed off enough to see the bands clearly without a great deal of background staining. A new, clean transparency was cut in half and the membrane was placed on top. The other half of the membrane was used to cover the membrane. Using a Kimwipe, bubbles were removed by pushing them to the edge of the transparency. This was then photocopied or a photograph was taken. The photograph provided a clearer picture than the black and white photocopy.

When multiple 1° Abs were used, the Ponceau (pink) staining in combination with the molecular marker helped to judge the success of the protein loading and protein transfer and to show where the membrane needed to be cut. The membrane was then washed in TBST again until the pink stain was almost completely gone. The membrane was placed into the Perfect Western containers. Five percent non-fat skim milk block was added to the container, which was left for a minimum of 1hr on a rocker in the refrigerator at 4°C.

While the block is on, the 1° Ab dilution was made using the correct 1° Abs in the appropriate volume of Western blocking solution- 5% milk in TBST. The 1° Abs used were NR1-NMDAζ1 at 1:1000, 5μL abs to 5mL 5% milk in TBST, synaptophysin was used at 1:10000, 0.5μL to 5mL 5%milk in TBST, and NeuN was made 1:1000, 5μL ab to 5mL 5% milk in TBST. Four mL of blocking solution was used for the small trays.

After the block was on for at least an hour, the block was dumped off and the 1° Ab was added. The membrane with the 1° was incubated at 4°C overnight on a rocker.

Day 2:

The 1° Ab was rinsed off with TBST, then the membrane was washed three times, 10mins each time, on a rocker at full speed. During this time, a secondary antibody (2°Ab), AP106P rabbit anti-goat IgG antibody HRP conjugate, at a 1:5000 dilution was made in blocking solution- 5% milk in TBST and AP192P donkey anti-mouse at a 1:5000 dilution in 5% milk in TBST. After the three rinses, the membrane was incubated with the 2°Ab at room temperature on the rocker for 1hr. Then the 2°Ab was rinsed off with TBST, and then the membrane was washed three times, 10mins each time, on a rocker at full speed. After this, analysis of the membrane was done using film and a Chemidoc (described below).

If the 1°Ab or 2°Ab would react to the second set of antibodies applied, then stripping buffer (information in Appendix 1) was used to remove the first 1°Ab and 2°Ab that was used. Stripping buffer was added to the Perfect membrane containers after the TBST was dumped off. On a rotating platform at a speed of 70, the membrane was agitated for two periods of 15mins each. Next, the membrane was blocked for 1 to 2hrs with Block at 4°C.

Housekeeping proteins were examined to confirm how much protein was actually added to each well. First, the control 1°Ab (T3952-100UG, Anti-β-Tubulin III antibody) was made at 1:10000 in 5% milk in TBST. The 1° Ab was then added to the membrane, which was incubated on a rocker overnight at 4˚C.

Day 3:

The 1° Ab for the housekeeping control protein was rinsed off with TBST, then the membrane was washed three times, 10mins each time, on a rocker at full speed. A 2° Ab (AP192P donkey anti-mouse IgG antibody, HRP conjugate) was made at 1:5000 dilution in the Western blocking solution. The membrane was incubated with the 2° Ab at room temperature on the rocker for 1hr. The 2° Ab was rinsed off with TBST and washed three times at 10mins each time on a rocker at full speed. The analysis of the membrane was done using film and a Chemidoc (described below). The stripping buffer was then used to remove the antibodies; the membranes were re-blocked with skim milk in TBST and stored in plastic pouches filled with TBST at -20 degrees in the event further probing was desired.

Chemidoc Procedure

The beginning part of the procedure was done under a dim red light to see. The chemicals and film are light sensitive. Using forceps, the membrane was placed on to an overhead plastic sheet, which was cut in half. For each membrane, 500μL of lumin (Millipore Immobilin, Cat. no. WBKLS0500) and 500μL of perox (Amersham ECL, Cat no PRN2209) was added together in a 15mL Falcon tube. The mixture was pipetted onto the membrane. After waiting 30secs to one minute for the chemical reaction to occur, the excess solution was poured off and the blots were moved to the Chemidoc to start the exposures.

First, Quantity One was started. Under file, Chemidoc XRS was chosen. Next, the button "Select" was picked and the category White Epi Illumination was selected. The Epiwhite light on the Chemidoc machine was turned on. The iris was opened all the way and the membrane was centred. The frame was then frozen and auto exposure was clicked. This was then saved. The Epiwhite light was then turned off and "White Epi Illumination" was changed to "ChemiMax". Live acquire was then picked and, at the start, the settings were for 120secs, 10secs per exposure, and 12 exposures in total (one picture every 10 seconds). Over time, the NMDA NR1 antibody exposure was changed to a 300sec exposure, 30secs per exposure, and 10 exposures overall. For the housekeeping antibody, it was changed to a 30sec exposure, 5secs per exposure, with six pictures overall (one picture every five seconds). These pictures were then saved.

After the Chemidoc procedure was completed, another 1mL per blot of the Lumin/Perox mixture was made and placed on the membrane again for 30secs to a minute to allow the luminescence quality to be stronger. The membrane was then covered with the other half of the overhead sheet and the overhead-membrane sandwich was taped in place in the film Hypercassette (Amersham Biosciences, RPN 13649 8x10in Batch no. 1207). The lights were then turned off completely and the film box was taken out of the fridge. One sheet of film was removed from the foil bag and was placed on top of the overhead and the Hypercassette was closed for a variable amount of time, depending on how reactive the protein of interest was (time varied between 1sec and 1hr). The film was taken out of the cassette (still with the lights off) and placed in the automatic film processor. Once the machine beeped, and the film was properly put away, the lights could be turned on.

Almost every membrane that was completed has a film, except for approximately one set of seven membranes due to the film developer being broken.

Quantity One Analysis

The first step in Quantity One analysis was opening the file of interest obtained using the Chemidoc Quantity One program (version 4.6.5). This photo of interest was received from the Chemidoc and exposures that did not have any saturated signal (containing red) were chosen for analysis. If there were any bands that were saturated, that specific photo captured would not be used. Once the optimal photo was selected, the Volume button was selected, then Rect. Tool. This tool allows a box to be drawn around the protein band on the membrane. A box was drawn around the largest band first so all rectangle boxes were large enough to fit around the protein of interest, while keeping the boxes to the smallest size possible. This ensured all protein was captured without too much background. Next, the keyboard commands control+copy and control+paste were used to create the same size boxes around each protein band. The boxes were dragged into the correct position. After each protein of interest region had a box, one more box was made and placed over a region of the membrane where no protein was; this was used for a background calibrator. The Background box was double clicked on so a dialogue box would appear; in which "Background" was checked. Next, Report, then Volume Analysis Report was chosen. This brought up a new screen where name, type, volume, adj. volume, percent volume, and area were selected. Export and save were then chosen.

From this point, the data were imported into excel. The adjusted volume was then found by dividing the adjusted volume of the protein of interest by the adjusted volume of the housekeeping protein. This data was then saved.

In situ hybridisation film quantification:

Scanner:

The in situ films were cut into A4 size so they fit onto the scanner. The scanner (Canon CanoScan8600F) had film placed on the platen glass the correct side down. If the film is placed wrong, the scanning process causes swirls on the acquired image. The CanoScan program (CanoScan Toolbox 5.0, version 5.0.1.4 for MacOS X) "Photo 2" option was chosen. The following parameters were chosen: Platen, Grayscale, 300-800dpi. When the scan was completed, the preview image was shown and saved as a .tiff file. This process was repeated for all films.

Adobe Photoshop

The scanned film was opened up in Adobe Photoshop (Adobe Photoshop CS5 extended version 12.0x64). Each tissue section was then cropped into individual files by going into the "Rectangular marquee tool", then "Image", then "Crop". Any pen marks were taken out during the cropping process. If the analysed images have pen marks, this caused problems with the actual background colour. The cropped images were then saved as .tiff files.

Next a visual inspection of the in situ films was done, looking for the darkest and lightest signals on the film. The images were used to determine the level of adjustments required to maximise the dynamic range of the in situ signal. By going to "Image", "Adjustments", "Levels", "Adjust input level", then dragging the arrows closer to the black histogram adjustments were made. The most conservative levels were chosen and the same levels were set for all images before the files were again saved as .tiff. The background for the same subject was compared on different films. If backgrounds were not similar, adjustments were made to achieve this. Also, any potential artifacts were noted.

ImageJ

Determining the Standard Curve

The files were opened in ImageJ. To calibrate the images, the "Edit" table was selected, then "Invert", then "Image", then "Look up table", and then "Invert LUT". The calibrated image was saved in a new folder to keep the images separated from the originals. To get a calibration curve, the best standard from the in situ with the widest range was opened. A rectangle was drawn inside the darkest standard square and the optical density was measured. The rectangles were then moved and repeated for all standard squares in order from darkest to lightest squares. The means of the rectangles were then copied into a results table. Next, the "Analyse" tab was selected, then "calibrate", changing units to μCi/g . The measured means were then entered into the left column and the standard values were added to the right column. The standard values used are in Table A3.1 below.

Box 1 - 0.000	Box 9 - 0.29
Box 2 - 0.002	Box 10 - 0.53
Box 3 - 0.004	Box 11 - 1.11
Box 4 - 0.009	Box 12 - 2.15
Box 5 - 0.017	Box 13 - 4.47
Box 6 - 0.035	Box 14 - 8.98
Box 7 - 0.067	Box 15 - 18.41
Box 8 - 0.130	Box 16 - 35.00

Table A3.1: Standard values used for ImageJ analysis. The entered standard values noted.

This text file was saved globally. After the exponential function was chosen, "Ok" was then selected. The aim was to get an R^2-value as close to 1.0 as possible.

Each section was then calibrated using the best-fit exponential function. This was used to calibrate all of the brain tissue images and convert the OD to μCi/g.

Determining the μCi/g of NMDAR NR1/cortical layer

The line tool was chosen for our analysis of mRNA levels within BA46 cortex. The line width was set to 10 pixels, and drawn from the pial surface to the white matter. The μCi/g was then measured by averaging the signal from three lines of the same width and approximate length. This image was saved. The same standard calibration curve was used for all sections.

Excel

Next, the raw data density was copied into excel. The start and end points of each layer was highlighted in the y column per slide while looking at the plot. The first value was the lowest point on the way up the curve, and the last value was the lowest point after flattening. This data was saved.

The raw data was then transferred into a formatted excel sheet, with each individual case on a different sheet. The Y column raw data (demarcating where the cortical surface started and stopped) was copied for each line separately. A previously developed macro program entitled "Personal" [231] was opened and the Macro enabled. The "Tools" tab was selected, then "Macros", then "Interpolate". The Y column raw data was selected. For output, the A1-B3 columns were selected starting at 0%. Then "Graph the density" was selected. This was then repeated for each line, and adjustments were made to best fit the data to the common cortical width. It was important not to "overfit" the data and it was important to compare the results to the picture. The layers were then lined up to see how the layers correlated with one another. Notice how the signal is aligned in layer II for all six sampling lines, but that there is quite a bit of variability in the signal in the middle

layers of the cortex for this case suggesting that the signal is more variable and that it is critical to average the signal across many lines (n=6) to get an accurate representation of the signal.

In situ hybridisation silver grain analysis:

Stereo Investigator:

To do silver grain analysis, Stereo Investigator version 8.27, 32-bit program was used. First, the microscope, microscope light, camera, and the box to control the joystick were all turned on. In the Stereo Investigator program, the "live image button" was clicked to bring up the live picture from the slide positioned under the objective. Then, the condenser on the microscope was adjusted in order for the picture to be visible on the computer screen. To bring the picture into correct lighting, the "Adjust video type" button was clicked, and then the "turns video exposure on or off" button was clicked. It is important to use consistent lighting while using the microscope, so this the AWB in the Adjust Video screen was used on each slide. Using the joystick, under 2x power, the slide was scanned to find the area of interest, which was indicated by pre-marked boxes. The boxes were drawn on the slides based on Nissl-stained images defining where BA46 was located using the cytoarchitecture of the brain.

When the correct area was found, and the cortex between the pial surface and white matter was visible in one screen, "Image", then "Quick Measure Line" was chosen and a line drawn across the cortex producing the distance (in μm). This was to measure the width of the cortex, to determine if there is an increase or decrease in cortex thickness between schizophrenia patients and controls and to confirm that the correct layer was being sampled from. The distance varied greatly between slides and parts of individual brain slices. The cortical width was

measured three times and averaged and then the approximate position of the cortical layer of interest was calculated: layer II- 10-20% from the pial surface, layer III- 20-46% from the pial surface, and layer V- 54-70% from the pial surface [58]. From these estimates, and after confirming the appropriateness of the cytoarchitecture within each layer, photos were taken at 20x, generally three photos for each layer. These photos were captured by going to "Acquire Image", then a scale bar was added by going to "Imaging", "Add Scale Bar", and set the scale bars to 20μm. The photos were saved as Tiff images.

ImageJ:

Photos were opened using Image J (version 1.44o, 32-bit) with the Lipschitz filter plug-in installed from the internet: <http://rsbweb.nih.gov/ij/plugins/lipschitz/index.html>.

Having an extremely dark area on the image to be analysed causes the Lipschitz filter to over work and the image to show fewer silver grains. Therefore, to ensure all images were consistent, once the images were opened in Image J, the colour of the scale bar was changed to the background colour of the slide by clicking on an area of the background with no silver grains with the "Eye Drop" tool. Then, with the "Paint Can" tool, the scale bar was selected, causing the scale bar to take on the background colour, eliminating extra black colouration on the screen. This allowed the Lipschitz filter to ignore all the scale bars added to the image and not contribute to the "silver grain" count in the end.

Cell counts and nuclear diameter measurements

Next, I measured the scale bar to enable measurement of the size of the nuclei of cells that were being analysed. Since the pyramidal neuron nuclei were larger than interneuron nuclei, this was one way to differentiate between the cell

types. The distance of the scale bar in pixels was measured by selecting the "Straight" line button and then a line was drawn over the top of the scale bar. At 20x, it was 58 pixels for 20μm. Next, the "Analyse" tab was selected and then "Set scale" was clicked. The distance in pixels equalled the length of the line that was drawn. This automatically showed up in the set scale box. The known distance was the length the scale bar was set to. The "Global" selection set all images the same scale. Next, "Edit" was selected, "Selection", then "Specify". On this screen, the "Oval" and "Scaled Units (μm)" were selected.

The density of glial cells, interneurons and pyramidal cells were counted in each analysed image. This was done by going to "Plugins", "Analyse", "Cell counter". On the new screen, the "Keep Original" box was selected, then the "Initialize" button was pressed. Any of the counter types could be used. Once a "Counters Type #" was selected, each of the glial cells were marked, then the interneurons and pyramidal cells. All cells in the image were counted excluding those whose nuclei touched the top and left boundary. This was done to consistantly capture only half of the cells which were going off the image. If all the cells were counted, that would give a higher purportion of cells to area size ratio then there actually is in reality. Next, nuclear diameters of 10 glial cells, 10 interneurons, and 10 pyramidal neurons were measured by clicking the "Line" tool then dragging the line from one end of the nuclei of interest to the other. Next, a line was placed and 30 nuclei were measured by clicking the "Measure" button on the "ROI Manager" screen. The "Results" information was then pasted into an excel document for further analysis.

Silver grain counts

To analyse the number of silver grains/cell, the "Oval" button was clicked. The first step was to set the background. A circle was drawn over an area with no

silver grains and no visible nuclei. Next, the size of the circle was set by going to the "Edit" tab, "Select", then "Specify". The circle was then corrected for size of background (either 15μm for interneurons or 35μm for pyramidal cells). These sizes were chosen based on the known human neuron sizes[224]. Five circles of each size were obtained to measure background. Control+T was pressed, which allowed for more circles to be replicated at the exact required size. The new circle appeared directly over the old circle. Clicking inside the drawn circle allowed one to move a new circle so it could be placed around the next cell of interest. This method was used to draw the number of circles needed per background, interneuron, or pyramidal neuron. The circle that was corrected in size was moved completely into an area without any or minimal silver grains. When counting the number of silver grains per cell for pyramidal cells and interneurons, all neurons in the field of view were circled. This is important so as to not over count the number of cells per viewing area, 200x. If every cell were counted, then it would overestimate the number of neurons present per viewing area. The first circle Control+T brought up the ROI manager. "Show all" mode was checked to see where the circles were placed. The co-ordinates in picture were saved.

The next step was to open image that had the background circles of either size, the interneuron circles, or the pyramidal neuron circle. Then the Lipschitz filter was enabled by going to the "Filter" tab, "Plugins", then "Lipschitz". On the next screen that popped up, "Top down" and "Top hat" were selected, and the slope was set to 10.00. Next, the "Process" tab was selected, then "Binary", then "Make binary". These changes to the image adjusted the contrast to a black and white image showing only the silver grains. When the image was in black and white mode, the "Measure" button on the ROI Manager was clicked. The data which came

up were then copied and pasted into an excel document. The data provided the percentage of the circle that was covered by silver grains from which an average of all numbers were taken.

Next, five individual silver grains were measured by drawing a circle 5μm x 5μm around a single silver grain in order to determine the number of pixels a single silver grain comprised for each slide.

Excel:

In the excel file, the lengths of each nuclei type were averaged per sample to give an overall average, along with the how many glia, interneurons and pyramidal neurons per slide there were. Also, the background and silver grain size for each image were averaged. After this was completed for the images from the slides of interest, the "Cell-Background" for each neuron was calculated, along with the "Area covered", and "Number of silver grains".

Data analysis

Data analysis was completed using IBM SPSS Statistics version 21. Figures were made using Excel for Mac 2011, version 14.3.8, along with Graph Pad Prism 6.0c for Mac OS X. I tested the data for normal distribution, homogeneity of variance, performed correlations between demographics of schizophrenia patients and controls, and ran cell counts and mRNA ANOVAs or ANCOVAs to test for effect of diagnosis, gender and hemisphere, and explored potential confounders like medication.